REFINING TOOLS FOR EVAPORATION MONITORING IN SUPPORT OF WATER RESOURCES MANAGEMENT

by

C. Jarmain[1], C.S. Everson[2], M.J. Savage[3], M.G. Mengistu[2], A.D. Clulow[2], S. Walker[4] and M.B. Gush[2]

[1] CSIR Natural Resources and the Environment, P.O. Box 320, Stellenbosch, 7599, South Africa
[2] CSIR Natural Resources and the Environment, c/o Soil-Plant-Atmosphere Continuum Research Unit, Agrometeorology Discipline, School of Environmental Sciences, University of KwaZulu-Natal, Private Bag X01, Scottsville, 3209, South Africa
[3] Soil-Plant-Atmosphere Continuum Research Unit, Agrometeorology Discipline, School of Environmental Sciences, University of KwaZulu-Natal, Private Bag X01, Scottsville, 3209, South Africa
[4] Soil, Crop and Climate Sciences, Faculty of natural and Agricultural Sciences, University of the Free State, P.O. Box 339, Bloemfontein, 9300

WRC REPORT NO 1567/1/08

ISBN 978-1-77005-798-2

JANUARY 2009

Acknowledgements

The research in this project was funded by the Water Research Commission, for whose assistance we are sincerely grateful.

We also wish to acknowledge contributions made by members of the steering committee:

Dr R Dube	*Water Research Commission (Chairman)*
Dr GC Green	*Private (ex Water Research Commission, initial Chairman)*
Prof RE Schulze / Prof G Jewitt	*University of KwaZulu-Natal*
Prof GS Pegram	*University of KwaZulu-Natal*
Dr JE Hoffman	*University of Stellenbosch*
Dr PJT Roberts	*Private / Forestry Industry*
Dr D Terblanche	*South African Weather Services*
Mr M Warren	*Department of Water Affairs and Forestry*
Mr E Nel	*Department of Water Affairs and Forestry*
Mr O Wilson	*Department of Water Affairs and Forestry*
Mr J Bosch	*Formerly with CSIR*
Dr Theresa Volschenk	*Agricultural Research Council*
Prof N Jovanovic	*CSIR (Formerly with University of the Western Cape)*
Dr N Lecler / Dr A Singels	*South African Sugarcane Research Institute*

The following people provided valuable technical assistance to the experiments:
Alistair Clulow, Lulethu Sinuka, Eric Prinsloo, Joshua Xaba, Lucas Ngidi and Vivek Naiken.

The following students provided assistance to the various trials:
Michael Mengistu, Nile Eltayeb, Angelo Mockie, Mpumelelo Shange, Moses Nape, Obed Phahlane and Manuel Mbuende.

Various land owners are acknowledged for allowing field work to be conducted on their property. We are very grateful for this and the assistance they provided during the various trails.

- The South African Sugarcane Research Institute (SASRI) and specifically Mr Francois Olivier from the Komatipoort research station and Dr Neil Lecler from the SASRI offices at Mt Edgecombe are thanked for making the lysimetry total evaporation data collected at the Pongola research farm, and other information regarding the lysimetry trial, available.

- Research staff from the Pongola research farm is thanked for their general assistance while conducting the field work.

- The managers of the Vumbuka Reserve at the AECI industrial complex at Umbogintwini are thanked for permission to conduct the research on their premises.

- Staff from the Department of Water Affairs and Forestry (DWAF) offices at Midmar Dam is thanked for making available the Symon's pan evaporation data.

- The managers of the Midmar Resort, Howick are thanked for allowing project team members free entrance to the site.

- Mr Mat Jackson is thanked for arranging permission to work on the Midmar Dam premises.

Dr Peter Dye and Dr Colin Everson are thanked for allowing integration of field work conducted during this project, with work conducted as part of other field experiments, specifically work conducted at the Ukulinga research farm, the Vumbuka Reserve at the AECI industrial complex and the Magoebaskloof *Podocarpus* research site.

Executive Summary

1. MOTIVATION AND BACKGROUND

The 1998 National Water Act, which proposes licensing of consumptive uses of water that result in streamflow reduction, implicitly requires that such uses be measured or estimated with an acceptable degree of accuracy. This makes it important to know the degree of accuracy and precision that can be achieved when estimating evaporation using currently available methods.

Most techniques for estimating evaporation have been around since the late 1940s, but only in the last 20 years has technology enabled them to come into their own as reasonably affordable and practically applicable methodologies. Their full potential has yet to be realized, especially in South African circumstances. At the same time new opportunities for improved measurement, such as through the complementary use of ground-based and remote sensing techniques, especially for larger scale water resource related applications, also need to be explored.

This project followed on from a research project by Savage *et al*. (2004) which investigated the operational use of scintillometry for spatial estimates of evaporation of a grassland surface (WRC Report No 1335/1/04).

2. PROJECT OBJECTIVE

The project objectives were:

- Classification and characterisation of land uses/units and water-resource management applications for which evaporation measurements/estimates are needed.
- Assessment of accuracy and precision requirements relating to evaporation measurement/estimation for various water-resource management applications.
- Assessment of appropriateness of evaporation measurement/estimation techniques for addressing a range of key water-resource management needs.
- Development of guidelines for the complementary use of measurement and estimation techniques (in order, e.g., to meet calibration or verification requirements).
- Development/refinement of evaporation measurement/estimation techniques for key water-resource management applications.
- Establishment of a sound basis for capacity building and skills development relating to evaporation measurement and estimation.

3. METHODS

A number of methods are used in South Africa to estimate either evaporation, transpiration or total evaporation. This project was aimed at testing the suitability and accuracy of a variety of techniques for total evaporation estimation, and also at suggesting improvements and/or changes in the application of these techniques for a range of land surfaces. Almost all of the evaporation methods used rely on the simplified energy balance, $R_n = LE + H + G$, where R_n is the net irradiance, *LE* the latent heat flux density associated with

transpiration, soil evaporation and evaporation of water, *H* the sensible heat flux density and *G* the soil heat flux density. When each term of the energy balance is measured independently, and the equation satisfied, energy balance closure is said to be achieved. The closure discrepancy is defined as $(LE + H)/(R_n - G)$.

A range of methods were applied and evaluated, including the eddy covariance technique, the surface renewal method, the heat pulse velocity method and the scintillometry method. The one-sensor eddy covariance system consisted of a three-dimensional sonic anemometer. The two-sensor (full) eddy covariance system included an infra-red gas analyser for absolute humidity measurement, for the direct estimation of total evaporation. The surface renewal system consisted of a fine-wire temperature sensor connected to a datalogger programmed to collect high frequency air temperature measurements. The scintillometer consisted of a laser beam (in the case of the surface layer scintillometer) or an infra-red beam (in the case of the boundary layer scintillometer) positioned horizontally over a distance, above the canopy. The optical characteristics of the atmosphere partly scatters the beam, allowing measurements from which evaporation can be estimated. The heat pulse velocity method consists of a heater probe and two thermistor probes. The ratio of the increase in temperature, following the release of a pulse of heat, at points equidistant below and above a heater probe, is linked to the sapflow (transpiration) of a tree.

Seven research sites were used in seven different case studies. The sites were geographically distributed over South Africa and represented different land surfaces and climatic conditions. Surfaces studied included a newly established "orchard-like" *Jatropha* surface, a tall narrow plantation of *Podocarpus* trees, an open sugarcane field, a grass/shrub mix, a *Chromolaena* stand, a tree/shrub mix and an open water surface. In Case studies 4 to 7, the suite of different techniques were only tested during one window period or season. But, the different techniques were tested in more than one season at both the *Podocarpus* and *Jatropha* sites (Case studies 1 to 3). For Case study 5, two different sites were used to test the suitablilty of the techniques to estimate total evaporation from a short heterogeneous (species rich) and aerodynamically rough surface.

In **Case study 1** the energy balance closure of an "orchard-like" surface consisting of young *Jatropha* trees was investigated. The In Situ Flux systems and modified Applied Technologies Inc. open path eddy covariance systems were used for this purpose. In addition, the sensible and latent heat flux densities of the two open path eddy covariance systems, were compared with flux estimates of the RM Young eddy covariance (EC) system and the surface (SR) renewal system. Measurements were performed from 11 November to 2 December 2005.

In **Case study 2** the suitability of a range of micrometeorological techniques in estimating total evaporation from a tall canopy under limited fetch conditions, were investigated. Field work was carried out at a plantation of *Podocarpus falcatus* trees. Three principle techniques were tested at the *Podocarpus* site: (1) the EC system for direct and indirect estimates of LE, (2) the SR method and (3) the Heat Pulse Velocity technique (HPV). Field work was conducted during three field campaigns: 21 to 28 September 2005 (Field trip 1), 09 to 15 February 2006 (Field trip 2) and 23 to 30 August 2006 (Field trip 3).

In **Case study 3** the suitability of a range of micrometeorological techniques in estimating total evaporation from an "orchard-like canopy" was investigated, and the impact of the height of sensors within the surface boundary layer on the total evaporation estimates investigated. Field work was again conducted at an "orchard-like" surface consisting of young *Jatropha* trees. In order to evaluate the effect of sensor installation height on energy flux estimates, sensors were installed at two reference heights within the surface boundary layer. Fluxes estimated with the In Situ Flux systems and RM Young EC system and that estimated with the SR system, were compared. Measurements were made from 6 to 20 March 2006.

In **Case study 4** the performance of the open path eddy covariance system, surface renewal method, surface layer scintillometer and a field scale lysimeter in estimating total evaporation from an open canopy was evaluated. A field of sugarcane with a thick trash layer on the surface (tops treatment) was used in this study. Measurements were made over a four-day period (2 to 5 October 2007).

In **Case study 5,** the suitability of the different micrometeorological techniques in estimating total evaporation for short heterogeneous and aerodynamically rough vegetation was investigated. Two sites were selected. The first site consisted of an extensive area covered by grasses and shrubs. The second site consisted of an extensive area completely invaded by *Chromolaena odorata*. Three different techniques were tested at both the grass/shrub site and at the *Chromolaena* site during two separate field campaigns. Fluxes from two EC systems were compared against fluxes from the SR system and the surface layer scintillometer. At the grass/shrub site the modified Applied Technologies Inc. EC system was used and at the *Chromolaena* site the In Situ Flux systems EC system. The RM Young system was used at both sites. Measurements were made from 23 June to 10 July 2006 at the grass/shrub site, and from 4 to 11 April 2006 at the *Chromolaena* site.

In **Case study 6** the suitability of a range of techniques in estimating total evaporation from a tall heterogeneous surface was investigated. An extensive area, dominated by trees and shrubs, was selected. Techniques used included the EC technique (In Situ Flux systems, RM Young), the SR technique, and scintillometry (surface layer scintillometer). Measurements were made from 23 June to 10 July 2006.

In **Case study 7** the performance of different micrometeorological techniques in estimating evaporation from an open water surface was investigated. Evaporation estimates from an automatic weather station using traditional reference type methods were compared with that from micrometeorological methods. Evaporation estimates with the boundary layer scintillometer, an In Situ Flux EC system, an EC system using an RM Young sonic anemometer and four SR systems, were compared with evaporation measured with a Symon's tank and the Penman equation. Field work was conducted at the Midmar Dam, Howick from 29 June to 13 July 2007.

4. RESULTS AND DISCUSSION

In Case study 1 it was found that differences existed in the diurnal pattern and the magnitude of the fluxes when the direct estimates of *LE* with two different systems were compared at an orchard-like surface. When direct and indirect estimates of *LE* were compared, differences in *LE* were

found especially for the In Situ Flux system, but also occasionally for the modified Applied Technologies Inc. (ATI) EC system. The *H* values estimated with the ATI and RM Young sonic anemometers, as well as the surface renewal estimates of *H* compared very well. The *H* values estimated with the In Situ Flux system (Gill sonic anemometer) differed greatly from other estimates of *H* at mid-day. Energy balance closure was generally not achieved at this site, and closure discrepancy values generally exceeded 1. Total evaporation accumulated over a 14 day period showed differences of up to 26%. Direct estimates of ET with the ATI system were the smallest, and the direct estimate of ET with the In Situ Flux EC system, the greatest.

In Case study 2, energy fluxes were compared in an area under tall *Podocarpus* trees with limited fetch, in three different seasons. The *H* values estimated with the EC and SR systems compared very well – both diurnally and in magnitude, especially in the first and third field campaigns, despite a difference of 6 m in the installation height in the first field campaign. The *H* values estimated in the second field campaign with the different techniques compared reasonably well, but showed more variation than in the other campaigns. This suggests that something was wrong with the eddy covariance sensor during this field campaign. The *LE* values estimated with the three systems agreed reasonably well. Generally indirect estimates of *LE* with the In Situ Flux EC systems showed the greatest variation, and the greatest *LE* values. Energy balance closure was often reached, with closure discrepancy values often equal to one, but for some 30 min periods, exceeding 1. Total evaporation accumulated over the three field campaigns showed that total evaporation estimates agreed to within 18%. The ET estimated with the SR method was the greatest (26 mm), and that with the direct estimate with the In Situ Flux EC system the smallest (22 mm). The ET estimates from the heat pulse velocity techniques (up-scaled from sap-flux measurements), compared well with the ET estimates from the micrometeorological methods.

In Case study 3 the *LE* values estimated at different heights above an orchard-like Jatropha canopy showed some differences in magnitude and the diurnal pattern, but nonetheless compared favourably. Differences in the *LE* values estimated with systems installed at the same heights were similar to those estimated with systems installed at different heights. Over a four-day period, the direct estimates of ET (sub-daily) (using the In Situ Flux EC system) exceeded ET from all other systems by up to 19%, with the exception of the SR system installed at the lowest reference height. Over a four-day period, sub-daily estimates of ET with all the systems varied by up to 25%.

In Case study 4 it was found that despite the open canopy of the sugarcane field studied, soil heat flux densities were very low (<15% of R_n), possibly because of the thick mulch present. Areally-averaged and point-based *H* estimates were within 30% of each other. Areally-averaged estimates of *H* were generally slightly underestimated. Areally-averaged estimates of *LE* and point-based estimates of *LE* also compared favourably (to within 16%). Areally-averaged estimates of *LE* generally slightly exceeded the point-based estimates. For a corresponding day, estimates of ET with the EC method, the SR method and the scintillometer, were within 11% of each other. But, ET estimated with the lysimeter was 50% less than the spatial estimate of ET, because of reduced transpiration rates by the sugarcane plants in response to waterlogged conditions in the

lysimeter following significant rainfall (91 mm).

In Case study 5, it was shown that the *H* values estimated with different techniques applied at two short heterogeneous canopies compared favourably (to within 36%). But, large differences in the magnitude of *H* existed on sunny days. Similarly, *LE* values, with the exception of the direct estimates of *LE* at the grass/shrub site, compared favourably. Generally, spatially averaged estimates of the *LE* values exceeded point-based estimates thereof. Direct estimates of ET (using the ATI EC system) were significantly smaller (up to 61%) than other estimates of ET, and likely because of a malfunctioning infra-red gas analyser sensor. The ET estimates from the other systems were generally within 20 and 39% of each other, depending on the site and monitoring system.

In Case study 6 point-based and spatial estimates of *H* estimated at a tall heterogeneous surface agreed to within 28%. *LE* values agreed to within 11%. Estimates of *H* with the In Situ Flux EC system generally exceed that from other systems. No single method consistently over- or underestimated H, *LE* or ET. The estimated ET with five different systems over a four-day period was within 14% of each other.

In Case study 7, highly variable heat storage values of an open water surface were measured at a 2 min interval. Heat storage values were smoothed for use in the calculation of LE, and sometimes accounted for up to 40% of the net irradiance. Sensible heat flux densities estimated with all techniques were generally very small (< 40 W m^{-2}). The *LE* values estimated with different micrometeorological techniques compared very well (to within 9% of each other). Daily estimates of evaporation (E) from the Symon's pan were generally within 7% of the estimates of E with the other techniques. Evaporation calculated with the Penman equation, however, was significantly higher than all other estimates of evaporation. Over a six-day period the Penman E was up to 46% higher than the other evaporation estimates.

Guidelines for estimating total evaporation: A Decision Support System

Another major output from this project, is the Guidelines developed to aid users in the selection of a suitable technique for estimating total evaporation from a specific surface. The Guidelines also provides users with basic information on the selected technique(s). A simple Decision Support System (DSS), in EXE format, was created in the Visual Mind™ software programme. The Guidelines DSS runs through a web browser installed on the computer. The DSS was designed so that the user is prompted with simple questions that ultimately lead to the selection of a suitable technique for estimating evaporation. The first question the user is asked is whether the technique to be used is known to the user. If that is the case, the user can select the technique from a list provided. More information on the specific technique can be obtained by opening or downloading an associated PDF file, which takes the form of a technique specific fact sheet. If the user is unsure of the suitable method for total evaporation estimation, the user is guided in the selection of a suitable technique through a set of questions, first of all relating to the dominant surface to be studied, e.g. whether the surface to be studied is a bare soil surface, open water surface or a vegetated or partly vegetated surface. The user is prompted with more questions relating to the surface to be studied, which lead to the selection of one or more suitable techniques.

5. CONCLUSIONS AND RECOMMENDATIONS FOR FUTURE RESEARCH

Evaporation estimation remains one of the important challenges for the agricultural and environmental sciences. Determination of reliable and representative evaporation data are an important issue of atmospheric research with respect to applications in agriculture, catchment hydrology and the environmental sciences, not only in South Africa but also elsewhere in the world. Techniques for long-term measurements of evaporation at different spatial and time scales and from different climatic regions are not yet readily available, though a number of different methods are available for shorter term measurements. Methods like the scintillometer and temperature-based aerodynamic methods are becoming more popular and hold great potential for long-term application and estimation of evaporation over different spatial scales. The scintillometer has the advantage of a large areal representation of the evaporation measured and real-time monitoring but the method is costly. The temperature-based methods, such as the SR method, have lower costs and low power requirements. In some cases real-time estimations of evaporation are possible for the temperature-based methods.

Eight possible areas for future research and activities are presented here in relation to the progress made in the current programme of research:

1. There is a dearth of technologists trained in the field of evaporation estimation. This has negative long-term consequences. This current project attempted to address this through conducting a training workshop. This should be aggressively pursued through regularly conducting similar workshops. Different agencies within South Africa are using different methods for estimating evaporation – hopefully there can be some sharing of knowledge and data and working towards a common approach in the future.

2. The aspect of fetch and the footprint of evaporation estimates were not the main focus of this report. However, these important aspects must receive continuing attention especially since more and more research is conducted on indigenous and invasive vegetation. Some of the sites chosen for evaporation measurement were at the limit of inadequate fetch and this aspect needs to be considered in more detail in relation to footprints. For example only one footprint model was applied in this study.

3. The lack of energy balance closure is another area that has frustrated energy balance methods and the consequential estimation of evaporation. This aspect needs to be further pursued and in addition, needs further research and must involve the estimation of evaporation from the high frequency measurements of water vapour pressure using an approach similar to the Surface renewal approach for high frequency air temperature.

4. The contribution and importance of advected energy (local and regional) to the energy balance of arid environments, especially where total evaporation from riparian zones needs to be estimated, also need to be assessed. With an increased interest in these arid environments and especially the water use requirements of ground water dependent ecosystems, it is important to understand limitations of micrometeorological evaporation estimation systems if applied under these climatic conditions.

5. Ground-based methods for estimating evaporation will always be in demand. These measurements are required to validate the remote estimates determined using spatial methods. The merging of these technologies will see much progress in the near future for near real time water resources management.

6. Water resources management on a catchment scale is normally based on catchment water balance modelling. Advances in technologies like the microwave scintillometry system which provides estimates of evaporation over several kilometres (< 15 km) can provide opportunities for improved catchment water balance modelling. Estimated and measured evaporation from small catchments can be compared directly for the first time ever. Especially when linked to remotely sensed data, this combination of measurement and modelling could hold great potential and needs to be investigated.

7. A complete, on site, real-time, sub-hourly, inexpensive and simple method for estimation evaporation has not yet been achieved. It has been suggested that high frequency air temperature-based methods, of which the SR method is one, may pave the way for evaporation stations from which real-time and sub-hourly estimates may be obtained relatively inexpensively. It is in this area that future research should also be continued.

8. Especially for water resources management of dams and reservoirs, a real-time, sub-hourly, inexpensive and simple method for estimation evaporation is required. Since the size of the dam or reservoir can differ greatly, and so the water quality, all affecting evaporation rates, it is in this area that future research should also be continued.

6. EXTENT TO WHICH THE CONTRACT OBJECTIVES HAVE BEEN MET

This project aimed at identifying key land uses for which accurate estimates of evaporation are required, and to establish an acceptable degree of accuracy for these estimates.

Interested stakeholders were invited to a workshop to provide input into the selection of the key land uses to be studied. From the workshop list a final list of study sites were selected by the project team.

A range of techniques for estimating evaporation were assessed as part of seven case studies in which different study sites were used. The application of a range of techniques, including the EC, SR, scintillometry and HPV techniques, were evaluated successfully. Sites used included a *Jatropha* orchard, a narrow plantation of *Podocarpus* trees, a sugarcane field with open canopy, two short heterogeneous, aerodynamically rough surfaces (a *Chromolaena* invaded area, a grass /shrub canopy), a tall heterogeneous, aerodynamically rough surface (a mixed tree and shrub canopy), and lastly a large dam.

The project further aimed at developing guidelines for the use of evaporation estimation techniques. A simple Decision Support System was developed to aid users in the selection of a suitable technique for the estimation of total evaporation for a specific surface. The DSS also provides users with basic information on the selected technique(s).

7. CAPACITY BUILDING & TECHNOLOGY EXCHANGE

Student involvement

This project had a very strong focus on capacity building and skills development in the use of techniques for evaporation estimation, as the current skills base is small. It also focused strongly on knowledge dissemination of the techniques available to estimate evaporation.

A number of students from both the University of KwaZulu-Natal and the University of the Free State contributed to and benefited from this project through their post-graduate studies. Mr. Dumisani Shezi was appointed to the CSIR as an intern for the period 1 January 2006 to 31 December 2006 to work specifically on this project. Mr. Shezi completed several courses in the field of Agrometeorology, and was going to start his M.Sc. project work during 2007, but accepted a position at DWAF in Pretoria as Hydrologist in 2007 and did not continue with his studies.

A number of Agrometeorology (PhD) students from the University of KwaZulu-Natal were involved in a number of field campaigns. The various field campaigns have been crucial in the development of these students and have provided a unique opportunity to test various techniques for the estimation of evaporation. Mr. Michael Mengistu, has successfully completed his PhD on the use of the surface renewal method for estimating sensible heat. The data analysis from his thesis included data from a previously funded WRC report (Savage *et al*., 2004), data from this project as well as data from the Ukulinga *Jatropha* project. As such, it is an output from three WRC projects but mostly from this current project. Mr. Nile Eltayeb is concentrating on evaporation from water bodies and sugarcane for his PhD and collected data during two field campaigns. Mr. Alistair Clulow has been involved in most of the field campaigns of this current project. He completed his Masters thesis in 2008, though as part of another WRC project, he benefited greatly from this project.

Agrometeorology students from the University of the Free State had the opportunity to see how the techniques for the estimation of evaporation are tested above a mixed canopy of *Chromolaena* and an open water surface. Mr. Angelo Mockie participated in the measurements of water use over *Chromolaena*. Students Mr. Mpumelelo Shange, Mr. Moses Nape, Mr. Manuel Mbuende and Mr. Obed Phahlane, assisted with the set-up and maintenance of instruments for the measurement of evaporation from the surface of Midmar Dam. This gave them the hands-on experience of the various instruments as they worked side-by-side with the experienced researchers.

Winter school and workshop

A week-long Winter school focussing on evaporation and aimed at students was presented from 17 to 21 July 2006. The Winter school aimed at exposing students to techniques that can be used to estimate evaporation, the theory supporting these techniques, and potential applications of such techniques. To complement the Winter school, a one-day Workshop aimed at water resources managers and practitioners, was also held. A total of 41 students and researchers attended the Winter school and represented eleven different institutions (Universities and research organisations). Most of these students were at post-graduate level, and were students from related fields. An additional ten people from universities, research institutions and governmental organisations joined the students for the Workshop on the final day.

Prof. Mike Savage (UKZN) presented the lectures on techniques for evaporation estimation, and a few other people were asked to do selected presentations (Dr. Caren Jarmain, Mr. Mark Gush, Dr. Colin Everson Dr. George Green and Mrs. Jenny Blight).

8. DATA

All processed data used in the report have been catalogued. A copy of the data is included on a CD accompanying this report. The raw data are stored at Natural Resources and the Environment Unit, CSIR, P.O. BOX 320, Stellenbosch, 7599.

Contact person: Dr. C. Jarmain.

The raw data are held on a hard drive and DVDs. All data can be supplied to researchers and managers on DVDs if required.

9. PUBLICATIONS

A popular article was published in a WRC publication during this project. The feature article in the July/August 2006 edition of the Waterwheel is on evaporation: "Building an evaporation monitoring toolkit". The article provides general information on evaporation estimation in South Africa, and refers to this research project. A copy of this article can be obtained from the WRC website (http://www.wrc.org.za/downloads/waterwheel/jul-aug%2006/evaporation%20p12-15.pdf)

A lot of the results from this study are also published in the PhD dissertation of Michael Mengistu (Mengistu, 2008).

Table of Contents

CHAPTER 4: ASSESSMENT OF THE SUITABILITY OF SELECTED TECHNIQUES FOR THE ESTIMATION OF TOTAL EVAPORATION 31

List of figures

List of tables

Symbol list

Symbol	Description	Unit
A	Area	m^2
A_{pan}	Class-A pan area	m^2
$A_{lysimeter}$	Lysimeter cross-sectional area	m^2
c_p	Specific heat capacity of air at constant pressure	J kg^{-1} K^{-1}
C	Energy balance closure	W m^{-2}
$\bar{c}$	Average closure value	W m^{-2}
C_n^2	Structure parameter for refractive index fluctuations	$m^{-2/3}$
D	Closure discrepancy	Unitless
dt	Time difference	S
dT_a	Air temperature difference	^oC
e_1, e_2	Water vapour pressure measured at two profile positions z_1 and z_2	Pa
ET_o	Reference evaporation	mm
G	Energy per unit time interval per unit area required to heat soil – referred to as soil heat flux density or in the case of water surface heat density stored in the water	W m^{-2}
H	Energy per unit time interval per unit area required to heat the atmosphere above the soil – referred to as the sensible heat	W m^{-2}
H_{BR}	Sensible heat flux density estimated using the Bowen ratio method	W m^{-2}
H_{EC}	Sensible heat flux density estimated using the eddy covariance method	W m^{-2}
H_{SR}	Sensible heat flux density estimated using the surface renewal method	W m^{-2}
K_h	Exchange coefficient for sensible heat flux density	M^2 s^{-1}
K_w	Exchange coefficient for latent energy flux density	
L	Specific latent energy of vapourisation	J kg^{-1}
LE	Energy per unit time interval per unit area required to evaporate water – referred to as latent energy or evaporation	W m^{-2}
LE_{BR}	Latent energy flux density estimated using the Bowen ratio method	W m^{-2}
LE_{EC}	Latent energy flux density estimated using eddy covariance	W m^{-2}
M_a	Mass of air heated (or cooled)	kg
q'	Fluctuation in absolute humidity	kg m^{-3}
R_n	Net irradiance above the surface	W m^{-2}
r_m	Time lag corresponding to maximum of S_T^3	s
r_s	Surface resistance	s m^{-1}
S	Air temperature quiescent period used with the surface renewal method	s
S_r^3	Third order air temperature structure function for time lag r_m	$^oC^3$
T_1, T_2	Air temperature measured at two profile positions z_1 and z_2	^oC
T_{sonic}	Sonic temperature	^oC
T_z	Air temperature at height z	^oC
$\bar{T}_{sonic}$	Average sonic temperature	^oC
T'	Fluctuation in sonic temperature	^oC

Symbol	Description	Unit
u, v and w	Three-dimensional components of wind velocity, u and v orthogonal and in the horizontal plane and w in the vertical	m s^{-1}
u_*	Friction velocity	m s^{-1}
U_2	Horizontal wind speed at a height of 2 m	m s^{-1}
V_a	Volume of air	m^3
w'	Fluctuation in vertical wind speed	m s^{-1}
$\overline{w}$	Average vertical wind speed	m s^{-1}
z_1	Profile height	m
z_2	Profile height	m
$\delta W / \delta t$	Rate of change in lysimeter weight	kg s^{-1}
ρ_w	Density of water	kg m^{-3}
α, β, γ	Empirical constants used for the surface renewal method	
β	Bowen ratio	Unitless
σ_T	Temporal air temperature standard deviation	^oC
γ	Psychrometric constant	Pa K^{-1}
a	Air temperature amplitude	^oC
ℓ	Air temperature ramp period used with the surface renewal method	s
τ	Total ramping period	s

List of definitions

Bowen ratio

The Bowen ratio can be defined as the ratio of heat energy used for sensible heating (conduction and convection) to the heat energy used for latent heating (evaporation of water or sublimation of snow). The Bowen ratio generally ranges from about 0.1 for the ocean surface to more than 2.0 for deserts and negative values are possible when reversing fluxes occur. In the early 1940s, Hararld Sverdrup named the ratio of heat conduction to evaporative flux at the air-water interface the Bowen ratio, after Ira S. Bowen (1898-1978), an American astrophysicist (http://earthstorm.mesonet.org/materials/b.php, Lewis, 1995).

Closure discrepancy

Energy balance closure can be assessed by looking at the energy balance closure discrepancy. Closure discrepancy can be defined as the ratio of the sum of the sensible and latent heat flux densities ($LE + H$) to the available energy (R_n-G).

Energy balance closure

If all four components of the energy balance (R_n, LE, H and G) are measured independently and correctly, energy balance closure (c) can be determined using the equation

$$c = R_n - LE - H - G$$

where c is termed the energy balance closure (W m^{-2}). Closure is said to be satisfied if $c = 0$ W m^{-2}.

Evaporation

Evaporation is the "physical process by which a liquid or solid is transferred to the gaseous state" (Huschke, 1959).

Fetch:height ratio

A number of micrometeorological methods require extensive fetch (homogeneity in surface conditions) in the upwind direction. The fetch requirements relate to the boundary layer requirements. The necessary fetch required to establish equilibrium conditions has often been assumed to have a relationship to the maximum measurement height above the ground. An ideal fetch:height ratio is often defined as 100:1.

Reference evapotranspiration

Allen *et al*. (1998) defines reference evapotranspiration (ETo) as "*The evapotranspiration from a reference surface, not short of water …The reference surface is a hypothetical grass reference crop with specific characteristics…The only factors affecting ETo are climatic parameters. Consequently, ETo is a climatic parameter and can be computed from weather data. ETo expresses the evaporating power of the atmosphere at a specific location and time of the year and does not consider the crop characteristics and soil factors.*" Other definitions specify that the reference surface should fully cover the soil surface. In this document we refer to it as reference evaporation.

Simplified energy balance

The simplified version of the energy balance of a specific surface is given by the equation

$$R_n - G - LE - H = 0$$

where R_n is the net irradiance, LE the latent (evaporation) energy flux density, H the sensible heat flux density and G the soil heat flux density. All terms are in W m^{-2}. The specific latent energy of vapourisation L is (2.501-0.00237 T_z) (MJ kg^{-1}), where T_z is the air temperature (^oC) at height z.

Total evaporation

Total evaporation (ET) can be defined as the total process of water movement into the atmosphere. Soil evaporation (E) and transpiration (T) occur simultaneously and are determined by the atmospheric evaporative demand (available energy and water vapour pressure deficit), soil (soil water availability), windspeed and canopy characteristics (canopy resistances) (Rosenberg *et al*., 1983). Others (Kite and Droogers, 2000) refer to total evaporation as evapotranspiration.

In this experiment total evaporation refers to the sum of (a) evaporation from the soil surface, (b) transpiration by vegetation, and (c) evaporation of water intercepted by vegetation.

Transpiration

Transpiration can be defined as evaporation of water that has passed through the plant. Transpiration therefore consists of vaporization of liquid water contained in the plant tissues and vapour removal to the atmosphere (Allen *et al*., 1998).

Chapter 1: Background

C.S. Everson

The need for increased food and timber production has led to dramatic increases in land under irrigated agriculture and forestry in South Africa. Agriculture and forestry faces increased competition for water by industries, municipalities and other groups. This ever-growing demand for water makes it imperative that water resource management procedures and policies be wisely implemented and improved. The accurate assessment of total evaporation from land surfaces is essential if this is to be done.

Since Dalton first introduced the mass transport equation in 1801 (Dalton, 1801), numerous methods for estimating or measuring evaporation have been developed. In certain instances, these methods are accurate and reliable; in others, they are unsuitable or provide only rough approximations. It is therefore over 200 years since the physical process of evaporation was described and 60 years since the formulation of the Penman equation (Penman, 1948). The latter included certain empiricisms to account for the aerodynamic and net radiation terms involved in the evaporation processes. Prior to this, most ecological studies on the water relations (transpiration) of plants were based on the "cut shoot" method using short term measurements of excised plant parts (Slavik, 1974). In South Africa the method was used by Mes and Aymer-Ainslie (1935), Henrici (1940, 1942), Brueckner (1944), Weinmann and le Roux (1946), Du Preez (1964), Van Zinderen Bakker (1971) and Everson (1979). It was also at about this time that weighing lysimeters for measuring evaporation were coming into use (Green *et al*., 1974; Hutson *et al*., 1980).

Even as late as 1989 the estimation of total evaporation by the measurement of the water vapour gradient was considered not yet ready for general application, despite being theoretically attractive (Scholes and Savage, 1989). The first micrometeorological attempts to measure total evaporation in South Africa were made on wheat using reiterative methods to solve the energy balance equation using an aerodynamic treatment of momentum, mass and heat exchange (Bristow and De Jager, 1981). The data were collected by means of multi-channel strip chart recorders.

In the early 1990's the development and increasing availability of more sophisticated electronic equipment and sensors allowed researchers to focus on the measurement of hydrological processes in South Africa (Dye and Bosch, 2000). This equipment enabled the direct measurement of the site energy balance and canopy microclimate (e.g. Bowen ratio, eddy covariance methods) and sap flow in trees (e.g. heat pulse velocity method, HPV). The operational use of the former techniques were pioneered in Water Research Commission funded studies in Catchment VI at Cathedral Peak (Savage *et al*., 1997, Everson *et al*., 1998), while the routine measurement of transpiration and plant water stress in trees using the heat pulse velocity technique (Green and Clothier, 1988; Olbrich, 1994; Dye *et al*., 1997a, b) has become a standard measurement in South Africa.

From the above discussion we can conclude that there is currently no single method capable of providing both good spatial and temporal data of evaporation. South African researchers have had good success with the heat pulse velocity and energy balance techniques. However, the HPV technique is suited only to mono-specific stands of trees, is problematic when scaling from single trees to whole stands and is a destructive technique (trees must be felled to calculate sapwood areas and wound size). The latter makes accurate calculations of transpiration only possible at the end of an experiment. The Bowen ratio energy balance (BREB) technique on the other hand, is well suited to mixed species communities such as grassland, but is limited by constraints imposed by both fetch distances and measurement height. Thus, the technique is not well suited to narrow strips of vegetation (e.g. riparian zones and wetlands) where fetch distances are short, or above tall vegetation where there are small gradients of temperature and humidity (caused by the increased wind turbulence above tall canopies). These gradients are often outside the measurement resolution of the instrumentation.

In recent years, direct measurements of turbulent fluxes have been achieved by local eddy correlation measurements. However, the application of this technique is often problematic. The necessary sensors for wind, temperature and humidity must respond very quickly (resolution 10 Hz or better) and at the same time must not show noticeable drift. This makes them delicate, expensive and in many cases difficult to calibrate. In addition, flow distortions by the sensor, mast, etc., as well as horizontal misalignments often cause significant errors. Moreover, there are technical problems, because temporal co-spectra, measured at a fixed local sensor, extend to very low frequencies. To achieve acceptable significant means often demands averaging periods of several tens of minutes. Such long averaging periods reduce the temporal resolution and conflict with the requirement of atmospheric stationarity within averaging periods. Due to these difficulties, alternative flux measurement methods have been sought.

Recent investigations have demonstrated the potential of using scintillometers to measure areally-averaged sensible heat fluxes over path lengths which range from 50 m to satellite pixel scale i.e. several kilometres. In one such study, Savage *et al*. (2004) investigated the use of the surface layer scintillometers for estimating spatially averaged energy fluxes and total evaporation. A scintillometer measures the intensity fluctuations of visible or infrared radiation after propagation over the plant canopy of interest. The fluctuations are caused by interference after the radiation has been scattered by inhomogeneities in the refractive index of the air, the latter caused by turbulent fluctuations of temperature and humidity. In contrast to local or point-based measurements, scintillometers provide spatially averaged results. An important significant advantage of the scintillometer is that the temporal resolution achievable is one order of a magnitude higher than that of point measurements obtained by instruments such as eddy covariance. Typical averaging times are 2 to 10 minutes for the fluxes and 10 to 60 s for the other turbulence statistics, with virtually no statistical noise. Due to the spatial averaging, extended experimental areas can be representatively characterized with a single instrument. With surface layer scintillometers it is therefore possible to measure the turbulent sensible heat (and hence calculate evaporation) for small areas, such as riparian zones, dams, slime dams and urban environments, while the large aperture scintillometers are suitable for large scale measurements of up to five kilometres. The expanded range of these instruments has opened up many avenues of research not previously possible.

The wide array of instrumentation available to researchers has made the choice of a suitable technique much more difficult, as each technique has advantages and disadvantages depending on the canopy type, fetch distances, available budget and the research objective. Equally important is the degree of expertise required or difficulty involved in operating the different technologies.

The objective of this project was to compare the various techniques over a wide range of canopy and climatic conditions in order to provide a better understanding of the advantages and disadvantages of each technique. The specific objectives set out for the project include:

- Classification and characterisation of land uses/units and water-resource management applications for which evaporation measurements/estimates are needed.
- Assessment of accuracy and precision requirements relating to evaporation measurement/estimation for various water-resource management applications.
- Assessment of appropriateness of evaporation measurement/estimation techniques for addressing a range of key water-resource management needs.
- Development of guidelines for the complementary use of measurement and estimation techniques (in order, e.g., to meet calibration or verification requirements).
- Development/refinement of evaporation measurement/estimation techniques for key water-resource management applications.
- Establishment of a sound basis for capacity building and skills development relating to evaporation measurement and estimation.

This project falls within the Hydroclimatological research programme of the Water Research Commission. In this program the project will contribute to research support for water resources assessment, management and sustainable utilisation in South Africa, by improving the methodologies and capacity for monitoring evaporation from both land and water surfaces.

Chapter 2: Theory and Practice of Evaporation Measurement

M.J. Savage

2.1 Introduction

Evaporation estimation remains one of the important challenges for the agricultural and environmental sciences. Different methods for measuring or estimating total evaporation include the pan methods, the reference evaporation and crop factor approach, lysimetry, atmometers such as the ETgage, and a whole range of aerodynamic methods that estimate sensible heat from which evaporation is estimated as a residual using the shortened energy balance equation. Excluded from this list are the climate based methods that operate at daily, weekly or even monthly time scales. Also excluded are the canopy enclosure methods using infrared gas analysers that allow for the measurement of transpiration rate of whole plants or plant parts. Microlysimeters allow measurement of soil evaporation, while heat pulse velocity or sap flow methods measure transpiration rate. The reference evaporation method (ETo), based on the Penman-Monteith approach, has recently been updated to allow hourly estimations of ETo. Estimations of ETo require measurements or estimations of solar irradiance, air temperature, atmospheric humidity and wind speed. Hourly reference evaporation is now possible for short grass (0.1 m tall) and short crop (0.5 m tall). For these two situations, different surface resistances and aerodynamic resistances are used. The disadvantage of the reference evaporation method is that for estimating the actual evaporation, a crop factor is required. The dual crop factor approach, as would be required for row or orchard cropping situations, allows two factors, one for soil evaporation estimations and one for the crop. Lysimeters are generally regarded as the standard for total evaporation measurement but they are expensive and not portable. Aside from the ETo estimations, the aerodynamic methods for estimating sensible heat or latent energy have received much attention over the last decade or so. Improvements in datalogging, improvements in sensors and their reduced cost have made their *in situ*, long-term, and unattended use in remote areas attractive. The eddy covariance and Bowen ratio methods have received the most attention but increasingly, the scintillometer and temperature-based aerodynamic methods are becoming more popular. The scintillometer has the advantage of the large areal representation of the measurements and real-time monitoring but the method is costly. The temperature-based methods, such as the surface renewal method, have low cost and low power requirements. In some cases real-time estimations of evaporation are possible for the temperature-based methods. Each of the aerodynamic methods is described and their advantages and disadvantages compared. The use of the heat pulse velocity and stem steady state heat energy balance methods are also discussed. Aspects of the closure of the energy balance and aspects of measurement footprints are discussed in relation to the different measurement methods.

2.2 Background

"The 1998 Republic of South Africa National Water Act refers to the possible prescription, by government, of methods for making a volumetric determination of water for purposes of water allocation and charges in the case of activities resulting in stream flow reduction. Given this scenario and the demand on water resources it is important to consider how evaporation, one of the main components of the water balance, and of the energy balance, is to be measured or estimated with reliable accuracy and precision. Determination of reliable and representative evaporation data are an important issue of atmospheric research with respect to applications in agriculture, catchment hydrology and the environmental sciences, not only in South Africa. Long-term measurements of evaporation at different time scales and from different climate regions are not yet readily available (Savage *et al*., 2004; Savage, 2008)".

There is a lack of evaporation data nationally with the result that evaporation models are used for its estimation. The term total evaporation includes evaporation from water and soil and transpiration from plants – also referred to as evapotranspiration in the literature. Evaporation measurements aid in planning land use changes, investigating human impacts on the environment and investigating impacts of global climate changes on water resources. Evaporation models need validation and calibration using actual evaporation data. There is a need for methodologies that would allow evaporation to be measured with spatially explicit models used to routinely estimate evaporation over time and space. Various type of models have been used, including deterministic type models (for example, Evett and Lascano, 1993) and adaptive neural-based fuzzy inference systems that process past data, mainly microclimatic, and adapt so as to provide estimates as new data become available (Terzi *et al*., 2006; Kii and Öztürk, 2007).

Evaporation measurements are also important for ground truthing remotely sensed evaporation estimates using models such as SEBAL (Bastiaanssen *et al*., 2005) and METRIC (Allen *et al*., 2007 a, b). Remote sensing numerical and empirical algorithms for the estimation of crop evaporation are detailed in the review of Corault *et al*. (2005). Some studies have combined ground- and aircraft-based estimates of evaporation with aircraft measurements providing vegetation cover and surface temperature information 30 m resolution (Kustas *et al*., 2006). In another aircraft study, spatial variability of the surface energy balance was at scales from 10 to 100 km (Isaac *et al*., 2004) and in a study using MODIS satellite data, monthly water balances from 1-km to continental spatial scales were demonstrated (Cleugh *et al*., 2007).

The field-measurement of total evaporation (mainly soil evaporation and transpiration) is of paramount importance in determining the water use of vegetation. In general, total evaporation studies are limited due to the high cost of instrumentation and sensors, instrumentation battery power requirements including the difficulty in obtaining real-time measurements in remote areas. Furthermore, many micrometeorological measurement methods require site homogeneity, adequate fetch, neglect of advection influences and application of the Monin-Obukhov similarity theory, MOST, which is described in detail by Foken (2006).

Point (single-level), profile and line-averaged atmospheric measurements have been used to measure sensible heat. Sensible heat is driven by vertical temperature differences between the canopy or soil surface and overlying air. By contrast, latent energy transfer (evaporation) is driven by vertical water vapour pressure differences between just above the canopy or soil surface and the overlying air.

2.2.1 The shortened energy balance

The sun provides energy to the earth's surface and the amount of energy is expressed as an energy amount per unit time interval per unit area. Solar irradiance, in J s^{-1} m^{-2} or W m^{-2}, is an important driver for many physical and physiological processes in the natural environment. Not all of the solar irradiance is utilised at the earth's surface. Some of it is reflected back to the atmosphere and some converted into infrared irradiance, invisible to the eye, and emitted to the atmosphere. A fraction of this emitted amount is returned to the surface by greenhouse gases, clouds and other particles. The net irradiance R_n (W m^{-2}) at the earth's surface is defined as the balance between incoming and reflected solar irradiance and outgoing and returned infrared irradiance.

The net irradiance at the surface of the earth is used to evaporate water, heat the air above the soil, heat the soil and vegetation and is also used by plants for photosynthesis. The energy associated with photosynthesis is usually small over a period of less than a day compared to the other components of the energy balance. For tall crops with a dense canopy, the heat stored in the canopy and the surrounding air may have to be taken into account. The evaporation of water requires energy to cause a change in the phase of water from the liquid form to water vapour. The symbols used for these forms of energy per unit time interval per unit area and information about each term are as follows:

R_n (W m^{-2}): net irradiance above the surface. This is measured directly using a net radiometer placed above the surface, typically between 1 and 3 m;

G (W m^{-2}): energy per unit time interval per unit area required to heat soil – referred to as soil heat. Generally G is positive during the day and negative during the night. This term is estimated using soil heat flux plates, temperature and water content sensors buried in the soil;

H (W m^{-2}): energy per unit time interval per unit area required to heat the atmosphere above the soil – referred to as the sensible heat. Generally H is positive during the day and negative during the night if the sign convention of Eq. (1) is used. Many methods have been used to estimate H;

LE (W m^{-2}): energy per unit time interval per unit area required to evaporate water – referred to as latent energy or evaporation. Generally LE is positive during the day corresponding to evaporation and negative at night corresponding to condensation. This term may be estimated using the simplified energy balance assuming that every other term is known but may also be estimated directly.

These energy balance terms, excluding stored heat in vegetation and photosynthesis, constitute the simplified energy balance:

$R_n = LE + H + G$	*1*

The specific latent energy of vapourisation L = (2.501–0.00237 T_z) MJ kg^{-1} where T_z is the air temperature (^{o}C) at height z.

There are many methods used for estimating evaporation (**Table 1**). A review on evaporation estimation methods by Drexler *et al*. (2004) mentioned that very few of the evaporation estimation methods work well for an hourly time-step, and in some cases, do not work well even for a daily time-step. There is perhaps only one method, the lysimetric method, that allows for the direct measurement of the total water loss from a vegetated surface. Virtually all of the methods rely on a theoretical framework for arriving at an expression for the latent energy flux density, in terms of other measurable quantities, based on certain assumptions or approximations. Many of the methods invoke use of the simplified surface energy balance equation (Eq. 1).

Terms ignored in the shortened energy balance include advection (horizontal transport of energy and water vapour into or out of the area under consideration), and stored heat and water vapour in the vegetation and surrounding air.

The term associated with evaporation, *LE*, could be estimated using the shortened form of the energy balance from:

$LE = R_n - H - G$	*2*

In words, evaporation (*LE*) is estimated as the net irradiance (R_n) less the sensible heat (*H*) less the soil heat (*G*).

In summary, evaporation may be estimated if R_n, *H* and *G* are known, assuming that other terms that may contribute are negligible over time periods of less than a day. Alternatively, *LE* may be determined directly without the use of the energy balance equation.

Table 1[1] Selected methods used for measurement (or estimation) of the sensible heat (*H*) and/or latent heat flux density (evaporation) (*LE*) terms of the surface energy balance, where $R_n = LE + H + G$ with R_n the net irradiance and *G* the soil heat flux density. Information is given on the spatial extent of the measurement, and temporal representation, and also the theoretical basis. A comment is also included on energy balance closure (see Section 2.4 for more detail).

Method	Measurement area, distance or height	Averaging period	Theoretical basis/comment	Closure statement/ Comment
Class A-pan/ Symon's tank	< 5 m^2	Usually daily	$LE_{pan} = L\rho_w(\delta W/\delta t)/A_{pan}$ where ρ_w is the density of water, $\delta W/\delta t$ is the rate of change in lysimeter weight and A_{pan} is the pan area	Only pan evaporation measured
Reference evaporation	Point measurements at 2 m above short grass of solar irradiance, air temperature, wind speed, water vapour pressure	Hourly/ daily	Penman-Monteith method for estimating reference evaporation (FAO 56), and use of a crop factor (Allen *et al.*, 2006) for short grass (0.1 m tall) and **tall** crops (0.5 m tall)	Only reference evaporation and estimated crop evaporation calculated
ETgage atmometer	< 0.01 m^2 Placed about 1 m above the surface	Hourly or daily	A porous surface covered with material cover of known pore size or known material supplied with water from a reservoir. Differences in reservoir depth correspond to the evaporation amount	Not applicable – only short grass or tall crop reference evaporation is estimated
Lysimeter	< 10 m^2	Usually 20 to 60 min	$LE_{lysimeter} = L\rho_w(\delta W/\delta t)/A_{lysimeter}$	By definition, $H = R_n - G - LE$
Micro-lysimeter	< 1 m^2	Usually daily	$LE_{lysimeter} = L\rho_w(\delta W/\delta t)/A_{lysimeter}$. Used for measuring soil evaporation	By definition, $H = R_n - G - LE$
Bowen ratio (BR) energy balance (BREB)	Vertical measurement distance of 1 m (grassland) to 2 m for forests	Usually 20 to 30 min	$LE = (R_n - G)/(1+\beta), \beta \neq -1$ where β is the Bowen ratio; $H = \beta LE$	By definition, $LE + H = R_n - G$ Assumes equality between exchange coefficients: $K_h = K_w$

[1] Taken from Savage *et al*. (2004)

Method	Measurement area, distance or height	Averaging period	Theoretical basis/comment	Closure statement/ Comment
Eddy Covariance (EC) (2 sensors)	Sensor path length of 100 to 150 mm	Usually between 20 and 60 min	$LE = L\overline{w'q'}$, $H = \rho_a c_p \overline{w'T'}$ (ρ_a is the air density and w', q' and T' are fluctuations in vertical wind speed, absolute humidity and air temperature respectively)	Generally, $LE + H < R_n - G$
Eddy Covariance (EC) (1 sensor)	Sonic path length of 100 to 150 mm	Usually between 20 and 60 min	$H = \rho_a c_p \overline{w'T'}$ $LE = R_n - H - G$	By definition, $LE + H = R_n - G$
Surface layer scintillometer (SLS)	SLS beam length between 50 and 250 m	2 min and 60 min	Monin-Obukhov similarity theory (MOST) used to estimate *H* and *LE* using $LE = R_n - H - G$	By definition, $LE + H = R_n - G$
Large aperture scintillometer (LAS)	Path length: 0.25 to 3.5 km (up to 10 km for boundary layer scintillometers)	2 min to 60 min	Measures C_n^2, the structure parameter for refractive index fluctuations; MOST is assumed	By definition, $LE + H = R_n - G$
Surface renewal (SR)	Point measurement at known height	2 min and 60 min	$H \propto$ amplitude of the air temperature ramps/(ramp period)	By definition, $LE + H = R_n - G$
Temperature variance	Point measurement of the friction velocity and the standard deviation in air temperature at known height	30 min	$H \propto \sigma_T$ and u_* where σ_T is the temporal air temperature standard deviation and u_* is the friction velocity (m s^{-1}); MOST is assumed	By definition, $LE + H = R_n - G$
Temperature method	Point measurement of u_* and air temperature at known height	30 min	*H* is related to the weighted average of the time history of air temperature and u_*	By definition, $LE + H = R_n - G$ Assumes equality between exchange coefficients: $K_h = K_w$
Infrared method	Areal measurement (< 25 m^2) of canopy temperature and wind speed	Hourly	Fick's Law to estimate *H*	By definition, $LE + H = R_n - G$
Chamber methods	Chambers enclosing entire canopies or canopy parts	Hourly	Infrared gas analysers and/or porometers monitor gas exchange between plants and surrounding atmosphere	Transpiration measurements only

Method	Measurement area, distance or height	Averaging period	Theoretical basis/comment	Closure statement/ Comment
Heat pulse /sap flow	Measurements made in or surrounding the stem of plants (< 200 mm)	Hourly	Rate of movement of stem heat pulse; stem energy balance with continuous heat applied	Transpiration measurements only
Cut stem method	Destructive weight measurements of a plant part	Hourly	Change in stem mass per unit time = transpiration rate	Transpiration measurements only

2.3 Selected methods for estimating evaporation

Different methods for measuring or estimating evaporation include the Class-A pan (Stanhill, 2002) and Symon's tank methods, the reference evaporation and crop factor approach, lysimetry, atmometers such as the ETgage from ET-gage Company, Loveland, USA (Altenhofen, 1985; Broner and Law, 1991) and Piche, and a whole range of aerodynamic methods. Microlysimeters allow measurement of soil evaporation usually at daily time intervals and sap flow or heat pulse velocity methods allow hourly measures of transpiration rate.

Excluded from this list are the climate-based estimation methods such as the many empirical methods, not listed in **Table 1**, used to estimate the grass reference evaporation which use the crop factor approach to calculate evaporation. These include empirical temperature- and radiation-based models of Thornthwaite (1948), Blaney and Criddle (1950), Holdridge (1962), Priestley and Taylor (1972), Linacre (1977) and Hargreaves and Samani (1982). These methods are based largely on daily maximum and minimum air temperature, and operate at daily, weekly or even monthly time scales and in some cases large areas. Also excluded from the list are the canopy or part-canopy enclosure methods using infrared gas analysers that allow for the measurement of transpiration rate at canopy or leaf-level.

While the use of evaporation pans together with crop or water-body factors is often of historical interest, Stanhill (2002) encourages the continued use of the Class-A pan for determining crop irrigation requirements.

The reference evaporation method, based on the Penman-Monteith approach, has recently been updated to allow hourly estimations of reference evaporation ETo. Hourly estimations of ETo require measurements of solar irradiance, air temperature, atmospheric humidity and wind speed. Hourly reference evaporation estimation is now possible for short grass (0.1 m tall) and short crop (0.5 m tall). For these two situations, different surface and aerodynamic resistances are used and the partitioning of the available energy flux density $R_n - G$, between R_n and G, is different. The disadvantage of the reference evaporation method is that for estimating *LE*, a crop factor is required. The dual crop factor approach, as would be required for row or orchard cropping situations, allows use of two factors, one for soil evaporation estimations and one for the crop.

Weighing lysimeters are generally regarded as the standard for *LE* measurement but they are expensive and not portable as they are constructed at a specific place with specific soils being used.

Aerodynamic methods, such as eddy covariance (EC), involve the measurement of at least two atmospheric variables and a theoretical framework and assumptions that allow for the direct calculation of *LE*. The Bowen ratio (BR) method involves up to eight measurements and a theoretical framework and K-theory similarity assumptions to estimate *H* and *LE* (Savage *et al*., 1997, 2004). The temperature-based aerodynamic methods such as the surface renewal method involve high frequency measurement of a single air temperature from which *H* is calculated and *LE* is determined using the

energy balance (Eq. 2). The SLS or LAS measurement methods, which rely on MOST and are therefore height-sensitive, allow for the estimation of *H* over distances between 50 and 250 m and 0.25 to 10 km respectively.

Heat pulse velocity or stem steady state heat energy balance methods allow transpiration to be measured at the individual plant-stem level. These methods involve the application of heat to a plant stem following which temperatures are measured using inserted sensors or sensors attached to the stem.

2.3.1 Reference evaporation estimation

The most common method used for estimating *LE* is the method using grass reference evaporation (Allen *et al*., 1998: FAO 56; Allen *et al*., 2006) based on atmospheric measurements at a single level, usually at a 2 m height, at an automatic weather station from measurements of solar irradiance, air temperature, water vapour pressure and wind speed. In addition, a crop factor is used as a multiplying factor for reference evaporation to obtain *LE*, the crop factor effectively distinguishing the vegetation under consideration from a grass reference crop. The dual crop factor approach uses one crop factor for the soil surface and another for the basal crop cover, allowing evaporation estimates for soil evaporation and transpiration components. The extension of reference evaporation from daily (Allen *et al*., 1998) to hourly estimates has been recommended (Allen *et al*., 2006) for both grass (0.1 m tall) reference evaporation and tall vegetation (0.5 m lucerne). Allen *et al*. (2006) recommend that if the FAO-Penman-Monteith ETo method from FAO56 is applied for hourly or shorter time intervals for short grass, a surface resistance (r_s) of 50 s m^{-1} is recommended for daytime and 200 s m^{-1} for night time periods. An aerodynamic resistance of $208/U_2$ is used, where U_2 is the horizontal wind speed at a height of 2 m. These adjustments are based on best agreements with lysimeter evaporation measurements made on a 24 h time interval. The daytime r_s value of 50 s m^{-1} recommended by Allen *et al*. (2006) is also similar to that found by Savage *et al*. (1997) for a short grass surface.

For hourly or shorter time intervals for a 0.5 m tall canopy, an r_s of 30 s m^{-1} for daytime and 200 s m^{-1} for night time periods and an aerodynamic resistance of $118/U_2$ is recommended by Allen *et al*. (2006).

The partitioning of the available energy flux density is slightly different for short grass reference evaporation compared to that for tall-crop reference evaporation. For short grass, $G = 0.1R_n$ when R_n is positive (daytime) and $G = 0.5R_n$ (night time). For tall-crop reference evaporation, it is assumed that $G = 0.04R_n$ when R_n is positive (daytime) and $G = 0.2R_n$ (night time).

2.3.2 Microlysimeters for measurement of soil evaporation

The weighing lysimetric method is often regarded as the standard for *LE* measurement (Table 1). Weighing lysimeters are large containers, filled with soil, water, other chemicals and entire plant(s). Weight measurements are made at regular time intervals. The weight difference per unit time difference (in s, min, h or day) divided by the density of water (1000 kg m^{-3}) and divided by the cross-sectional area (m^2) of the lysimeter yields the evaporation rate which equates to evaporation losses if

there is no drainage or leakages. Lysimeters allow the water loss from such containers to be measured for very short time intervals such as from hours to days or longer. The main component of water loss from a lysimeter is due to transpiration and evaporation from the exposed soil surface. The disadvantages of the lysimetric method include the cost, the destructive nature of the measurements since a relatively large volume of disturbed or undisturbed soil is placed in a container usually of metal construction and the non-portable nature of the measurement method. Also, the representation or the so-called footprint of *LE* is localised to the cross-sectional area of the lysimeter. The microlysimetric method for measuring soil evaporation is much less expensive but the surface area is an order of magnitude less than that of a large weighing lysimeter. It is still a destructive method and not designed to contain whole plants.

2.3.3 Eddy covariance

Methods like the EC, BR and scintillometer methods (Table 1) are attractive since they are non-invasive and can be used for the estimation of *H* and *LE*, the latter estimated using the shortened energy balance (Eq. 2). Furthermore, these are portable methods that can be used to collect unattended measurements for extended periods of time. These methods are the focus of previous research reports (Savage *et al*., 1997, 2004). Eddy covariance measurements (Swinbank 1951) allow for absolute point measurements of *H* and *LE* at a defined height above canopy. The EC method is a popular method since it is a direct method that also allows sensible heat estimates in real-time. The calculation of fluxes, $H = H_{EC}$, for example, using the EC method is based on the covariance between vertical wind speed w and a scalar property such as air temperature T. The covariance between w and T is expressed as $\Sigma(w-\overline{w})(T-\overline{T})$ where the means indicated by the bars are for short time periods, typically 30 minutes. If the covariance is very small, then H_{EC} is small. The EC method may also be used to directly measure LE_{EC} from the covariance between w and absolute humidity q (kg m^{-3}). Alternatively, *LE* may be estimated as a residual from the simplified energy balance (Eq. 2) by measuring H_{EC} and R_n and G.

Sensible heat H_{EC} may be estimated using a three-dimensional sonic anemometer. This instrument gives measurements of the three components of wind velocity (u, v and w) as well as an estimate of air temperature using sonic temperature (T_{sonic}) corrected for the influence of water vapour pressure on the speed of sound (Schotanus *et al*., 1983). Sensible heat is estimated as

$$H_{EC} = \rho_a \, c_p \, \Sigma(w-\overline{w})(T_{sonic} - \overline{T}_{sonic})$$	*3*

where ρ_a is the density of air (approximately 1.12 kg m^{-3}) and c_p is the specific heat capacity of air at constant pressure (approximately 1040 J kg^{-1} K^{-1}). The EC method has been used successfully in South Africa to estimate evaporation from mixed grassland communities for extended periods by Savage *et al*. (1997, 2004) and Savage (2008) with aspects of fetch, placement height and the footprints of EC measurements investigated by Savage *et al* (2005, 2006, 2007).

2.3.4 Bowen ratio method

The calculation of sensible heat flux density ($H = H_{BR}$) and latent energy flux density ($LE = LE_{BR}$) using the Bowen ratio (BR) method (Bowen, 1926; Sverdrup, 1943) is based on the shortened energy balance and the definition of the Bowen ratio β:

$LE_{BR} = (R_n - G)/(1+\beta)$	*4*

and

$H_{BR} = \beta LE_{BR}$	*5*

where, β, with the condition $\beta \neq -1$, is calculated using:

$\beta = \gamma(\overline{T_2} - \overline{T_1})/(\overline{e_2} - \overline{e_1})$	*6*

where γ (= 66 Pa K^{-1}) is the psychrometric constant, $\overline{T_2}$, $\overline{e_2}$ and $\overline{T_1}$, $\overline{e_1}$ are the time-averaged air temperature (K) and water vapour pressure (Pa) at profile heights z_2 and z_1 above the canopy surface, respectively. Assuming that the air temperature and water vapour pressure gradients and *H* and *LE* fluxes are in local equilibrium, with the assumption that the exchange coefficients K_h for *H* and K_w for *LE* are equal, the atmospheric stability dependence of the BR method is removed (Savage, 2008).

Two different types of BR systems have commonly been used. The single-sensor method involves using one hygrometer and two sensors for air temperature, with air being pumped alternately from the one level and then from the other (Tanner *et al*., 1987; Cellier and Olioso, 1993). The other type involves an oscillating system in which two sensors, one at each measurement level, are used for air temperature and water vapour pressure determinations (Gay and Greenberg, 1985; Fritschen and Fritschen, 2005).

Unlike the EC method, the BR method is more difficult to set up and it requires more maintenance: filters need changing, hoses need to be checked regularly for internal condensation and usually, the power requirements are greater, necessitating regular changes in large capacity batteries, since pumps are used to flow air across the humidity sensor or motors used to alternate the humidity sensor from one level to the other.

The BR method has been used successfully in South Africa for many years by Metelerkamp (1993), Savage *et al*. (1997, 2004) and Everson (2001) for the measurement of evaporation in grassland areas. Other studies include BR evaporation measurement for cabbage (Lukangu, 1998), for sugarcane, black wattle and eucalypt trees (Burger, 1999; Jarmain and Everson, 2002), and open water river losses from the Orange river (Everson, 1994).

2.3.5 Scintillometer method

A scintillometer is used to measure path-weighted *H* with a transmitter and a receiver at each end of the path of a radiation beam. The instrument measures the intensity fluctuations of a visible or infrared radiation beam after it has been propagated above the plant canopy of interest. It optically measures the structure parameter of the refractive index of air, C_n^2 (Thiermann, 1992), that is a measure of the atmospheric turbulence structure. The sensible heat flux density *H* is estimated using the empirically-based MOST. Surface layer scintillometers (SLS) operate over horizontal distances between 50 and 250 m. Large aperture scintillometers (LAS) operate typically over distances between 0.25 and 5 km and employ a near-infrared radiation beam. In the case of the SLS, a laser beam (low power class 3a as used in laser pointers, 670-nm wave length that minimises beam divergence) is split into two parallel, displaced (2.7 mm separation) beams with orthogonal polarizations. The receiver unit measures the radiation intensity fluctuations, for weak scattering conditions, from the transmitter at a very high frequency, typically 1 kHz. The radiation intensity fluctuations are caused by refractive scattering of small air parcels in the scintillometer path emitted by the transmitter. Changes in the intensity and the phase of the light beam are detected at the receiver position. A term referred to as the inner scale of refractive index fluctuations (l_o) and C_n^2, is calculated from the variances of the logarithm of the amplitude of the two beams, and the covariance of the logarithm of the amplitude fluctuations between the two beams. Using an iterative technique, and applying MOST, H_{SLS} can be calculated. In the case of the LAS method, lower measurement frequencies are used. Except for the boundary layer scintillometers which employ hundreds of light emitting diodes, the LAS method does not allow l_o to be estimated. Instead, independent wind speed measurements are used for this estimation.

The key to the implementation of the LAS and SLS methods is the interaction between eddy (air parcel) size, beam distance, beam wavelength and aperture diameter and for some of the estimates also effective beam height, air temperature and atmospheric pressure. The SLS system is specifically targeted for short path lengths compared to LAS units that operate over kilometres. As with the other evaporation estimation methods, measurement of R_n and G allows LE to be estimated using the shortened energy balance (Eq. 2).

The SLS methodology is discussed in detail by Savage *et al*. (2004) and Savage (2008). The discussion here is based mainly on Savage (2008). Unlike the BR and EC methods, the LAS and SLS methods are based on the semi-empirical MOST and are therefore height dependent. The beam height is referenced to the height at which wind speed was estimated to be 0 m s^{-1}. Using the neutral wind profile equation, this height was assumed to be $d + z_o$ where $d = 0.67h$ is the zero plant displacement and $z_0 = 0.1h$ the roughness length (Brutsaert, 1982; Mölder, 1997). If the vegetation height varies seasonally, this needs to be noted. The canopy height should be measured regularly. These heights are then weighted according to a path-weighting function used for the log-amplitude variances (Thiermann, 1992) and normalised so as to have an area under the curve of 1. The weighting process favours effective beam heights midway between the transmitter and receiver units with vegetation height near the transmitter and receiver carrying little weight.

The frequency of SLS measurements is 1 kHz compared to typical frequencies of 1 Hz for BR measurements, 10 Hz for EC measurements, 8 Hz for LAS measurements, and 125 Hz for boundary-layer scintillometer measurements if crosswind measurements are included. For LAS and SLS measurements, the averaging period can be as short as 1 or 2 min compared to the commonly-used 20 min or longer for BR and EC averaging periods. Lidar (light detection and ranging) methods (Eichinger *et al*., 2006) also use MOST and allow, typically over distances of kilometres, spatially-integrated measures of sensible heat but the equipment is very expensive.

Unlike the EC method, no corrections are applied to the LAS or SLS data, other than the use of MOST and a possible correction for the influence of water vapour pressure on beam transmission, through the Bowen ratio.

Saturation of the voltage signals, which results in low measured voltages under conditions of strong turbulence (Gracheva *et al*., 1974), invalidate the assumption of weak scattering (Lawrence and Strohbehn, 1970) upon which the LAS and SLS methods depend. The manufacturer recommends that should saturation occur frequently, then the effective beam height should be increased and/or the beam path length decreased (Scintec, 2006). In the unlikely event that following these procedures the voltage signals are still too low, then the voltage range setting needs to be altered.

One disadvantage of the scintillometer method, is that it cannot distinguish between the upward or downward direction of H without additional estimates of atmospheric stability. This disadvantage is overcome by using a pair of fine-wire thermocouples to measure air temperature at two vertical positions to determine the direction of H. This however necessitates use of additional logging equipment. A portable automatic weather station system located near the centre of the beam can be used for this air temperature differential measurement. Alternatively, EC measurements of H can be used to ascertain the direction of H or the assumption can be made that unstable conditions corresponding to positive H occurs between sunrise and sunset.

The second major disadvantage of the scintillometer method is that the method is based on the theory of weak scattering of the scintillometer beam, which may not always apply. Strongly turbulent conditions causes more severe scattering, invalidating the assumption of weak scattering.

A third disadvantage of many scintillometer systems, with the exception of the boundary layer scintillometer and SLS instruments, is that a term known as the friction velocity needs to be known at the time H is measured. From voltage covariance between both beams and voltage variance measurements of each beam for the SLS, the friction velocity is estimated. The SLS method allows H to be calculated directly – for the LAS method, additional measurements of wind speed are required.

The SLS method has been used in South Africa by Savage *et al*. (2004, 2005), Odhiambo (2007) and Savage (2008) to estimate H and LE for extended periods of time for a mixed grassland community. The LAS method has also been used above sugarcane (Wiles, 2008), wattle (Clulow, 2008), *Podocarpus* trees (Dye *et al*., 2008), savanna (Dye *et al*., 2008), Renosterveld and wheat (De Clercq and Fey, 2007), riparian vegetation (Everson et al., 2008), fynbos (Dye *et al*., undated).

2.3.6 Surface renewal

The surface renewal (SR) method (Paw U, 1992; Paw U *et al*., 1992; Zhang *et al*., 1992; Paw U *et al*., 1995; Qiu *et al*., 1995; Snyder *et al*., 1996; Anandakumar, 1999; Spano *et al*., 2000; Castellvi 2004; Castellvi *et al*., 2006) for estimating H is relatively new compared to EC and BR methods. The SR method has been reviewed by Savage *et al*. (2004) and Mengistu (2008). The SR method is based on the idea that an air parcel near a surface is renewed by an air parcel from above. Air temperature fluctuations exhibit organized coherent structures which resemble ramp events (Paw U *et al*., 1992). The SR analysis involves evaluation of high frequency air temperature measurements at a single level and considering air temperature ramps (positive or negative) consisting of quiescent periods (for which there is no change in air temperature with time) and ramping periods for which there is an air temperature ramp for unstable conditions (that is, an air temperature increase) or for stable conditions for which there is an air temperature decrease. The high frequency air temperature measurements are usually obtained using unshielded fine-wire thermocouples – 75 μm in diameter – placed at various heights above the canopy surface. Frequency of measurement for the SR method is typically 8 Hz and post-measurement calculations are used to estimate $H = H_{SR}$. Measurement of R_n and G allows LE to be estimated using the shortened energy balance equation (Eq. 2). The SR method is attractive due to its simplicity (few parameters need to be measured), and it is relatively low cost. The method requires knowledge of the measurement height, the rate of change in air temperature, and a weighting factor. The weighting factor needs to be determined, *a priori*, for the vegetation type, thermocouple size and measurement height (Paw U *et al*., 2005) by comparison of the estimated H_{SR} with H measurements from other methods such as EC or SLS. The weighting factor is 0.5 for coniferous forests, orchards and maize when the sensor is at canopy level and 1 for short grass for a sensor height of about 1 m (Paw U *et al*., 1995).

Paw U and Brunnet (1991) proposed the SR model by assuming that under unstable atmospheric conditions when the canopy is warmer than the air, any air temperature increase represents air being heated by the canopy. Under stable conditions, when the canopy is cooler than the air, any air temperature decrease represents air being cooled by the canopy. For a given measurement period, H_{SR} can be expressed as the change of heat energy content of air with time per unit area

$$H_{SR} = M_a \, c_p \, dT_a / (dt \, A)$$	7

where M_a is the mass of air heated (or cooled) by the rate of change in the air temperature difference dT_a in time dt and A the horizontal area of the heated or cooled volume of air. Expressing the mass of air in terms of air density ρ_a and the volume of V_a,

$$H_{SR} = \rho_a \, c_p \, (V_a / A) \cdot (dT_a / dt)$$	8

Snyder *et al*. (1996) simplified and modified the above-mentioned SR analysis by substituting V_a/A by the measurement height z and dT_a/dt in Eq. 8 by a/τ ($^oC\ s^{-1}$) where a is the air temperature amplitude (^oC) and τ the total ramping period (s) for the average rate of change in air temperature for the total ramping period:

$$H_{SR} = \rho_a c_p z \cdot a/\tau$$	*9*

The amplitude a of the air temperature ramp and the ramp period τ is estimated using an air temperature structure parameter approach of van Atta (1977). For the calculation of H, the average of the second, third and fifth order air temperature deviations from the mean is calculated by the datalogger following which the van Atta approach is applied on a PC. To obtain the rate of change in air temperature, dT/dt, the method assumes that the variation in air temperature consists of an air temperature quiescent period s, for which there is no change in air temperature with time, followed by a ramp period l. A ramp with a positive amplitude a occurs during unstable conditions and a negative amplitude for stable conditions. The ratio $a/(s + l)$ is therefore used as the air temperature change with time, dT/dt. Hence,

$$H_{SR} = \alpha z \rho c_p \frac{a}{s+l}$$	*10*

Currently, there are three SR methods used for determining H_{SR} (Mengistu, 2008):

1. an ideal SR analysis model based on an air temperature structure function analysis for which a, s and l are determined (Eq. 10) from high frequency air temperature measurements from second, third and fifth order air temperature structure function values. In addition, α and z are required for estimating H_{SR} (Paw U *et al*., 1995). For this SR method, MOST is not applied but the method is still height dependent. The SR method based on air temperature structure function analysis (Paw U *et al*., 1995) must be calibrated against another standard method, such as the EC method to determine the weighting factor α which accounts for unequal heating of air parcels below the air temperature sensor;
2. the SR analysis model with finite micro-front period based on Chen *et al*. (1997a). For this SR method, the quiescent period is replaced by a finite micro-front period with an insignificant quiescent period. MOST is assumed and the method is also height dependent. For the micro-front SR method of Chen *et al*. (1997b), a constant value of 0.4 is used for their empirical combined coefficient $\alpha\beta^{2/3}\gamma$, as well as the third order of the structure function of air temperature $S_{rm}{}^3$, where r_m is the time lag at which $S_{rm}{}^3$ is a maximum, and their value of $S^3_{(r)}/r$ can be determined from the high frequency air temperature data and constant values of $1/r_m$ = 1, 2, 2.5, and 10 Hz. Chen *et al*. (1997b) used a value of 1 for parameter γ for their experiment in a Douglas-Fir forest;

3. an empirical SR analysis model based on similarity theory (Castellvi *et al*., 2002). The main advantage of this empirical SR approach is that it appears not to require calibration of H_{SR} measurements against another method (Castellvi, 2004). However, this method is not as attractive as the original ideal SR analysis model proposed by Paw U *et al*. (1995), as it requires additional wind speed measurements to estimate H_{SR}.

The disadvantage of the SR method is that high frequency air temperature measurements are required, necessitating use of expensive datalogging equipment. Furthermore, the sensors are fragile and easily damaged and prone to error due to dirt and cobwebs adhering to the thermo-junction. Some of these disadvantages are overcome by employing a number of sensors at one location. A severe disadvantage of the SR method however, apart from the SR method of Castellvi (2004) which also requires wind speed measurements, is that the value for α (Eq. 10) needs to be known *a priori* for H_{SR} to be estimated. Therefore, in practice, simultaneous SR and EC measurements, for the same canopy, are required if the SR method is used apart from SR method 3.

The SR method, previously untested in South Africa apart from the work by Savage *et al*. (2004), has been evaluated in detail by Mengistu and Savage (2006, 2007) and Mengistu (2008) for a wide range of canopies and above water. Savage (2007) suggested that high frequency air temperature-based methods, of which the SR is one, may pave the way for evaporation stations from which real-time and sub-hourly estimates may be obtained relatively inexpensively. Other temperature-based methods for estimating *H* have also proved satisfactory (Savage and Mengistu, 2006; Savage, 2007).

2.4 The heat pulse velocity and stem steady state heat energy balance methods for estimating transpiration

Simultaneous measurements of transpiration and evaporation allow soil evaporation to be calculated by subtraction of these two measurement estimates. This subtraction method is particularly useful for sparse canopies (Heilman *et al*., 1994, 1996) and has been validated in a vineyard using soil microlysimeter measurements of soil evaporation (Heilman *et al*., 1994). The methods used for transpiration are few in number and include the heat pulse velocity (Swanson and Whitfield, 1981) and stem steady state heat energy balance (Sakuratani, 1984) methods.

The heat pulse velocity (HPV) method is recognised internationally as an accepted method for the measurement of sap flow in woody plants and has been extensively applied in South Africa (Dye and Olbrich, 1993; Dye *et al*., 1996). The heat ratio method (HRM) of operation applied in the HPV method is fully described in Burgess *et al*. (2001), and the description below is drawn largely from that reference.

The heat ratio method measures the ratio of the increase in temperature, following the release of a pulse of heat, at points equidistant below and above a heater probe. In order to achieve this, three parallel holes are accurately drilled (with the help of a drill guide strapped to the tree) into the sapwood (xylem) portion of tree trunks. The upper and lower holes are both situated 5 mm from the central hole (above and below, respectively). Copper-constantan thermocouples, connected to a

multiplexer or logger, are inserted into the upper and lower holes to a specific depth below the cambium (below-bark insertion depth). A heater probe, wired to a relay control module, is inserted into the central hole.

At a pre-determined time interval (usually hourly), the temperatures in the upper and lower thermocouples are measured and the ratio (upper over lower) is logged. Directly thereafter, the central (heater) probe releases a short (0.5 s) pulse of heat, which diffuses through the adjacent wood and is convected by the sap moving upwards through the xylem of the tree. As the heat pulse is carried up the tree by the sap, the upper thermocouple begins to warm. Logging of the changing heat ratio commences 60 s after the initiation of the heat pulse and is measured continuously (approximately every second, depending on the processing speed of the logger) until 100 s after the heat pulse. The average of these ratios is calculated and utilised in subsequent formulae to derive the sap velocity. These formulae are described in Burgess *et al*. (2001).

Further measurements of sapwood area, water content and density, as well as the width of wounded (non-functional) xylem around the thermocouples, are used to convert sap velocity to a total sap flow rate for the entire sample tree. These measurements are usually taken at the termination of the experiment due to the destructive sampling required to obtain them. Heat pulse velocities derived using the heat ratio method are corrected for sapwood wounding caused during the drilling procedure, using wound correction coefficients described by Swanson and Whitfield (1981). The corrected heat pulse velocities are then converted to sap flux densities according to the method described by Marshall (1958). Finally, the sap flux densities are converted to whole-tree total sap flow by calculating the sum of the products of sap flux density and cross-sectional area for individual tree stem annuli (determined by below-bark individual probe insertion depths and sapwood depth). In this way, point estimates of sap velocity are weighted according to the amount of conducting sapwood in the annulus they represent. Hourly sap flow values are aggregated into daily values.

The number of probe sets (two thermocouples and one heater) utilised per tree is determined arbitrarily by the diameter of the tree, but typically range from four to twelve. The thermocouples are typically inserted to four different depths, since velocities tend to be greatest in the younger xylem near the cambium and slower in the older, deeper xylem. Data loggers are programmed to initiate the heat pulses and record the heat ratio changes in the respective thermocouple sensor pairs.

Unlike the HPV method, for the stem steady state heat energy balance (SSSHEB) method (Sakuratani, 1984), constant and continuous power is applied to a heater surrounding the stem of a plant under steady state energy conditions. The method is described in detail by Savage *et al*. (1993, 2000) and the summary below is taken from these references. Unlike the HPV method, the SSSHEB does not involve the implanting of sensors into the stem but rather has sensors in contact with the stem. There are therefore no wound corrections applied. A heater completely surrounding the stem is used as the source of continuous heat energy. In order to attain the steady state condition, a portion of the stem and the sensors are heavily insulated from external heating or cooling, usually solar irradiance and wind effects. The insulation also reduces the possibility of water entering the system, causing possible corrosion of the sensors. The heat energy flux supplied by the heater must be accounted for according to the conservation of energy. The components of heat energy flux are as follows: heat energy flux

may be conducted radially outward, conducted vertically upward through the stem, conducted vertically downward through the stem, and may be convected with the vertical ascent of sap flow. If each of these energy flux terms, except that convected with the sap, can be calculated, then this convection heat term may be determined. For larger diameter stems, the stored heat in the stem would need to be accounted for. A datalogger is used to control the heater power and measure the temperature differences at various positions within the gauge. These temperature measurements together with the heater power allow real-time estimates of sap flow, in kg h^{-1}. A disadvantage of the SSSHEB method is that under conditions of high sap flow, temperature differences associated with the convected energy flux are small and this results in estimated sap flows that are unrealistically high. Furthermore, the same power is applied to the stem, irrespective of sap flow with the result that the stem may be overheated at night when the convected energy flux is small. Some of these disadvantages have been overcome by the use of a variable power but constant temperature difference method (Ishida *et al*., 1991).

In South Africa, the SSSHEB has been used to estimate the water use in *E. Grandis* (Savage *et al*., 1993, 2000) as well as for the measurement of sap flow rate in lateral roots (Lightbody, 1994; Lightbody *et al*., 1994).

2.5 Energy balance closure and measurement footprints

The application of the surface energy balance is fundamental to many of the evaporation methods outlined. Each term of the energy balance is measured separately and therefore has a different spatial representation. If all four components of the energy balance (R_n, LE, H and G) are measured independently and correctly and sum to 0, then Eq. 1 is satisfied and closure is said to exist. Fortuitously however, closure could still exist even if two or more terms have incorrect values and the terms still sum to 0 W m^{-2}. It would be unlikely however that an incorrect set would always sum to 0 W m^{-2} for each time interval. Use of the energy balance equation for independent measurements of the component terms results in:

$c = R_n - LE - H - G$	*11*

where c is termed the energy balance closure (W m^{-2}). Closure exists if c = 0 W m^{-2}. A non-zero value for c may be due to measurement errors in one or more of the component energy balance terms, although a near-zero value for c may be due to two or more of the component terms with incorrect value tending to cancel each other. According to Stannard *et al*. (1994), a near-zero value for c only increases confidence in the flux density measurements but does not necessarily verify them.

The differing spatial scales, or footprints, of the energy balance component measurements tend to counter the achievement of closure especially for heterogeneous terrain (Stannard *et al*., 1994). The spatial scales of the measurements of the energy balance component terms are different due to the nature of their measurement. For example, while the EC measurements of H are point measurements, they are influenced by upwind source areas of hundreds of square metres, depending on atmospheric

stability (Savage *et al*., 1995, 1996). Other examples: the source area of soil heat flux density measurements using a heat flux plate which is small in area, is very much less than 1 m^2; a net radiometer at measurement height of 2 m above canopy with a source area radius of 6 m is equivalent to a footprint measurement area of 113 m^2.

2.5.1 Closure not satisfied?

For relatively homogeneous terrain, Savage *et al*. (1997) found that the average closure value $\bar{c}$ for their EC measurements of H_{EC} and LE_{EC}, the latter from an open-path infrared analyser system, was positive. For heterogeneous terrain using eddy covariance (EC) measurements, Stannard *et al*. (1994) also found that the mean closure value $\bar{c}$ was positive. Stannard *et al*. (1994) listed a number of possible mechanisms resulting in $\bar{c} > 0$ W m^{-2}:

- the magnitude of one or both of *H* and *LE* is underestimated;
- the available energy flux density, $R_n - G$, is overestimated;
- the sensible heat or latent energy content, or both, of the air advected into the source area of the flux density measurements by the mean wind speed is less than that leaving the source area - referred to as horizontal flux divergence;
- mismatched source areas for the different measurements of the energy balance component terms.

According to Stannard *et al*. (1994), the influence of horizontal flux divergence on $\bar{c}$ would be small as the divergence of *H* would tend to be opposite in sign to the divergence of *LE* since wetter areas tended to be cooler and drier areas tended to be warmer. Therefore in total, these divergences would tend to cancel. In order to determine the net effect of divergence at any site, a detailed network of air temperature, relative humidity and wind speed sensors would be required. They also concluded that the underestimation of *H* and *LE* was the major cause of the tendency for $\bar{c}$ to be positive.
Another measure of the lack of closure is the closure ratio, which is given by:

$D = (LE + H)/(R_n - G)$	*12*

for which a closure ratio of 1 yields the shortened energy balance equation (Eq. 1). Ham and Heilman (2003) found that the energy imbalance persisted in different surfaces with an average of about 20%, corresponding to $D = 0.8$, but that the energy balance closure was better on average in the afternoon than in the morning. This indicates the underestimation of storage terms, which are usually larger in the morning. Finnigan *et al*. (2003) found that filtering of the low frequency eddy covariances by the averaging-rotation operations is a large factor contributing to the failure to close the energy balance over tall canopies. According to Cava *et al*. (2008), the use of a 'long term coordinate system', together with spectral analysis, with the usual 30 min averaging time is too short to include the entire contribution of the turbulent heat fluxes and that a 2 h averaging period is more suitable if larger scale

motion effects are to be included. In contrast however, Savage (2008) found that there was good agreement between H_{EC} and H_{SLS} even when using a 2 min averaging period.

Liu *et al*. (2006) pointed out that a lack of closure of the surface energy budget by 10% or more $(CR \geq 0.9)$ is not uncommon at eddy covariance flux sites. It is postulated that site heterogeneities, under conditions that are not perfectly ideal, introduce horizontal and vertical advective flow terms that cannot be resolvable by single point vertical flux tower measurements. If these advective terms contribute to vertical fluxes at the site, non-closure of the surface energy balance would be inevitable even though appropriate adjustments are made for high/low frequency losses to the EC data and the canopy storage terms of the energy balance is accounted for. The lack of energy balance closure could also be due to the effect of the roughness sub-layer on the flux measurements.

In the case of the BR method, for which by definition $\beta = H / LE$ and Eq. 4 applies, D is necessarily always 1. Other methods for estimating H such as the EC and SLS methods often involve measurements of H and estimation of LE by assuming D = 1. The EC systems that measure H and LE independently of each other make no assumption of the value of the closure ratio.

2.5.2 Differing footprints responsible for the lack of closure?

Given the limitations of the lysimetric method (refer to Section 2.3.2), the search for an alternative standard for evaporation estimation has been the focus of many studies for several decades. The EC, BR and aerodynamic temperature-based methods essentially yield point estimates of H and LE although these estimates are influenced by events upwind from the point of measurement. In the case of H, the measurement footprint refers to the relative contribution of upwind surface sources to the H measured at a height above the canopy surface. The extent of the area of influence on the measurement using both EC and BR methods has received attention. For example, Savage *et al*. (1995, 1996, 1997) investigated the footprints of EC measurements and Stannard (1997) investigated that of BR measurements. Agreement between BR, EC and SLS measurements, for example, may be dependent on the footprint of the measurements which in turn depends on the state of atmospheric stability.

Wilson *et al*. (2002) and Ham and Heilman (2003) report on the inadequacy of the EC method for the direct estimation of LE with the result that $LE + H < R_n - G$ (**Table 1**) resulting in a closure ratio less than 1 (Eq. 12). This situation is referred to as a lack of closure. As an alternative therefore, the EC method could be used to measure H from which LE may be estimated from simultaneous measurements of R_n, G and H_{EC}.

Each of the methods presented in **Table 1** result in measurements with different footprints. For example, the footprint of the lysimetric measurements is the area of the lysimeter. In the case of the EC method, the footprint is defined as the relative contribution of upwind surface sources to the measured H.

By theoretical definition and making certain assumptions, the BR measurements always produce exact closure (**Table 1**). Problems associated with EC and BR methods include the following:

- that EC measurements of *LE* are often underestimated, as claimed by a number of authors (for example, Twine *et al*., 2000);
- that both the EC and the BR estimates of *LE* are based on point measurements;
- that due to the theoretical assumptions made using the BR method, exact measurement comparisons between the BR and EC measurement methods have been frustrated by differing assumptions, differing footprint areas, measurement limitations and often-times poor agreement between *LE* and *H*;
- a comparison of two methods does not indicate which method is correct especially if the methods do not consistently agree.

2.6 Summary

Increasingly in South Africa, evaporation, one of the main components of the water balance, and of the energy balance, needs to be measured or estimated with reliable accuracy and precision. Selected measurement methods for the estimation of either the sensible heat or the latent energy flux terms of the shortened energy balance are discussed. The various methods discussed have differing assumptions, theoretical basis, requirements, ease of use, complexity, cost and relative advantages/disadvantages. Many of the methods allow sensible heat flux to be estimated from which evaporation is calculated from additional measurements of net irradiance and soil heat flux. These methods include the eddy covariance (without a fast-responding hygrometer), scintillometer, surface renewal, temperature variance and infrared methods. Lysimeters, microlysimeter and eddy covariance (with a fast-responding hygrometer) methods allow evaporation to be estimated directly without requiring net irradiance and soil heat flux measurements. The Bowen ratio method is a combination method that allows sensible heat and evaporation to be estimated. Other methods such as the class-A pan, ETgage and grass reference evaporation methods also differ in assumptions, requirements and cost. These methods require knowledge of a crop factor for the estimation of evaporation. Perhaps the most popular method routinely used is the grass reference evaporation method based on measurements of solar irradiance, air temperature, water vapour pressure and wind speed obtained from an automatic weather station. This method may now be applied using hourly data. Chamber, heat pulse/sap flow and cut stem methods allow estimation of transpiration of canopy parts or whole-canopies. Simultaneous evaporation and heat pulse or sap flow measurements allow soil evaporation to be calculated by subtraction. The many measurement evaporation methods have differing spatial scales, or footprints. The aspect of footprints in relation to the often-times lack of closure of the energy balance is discussed.

Chapter 3: Description of Instrumentation Used

A number of methods are used in South Africa to estimate evaporation, transpiration and total evaporation. A brief summary of the theoretical basis of these methods are given in Chapter 2. Of the range of methods available, the scintillometry and the surface renewal methods have been developed most recently. Although these two techniques have only been applied in South Africa in more recent years, they hold great potential for evaporation estimation.

This project was aimed at testing the suitability and accuracy of a variety of techniques for total evaporation estimation. It was also aimed at suggesting improvements and/or changes in the application of these techniques for a range of land surfaces to ensure a high level of accuracy in the estimated evaporation (Objectives 2 to 5).

Therefore, a range of methods were applied under different conditions (surface, climates), and their performance evaluated. The instrumentation used in this project is described in this section to give the reader an idea of the degree of sophistication of the different techniques.

Although used in this project, none of these systems are endorsed by the CSIR or the Water Research Commission or the University of KwaZulu-Natal.

Detailed information on the application of these systems at the various research sites, as part of seven case studies, is given in Chapter 4.

3.1 Net irradiance and soil heat flux

Net irradiance was generally measured using a NR-Lite net radiometer (Model 240-110, Kipp & Zonen). Soil and water temperatures were measured using type E thermocouples, and heat flux in the soil and water were measured with REBS heat flux plates. The sensors were all connected to a CR23X datalogger (Campbell Scientific, Logan, Utah, USA) and measurements were performed every 1.0 s and averages obtained every 2 minutes which were in turn used to calculate 30 min averages for the latent energy flux calculations.

Where the Scintec Optical Energy Balance Measurement System (OEBMS1) laser scintillometer was used, the net radiation, solar radiation, soil temperature and soil heat fluxes were measured using the free standing OEBMS tower. Mounted onto the tower was a Schenk Pyrradiometer (model 8111), a Schenk Pyranometer (model 8101), two Gill aspirated radiation shields with thermometers (PT 1000) (to determine the direction of energy fluxes) and three Hukseflux soil heat flux plates (model HFP01SC) to estimate soil heat flux density. These were all connected to separate controller boxes on the tower and interfaced to a central multiplexer. The latter was connected by a 100 m cable, to the Signal Processing Unit (SPU) (see more details in Section 3.6).

3.2 Open path Eddy covariance systems

Two types of In Situ Flux open path eddy covariance systems were used in this experiment. The In Situ Flux systems open path eddy covariance system (In Situ Flux systems, Sweden), and an Applied Technologies Inc. (Applied Technologies Inc., USA) eddy covariance system that was later modified into the In Situ Flux systems format. The former system is referred to as the In Situ Flux system and the latter as the Applied Technologies Inc. or ATI system. Both systems are described below.

In Situ Flux systems open path eddy covariance system components

The In Situ Flux systems eddy covariance system, consists of a number of units that were integrated into a complete ready-to-run system:

- Gill Solent R3 three dimensional sonic anemometer with inclinometer for remote levelling of the anemometer.
- Analogue Signal Input Unit, (SIU) for interfacing the Gill and other sensors.
- Li-Cor Li-7500 open path gas analyzer was interfaced through the SIU.

A platinum resistance thermometer was included to provide more accurate measurements of the sonic anemometer derived temperatures. The System box was insulated and cooled to offer the optimal environment for the enclosed components.

In Situ Flux open path system (Gill R3 Anemometer)

The open path flux system GR3-L7500 was a complete system for measurement of momentum, heat, CO_2 and H_2O fluxes. The sensors were a Gill R3 anemometer and Li-Cor 7500 Analyzer (Li-cor Inc., Lincoln, Nebraska, USA). The system was designed for continuous monitoring in harsh environments and included transient protection, with 12 VDC for safe and flexible power supply. Components inside the system box included AC/DC Converters, Deep Discharge Protection, transient protection and thermostat overheat protection. The box temperature sensor was a Vaisala PTB101B. The Westermo MD-54LV Flux Computer (12 VDC) with display and keyboard included a CD-RW drive and 4xRS232 serial card with an on board microprocessor. There were four USB ports and a 20 Gbyte 2.5" auto heated hard drive. An internal battery prevented unplanned power shut downs. The Flux card with on board microprocessor, cooperated with the PC software for control of data processing, system shutdown, system auto start and operating temperatures. Data were copied once a day during the night. Two mobile USB drives were used for downloading the processed and raw data from the flux system computer.

EcoFlux software package:

The EcoFlux software handled the collection and storage of raw data, calculation and storage of mean fluxes, variances, co-variances, wind direction and wind speed, stability and friction velocity. The software made all the necessary corrections, filtering and co-ordinate rotations that were needed for accurate measurements. The software included long term rotation angles and average tilt angle for every wind direction (planar fit). Software included a view of instantaneous values and graphs.

In Situ Flux open path system (Applied Technologies Inc. anemometer)

The Applied Technologies Inc. eddy covariance system was identical to the In Situ Flux system described above with the exception that an Applied Technologies Inc. 3-D SATI-3VX sonic anemometer replaced the Gill R3 and a model PAD-802 data packer replaced the SIU.

3.3 RM Young eddy covariance system

In addition to the use of the open-path eddy covariance systems, described above, an RM Young three-dimensional ultrasonic anemometer (model 81000, Traverse city, Michigan, USA – path length of 150 mm) was used to estimate sensible heat flux density. Measurements of net irradiance and soil heat flux densities were used to estimate latent energy flux density using the shortened energy balance equation. The anemometer was connected to either a Campbell CR5000 or a CR3000 datalogger. The ultrasonic anemometer data were sampled at a frequency of 10 Hz and data processed online in the datalogger and stored for further analysis. Differential voltage measurements on the 5 V range with a settling time of 100 μs and an integration period of 100 μs were used. The anemometer was powered by the datalogger.

Where necessary, measurements for the three components of wind velocity and sonic coordinate rotations were performed after the data collection period using a Fortran program. The high frequency measurements of the three components of wind velocity and sonic temperature were stored on a 1 GB PC card for further analysis.

3.4 Surface renewal system

The SR method allows sensible heat flux density to be estimated from high frequency measurements of air temperature at a single measurement level using an unshielded fine-wire thermocouple. Frequency of measurement for the SR method is typically 8 or 10 Hz and post-measurement calculations are used to estimate sensible heat flux density. Measurements of net irradiance and soil heat flux densities were used to estimate latent energy flux density using the shortened energy balance equation. The surface renewal method is attractive because of its simplicity (few parameters need to be measured) and relatively low cost.

For the SR method, we used several unshielded type-E thermocouples (75-µm diameter) to measure air temperature, placed at various heights above the canopy surface. Each sensor consisted of a pair of thermocouples in parallel. For thermocouples connected to a Campbell CR10X datalogger, a reference thermistor was used. Differential thermocouple measurements on the slow 2.5 mV voltage range were performed and the reference thermistor was well insulated to prevent unwanted thermal gradients. The thermocouple arms were pointed into the predominant wind direction. In the case of the CR10X, measurements were made every 0.125 s (equivalent to a frequency of 8 Hz) and then lagged, typically by 0.125 and 0.25 s, before obtaining the second, third and fifth order of the air temperature structure function values required by the Van Atta (1977) approach for SR analysis. These values were averaged every two minutes. For the CRBasic dataloggers (CR3000 OR CR5000, Campbell Scientific Inc., USA), thermocouple measurements were at 10 Hz and done differentially with a settling time of 0.1 ms and an integration time of 0.1 ms.

Various time lags were used: for *Chromolaena* (Case study 5), the performances of the three SR analysis approaches were evaluated for unstable conditions using four time lags: 0.1, 0.4, 0.5 and 1.0 s. For the open water study (Case study 7), time lags of 0.4 and 0.8 s were used. For the *Jatropha* study at the Ukulinga Research Farm (Case studies 1, 3), the air temperature time lags used were 0.5 s and 1.0 s. In all cases, the second, third and fifth order air temperature structure function values were averaged every two minutes.

For the CRBasic dataloggers, the raw SR data were stored on a 1 Gbyte PC card and output files created at midnight every second day. Subsequently, from the data stored on the card, 30-min air temperature means of the air temperature structure function values were calculated using Split (part of LoggerNet version 3.2.2) available from Campbell Scientific. Since measurements from a number of thermocouples were stored in one datalogger, it was necessary to split the data so that each data file corresponded to data from just one thermocouple. For this purpose, the Split program, part of PC208 (version 3.08) or LoggerNet 2.1, both from Campbell Scientific, was used. Software calculations, post-data collection, were used to calculate two-minute sensible heat flux density using the Van Atta (1977) approach. For this purpose, QuickBASIC 4.0, under MS-DOS, was used to modify and compile a program used to solve the parameters from which the sensible heat flux density may be estimated using α and the measurement height z.

3.5 Heat pulse velocity system

The heat pulse velocity technique was used to estimate transpiration from six *Podocarpus* trees as part of case study 2. Six representative trees were selected. A CR10X datalogger (Campbell Scientific Inc., USA) with AM 16/32 multiplexer was used to measure the velocity at which a heat pulse moves through the tree stem at different depths below the cambium. Measurements were made at hourly intervals. Sets of heater and thermistor probes were implanted to different depths within the sapwood. Four sets of probes (a set consisting of a heater probe and two thermistor probes) were installed at different depths below the cambium. This ensured that the variation in sap flux over the sapwood was covered.

The accuracy of the sap flux measurements and heat pulse velocity depends on the distance between the probes. A drill jig with three aligned holes was therefore used to install the probes accurately and parallel to each other. The heater probe was installed in the centre hole, and the two thermistor probes were installed at 5 mm below and above the heater probe.

3.6 Scintec laser scintillometer

Two Scintec AG (Atmospärenmessetechnik, Tübingen, Germany) Surface Layer Scintillometer (SLS) models were used in this study – the SLS40-A and the SLS40-A with the OEBMS1 system. The surface layer scintillometer (SLS40-A) is an optical instrument used to measure path weighted estimates of sensible heat flux density, typically every 2 min (Thiermann and Grassl, 1992). The SLS40-A used in this project, consisted of a dual-beam transmitter with a laser diode source (lifespan 20 000 hours) and at the receiver a photo diode for the measurement of the structure function constant (C_n^2) and inner scale (ℓ_0) of refractive index fluctuations. Operation of the SLS40-A is possible over pathlengths from 50 to 300 m. The frequency of the SLS measurements is 1 kHz and the wavelength is 670 nm. The SLS40-A system includes automatic alignment, a correction for transmitter vibration and heated windows to prevent dew and ice deposits. The SLS's are connected to a Junction Control Box (JCB) which provides power to the transmitter and receiver and allows for contol of the transmitter unit by the PC for optical alignment.

The OEBMS1 is used for the measurement of soil heat flux (Hukseflux soil heat flux plates - model HFP01SC), net radiation (Schenk Pyrradiometer - model 8111) and global radiation (Schenk Pyranometer (model 8101). Air temperature is measured at two heights (approximately 1.0 m apart) to determine the direction of the fluxes using Gill aspirated radiation shields with PT 1000 thermometers). The sensors are mounted on a tower and are connected to separate controller boxes that are all wired into a single multiplexer. The multiplexer and JCB are connected to a signal processing unit (SPU). The SPU performs the filtering and demodulation of the signals. It includes a microprocessor which controls the communication with a PC via a serial cable. The SPU interfaces with all sensors including a RM Young barometric pressure sensor (model 61202V) and communicates with the PC. The SLSRUN software is used to configure the system and display real-time and historic outputs of sensible heat flux, latent energy, solar radiation, net radiation and soil heat flux. Data are stored on the PC in three file formats, namely, the main data output file, the diagnosis output file and the OEBMS output file, all in text format.

3.7 Scintec boundary layer scintillometer

Scintec AG is the supplier and manufacturer of the BLS900 Boundary Layer Scintillometer used in this study. This sophisticated scintillometer system, evaluates the atmospheric scintillation caused by refractive index fluctuations, which is linked to sensible heat flux density. The BLS900 system can be operated over distances ranging from 0.5 to 5 km. The BLS900 consists of (a) an optical transmitter, (b) an optical receiver, (c) an SPU and (d) data evaluation software (BLSRUN). Both the optical transmitter and receiver units are equipped with positioning devices. The signal processing unit is equipped with an integrated datalogger, and the evaluation software runs in Microsoft Windows based operating systems.

The BLS900 transmitter sensor emits radiation through 924 light emitting diodes (LED) on two disks. The LEDs can emit radiation in 4 different pulse repetition rates (1, 5, 25 and 125 Hz). A pulse rate of 125 Hz provides maximum accuracy and transverse wind speed measurement capability. A pulse rate of 1 Hz results in a very low power consumption. The two-disk configuration of the BLS900 allows for a correction of absorption fluctuations which is performed in the BLSRun software and increases the accuracy of the measurement. Although the two-disk configuration could provide crosswind measurement capability, this feature was not used in this project.

In the BLS900 receiver radiation is collimated by a lens onto two photodiodes. The lens is convex and made of glass. One of the photodiodes is used for sensing the turbulence-induced fluctuations, and the auxiliary detector is used as an alignment aid. For alignment purposes both the transmitter and receiver sensors were mounted onto 3 axis-positioning devices and the receiver sensor were also equipped with a mounted telescope. The receiver electronics pre-amplifies and filters the signals. The transmitter and receiver sensors were mounted on standard surveyors' tripods.

The SPU houses two plugged-in cards: (a) a signal processing card that filters, demodulates and digitises the received signals, and (b) a microprocessor card for evaluating and storing the converted data. The microprocessor also handles the communication to a PC via a serial interface. The SPU is also equipped with non-volatile flash memory for storing up to approximately 700 days of measurement data.

The BLSRUN software is used in part to configure the system, and also reads the measured data either in real-time, from volatile SPU memory or from the non-volatile SPU/DL storage. BLSRUN requires input on a number of parameters. For the open water field campaign, the path length was set to 2.5 km, the path averaged height of the sensors to 8.99 m and the data averaging period to 10 minutes. More information on the BLS900 scintillometer can be obtained from the Users manual (Scintec, 2006).

The spatial estimates of sensible heat flux density obtained with this system were integrated with the net irradiation and soil heat flux density estimates, through the simplified energy balance equation.

Chapter 4: Assessment of the Suitability of Selected Techniques for the Estimation of Total Evaporation

This project was aimed at testing the suitability and accuracy of a variety of techniques for total evaporation estimation. It was also aimed at suggesting improvements and/or changes in the application of these techniques for a range of land surfaces to ensure a high level of accuracy in the estimated evaporation. Objectives 2 to 5 of this project stated in the executive summary relates directly to this. To evaluate the accuracy of a range of micrometeorological techniques, the basic outputs of these techniques (sensible heat flux density and latent heat flux density), and daily total evaporation, were evaluated.

Seven research sites were used as part of seven different case studies (**Table 2**). The sites were geographically distributed across South Africa (**Fig. 1**), and represented different land surfaces and climatic conditions. Surfaces studied include a young *Jatropha* orchard, a tall narrow plantation of *Podocarpus* trees, an open sugarcane field, a grass/shrub mix, a *Chromolaena* stand, a tree/shrub mix and an open water surface. At most of these sites, a suite of different techniques was tested only during one window period or season – Case studies 4 to 7 (**Table 2**). The different techniques were however tested in more than one season at both the *Podocarpus* and *Jatropha* sites (Case studies 1 to 3). For Case study 5, two different sites were used to test the suitability of the techniques.

Table 2 A list and description of the different case studies with the associated land surfaces studied as part of the specific case study. Generally techniques were only tested at one site, in one season (measurement period). However, for Case study 2, three season's measurements were used. For Case study 5, two different sites were used with one measurement period each. The description of each case study gives the objective of the specific case study.

Case study no	Case study Description	Land surface / canopy cover	Measurement period	Section of this report
1	Energy balance closure	*Jatropha* orchard	11 November - 2 December 2005	4.1
2	Limited fetch	Narrow plantation of *Podocarpus* trees	21-28 Sep. 2005: Field trip 1 09-15 Feb. 2006: Field trip 2 23-30 Aug. 2006: Field trip 3	4.2
3	Orchard-like canopy	*Jatropha* orchard	06-20 March 2006	4.3
4	Open/incomplete canopy: row crops	Open canopy sugarcane field	2-5 October 2007	4.4
5	Short heterogeneous [2]surface/aerodynamically rough canopy	Grass/shrub canopy	23 June – 10 July 2006	4.5
		Chromolaena stand	4-11 April 2006	
6	Tall heterogeneous [3]surface/aerodynamically rough canopy	Tree/shrub canopy	22 June – 10 July 2006	4.6
7	Open water surface	Large dam	29 June to 13 July 2007	4.7

[2] A short heterogeneous surface is defined as a surface where the average canopy height did not exceed 2 m.
[3] A tall heterogeneous surface is defined as a surface where the average canopy height exceeds 2 m.

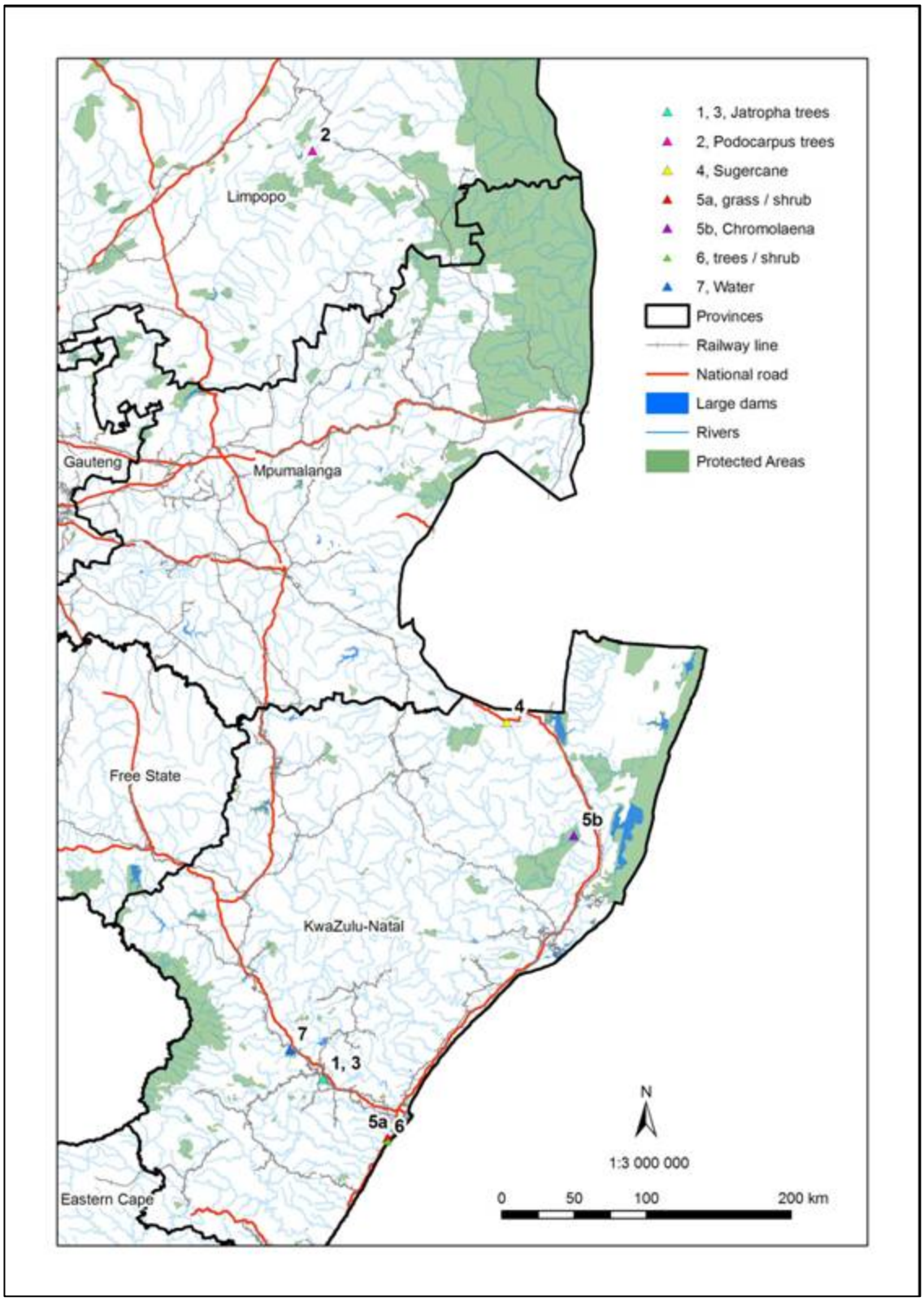

Figure 1 The geographical distribution of the research sites used in this study as part of the different case studies listed in Table 2. The research sites shown include the *Jatropha* orchard, the *Podocarpus* plantation, the sugarcane site, the shrub /grass and the shrub/trees sites, the *Chromolaena* site and open water surface.

4.1 Case study 1: Energy balance closure

In Chapter 2 (Section 2.4), the problem around energy balance closure with the eddy covariance systems, and the effect of flux footprints on the accuracy of total evaporation estimates are discussed. The eddy covariance system with an infra-red gas analyser as described in Table 1 is one of only two types of systems, the other being a lysimeter, that can provide direct and independent (not based on the energy balance) estimates of latent heat flux density and hence total evaporation.

A "two sensor" eddy covariance system was used in all the case studies to provide a direct estimate of latent heat flux density and total evaporation, as reference estimates. Therefore, in Case study 1 the outputs of the two eddy covariance systems used (In Situ Flux systems and Applied Technologies Inc.) were compared to ensure that they were operating correctly. The eddy covariance fluxes were also compared with fluxes from the other systems and the level of energy balance closure achieved was determined. An orchard-like surface consisting of young *Jatropha* trees was used.

Aims of case study:

- Compare sensible and latent heat flux densities estimated with two independent eddy covariance systems;

- Calculate energy balance closure of an orchard-like surface.

4.1.1 Materials and methods

4.1.1.1 Site description

Field work was conducted at an agroforestry stand (29° 40' S, 30° 24' E, 781.5 m a.m.s.l.), with different *Jatropha* and *Kikuyu* treatments. Two research plots (plot 11 and 13) with *Jatropha* trees only, were used to study the suitability of a range of micrometeorological techniques to estimate total evaporation.

Jatropha trees were planted at a density of 1110 trees per ha (3 m x 3 m). The plots were 0.125 ha (50 m x 25 m) in size, with a total study area of 60 m x 50 m (inter plot length included). At the time of measurement (11 November to 2 December 2005), the trees were 15 to 18 months old, and at an average height of 0.8 to 1.2 m and average stem diameter of 30 to 50 mm (**Fig. 2**).

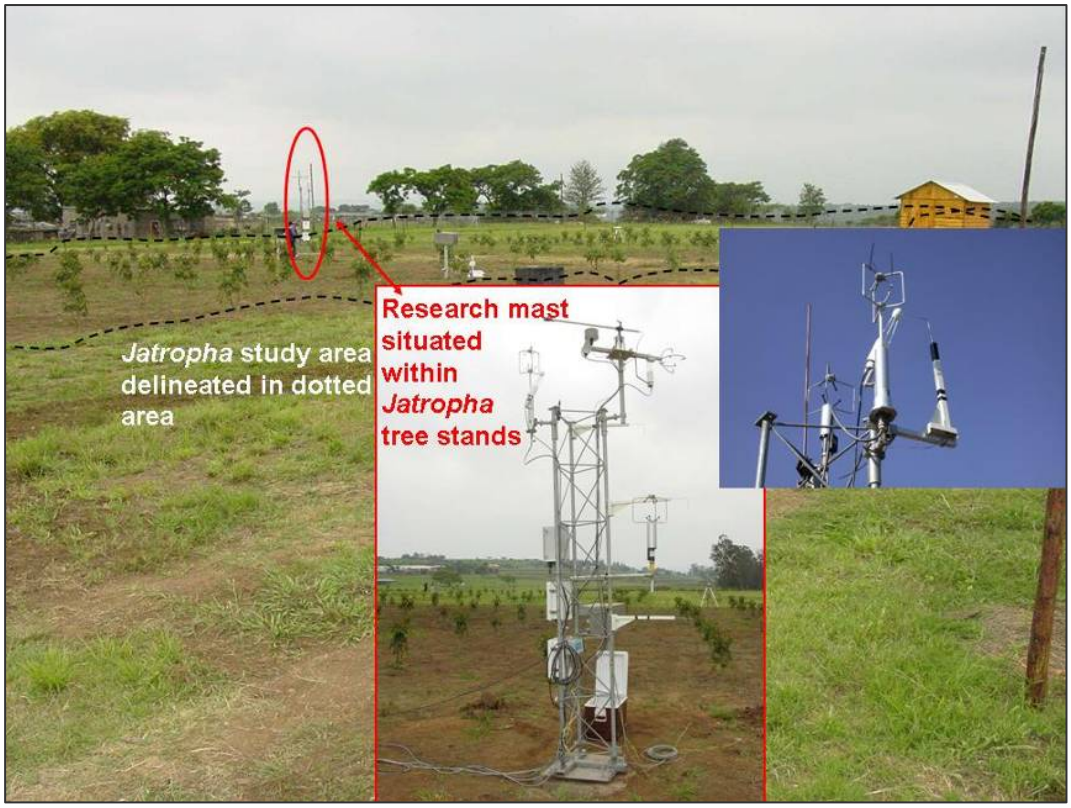

Figure 2 The orchard-like *Jatropha* research site (Ukulinga Research Farm, UKZN, Pietermaritzburg) delineated by the black dotted lines, with research mast and equipment used to estimate total evaporation in the foreground.

4.1.1.2 Techniques applied

In Case study 1, an orchard-like surface was used. Fluxes estimated with the In Situ Flux systems, Applied Technologies Inc. and RM Young eddy covariance systems and that estimated with surface renewal systems were compared. The In Situ Flux eddy covariance system was installed at an average height of 3.6 m above ground, and an RM Young sonic anemometer (as part of a separate eddy covariance system) was installed at a height of 2.15 m. Fine wire thermocouples for the surface renewal technique were installed at three heights above the soil surface: 1.22, 2.15 and 3 m. An Applied Technologies (ATI) eddy covariance system was also installed at 3.6 m. Detailed energy flux measurements took place from 11 November to 2 December 2005. Flux measurements continued following this field campaign as part of an ongoing WRC project (Everson et al., 2007).

Table 3 Summary information on the techniques applied in Case study 1 at the orchard-like surface. Techniques applied include the In Situ Flux systems and Applied Technologies Inc. eddy covariance systems which provide direct estimates of latent heat flux density, and an independent eddy covariance system (1 sensor only – RM Young sonic anemometer), and lastly three surface renewal systems.

Techniques applied	**Eddy covariance (In Situ Flux systems)**	**Eddy covariance (Applied Technologies Inc.)**	**Eddy covariance (RM Young)**	**Surface renewal**
Abbreviation	**IS EC (with IRGA), ECEB (without IRGA)**	**EC ATI**	**RMY**	**SR**
Measurement period	11 November to 2 December 2005			
Data used in comparisons	Field trip 1: 23-24 November 2005 (Sunny) + 30 November and 1 December 2005 (Partly cloudy)			
Output interval	30 min	30 min	2 min averaged to 30 min	2 min averaged to 30 min
Installation height/s	3.6 m	± 3.6 m	2.15 m	1.22, 2.15 and 3 m
Make and model of sensors (if applicable)	In Situ Flux with R3 Gill sonic anemometer, and Licor 7500 Infra-red gas analyser	Applied Technologies with ATI sonic anemometer and Licor Infra-red gas analyser	RM Young 8100 sonic anemometer	Chromal-constantan thermocouples
Complementing project	Everson et al. (2007)			
Additional measurements	Net radiometer, REBS soil heat flux plates, Chromal-constantan thermocouples, Complete automatic weather station with Solarimeter, RM Young windsentry, Vaisala Temperature and Humidity sensor, Tipping bucket raingauge			

4.1.2 Results

Two sunny (23, 24 November 2005 - DOY 327, 328) and two cloudy days (30 November and 1 December 2005 - DOY 334, 335) were selected for detailed analysis of energy fluxes and energy balance closure at an "orchard-like" surface.

4.1.2.1 Climatic conditions

Daily average temperatures ranged between 18.74 and 24.02°C, with the highest temperatures recorded on DOY 334. Daily total solar radiation values were 23.23 and 25.78 MJ m^{-2} on the two sunny days studied, and 18.76 and 12.47 MJ m^{-2} on the two cloudy days. The average windspeed over the four days was 2.07 m s^{-1}, with the higher wind speeds recorded on the two cloudy/partly cloudy days. No rainfall was recorded on the four days studied in detail, and only 0.1 mm was recorded during the entire measurement period.

4.1.2.2 Net radiation and soil heat flux density

The net irradiance (*Rn*) and soil heat flux density (G) measurements represented single point measurements. Great care was taken during installation (in terms of position and orientation of sensors), and it is therefore believed that these estimates were representative of the research site. Mid-day maximum net irradiance values exceeding 700 W m^{-2} were measured during the study period. During the day a significant amount (20-50%) of the net irradiances (*Rn*) was converted at the soil surface into soil heat flux density (G) (**Fig. 3**). These high *G* values were expected as the *Jatropha* trees were planted in this orchard configuration were still very young at the time of measurements, and thus the canopy was still undeveloped, leaving large areas of bare soil unshaded in this "tree only" treatment.

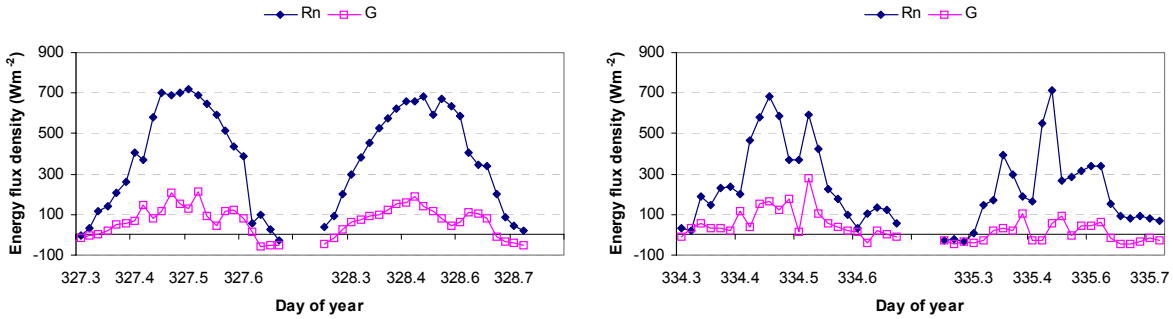

Figure 3 Net irradiance (*Rn*) and soil heat flux density (G) estimated at the orchard-like *Jatropha* site as part of Case study 1, on DOYs 327 and 328 (sunny), and 334 and 335 (partly cloudy). Only data for the time period 06h00 to 17h00 are plotted. The X-axis shows the day of year (DOY) divided into fractions of time, e.g. 327.5 refers to DOY 327 at 12h00.

4.1.2.3 Sensible and latent heat flux density from two independent eddy covariance systems

Sensible (H) and latent heat flux densities (LE) measured with the In Situ Flux systems (IS) and Applied Technologies Inc. (ATI) eddy covariance systems are compared for two sunny and two cloudy/partly cloudy days. These two systems provided both direct[4] and indirect[5] estimates of latent heat flux density. The focus in this section will be on the direct estimates of LE.

The sensible heat flux densities, based on measurements of sonic temperature and windspeed from two different makes of sonic anemometers (Gill and ATI) (**Table 3**), show some differences. On sunny days (DOY 327, 328) the differences in *H* (**Fig. 4a**) are more prominent and significant than during cloudy days (DOY 335, 326) (**Fig. 4b**). The In Situ Flux system estimates of *H* (IS H) consistently exceeded the sensible heat flux density estimates made with the ATI system (ATI H) (**Fig. 4**), on both sunny and cloudy/partly cloudy days. The latent heat flux density estimates (**Fig. 4**) show similar trends. The In Situ Flux systems estimates of *LE* (IS LE) consistently exceeded the latent heat flux densities estimated with the ATI system (ATI LE), both on sunny and cloudy days. Again the differences in the *LE* estimates are greater during sunny days (**Fig. 4**). It appears, from **Fig. 4**, that the *H* and *LE* values estimated with the IS eddy covariance system showed a larger diurnal variation than the values estimated with the ATI system.

[4] A **direct** estimate of latent heat flux density is obtained when an infra-red gas analyzer is used to directly obtain an estimate of the latent heat flux density (also referred to as EC 2 sensor method - see Table 1).

[5] An **indirect** estimate of latent heat flux density is obtained when a sonic anemometer is used to estimate sensible heat flux density first, where after latent heat flux density is calculated as the residual of the energy balance equation (also referred to as EC 1 sensor method – see Table 1).

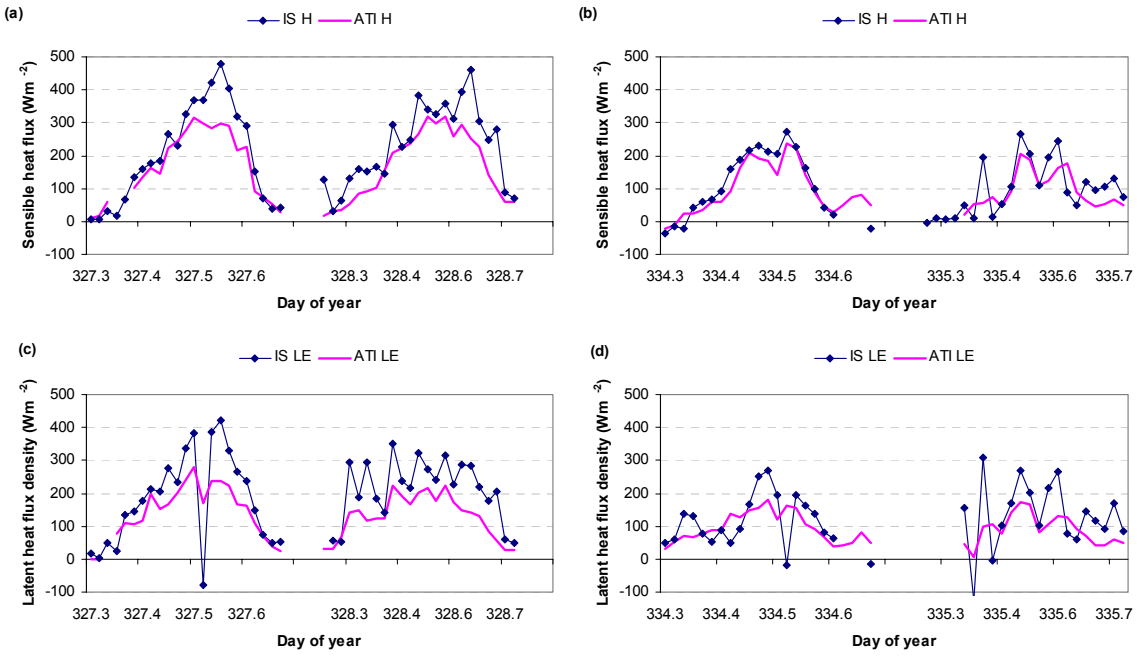

Figure 4 Sensible (a, b) and latent heat flux densities (c, d) estimated at the orchard-like *Jatropha* site as part of Case study 1, on DOYs 327 and 328 (sunny), and 334 and 335 (partly cloudy). a and b are the sensible heat flux densities estimated with the In Situ Flux system and the Applied Technologies Inc. eddy covariance system (IS H and ATI H respectively); c and d are the latent heat flux densities estimated with the In Situ Flux system and the Applied Technologies Inc. eddy covariance system (IS LE and ATI LE respectively). Only data for the time period 06h00 to 17h00 are plotted. The X-axis shows the day of year (DOY) divided into fractions of time, e.g. 327.5 refers to DOY 327 at 12h00.

4.1.2.4 Latent heat flux density of eddy covariance systems: Direct and indirect estimates

In **Fig. 4** sensible and heat flux densities estimated with the IS and ATI eddy covariance systems are compared. Only direct estimates of latent heat flux densities were compared in **Fig. 4c & d**. In **Fig. 5**, however, the direct (IS LE, ATI LE) and indirect estimates of latent heat flux density (IS LE(EB), ATI LE(EB)) are compared. The diurnal trends of the direct and indirect estimates of *LE* differ most of the time. For example in the afternoon of DOY 327, direct and indirect estimates of *LE* with the In Situ Flux system, differ by up to 400 W m^{-2} (**Fig. 5a**). However, for the early parts of DOY 327, there is a very good agreement between the direct and indirect estimates of *LE* (**Fig. 5a**).

The direct (ATI LE) and indirect estimates of *LE* (ATI LE(EB)) using the Applied Technologies Inc. eddy covariance system compared better, but differences were still apparent (**Fig. 5c & d**). The direct and indirect estimates of *LE* follow a similar diurnal trend, with the exception of short periods generally during mid-morning (e.g. DOY 327, 334 and 335) (**Fig. 5c & d**).

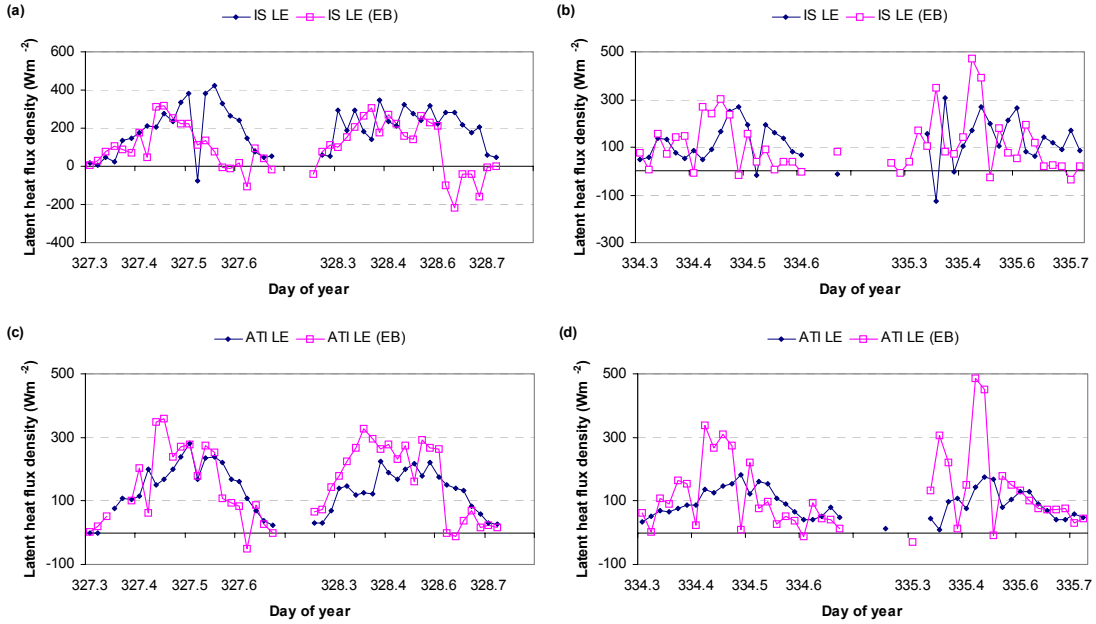

Figure 5 Direct and indirect estimates of latent heat flux densities estimated at the orchard-like *Jatropha* site as part of Case study 1, on DOYs 327 and 328 (sunny), and 334 and 335 (partly cloudy). a & b show direct (IS LE) and indirect (IS LE(EB)) estimates of latent heat flux density using the In Situ Flux systems eddy covariance systems on the sunny and cloudy/partly cloudy days. c & d show direct (ATI LE) and indirect (ATI LE(EB)) estimates of latent heat flux density using the Applied Technologies Inc. eddy covariance system on the sunny and cloudy/partly cloudy days. Only data for the time period 06h00 to 17h00 are plotted. The X-axis shows the day of year (DOY) divided into fractions of time, e.g. 327.5 refers to DOY 327 at 12h00.

4.1.2.5 Energy balance closure discrepancy and Bowen ratio of two independent eddy covariance systems

Energy balance closure can be evaluated by looking at the energy balance closure discrepancy (D)[6]. The closure discrepancies calculated for both the In Situ Flux (IS D) and Applied Technologies Inc. eddy covariance system (ATI D) exceeded 1 for a great part of the day (**Fig. 6a & b**). This means that the sum of the sensible (H) and latent heat flux densities (LE) exceeded the available energy (*Rn*-G), but more importantly that closure was not satisfied. The closure discrepancy estimated for the In Situ Flux system showed greater diurnal variation when compared to the D values estimated for the Applied Technologies Inc. system (ATI) (**Fig. 6a & b**). This is a direct reflection of the differences in the sensible and latent heat flux densities estimated by the systems and shown in **Fig. 4**.

Though differences existed in the closure discrepancies estimated for the two eddy covariance systems, the Bowen ratios (β) calculated for the In Situ Flux system (IS B) and Applied Technologies eddy covariance systems (ATI B) compared favourably (**Fig. 6c & d**). An exception is the afternoon of DOY 328 (**Fig. 6c**). On both sunny and partly cloudy days, the Bowen ratio values calculated vary around 1 (**Fig. 6**). A β value of 1 means that the sensible and latent heat flux densities are divided equally. A $\beta > 1$ means that the sensible heat flux densities exceeded the latent heat flux densities, which was often the case in the late afternoon. This is typical of atmospheric conditions experienced in late afternoons during summer. On partly cloudy days (DOY 334-335) the β values were well below 1 during early morning and late afternoon (**Fig. 6d**), and suggest condensation which is likely during cloudy/rainy days.

[6] Energy balance closure is calculated as $(LE+H)/(R_n-G)$

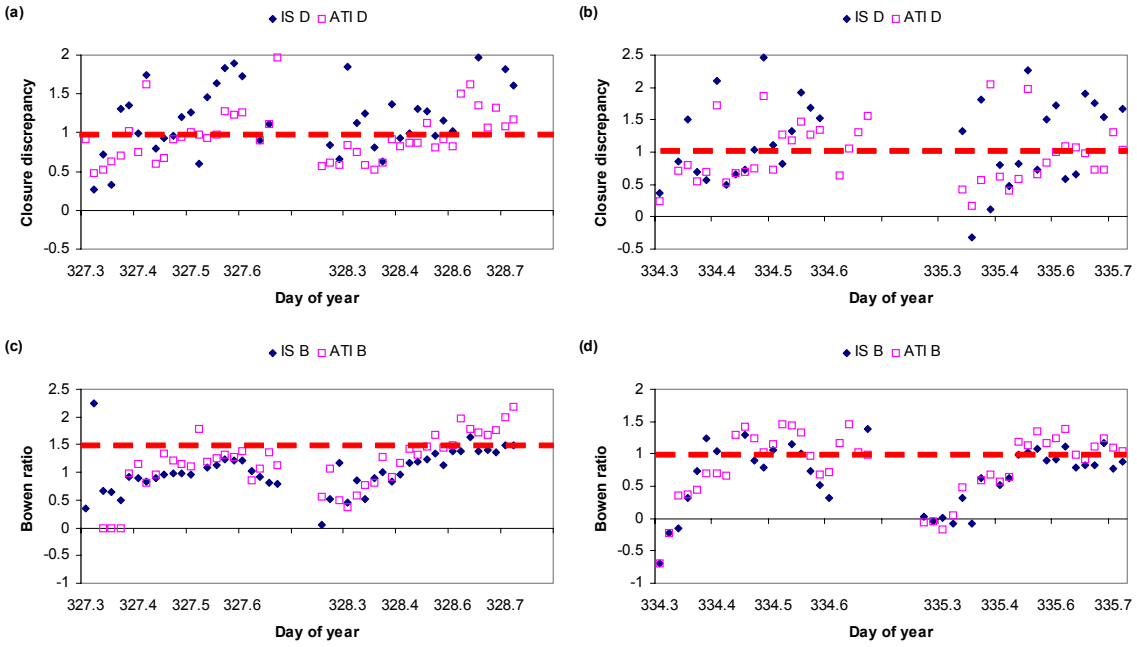

Figure 6 Closure discrepancy (D) and Bowen ratio (B) values estimated at the orchard-like *Jatropha* site as part of Case study 1, on DOYs 327 and 328 (sunny), and 334 and 335 (partly cloudy). a & b show the closure discrepancy (D) estimated for the In Situ Flux systems (IS D) and the Applied Technologies Inc. eddy covariance systems (ATI D) on the sunny and cloudy/partly cloudy days. c & d show the Bowen ratio values (B) estimated for the In Situ Flux systems (IS B) and the Applied Technologies Inc. eddy covariance systems (ATI B) on the sunny and cloudy/partly cloudy days. Only data for the time period 06h00 to 17h00 are plotted. The X-axis shows the day of year (DOY) divided into fractions of time, e.g. 327.5 refers to DOY 327 at 12h00.

4.1.2.6 Sensible and latent heat flux densities (direct and indirect) estimated with a range of micrometeorological systems

The sensible heat flux densities estimated with systems using sonic anemometers (including the In Situ Flux systems, Applied Technologies Inc. and RM Young eddy covariance system) (**Table 3**) compared well (**Fig. 7a & b**). This was partly because these systems all used sonic windspeed and temperature data in the calculation of the sensible heat flux densities. The sensible heat flux density values (H) compared well on cloudy days (DOY 334, 335) (**Fig. 7b**), and it appeared as if the sonic anemometers detected atmospheric changes similarly. However, bigger differences exist between the *H* values estimated with the different systems on sunny days (DOY 327, 328) (**Fig. 7a**). On sunny days, the sensible heat flux densities estimated with the In Situ Flux system consistently exceeded the *H* values of the ATI system, even though the sensors were installed at the same height (**Fig. 7a & b**).

The sensible heat flux densities estimated with the ATI and RM Young eddy covariance system compared favourably with the sensible heat flux densities estimated with the surface renewal system installed in the lowest position (SR1) (**Table 3**) (**Fig. 7a & b**), whereas, the *H* values estimated with the surface renewal systems installed at the greater heights (SR2, SR3) compared more favourably with the IS eddy covariance system. These trends are consistent for sunny days (DOY 327, 328), but not for partly cloudy days (DOY 334, 335), when the sensible heat flux densities estimated with the SR2 and SR3 systems exceeded the sensible heat flux densities of all other techniques (**Fig. 7a & b**).

A bigger variation was observed in the estimates of LE, than in the estimates of *H* (**Fig. 7c & d**). Only the direct estimates of *LE* for the IS and ATI systems are shown. Noticeable was that the peak values of the six systems were not reached at the same time (**Fig. 7c & d**). Generally, the *LE* data from the RMY system compared well with the SR data (specifically SR1) (**Fig. 7c & d**), as was the case for the *H* data. Apart from that there was a lot of variation in the *LE* values estimated with the different systems.

The fair agreement in the sensible heat flux densities estimated with the different systems, is illustrated in scatter plots (**Fig. 8a & b**). Good agreements existed between the sensible heat flux densities of the In Situ Flux (IS) and other systems (ATI, RMY, SR) on sunny days, with $R^2 > 0.78$ (**Fig. 8a**), and little scatter around the 1:1 line. Generally, the sensible heat flux estimates from the In Situ Flux eddy covariance system exceeded that of the other systems (by 19 to 32%), with slopes $(m)^7$ values exceeding 1 (**Fig. 8a**). On cloudy days there was more scatter around the 1:1 line, but the sensible heat flux densities still agreed reasonably well ($R^2>0.7$) (**Fig. 8b**). These scatter plots reflect the diurnal variation in the sensible heat flux density data shown in **Fig. 7a & b**.

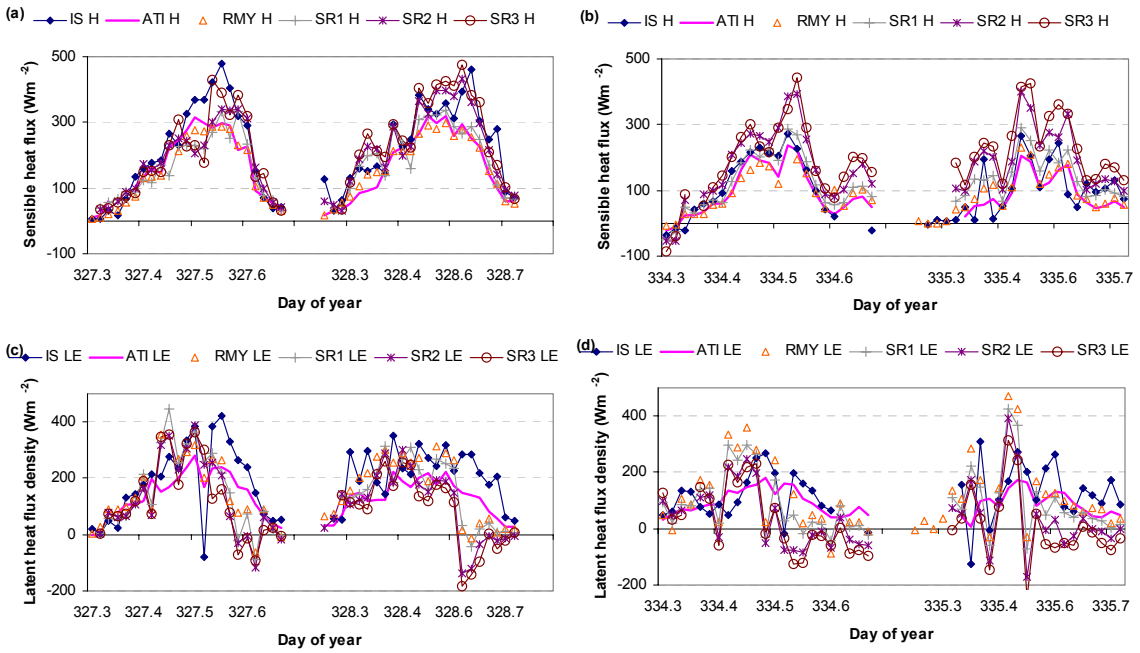

Figure 7 Sensible (a & b) and Latent heat flux densities (c & d) as estimated at the orchard-like *Jatropha* site as part of Case study 1, on DOYs 327 and 328 (sunny), and 334 and 335 (partly cloudy). a & b show the sensible heat flux density estimated for the In Situ Flux systems (IS H), the Applied Technologies Inc. system (ATI H), the RM Young eddy covariance systems (RMY H), and three different surface renewal systems installed at different height (SR1 H, SR2 H, SR3 H)(see heights in Table 3) on the sunny and cloudy/partly cloudy days. c & d show the latent heat flux density values estimated for the In Situ Flux systems (IS LE), the Applied Technologies Inc. system (ATI LE), the RM Young eddy covariance systems (RMY LE), and three different surface renewal systems installed at different height (SR1 LE, SR2 LE, SR3 LE)(see heights in Table 3) on the sunny and cloudy/partly cloudy days. (Only direct estimates of *LE* with the IS and ATI systems are shown). Only data for the time period 06h00 to 17h00 are plotted. The X-axis shows the day of year (DOY) divided into fractions of time, e.g. 327.5 refers to DOY 327 at 12h00.

[7] Linear relationship given by y=mx+c is assumed.

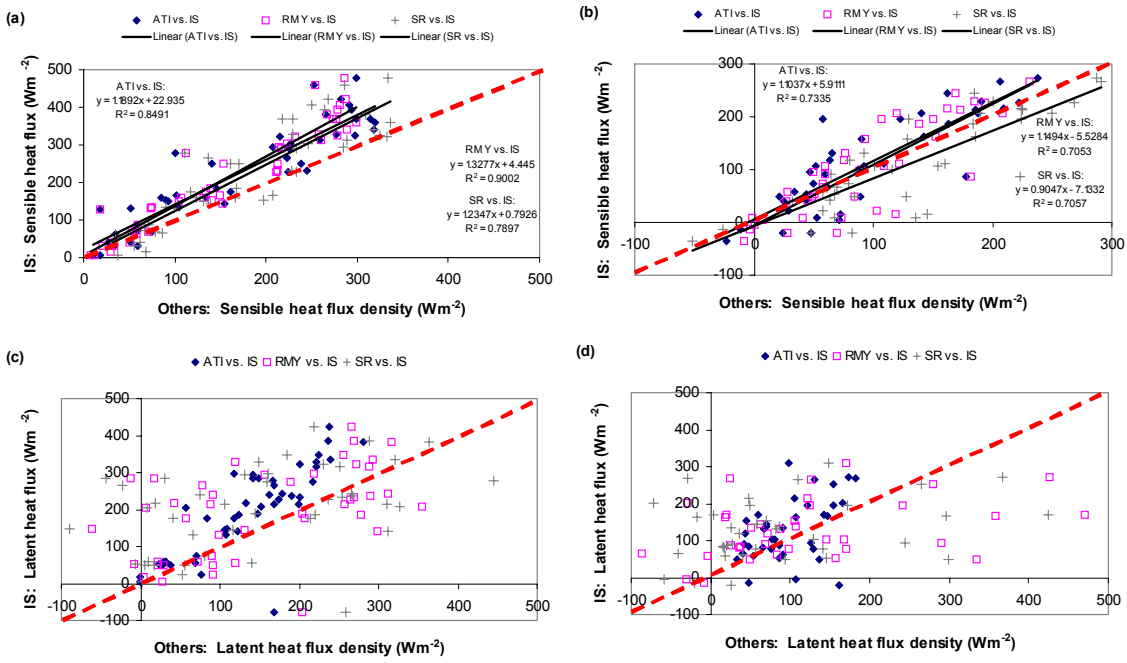

Figure 8 Scatter plots of sensible (a & b) and latent heat flux densities (c,b) estimated at the orchard-like *Jatropha* site as part of Case study 1, on DOYs 327 and 328 (sunny), and 334 and 335 (partly cloudy). The In Situ Flux system (IS) data are presented on the Y-axis and the other systems, Applied Technologies (ATI), RM Young (RMY) and the Surface renewal system (SR1) on the X-axis. a & b show the relationship between the IS sensible heat flux density values compared to the sensible heat flux densities estimated with the ATI system (ATI vs. IS), the RM Young eddy covariance systems (RMY vs. IS), and one surface renewal system (SR vs. IS) (installed at lowest height). c & d show the relationship between the IS latent heat flux density values compared to the latent heat flux densities estimated with the ATI system (ATI vs. IS), the RM Young eddy covariance systems (RMY vs. IS), and one surface renewal system (SR vs. IS) (installed at lowest height). (Only direct estimates of *LE* with the IS and ATI systems are shown). Only data for the time period 06h00 to 17h00 are plotted.

However, the latent heat flux scatter plots (In Situ Flux system *vs* others) show a much greater scatter around the 1:1 line (**Fig. 8c & d**). Here the *LE* estimates with both the IS and ATI systems represent direct estimates of LE. The comparison of the latent heat flux densities reflects the diurnal variation in the *LE* values shown in **Fig. 7c & d**. More scatter is visible on cloudy days (**Fig. 7d**), than on sunny days (**Fig. 7c**).

4.1.2.7 Direct and indirect estimates of total evaporation

Fig. 9 shows the large variation in the daily total evaporation (ET) estimates at an orchard-like *Jatropha* site using different techniques, over a 14 day period. The accumulated ET over this period ranged between 27 mm with the ATI system where the direct estimates of *LE* were used, and 36.8 mm with the IS system where the direct estimates of *LE* were used (**Fig. 9**). Daily total evaporation averaged between 1.9 and 2.6 mm d^{-1}. Direct estimates of total evaporation with the ATI system and the indirect estimate with the IS flux systems were the lowest and similar (≈27 mm) (**Fig. 9**). The direct estimate of total evaporation with the In Situ Flux system was the highest, and the estimates with the SR1 and RMY systems and indirect estimate with the ATI system were similar (31.3, 33.7 and 34.1 mm respectively).

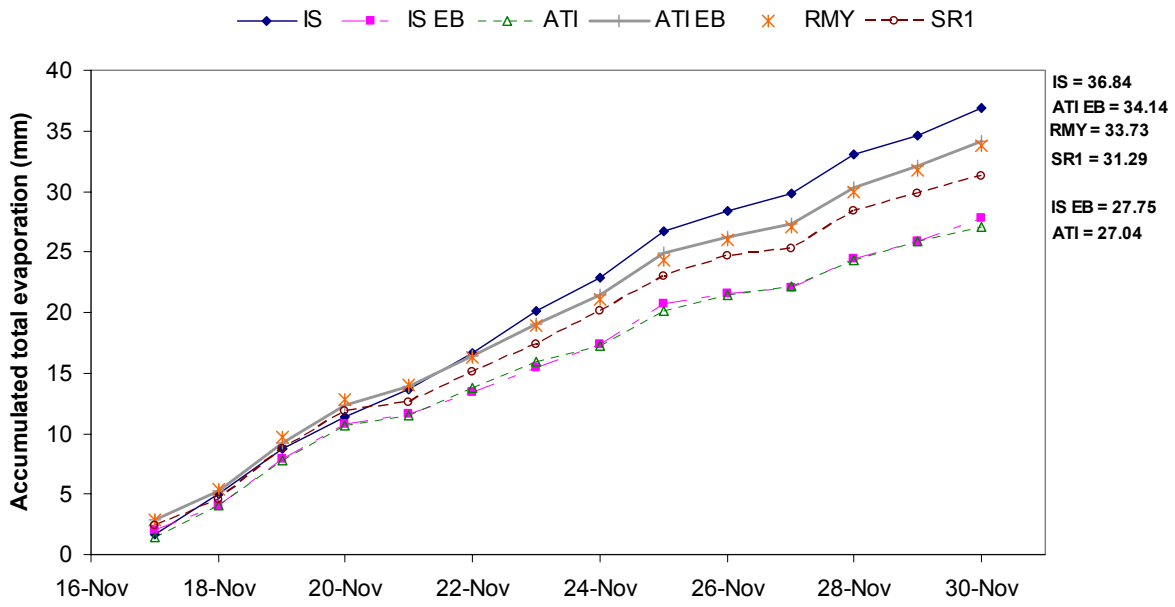

Figure 9 Daily total evaporation estimated at the orchard-like *Jatropha* site as part of Case study 1 over a period of 14 days (17 to 30 November 2005, DOY 322-335) using four techniques: Direct and indirect estimates with the In Situ Flux eddy covariance system (IS, IS EB), direct and indirect estimates with the Applied Technologies eddy covariance system (ATI, ATI EB), the RM Young system (RMY) and the surface renewal system installed at the lowest height (SR1).

The reasons for differences in evaporation estimates using different techniques cannot always be explained easily. However, small variations in sensor installation and design may contribute to differences in ET through for example flow distortion, while system differences (e.g. software, sampling frequency, etc.) will also result in minor differences of these estimates.

4.1.3 Summary and conclusions

Relatively small differences existed in the sensible heat flux estimates with three different sonic anemometers (Gill, ATI, RM Young). Generally the sensible heat flux density estimates with the In Situ Flux system exceeded those of all the other systems, with the largest differences at mid-day. Sensible heat flux densities estimated with the ATI, RMY and SR systems compared well with each other.

Similar differences to those above were noted when comparing the latent heat flux densities, with the In Situ Flux *LE* estimates exceeding those measured with the ATI system. The ATI estimates of *LE* compared well with the RMY and SR data. When comparing direct and indirect estimates of *LE* estimated with two different eddy covariance systems, large diurnal differences in *LE* (direct *vs* indirect) were noted, especially with the In Situ Flux system, but occasionally also with the ATI system.

Closure discrepancy values for the orchard-like *Jatropha* site generally exceeded 1. Energy balance closure was generally not reached (D=1).

Longer term ET estimates (over a period of 14 days) showed differences of up to 26%. Direct estimates of ET with the ATI system were the lowest (27.04 mm), and the direct estimate of ET with the IS system was the highest (38.84 mm).

It can be concluded that differences of up to 26% in the total evaporation estimated with different systems, can exist under similar conditions experienced in this study.

4.2 Case study 2: Limited fetch

4.2.1 Introduction

Various plants (trees, crops and others) are grown or occur naturally in narrow strips. Quite often, these narrow strips of plants occur around a stream. Total evaporation estimates from e.g. riparian vegetation (indigenous or invasive) are important when impacts of land use changes are assessed (due to invasions) and also in determining the requirements of the ecological reserve. Where total evaporation of tall vegetation grown in narrow strips needs to be estimated, the fetch:height requirements of most micrometeorological techniques might not be met.

***Aim of case study**:*

- To determine the suitability of a range of micrometeorological techniques in estimating total evaporation from a tall canopy under limited fetch conditions.

4.2.2 Material and methods

4.2.2.1 Site description

Field work was carried out on a plantation of *Podocarpus falcatus* trees (23.9°S, 30.06°E, 853 m a.m.s.l.) (**Fig. 10**). The plantation was situated in a riparian zone, and is located in the Tzaneen area. The relatively small *Podocarpus* plantation (200 m x 800 m = 16 000 m^2) consisted of a narrow strip of trees, with tree heights ranging from 8.15 m to 11.05 m. The average tree diameter estimated was 83 to 224 mm. The *Podocarpus* plantation was surrounded by extensive plantations of exotic trees (species like *Mahogany*, *Pinus* and others). The slope at this site was less than 5%.

Field work was conducted during three field campaigns: 21 to 28 September 2005 (Field trip 1), 09 to 15 February 2006 (Field trip 2) and 23 to 30 August 2006 (Field trip 3).

4.2.2.2 Techniques applied

Table 4 summarises the techniques used in the different field campaigns. Three principal techniques were tested at the *Podocarpus* site: (1) the eddy covariance technique (EC) (for direct and indirect estimates of LE), (2) the surface renewal method (SR) and (3) the Heat pulse velocity technique (HPV). In addition to these systems, a complete automatic weather station was installed in close proximity to the *Podocarpus* site (23.85°S, 30.14°E, 731 m a.m.s.l.). Total evaporation measurements

with the EC and SR systems were for the duration of window periods only. Transpiration was however estimated with the HPV technique for a longer period (Sept. 2005 to Aug. 2006).

During the first and second field trips, the Gill R3 sonic anemometer and Li-cor 7500 infra-red gas analyzer (IRGA) (part of an In Situ Flux systems eddy covariance system) were installed at a height of 18 m (**Table 4**). A second sonic anemometer (RM Young) was installed at 12.2 m during all three field campaigns. Three sets of thermocouples for the surface renewal systems were installed at different heights, but only the results from the 11.2 m height are shown. During the last field trip, the In Situ Flux system sensors were lowered to a height of 12 m. It was felt that the initial installation height might have been too high above the canopy, possibly sensing fluxes from the surrounding vegetation rather than the narrow *Podocarpus* plantation.

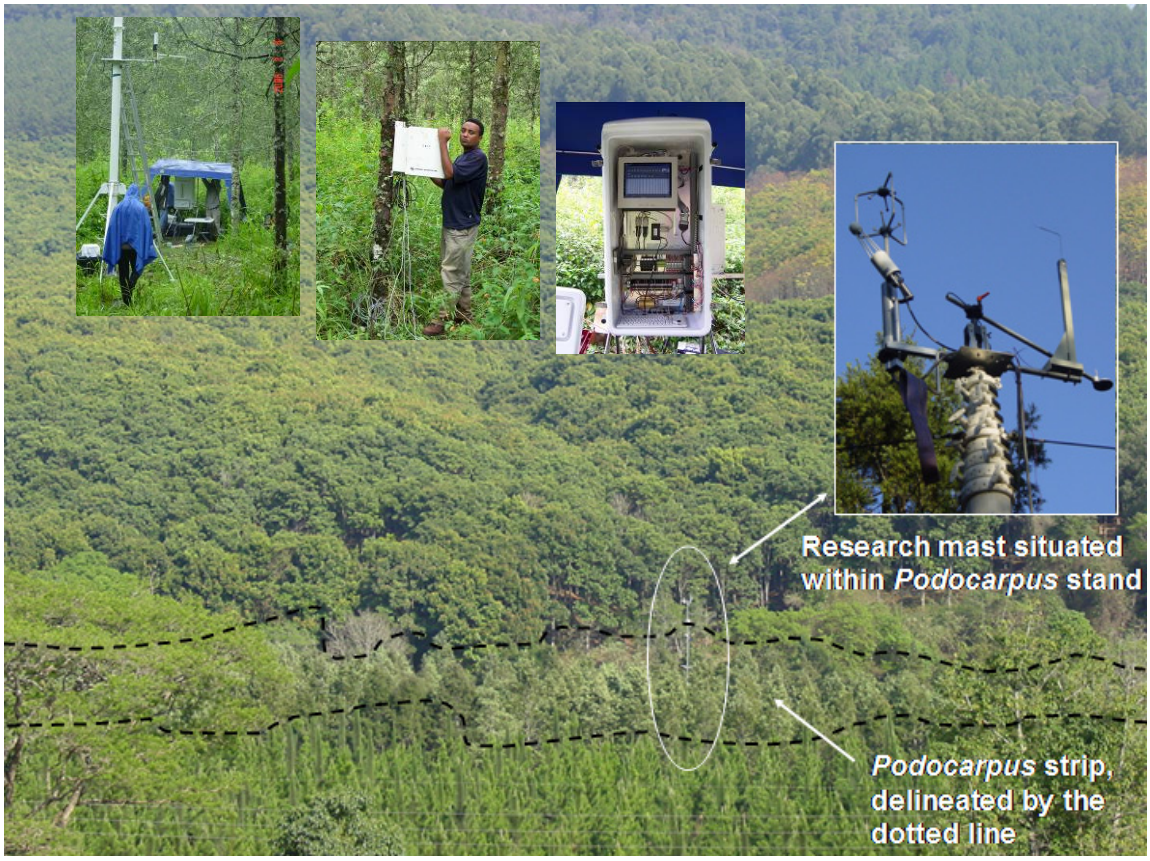

Figure 10 The *Podocarpus* plantation (Tzaneen area) used in Case study 2. Shown in the figure is the research mast and equipment used to estimate evaporation.

Table 4 Summary information on the techniques applied in Case study 2 at the narrow plantation of *Podocarpus* trees. Techniques applied include the In Situ Flux systems eddy covariance system, the RM Young eddy covariance system, the surface renewal system and the heat pulse velocity system.

	***Podocarpus* research site**			
Techniques applied	**Eddy covariance (In Situ Flux systems)**	**Eddy covariance (RM Young 8100)**	**Surface renewal**	**Heat pulse velocity**
Abbreviation	**EC (direct) ECEB (indirect)**	**RMY**	**SR**	**HPV**
Measurement period	21-28 Sep. 2005: Field trip 1 09-15 Feb. 2006: Field trip 2 23-30 Aug. 2006: Field trip 3			21 Sep. 2005 to Aug. 2006
Data used in comparisons	23-24 Sep. 2005 (Sunny); 22 and 25 Sep. 2005 (Partly cloudy) 11-12 Feb. 2006 (Cloud/Partly cloudy); 13-14 Feb. 2006 (Sunny/Cloudy) 28-29 Aug. 2006 (Sunny); 26-27 Aug. 2006 (Partly cloudy)			
Output interval	30 min	2 min averaged to 30 min	2 min averaged to 30 min	60 min
Installation height/s	Field trip 1,2: 18 m Field trip 3: 12 m	Field trip 1,2: 12.2 m Field trip 3: 12.2 m	Field trip 1,2: 11.2 m Field trip 3: 11.2 m	N/a
Make and model of sensors (if applicable)	In Situ Flux with R3 Gill sonic anemometer, and Licor 7500 Infra-red gas analyser	RM Young 8100 sonic anemometer	Chromal-constantan thermocouples	N/a
Complementing project	Dye et al. (2008)			
Additional	Net radiometer, REBS soil heat flux plates, Chromal-constantan thermocouples, Complete automatic weather station with Solarimeter, RM Young windsentry, Vaisala temperature and humidity sensor, tipping bucket raingauge			

4.2.3 Results

Sunny, cloudy and partly cloudy days were selected from the different field campaigns for the techniques comparison (**Table 4**). Only data from 07h00 to 17h00 are shown.

4.2.3.1 Climatic conditions

The three field campaigns experienced very different climatic conditions. During the first campaign, daily average air temperatures ranged between 21.49 and 26.03°C (average 23.17°C) over the four days studied (DOY 265-268), with maximum temperatures of 38.23°C recorded on DOY 268. No rainfall was recorded and the solar radiation values ranged between 14.68 and 22.53 MJ m^{-2}.

During the second field campaign, the temperature and humidity sensor malfunctioned, so no data were available for this period. Solar radiation values recorded over the four days studied (DOY 42-45) ranged between 9.67 and 23.48 MJ m^{-2}, with 63.3 mm of rainfall recorded over this time. During the last field campaign, daily average temperatures ranged between 15.57 and 19.24°C (average 16.94°C) over the four days studied (DOY 238-241). Maximum air temperatures of 30.39°C were recorded on DOY 241. Solar radiation values ranged between 15.37 and 21.76 MJ m^{-2}. A total of 0.1 mm of rainfall was recorded over the four-day study period.

During all three field campaigns, wind speeds measured were low – with daily averages less than 0.5 m s^{-1}, but maximum wind speeds of up to 6 m s^{-1} were recorded on DOY 267.

4.2.3.2 Net radiation and soil heat flux density

The net irradiances (*Rn*) changed significantly from one season to the next, with mid-day maximum net irradiances in September 2005 exceeding 600 W m^{-2} (**Fig. 11a**), and increasing to > 1000 W m^{-2} in February 2006 (**Fig. 11b**). By August 2006, values had decreased to mid-day maxima of < 600 W m^{-2} (**Fig. 11c**). The soil heat flux densities estimated during the three field campaigns accounted for 10 to 30% of the net irradiance (**Fig. 11**). An understorey canopy was present at all times. About 70% of the net radiation was therefore available for partitioning between sensible and latent heat flux densities.

4.2.3.3 Sensible and latent heat flux density

During the first field campaign the Bowen ratio values (for different 30 min periods) exceeded 1 for most of the day, meaning that more energy went into heating the air than into driving total evaporation (**Fig. 12**). The sensible heat flux densities (H) estimated during this field campaign using the In situ flux systems and RM Young eddy covariance system and the surface renewal system, showed similar diurnal trends and magnitudes especially on cloudy days (**Fig. 13a**), but varied greatly over any given day. The sensible heat flux densities estimated with the eddy covariance systems (H EC and HRMY) were similar at times despite an almost 6 m difference in installation height (**Fig. 13a & b**). These estimates of *H* occasionally differed greatly from the estimates of the surface renewal system (e.g. DOY 266) (**Fig. 13a & b**). Also, it appeared as if estimates of *H* with the eddy covariance system installed at the highest position above the canopy (H IS) (**Fig. 13a & b**), showed the greatest variation in *H* from one 30 min period to the next.

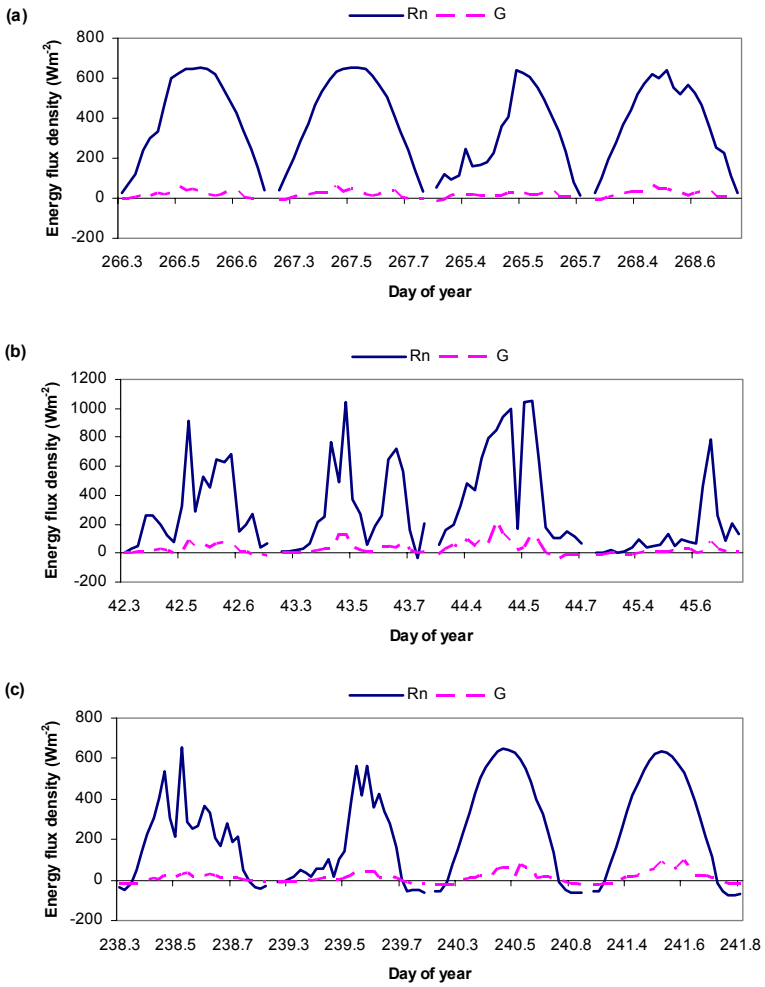

Figure 11 Net irradiances (*Rn*) and soil heat flux densities (G) estimated at the narrow plantation of Podocarpus trees on sunny and partly cloudy days of the three field campaigns. a – net irradiances and soil heat flux densities for DOYs 265-268 (Field trip 1); b – net irradiances and soil heat flux densities for DOYs 42-45 (Field trip 2) and c – net irradiances and soil heat flux densities for DOYs 238-239, 240-241 (Field trip 3). Only data for the time period 07h00 to 17h00 are plotted. The X-axis shows the day of year (DOY) divided into fractions of time, e.g. 42.5 refers to DOY 42 at 12h00.

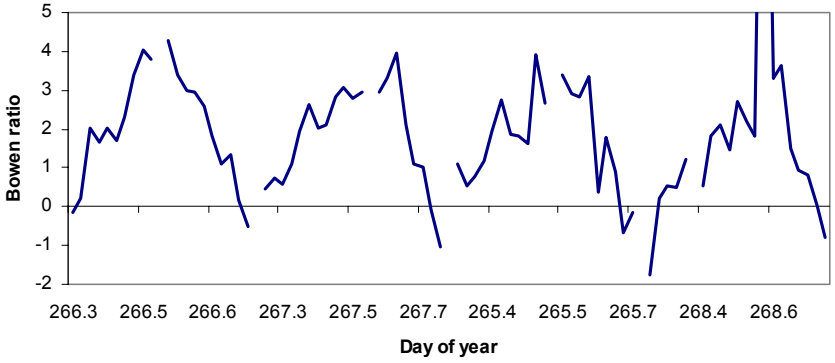

Figure 12 Bowen ratio values estimated at the narrow plantation of *Podocarpus* trees on sunny and partly cloudy days of the first field campaign (DOYs 265-268) using the In Situ Flux eddy covariance system. Only data for the time period 07h00 to 17h00 are plotted. The X-axis shows the day of year (DOY) divided into fractions of time, e.g. 266.5 refers to DOY 266 at 12h00.

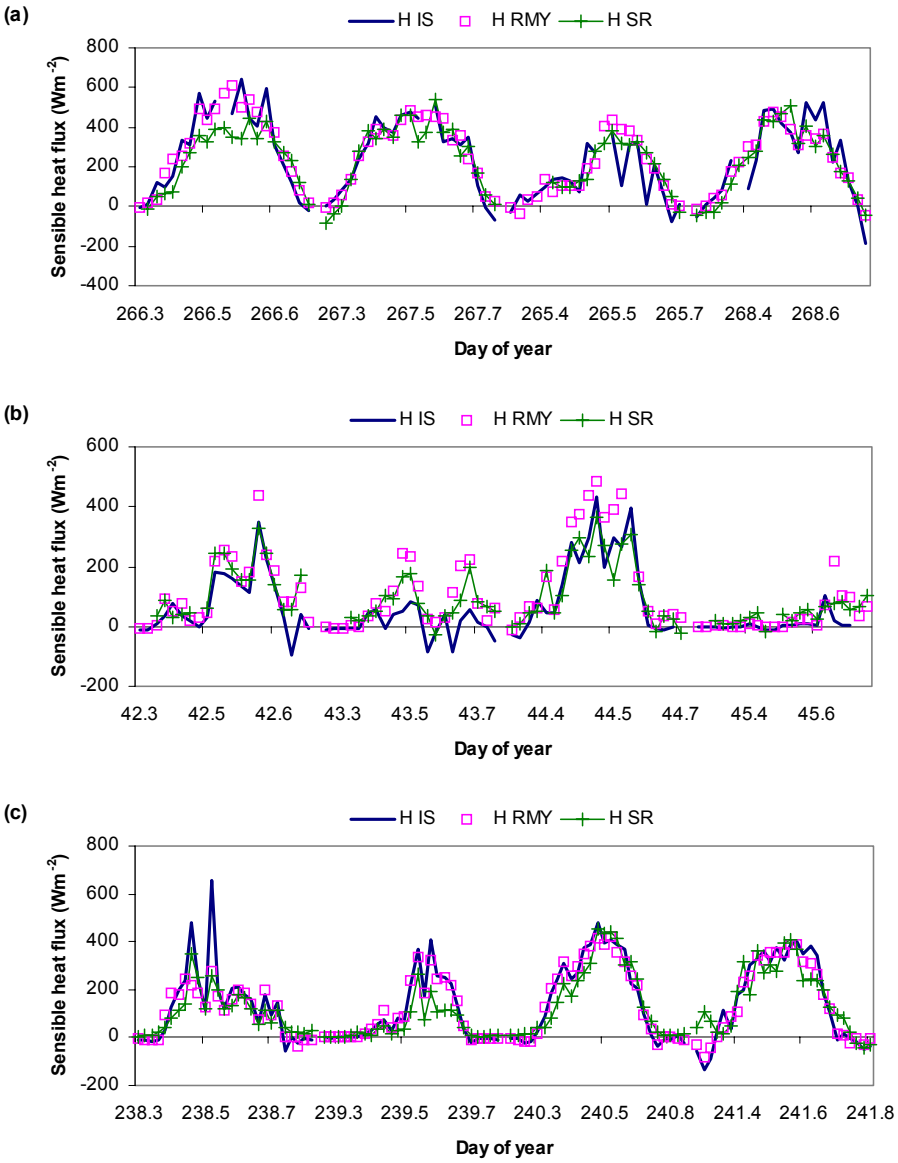

Figure 13 Sensible heat flux densities estimated at the narrow plantation of *Podocarpus* trees on sunny and partly cloudy days of the three field campaigns: Field trip 1 (DOYs 265-268), Field trip 2 (DOYs 42-45) and Field trip 3 (DOYs 238-241). Sensible heat flux density was measured with the In Situ Flux and RMY eddy covariance systems (H IS, H RMY) and with a surface renewal system (H SR). Only data for the time period 07h00 to 17h00 are plotted. The X-axis shows the day of year (DOY) divided into fractions of time, e.g. 42.5 refers to DOY 42 at 12h00.

During the first field campaign *LE* estimated with the different systems showed high diurnal variation over any given day (**Fig. 14a**). Interesting to note was the big difference in the direct and indirect estimates of *LE* using the In Situ Flux system (LE IS and LE IS EC), this despite the same installation height (**Fig. 14a & b**). Also, interesting to note was the fact that the closure discrepancy during this field campaign was generally around 1 (**Fig. 15**), meaning that energy balance closure was achieved at this site, and hence no additional source of energy contributed to the energy balance.

During the second field campaign, where there were still a large height difference between the In Situ Flux eddy covariance sensors and the other sensors (**Table 4**), *H* showed similar diurnal variations on

both sunny and cloudy days (**Fig. 13b**) to the first field campaign. The magnitude of the fluxes differed somewhat e.g. DOY 43 (**Fig. 13b**). The *H* values generally mimicked the changes in the net irradiances well (**Fig. 13b, 11**). The *H* estimates with the surface renewal and RMY system compared well (**Fig. 13b**), with the RMY system generally recording the highest estimates of sensible heat flux density. Similarly, the latent heat flux densities estimated with these systems compared reasonably well, but the direct estimates of *LE* (LE IS) were often lower than the other estimates of *LE* (**Fig. 14b**).

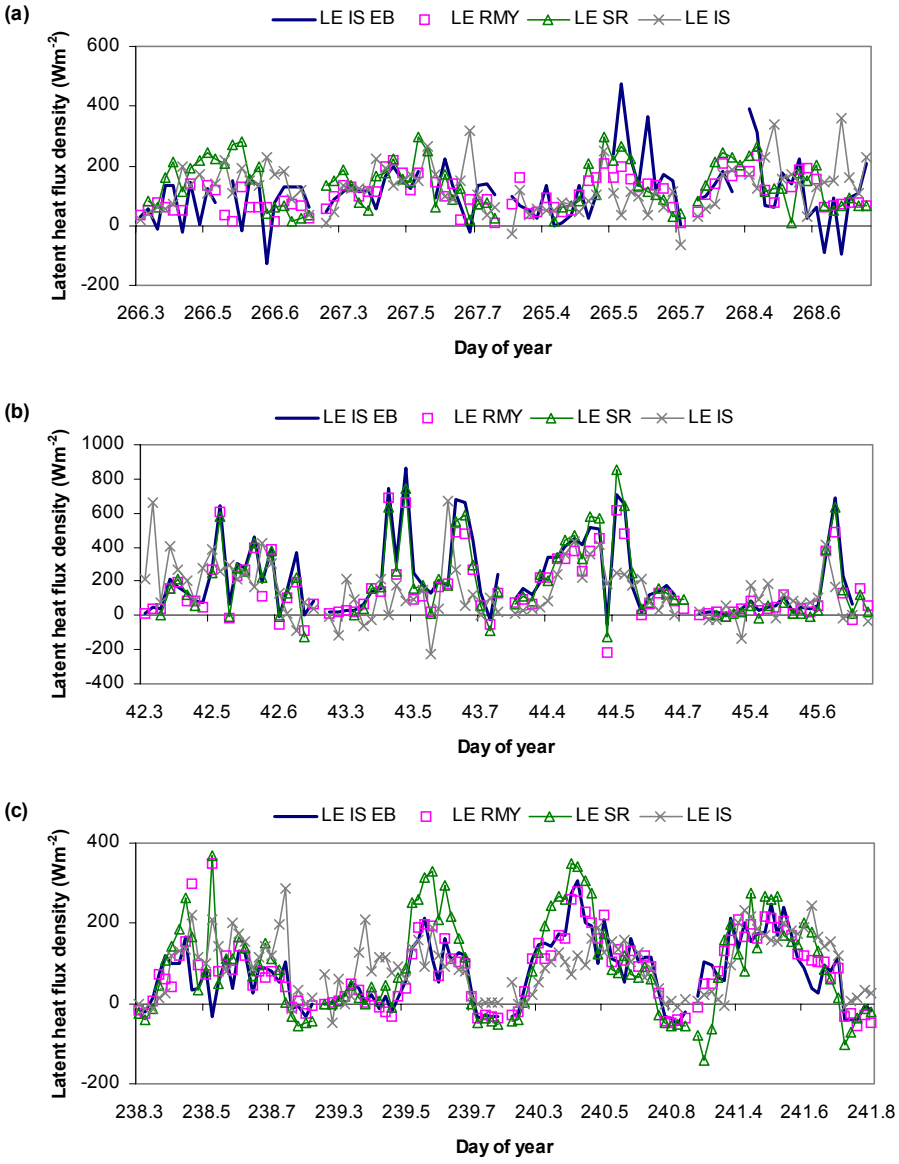

Figure 14 Latent heat flux densities estimated at the narrow plantation of *Podocarpus* trees on sunny and partly cloudy days of the three field campaigns: a - Field trip 1 (DOYs 265-268), b - Field trip 2 (DOYs 42-45) and c - Field trip 3 (DOYs 238-241). Latent heat flux density was measured with the In Situ Flux eddy covariance system (directly and indirectly - LE IS and LE IS EB), with the RMY eddy covariance system (LE RMY) and with a surface renewal system (LE SR). Only data for the time period 07h00 to 17h00 are plotted. The X-axis shows the day of year (DOY) divided into fractions of time, e.g. 42.5 refers to DOY 42 at 12h00.

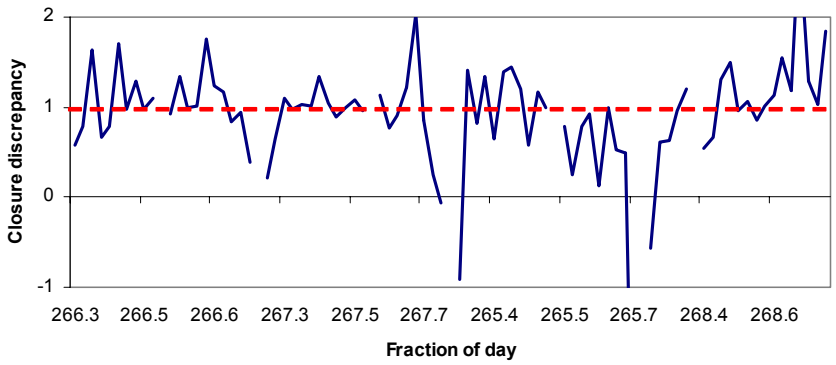

Figure 15 Closure discrepancy values estimated at the narrow plantation of *Podocarpus* trees as part of Case study 2, on sunny and partly cloudy days of the first field campaign (DOYs 265-268) using data from the In Situ Flux eddy covariance system. Only data for the time period 07h00 to 17h00 are plotted. The X-axis shows the day of year (DOY) divided into fractions of time, e.g. 266.5 refers to DOY 266 at 12h00.

During the last field campaign, the closure discrepancy values estimated again varied around 1, indicating that there were no major additional energy sources contributing to the available energy (**Fig. 16**). The sensible heat flux densities estimated (**Fig. 13c**) with the different systems, now installed to within 1 m of each other (**Table 4**) still showed similar diurnal variation to the previous field campaigns (**Fig. 13a & b**). Occasionally, as in the first campaign, the sensible heat flux densities estimated with the surface renewal system were much lower than the other estimates of *H* (e.g. DOY 238) (**Fig. 13c**). In contrast to differences in *H* observed in the previous field campaigns (**Fig. 13**), the *H* estimated with the eddy covariance systems (H IS and H RMY) now agreed very well (**Fig. 13c, 17**). This is also reflected in the good agreement of *LE* estimated by these two systems (LE IS, LE RMY) (**Fig. 14c**). The improved agreement in *H* and *LE* values from these two different eddy covariance systems can be directly related to the fact that the sonic anemometers were installed at similar heights (**Table 4**). In contrast, the direct estimate of latent flux density (LE IS EB) and the *LE* estimate with the surface renewal (LE SR) system still showed large diurnal variation and differences in the magnitude of the latent heat flux density (**Fig. 14c**), when compared to the indirect estimates of *LE* (LE IS, LE RMY).

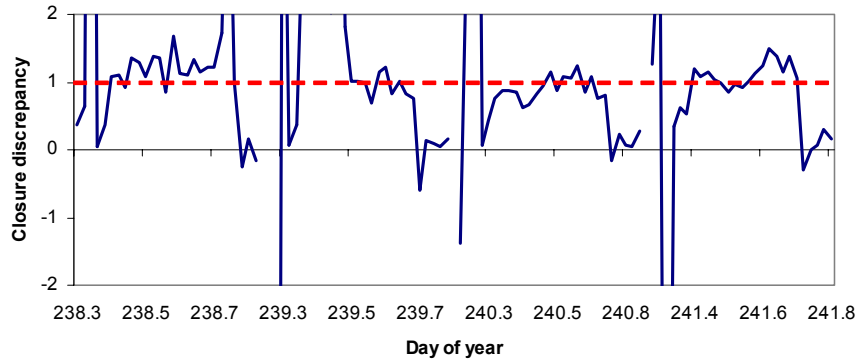

Figure 16 Closure discrepancy values estimated at the narrow plantation of *Podocarpus* trees as part of Case study 2, on sunny and partly cloudy days of the first third campaign (DOYs 238-241) using data from the In Situ Flux eddy covariance system. Only data for the time period 07h00 to 17h00 are plotted. The X-axis shows the day of year (DOY) divided into fractions of time, e.g. 238.5 refers to DOY 2238 at 12h00.

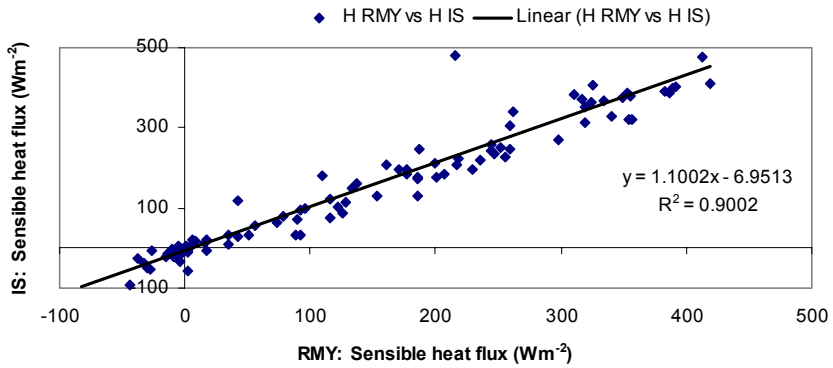

Figure 17 Sensible heat flux density estimated at the narrow plantation of *Podocarpus* trees as part of Case study 2, on sunny and partly cloudy days of the first third campaign (DOYs 238-241). Sensible heat flux densities estimated with the In Situ Flux systems eddy covariance system (Y-axis) are compared to sensible heat flux densities estimated with the RM Young eddy covariance system (X-axis) (H IS *vs* H RMY). Data shown are only for the time period 07h00 to 17h00.

4.2.3.4 Total evaporation

Daily rates of ET estimated with the eddy covariance, surface renewal and heat pulse velocity[8] systems showed great variation, especially during the first two field campaigns (**Table 5**). Generally, *LE* estimates agreed better on sunny days than on partly cloudy days. During the second field campaign (DOY 265-268), the accumulated ET differed by 35%. During this field campaign, wet and partly cloudy conditions prevailed. In all field campaigns, no technique consistently over- or underestimated ET.

Lowering the In Situ Flux eddy covariance sonic anemometer during the third field campaign improved the agreement of the indirect ET estimates using the two different eddy covariance systems (In situ EB and RMY) (**Table 5**). Over a four-day period the accumulated ET values for these two systems were within 8% of each other.

ET estimates over the three field campaigns (12 days) agreed to within 18% and ranged between 22 mm (direct estimate of ET with the In Situ Flux system) and 26 mm (surface renewal estimate) (**Table 5**). Average tree transpiration rates recorded using the HPV technique were generally less than 50% of the total evaporation rates measured with the micrometeorological techniques (**Table 5**).

4.2.4 Summary and conclusions

Large variations in estimates of latent heat flux density (i.e. ET), using different techniques, from a narrow strip of *Podocarpus* trees experiencing a range of climatic conditions (sunny, partly cloudy to rainy conditions), were found in this study.

[8] The heat pulse velocity system was used to estimate tree transpiration only. Transpiration values displayed in Table 5 represent the average transpiration rates of six sample trees, which were up-scaled to a unit surface. The transpiration values were up-scaled to total evaporation using a relationship of transpiration and total evaporation for the entire study period as described in Dye *et al*. (2007).

Indirect estimates of latent heat flux density (and ET) using two independent systems showed good agreement, but differed greatly from direct estimates of latent heat flux density during all three campaigns.

Table 5 Total evaporation (mm d^{-1}) estimated at a narrow plantation of *Podocarpus* trees as part of Case study 2. Total evaporation rates are displayed for sunny and partly cloudy days and were collected during three field campaigns (22-25 Sept.'05, 11-14 Feb.'06 and 26-29 Aug.'06). Total evaporation was estimated using different systems including two eddy covariance, a surface renewal system and a heat pulse velocity system. Transpiration rates (mm/d) were determined with the heat pulse velocity system and represent the average transpiration rate of six sample trees, scaled to a unit surface.

Year	DOY	Date	Total evaporation					Transpiration
			Eddy covariance (In situ)	Eddy covariance (In situ EB)	Eddy covariance (RMY)	Surface renewal	Heat pulse velocity	Heat pulse velocity
			mm d^{-1}	mm d^{-1}	mm d^{-1}	mm d^{-1}	mm d^{-1}	mm d^{-1}
2005	265	22-Sep-05	0.82	1.62	1.24	1.29	1.70	1.18
2005	266	23-Sep-05	1.65	1.21	0.93	1.80	1.00	1.75
2005	267	24-Sep-05	1.69	1.76	1.63	1.87	1.70	1.86
2005	268	25-Sep-05	2.25	1.79	1.76	1.92	1.76	1.84
SUM: DOY 265-268			6.41	6.38	5.56	6.89	6.16	6.63
2006	42	11-Feb-06	2.82	2.88	2.36	2.44	2.46	0.57
2006	43	12-Feb-06	1.55	4.01	2.94	3.25	3.07	0.50
2006	44	13-Feb-06	2.48	4.07	3.20	4.03	3.28	1.45
2006	45	14-Feb-06	1.15	1.52	1.17	1.10	1.40	0.21
SUM: DOY 42-45			8.00	12.48	9.67	10.82	10.22	2.73
2006	238	26-Aug-06	2.08	1.19	1.62	1.82	1.65	0.40
2006	239	27-Aug-06	1.55	1.07	1.07	1.83	1.11	0.32
2006	240	28-Aug-06	1.63	2.22	2.22	2.44	2.22	0.46
2006	241	29-Aug-06	2.33	2.05	2.16	2.20	2.25	0.42
SUM: DOY 238-241			7.59	6.53	7.08	8.29	7.24	1.60
Sum over entire period (DOY 265-268, 42-45, 238-241)			**22.00**	**25.39**	**22.31**	**26.00**	**23.62**	10.96
% total evaporation of In situ Eddy covariance total evaporation (entire period)			**1.00**	**1.15**	**1.01**	**1.18**	**1.07**	

4.3 Case study 3: "Orchard-like" canopy

4.3.1 Introduction

Many fruit and other trees (e.g. agroforestry species) are grown in an "orchard-like" layout. Initially, when the trees are young, the soil surface is not completely covered and soil evaporation contributes greatly to the total evaporation estimates. When the trees are young, fetch is generally not limiting (e.g. if tree heights are <1 m, and the distance from the leading edge is around 100 m). However, as the trees increase in size (height and leaf area), and depending on the management practices, the soil evaporation component can decrease significantly. For more mature trees, fetch will likely limit the application of some micrometeorological methods for estimating total evaporation.

Aims of case study:
- To determine the suitability of a range of micrometeorological techniques in estimating total evaporation from an orchard-like canopy/surface,
- Determine the impact of the height of sensors within the surface boundary layer on the total evaporation estimates.

4.3.2 Materials and methods

4.3.2.1 Site description

Field work was conducted at an agroforesty stand (29° 40' 10.7" S, 30° 24' 50.6" E, 781.5 m a.m.s.l.), with different *Jatropha* and *Kikuyu* treatments. Two research plots (plot 11 and 13) with *Jatropha* trees only, were used to study the suitability of a range of micrometeorological techniques to estimate total evaporation.

Jatropha trees were planted in plots of 0.125 ha (50 m x 25 m) in size. The total study area was 60 m x 50 m (inter plot length included). At the time of the study (6 to 20 March 2006), the trees had hardly any leaves as the leaves were severely damaged by insects (**Fig. 18**).

4.3.2.2 Techniques applied

In order to evaluate the effect of sensor installation height on energy flux estimates, sensors used to estimate total evaporation were installed at two "reference" heights within the surface boundary layer as part of Case study 3. An orchard-like surface was used. Fluxes estimated with the In Situ Flux systems and RM Young eddy covariance systems were compared against those estimated with the surface renewal systems. During the first part of the field campaign, the sensors were installed high above the vegetation (~ 2 m) and during the second part of the field campaign, at a lower height (~ 0.5 m above the vegetation), closer to the vegetation. The height of the In Situ Flux system was initially 2.75 m (sonic anemometer) and 3.6 m (infra-red gas analyser), where after the sensors were moved to 1.2 m (**Table 6**). The heights of the RM Young sonic anemometers were initially 3.75 and 1.68 m, where after the lower RM Young sensor was moved to 1.2 m, and the upper RM Young sensor was left at 3.75 m. The surface renewal sensors remained at the same heights throughout the measurement period - 1.2, 1.56, 2.2 and 3.72 m. Estimates of energy fluxes from different systems were compared for each of the "reference" heights - 3.75 and 1.2 m respectively.

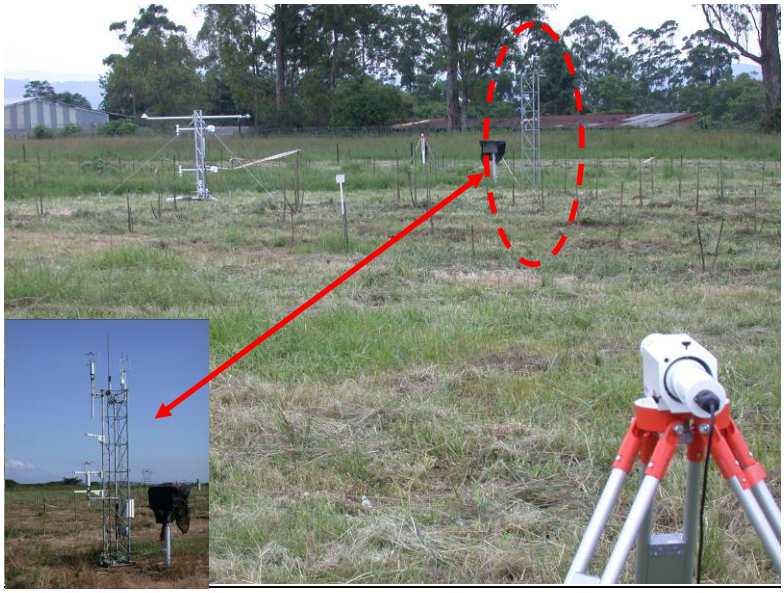

Figure 18 The orchard-like *Jatropha* research site (Ukulinga Research Farm, UKZN, Pietermaritzburg), with research mast and equipment used in Case study 3 to estimate total evaporation (insert). The *Jatropha* trees are barely visible. In the foreground (right hand corner) the surface layer scintillometer receiver sensor is seen, mounted on a tripod. (Note: The results from the surface layer scintillometer are not included in this report).

Table 6 Summary information on the techniques applied in Case study 3 at the orchard-like *Jatropha* site. Techniques applied include the In Situ Flux systems eddy covariance systems which provided direct and indirect estimates of latent heat flux density, an RM Young eddy covariance system, and a surface renewal system.

Techniques applied	**Eddy covariance (In Situ Flux system)**	**Eddy covariance (RM Young)**	**Surface renewal**
Abbreviation	**EC (with IRGA), ECEB (without IRGA)**	**RMY**	**SR**
Measurement period	06 to 13 March 2006: Field trip (upper height) 13 to 20 March 2006: Field trip (lower height)		
Data used in comparisons	Field trip (Upper): 9-10 March 2006 (Sunny and partly cloudy day respectively) Field trip (Lower): 14, 16 March 2006 (Sunny and partly cloudy day respectively)		
Output interval	30 min	2 min averaged to 30 min	2 min averaged to 30 min
Installation height/s	Field trip (upper): 2.75 m; 3.6 m (IRGA) Field trip (lower): 1.2 m	Field trip (upper): 3.75 and 1.68 m Field trip (lower): 3.75 and 1.2 m	Field trip: 1.2, 1.56, 2.2 and 3.72 m
Make and model of sensors (if applicable)	In Situ Flux with R3 Gill sonic anemometer, and Licor 7500 Infra-red gas analyzer	RM Young 8100 sonic anemometer	Chromal-constantan thermocouples
Complementing project	Everson et al. (2007)		
Additional	Net radiometer, REBS soil heat flux plates, Chromal-constantan thermocouples, Complete automatic weather station with Solarimeter, RM Young windsentry, Vaisala temperature and humidity sensor, Tipping bucket raingauge		

4.3.3 Results

Two sunny and two cloudy days were selected for detailed analysis. A set of days (one sunny and one cloudy day) was selected for the "upper reference" height data comparisons (9, 10 March 2006 - DOY 68, 29), and another set of days for the "lower reference" data comparisons (14, 16 March 2006 -DOY 73, 75).

4.3.3.1 *Climatic conditions*

Daily average air temperatures over the four days studied (DOY 68-69, 73 and 75) ranged between 19.59 and 22.06°C, with a maximum temperature of 31.8°C recorded on DOY 68. Over the corresponding period, the daily total solar radiation values ranged between 13.69 and 23.69 MJ m^{-2} (on DOY 75 and 73 respectively) (average = 18.54 MJ m^{-2}). During the first three days no rainfall was recorded, but on DOY 75, 17 mm of rainfall was recorded. Recorded wind speeds at the site were generally low (1.34 m s^{-1}).

4.3.3.2 *Net radiation and soil heat flux density*

The net irradiance (*Rn*) and soil heat flux density (G) measurements represent single point measurements. Care was taken during installation to position and orientate sensors such that *Rn* and *G* estimates should be representative of the research site. Net irradiance values at midday (on sunny days) were generally less than 600 W m^{-2} (**Fig. 19**). The soil heat flux density accounted for a large fraction of the net irradiance (up to 60% during mid-day) (**Fig. 19**). The high *G* values were expected at the time, as the plots studied consisted of a tree only treatment. Furthermore, the trees were severely damaged by insects prior to the measurements and as a result had lost nearly all their leaves, resulting in a high percentage of unshaded soil surface.

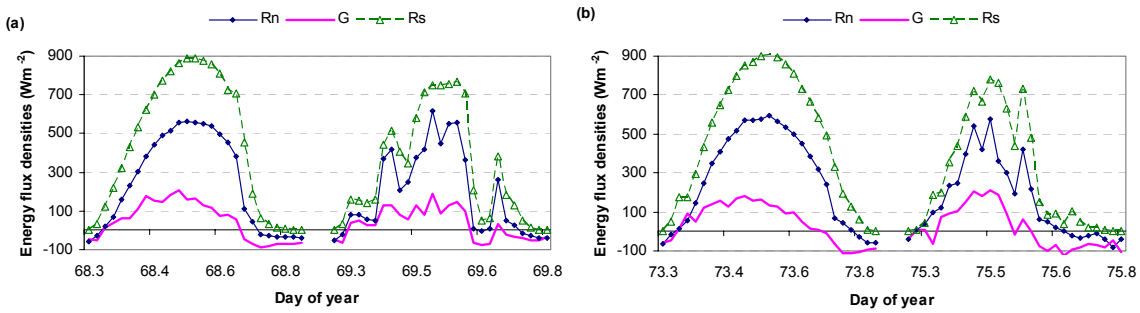

Figure 19 Net irradiance (*Rn*), soil heat flux density (G) and solar irradiance values estimated at the orchard-like *Jatropha* site as part of Case study 3. Data shown are for two sunny (DOYs 68, 73) and two cloudy/partly cloudy days (DOYs 69, 75). a - represents data from the upper reference height, whereas b represents data from the lower reference height. Only data for the time period 06h00 to 19h00 are plotted. The X-axis shows the day of year (DOY) divided into fractions of time, e.g. 69.5 refers to DOY 69 at 12h00.

4.3.3.3 *Sensible and latent heat flux density*

In Case study 3 the impact of sensor height on flux estimates was investigated. In the first part of the study (6 to 13 February 2006), sensors from the different systems were installed at a reference height (roughly 3.6 m), with some "control sensors" at a lower height (1.2 m) (**Table 6**). The reference height was considered as the correct/optimum height for sensor installation.

In the second part of the field campaign, the sensors were moved to a different "reference height" at 1.2 m, with some control sensors at roughly 3.6 m (**Table 6**). Energy fluxes from both partly cloudy/cloudy and sunny days are compared below.

4.3.3.3.1 Sensible heat flux density

In **Fig. 20 (a & b)** the sensible heat flux densities (H) measured with the two different eddy covariance systems (IS and RMY) and the surface renewal (SR) systems are shown. A top (approximately 3.6 m) and a bottom reference height (1.68 and 1.2 m for the RMY and SR respectively) were used in the comparison (**Fig. 20**). In **Fig. 20** (**c & d**) the sensible heat flux densities measured at a similar height (whether 3.6 or 1.2 m) are shown and the sensible heat flux densities measured at both reference heights, compared well. A few exceptions do exist, e.g. DOY 73. The similarities in the sensible heat flux estimates suggested that the different techniques do sample similar fluxes.

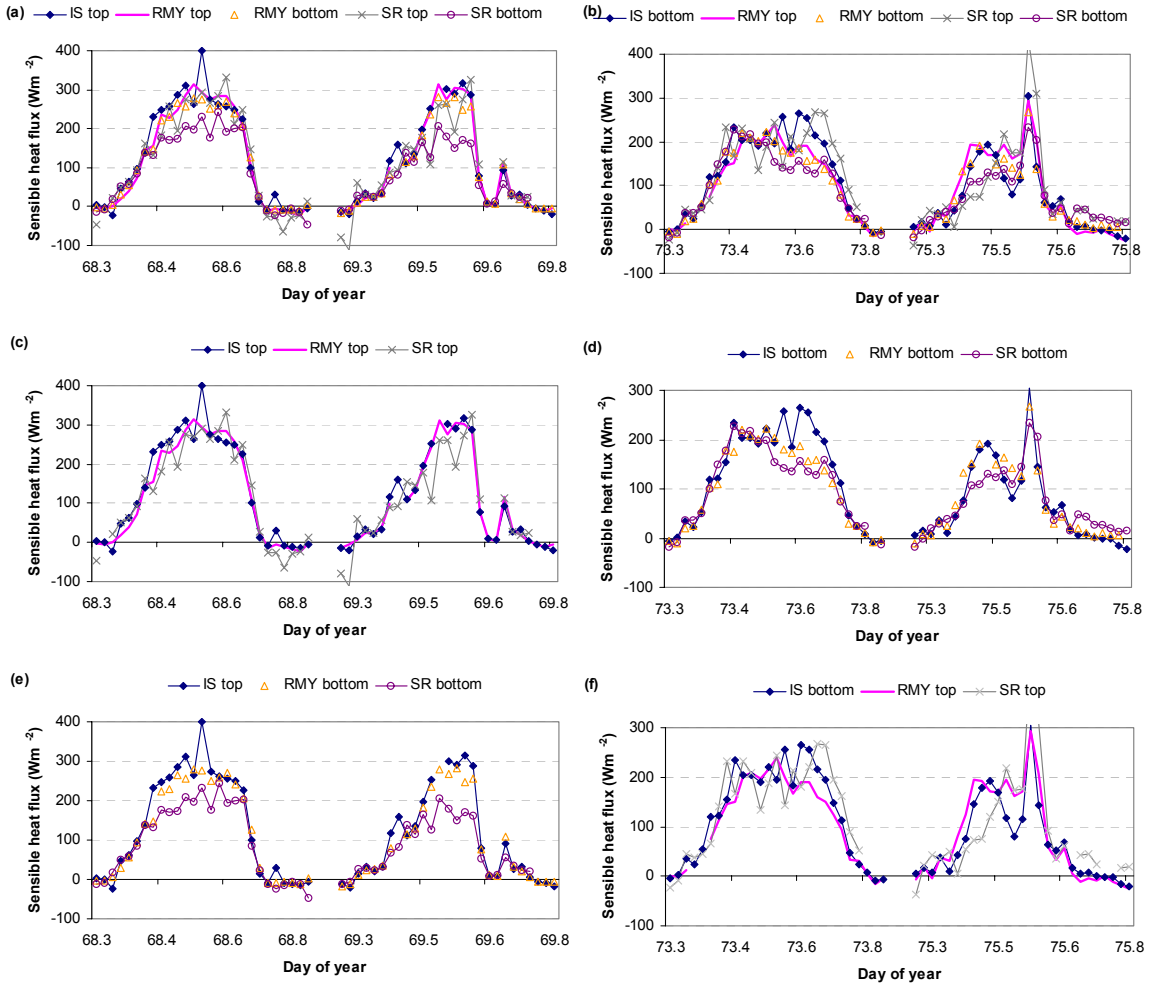

Figure 20 Sensible heat flux densities estimated at the orchard-like *Jatropha* site as part of Case study 3, using different techniques and with sensors installed at two reference heights. IS top refers to the In Situ Flux eddy covariance system installed at the top reference height (3.65 m), and RMY_top and _bottom refers to the RM Young sonic anemometers installed at top (3.75 m) and bottom levels (1.68 m), and SR_top and _bottom refers to thermocouples installed at two heights - 3.72 and 1.2 m above the soil. See Table 6 for more details. Data shown are for two sunny (DOYs 68, 73) and two cloudy/partly cloudy days (DOYs 69, 75). Only data for the time period 06h00 to 19h00 are plotted. The X-axis shows the day of year (DOY) divided into fractions of time, e.g. 69.5 refers to DOY 69 at 12h00.

In **Fig. 20e** the *H* values estimated with the In Situ Flux system at a height of 3.65 m, are compared with *H* values from the RMY and SR systems (1.68 m and 1.2 m respectively). The *H*'s of the two techniques based on high frequency windspeed measurements (IS and RMY) compared very well, and consistently exceeded the *H*'s of the SR technique which is based on high frequency temperature measurements. Note: The RMY and SR techniques were not installed at the same "lower" height.

Even smaller differences in *H* values were observed when In Situ Flux sensors were installed at 1.2 m and the RMY and SR at 3.75 and 3.72 m respectively (**Fig. 20f**). A few exceptions with larger differences in *H* existed, e.g. around DOY 75.5.

4.3.3.3.2 Latent heat flux density

In **Fig. 21** the latent heat flux densities estimated with different methods are shown. In **Fig. 21** (**a & b**) the *LE*s are compared for similar installation heights (3.65 m as top reference and 1.2 m as bottom reference). When the different systems were installed at a height of ≈ 3.65 m (canopy height about 1 m), the direct estimates of *LE* using the In Situ Flux eddy covariance system (IS top) (e.g. DOYs 68-69), with a few exceptions, consistently exceeded the *LE*s estimated with all the other techniques (**Fig. 21a**). In contrast, when all systems were installed lower (1.2 m above ground), the *LE*s of all the techniques agreed much better in their diurnal trends and in magnitude, see e.g. DOYs 73 (**Fig. 21b**). Changes in climatic conditions also seem to affect the magnitude of the *LE*s measured with the different systems, at the lower reference height. Bigger differences in the *LE*s using different techniques were evident on a partly cloudy day (DOY 75) than on a sunny day (DOY 73) (**Fig. 21b**).

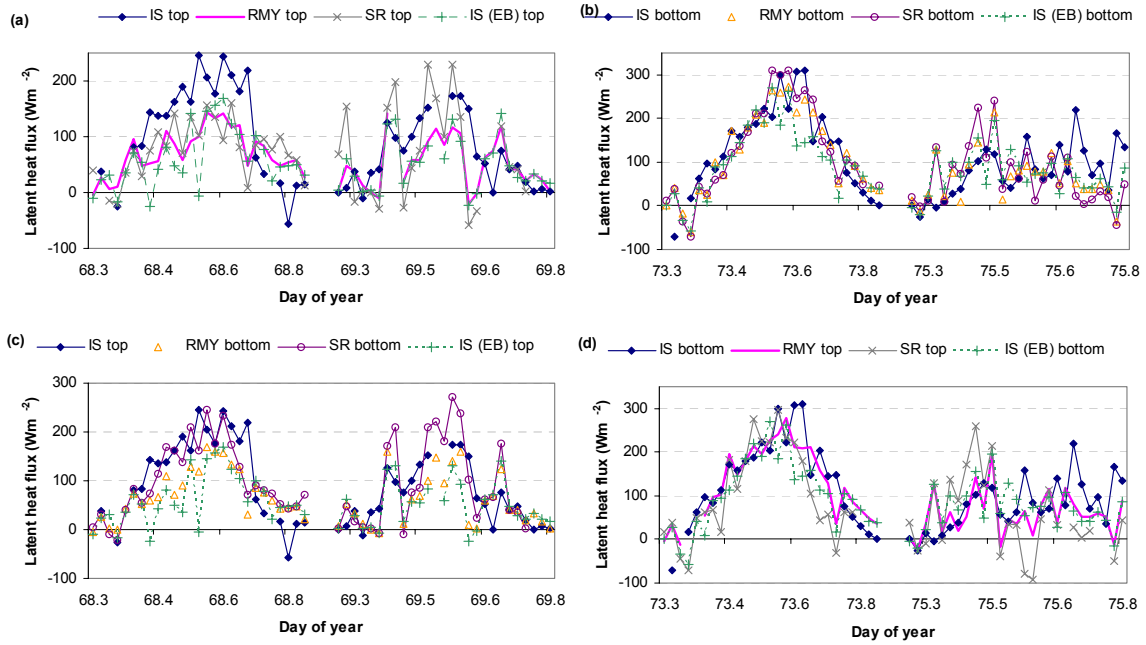

Figure 21 Latent heat flux densities (LE) estimated at the orchard-like Jatropha site as part of Case study 3, using different techniques and with sensors installed at two reference heights. IS top refers to the In Situ Flux eddy covariance system installed at the top reference height (3.65 m) which provided a direct estimate of LE. RMY_top and _bottom refers to the RM Young sonic anemometers installed at top (3.75 m) and bottom levels (1.68 m) and SR_top and _bottom refers to thermocouples installed at two heights - 3.72 and 1.2 m above the soil. See Table 6 for more details. IS (EB)_top and _bottom refers to the indirect estimate of LE using the In Situ Flux systems eddy covariance system. Data shown are for two sunny (DOYs 68, 73) and two cloudy/partly cloudy days (DOYs 69, 75). Only data for the time period 06h00 to 19h00 are plotted. The X-axis shows the day of year (DOY) divided into fractions of time, e.g. 69.5 refers to DOY 69 at 12h00.

When latent heat flux densities estimated with systems installed at different heights were compared, differences in the *LE*s were clear (**Fig. 21c & d**), both in terms of the diurnal pattern and in the magnitudes of the *LE*s. However, these differences in *LEs* were similar to those observed when the IS, RMY and SR systems were installed at the same height (**Fig. 21a & b**).

4.3.3.4 Bowen ratio and closure discrepancy

If the latent and sensible heat flux densities estimated with different techniques compare well, the β vales for different techniques for a given day, should also compare well. **Figure 22** (**a & b**) shows that for the two sunny days (DOYs 68 and 73), the β values for all three techniques (IS, RMY and SR), with the exception of RMY top on DOY 68, were very similar and ranged from 1.6 to 1.8. The β values estimated generally exceeded 1 and therefore that energy fluxes at the orchard-like *Jatropha* site were dominated by sensible heat flux densities and not by evaporative (latent heat) fluxes.

The β values estimated on partly cloudy days (DOY 69 and 75) were more variable than on sunny days (**Fig. 22a & b**). This greater variability in the β values is a result of greater fluctuations in the net radiation during partly cloudy days (**Fig. 19**).

The closure discrepancies estimated for the sunny days (DOY68 and 73) were consistently close to 1 (**Fig. 22c & d**), suggesting that the simplified energy balance does apply to this site under these conditions. Occasionally D was below 1. Even under conditions of varied cloudy cover, e.g. DOYs 96 and 75, the D values were very close to 1, suggesting again that the simplified energy balance applies to this site. A few exceptions (of individual 30 min periods where $D < 1$) are again shown in **Fig. 22** (**c & d**), but these only occurred in the early morning and late afternoon of DOYs 69 and 75, when the fluxes were very low.

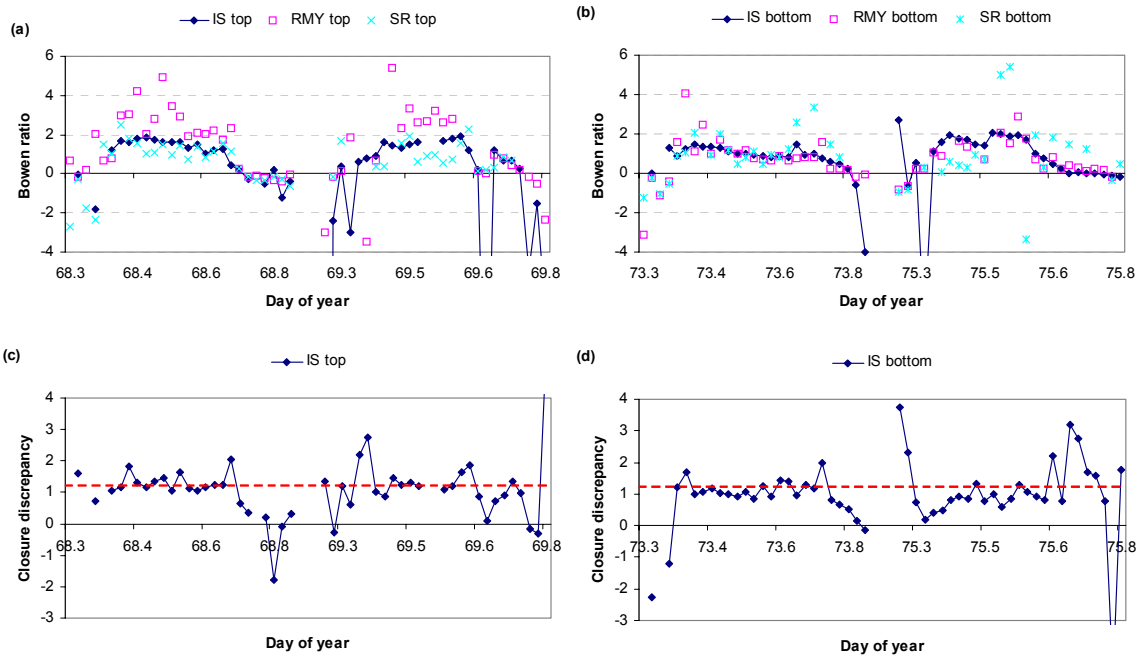

Figure 22 Bowen ratio values (a & b) and Closure discrepancy values (c & d) estimated at the orchard-like *Jatropha* site as part of Case study 3. IS top refers to the In Situ Flux eddy covariance system installed at the top reference height (3.65 m) , RMY_top and _bottom refers to the RM Young sonic anemometers installed at top (3.75 m) and bottom levels (1.68 m) and SR_top and _bottom refers to thermocouples installed at two heights - 3.72 and 1.2 m above the soil. See Table 6 for more details. Data shown are for two sunny (DOYs 68, 73) and two cloudy/partly cloudy days (DOYs 69, 75). Closure discrepancy values were estimated for the In Situ Flux system. Only data for the time period 06h00 to 19h00 are plotted. The X-axis shows the day of year (DOY) divided into fractions of time, e.g. 69.5 refers to DOY 69 at 12h00.

4.3.3.5 Total evaporation

ET estimated with the different micrometeorological systems generally showed good agreement (**Fig. 23**), whether at different or similar installation heights. Total evaporation estimates generally compared better when measurements took place close to the canopy (DOYs 73 and 75) (at a lower "reference height") (**Fig. 23b**), than from systems installed at a greater reference height. The latter *LEs* generally showed greater diurnal variation (e.g. DOY 68, 69) (**Fig. 23a**).

Daily total evaporation estimates were calculated for all the different systems. However, as a number of 30 min data points were "missing", the *daily* total evaporation estimates represents total evaporation for a period of less than a day (**Table 7**) (here after referred to as sub-daily estimates of ET). Differences existed in the sub-daily estimates of ET using the different systems. Generally the direct estimates of total evaporation using the In Situ Flux system (IS ET) exceeded the total evaporation from all other systems (**Table 7**) by up to 19% (11-19%). However, the total evaporation estimated with the surface renewal system installed at the lower reference height (SR bottom), always exceeded this direct estimate of ET by up to 7% (**Table 7**). Over the four-day period, the sub-daily estimates of total evaporation ranged between 4.67 and 6.07 mm (a variation of up to 25%) (**Table 7**). Total evaporation measured at the lower installation height (EC bottom, SR bottom) was generally greater than at the higher installation height (EC top, SR top) (**Table 7**).

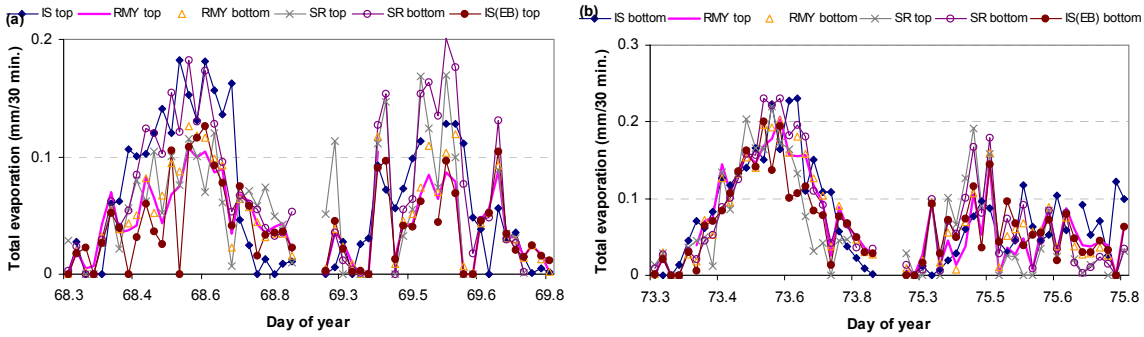

Figure 23 Total evaporation rates (mm/30 min) estimated at the orchard-like Jatropha site as part of Case study 3. IS top refers to the In Situ Flux eddy covariance system installed at the top reference height (3.65 m) which provided a direct estimate of total evaporation. RMY_top and _bottom refers to the RM Young sonic anemometers installed at top (3.75 m) and bottom levels (1.68 m) and SR_top and _bottom refers to thermocouples installed at two heights - 3.72 and 1.2 m above the soil. IS (EB) top and _bottom refers to indirect estimates of total evaporation using the In Situ Flux systems eddy covariance system. See Table 6 for more details. Data shown are for two sunny (DOYs 68, 73) and two cloudy/partly cloudy days (DOYs 69, 75). Only data for the time period 06h00 to 19h00 are plotted. The X-axis shows the day of year (DOY) divided into fractions of time, e.g. 69.5 refers to DOY 69 at 12h00.

Table 7 Sub-daily total evaporation rates (mm d^{-1}) and accumulated (sum) total evaporation over in four-day period (mm) estimated at the orchard-like *Jatropha* site as part of Case study 3. IS and IS (EB) refers to the direct and indirect estimates of ET using the In Situ Flux eddy covariance system. RMY_top and _bottom refers to the RM Young sonic anemometers installed at top (3.75 m) and bottom levels (1.68 m) and SR_top and _bottom refers to thermocouples installed at two heights - 3.72 and 1.2 m above the soil. Data shown are for two sunny (DOYs 68, 73) and two cloudy/partly cloudy days (DOYs 69, 75). On DOY 68-69, the systems were installed at the top reference height (3.65 m) and on DOY 73 and 75 at the bottom reference height (1.2 m above the soil surface). Sub-daily total evaporation estimates are also given as a percentage of the In Situ Flux ET estimates (%IS and %IS (EB)) respectively.

Year	DOY	IS	IS (EB)	RMY TOP	RMY BOTTOM	SR BOTTOM	SR TOP
		mm/period	mm/period	mm/period	mm/period	mm/period	mm/period
2006	68	1.73	1.18	1.24	1.30	1.79	1.30
2006	69	0.80	0.63	0.63	0.72	1.01	0.96
2006	73	2.36	1.94	2.26	2.27	2.34	1.93
2006	75	0.82	0.93	0.77	0.79	0.93	0.92
Sum (DOY 68-69, 73,75)		5.71	4.67	4.90	5.07	6.07	5.10
% IS		100.00	81.77	85.83	88.86	106.26	89.30
%IS (EB)		122.29	100.00	104.96	108.66	129.94	109.20

4.3.4 Summary and conclusions

Latent heat flux densities estimated with systems installed at different heights showed some differences in the magnitude of the fluxes and the diurnal patterns, but nonetheless compared favourably. These differences in *LE*s were similar to those observed when the different systems were installed at the same height.

Generally the direct estimates of total evaporation using the In Situ Flux system (IS ET) exceeded those from all other systems by up to 19%, except for the ET estimate with the SR system (bottom installation), which exceed the IS ET estimate by 7%. Over a four-day period, the sub-daily estimates of total evaporation varied by up to 25%.

4.4 Case study 4: Incomplete/open canopy: row crop

4.4.1 Introduction

Different types of agricultural row crops are cultivated in South Africa. In the early crop development stages, most of these crops have an open canopy (incomplete canopy cover). At these early stages soil evaporation can be a major component of the total evaporation from this surface. Certain crops like sugarcane are said to have a high water use. Because of its said high water use and economical importance, and in some areas its widespread occurrence, numerous studies have investigated the water use by sugarcane and the impact on streamflow in a catchment. A number of South African examples exist (Jarmain and Everson, 2002; Wiles *et al*., 2005; Olivier *et al*., 2006 and Bezuidenhout *et al*., 2006). An ongoing research project, funded by the Water Research Commission (K5/1577), and conducted by the South African Sugarcane Research Institute (SASRI) is aimed at investigating the water use efficiency (WUE) and yield of irrigated sugarcane under good agronomic practices. As part of this WUE project, total evaporation from a sugarcane field is measured using field scale lysimeters at the SASRI research farm in Pongola.

In this section we describe the results from a field campaign that was conducted at the Pongola research farm, where we investigated the suitability of a range of micrometeorological techniques to estimate energy fluxes and total evaporation (both spatially and at a single point in space). Total evaporation estimated with different micrometeorological techniques was also compared to that estimated with a field scale lysimeter.

Aims of case study:

- Determine the suitability of a range of micrometeorological techniques in estimating total evaporation from an open canopy,

-Compare total evaporation estimates with micrometeorological methods to that estimated with a field scale lysimeter.

4.4.2 Materials and methods

4.4.2.1 Site description

Total evaporation was estimated at a field of sugarcane with incomplete canopy cover using a range of techniques. Field work was conducted at the research station of the South African Sugarcane Research Institute (SASRI) situated in close proximity to the town of Pongola (27° 24'S; 31° 35'E, 308 m).

A field of sugarcane mulched with waste sugarcane tops (tops treatment) of size 18 m x 240 m was used in the experiment. Micrometeorological equipment was installed on block 319 (18 m x 240 m). Total evaporation estimated with the "tops lysimeter" (block 318) was compared to the total evaporation estimated with the micrometeorological techniques. **Figure 24** shows the trial layout of the WUE experiment.

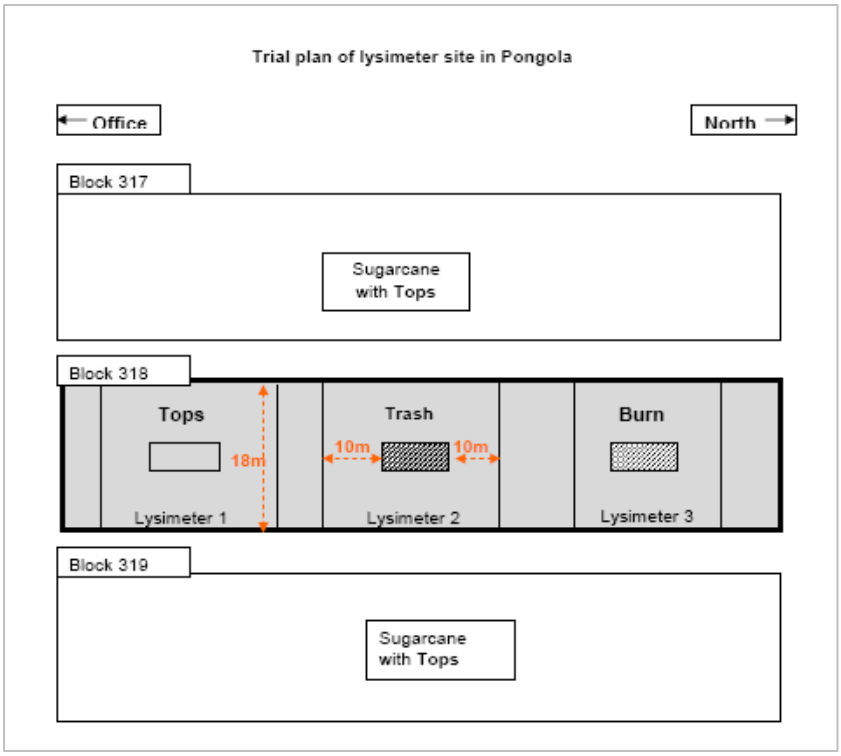

Figure 24 Trial plan of the sugarcane water use efficiency experiment conducted at the SASRI research station at Pongola (Oliver *et al*., 2006). To complement this work, Case study 4 was conducted at this site. Micrometeorological instrumentation was installed in Block 319. Total evaporation of this sugarcane block with an open canopy was compared to that estimated with the tops lysimeter (Lysimeter 1). Additional information: Block 317, 318 and 319 are each 18 m wide and 240 m long. These are separated by a 5 m path. Each lysimeters is 2.44 m long, 1.52 m wide and 1.22 m deep. The surrounding areas are also covered with tops (lysimeter 1) and trash (lysimeter 2).

The sugarcane cultivar N14 was planted on 24 April 2004 in rows 1.4 m apart in a Hutton soil with 30% clay. The crop is harvested annually at the age of 12 months. Evaporation measurements were conducted in the third ratoon crop, when the sugarcane was five months old (October 2007). The canopy cover was incomplete (25%) at the time of measurements, and the average canopy height was approximately 0.4 to 0.6 m.

4.4.2.2 Techniques applied

Table 8 gives a summary of the techniques used to estimate total evaporation from an incomplete sugarcane row crop over a four-day period (2 to 5 October 2007). The sugarcane research site with equipment installed is shown in **Fig. 25**.

Techniques used in this comparison included the Applied Technologies Inc. open path eddy covariance system (ATI), the surface renewal technique (SR) system, the surface layer scintillometer (SLS), the infra-red method (IR) and the lysimeter method (L). The ATI modified eddy covariance system was installed at a height of 2.1 m, and the RM Young sonic anemometer (as part of an eddy covariance system) at 1.57 m (**Table 8**). Thermocouples, as part of the surface renewal technique,

were installed at four different heights above the soil: 0.8, 1.2, 1.65, 2.2 m (**Table 8**). Average surface renewal fluxes and total evaporation rates (averaged for four heights) were used in the comparisons. The average weighted height of the dual laser beam of the surface layer scintillometer was 1.1 m above the canopy. Two Apogee infra-red temperature sensors were installed above the sugarcane at a 45° angle aimed at the canopy cover. Net irradiance and soil heat flux density estimates required by all the techniques, are based on single point measurements.

Lysimeter mass changes were detected electronically with load cells (Route Calibration Services), which were connected to a CR10X datalogger (Campbell Scientific Inc.). The lysimeter mass changes were measured at 15 min intervals at a resolution of 0.83 mm. A tipping bucket rain gauge (Texas Instruments) measured deep drainage under the lysimeter also at 15 min intervals. Daily total evaporation for the lysimeter was calculated using these mass change and drainage estimates, as well as daily rainfall estimates recorded at a nearby weather station (± 200 m).

The lysimeter is normally irrigated according to demand on reaching a deficit of 20 mm as indicated by the lysimeter readings. A watering can is used to apply exact irrigation amounts and to mimic an overhead irrigation system. The sugarcane fields surrounding the lysimeters were irrigated with a drip irrigation system according to the Canesim program (Singels *et al*., 1998) using weather data obtained from an on site automatic weather station. No irrigation was applied during the measurement period.

Table 8 Summary information on the techniques applied in Case study 4 at the open canopy sugarcane row crop. Techniques applied include the Applied Technologies Inc. eddy covariance system (ATI), the RM Young eddy covariance system (RMY), the surface renewal system (SR) and the Surface layer scintillometer (SLS). Data were also collected with the Infra-red method, but are not shown here.

Techniques applied	**Eddy covariance (ATI modified to IS system)**	**Eddy covariance (RM Young)**	**Surface renewal**	**Surface layer scintillometer**	**Infra-red**	**Lysimetry**
Abbreviation	EC and EC EB	RMY	SR	SLS	**IR**	Lys
Measurement period	2 October 2007- 5 October 2007					Long-term measurements (including 2 to 5 October 2007)
Sampling type	Point measurement	Point measurement	Point measurement	Spatial measurement (areal average)	**Point measurement**	Spatial measurement
Output interval	30 min	2 min averaged to 30 min	2 min averaged to 30 min	2 min averaged to 30 min	**2 min averaged to 30 min**	15 min summed to daily
Installation height/s	2.1 m (Sonic and IRGA)	1.57 m	0.8, 1.2, 1.65, 2.2 m (use average values)	1.1 m (average path height)	**1 m**	Installation depth 1.22 m
More information				Path length between sensors 100m Data loss due to power failures on site	**Data not shown**	
Make and model of sensors (if applicable)	In Situ Flux with R3 Gill sonic anemometer, and Licor 7500 Infra-red gas analyser	RM Young sonic anemometer	Chromal-constantan thermocouples	Scintec dual beam laser scintillometer	**Apogee**	Load cells (Route Calibration Services)
Data used in comparisons	2 October 2007- 5 October 2007					2 October 2007- 5 October 2007
Additional measurements	Net radiometer, REBS soil heat flux plates, Chromal-constantan thermocouples, Complete automatic weather station with Solarimeter, RM Young windsentry, Vaisala Temperature and Humidity sensor, Tipping bucket raingauge					

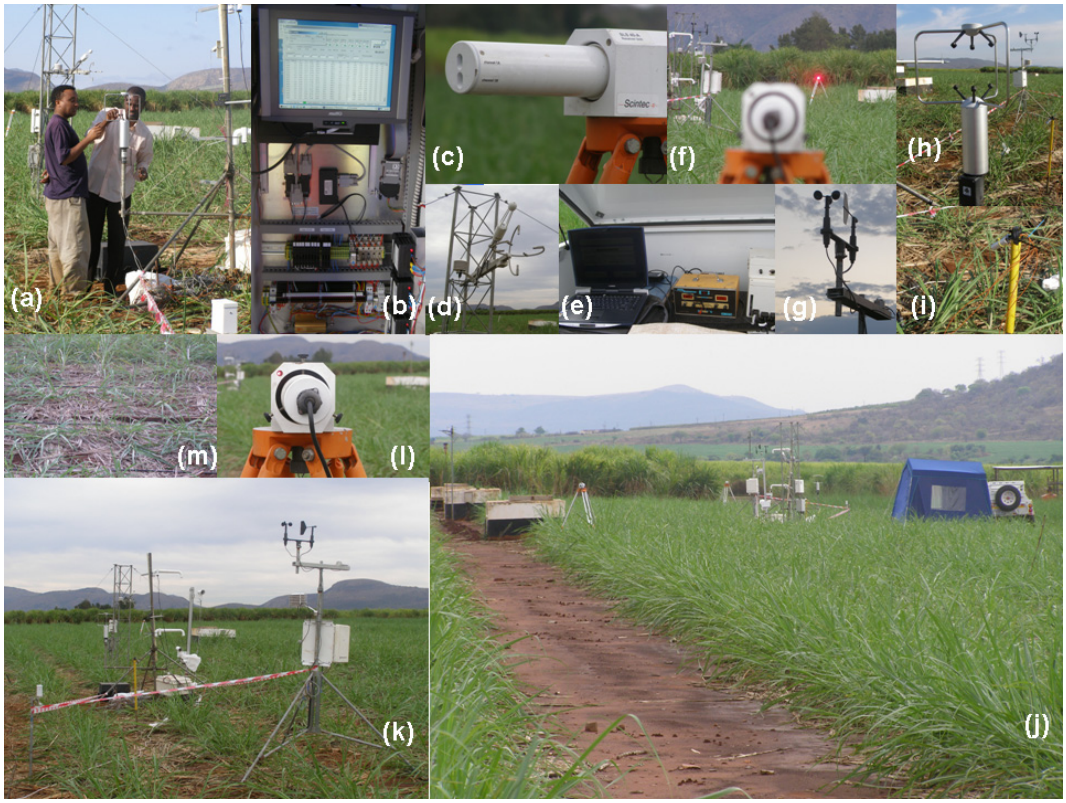

Figure 25 Equipment for the estimation of total evaporation installed at a sugarcane site with incomplete canopy cover. (a) Students Michael Mengistu and Nile Eltayeb tend to the RM Young sonic anemometer; (b) The ATI modified eddy covariance controlling and processing system; (c) Scintec scintillometer transmitter unit; (d) An ATI modified eddy covariance system consisting of an infra-red gas analyser and sonic anemometer installed onto a lattice mast in the sugarcane field; (e) Laptop computer, power regulating system and signal processing unit controlling measurements with the Scintec scintillometer; (f) Background - Red laser beam as transmitted by the scintillometer; (g) RM Young Windsentry consisting of a wind speed and direction sensor as part of the automatic weather station installed at the site; (h) RM Young sonic anemometer; (i) Apogee Infra-red sensor installed above sugarcane; (j) All equipment installed at sugarcane Block 19 – to the left is the entrances to the lysimeters; (k) Three masts with equipment installed at the sugarcane site – in the foreground the automatic weather station, towards the back the mast with the RM Young sonic and the Bowen ratio arms and at the back the lattice mast with the ATI eddy covariance system; (l) the receiver sensor of the scintillometer with the red beam visible thought the eye and (m) the top/edge of the lysimeter installed in the sugarcane field with tops treatment.

4.4.3 Results

Energy fluxes and total evaporation from a sugarcane field, estimated with different systems, are compared over a four-day period (2 to 5 October 2007 - DOYs 275 to 278). Only data for the period 08h00 to 17h00 are shown.

4.4.3.1 Climatic conditions

Daily average air temperatures ranged between 22.48 and 25.57°C over the four day studied (DOY 275-278). The maximum air temperatures were recorded on DOY 276 (35.94°C). Solar radiation was generally less than 16 MJ m^{-2}. The maximum windspeed was 3.51 m s^{-1}. A significant amount of rainfall was recorded on the first two days of measurement, with 23 mm on DOY 274 and 68 mm on DOY 275 (totalling 91 mm).

4.4.3.2 Net irradiance and soil heat flux density

Partly cloudy conditions were experienced during the entire period of measurements at the sugarcane research site. Climatic conditions improved (temperatures and solar irradiances increased) towards the end of the measurement period. Changes in cloud cover during the day are reflected in the variability of net irradiances (**Fig. 26**). Under fairly sunny conditions (e.g. DOY 277, 278) maximum mid-day net irradiance values exceeded 600 W m^{-2}.

Although the sugarcane canopy had an incomplete canopy cover (25%), the soil heat flux density during daytime was generally low (< 39 W m^{-2}) (**Fig. 26**) and accounted for less than 15% of the net irradiance. The relatively low soil heat flux density values are attributed to the heavy tops treatment (cover) at the site. Heat storage within this "tops layer" could possibly have been an additional heat source which was not estimated during this experiment.

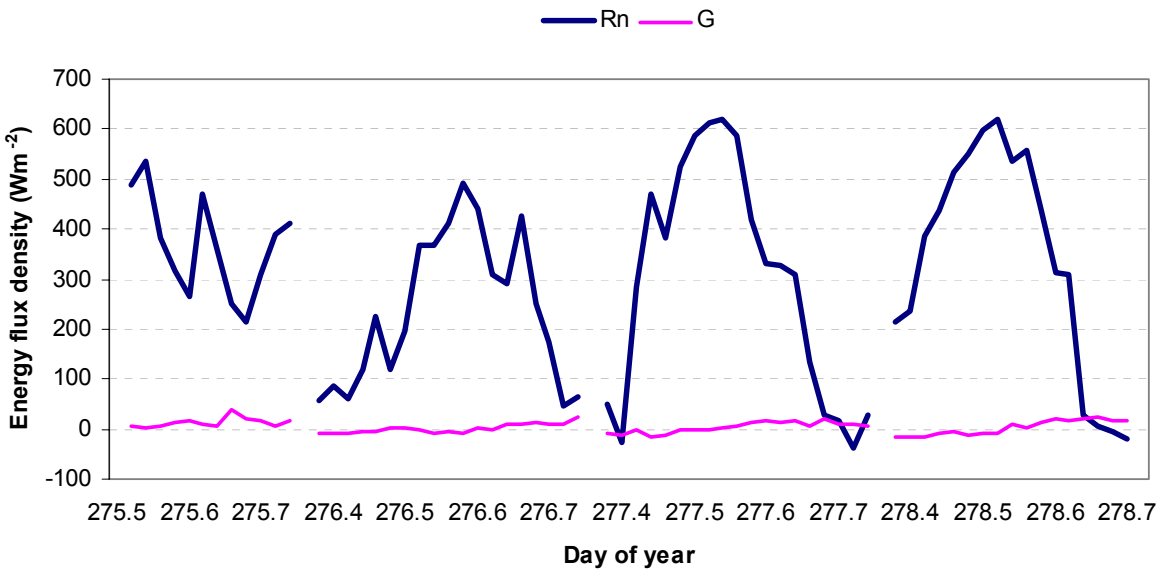

Figure 26 Net irradiances (*Rn*) and soil heat flux densities (G) estimated at a sugarcane site with incomplete canopy cover over a four-day period (DOY 275-278). Only data for the time period 08h00 to 17h00 are shown. The X-axis shows the day of year (DOY) divided into fractions of time, e.g. 275.5 refers to DOY 275 at 12h00.

4.4.3.3 Sensible heat flux density

Despite slight differences in installation heights of the different systems used to estimate total evaporation (**Table 8**), the sensible heat flux densities (H) estimated with the different micrometeorological techniques compared very well (**Fig. 27**). Diurnal variations in *H* (**Fig. 27**) tracked the changes in net irradiance (**Fig. 26**) due to changes in cloud cover. On a very cloudy day (e.g. DOY 276) the *H* values estimated with the four techniques were small (instantaneous daytime < 250 W m^{-2}), but compared well (**Fig. 26**). On more sunny days (DOY 277, 278), bigger differences were observed in the *H* values estimated with the different systems, with the *H* values estimated with the ATI system differing most from the other systems (RMY, SR and SLS) (**Fig. 26**). The *H* values estimated with the ATI system did not consistently over- or underestimate *H* - on DOY 277 the *H* values were underestimated compared to other techniques, whilst on DOY 278 the *H* values observed

during mid-day were overestimated compared to the other techniques (**Fig. 26**). The differences in the sensible heat flux densities might be the result of slight differences in installation height of the different sensors and therefore slightly different fluxes sensed by the different systems.

Point-based estimates of *H* (with the ATI, RMY and SR systems) compared remarkably well with areally-averaged (spatial) estimates of *H* (with the SLS system) (**Fig. 28**). A scatter plot of *H* values estimated with the surface layer scintillometer showed that SLS estimates were slightly lower compared to the other three methods – and up to 30% lower when compared to the ATI H estimates. However, small differences existed between the SLS, RMY and SR estimates of *H* which differed by about 15% ($R^2 > 0.83$) (**Fig. 28**).

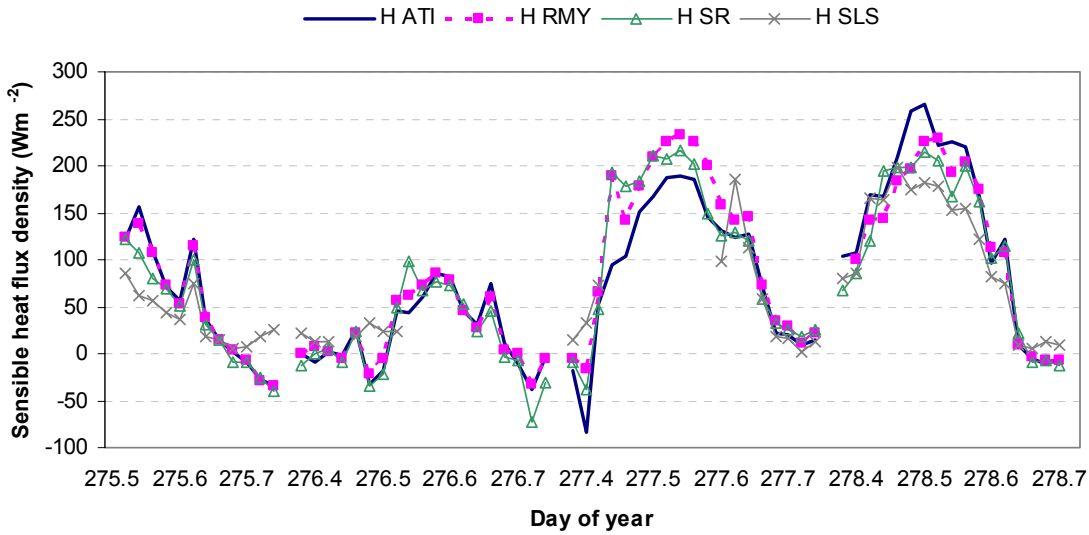

Figure 27 Sensible heat flux density estimated at a sugarcane site with incomplete canopy cover over a four-day period (DOY 275-278). Sensible heat flux density was estimated with the eddy covariance system (H ATI), the RM Young eddy covariance system (H RMY), the surface renewal system (H SR) and the surface layer scintillometer (H SLS). Only data for the time period 08h00 to 17h00 are shown. The X-axis shows the day of year (DOY) divided into fractions of time, e.g. 275.5 refers to DOY 275 at 12h00.

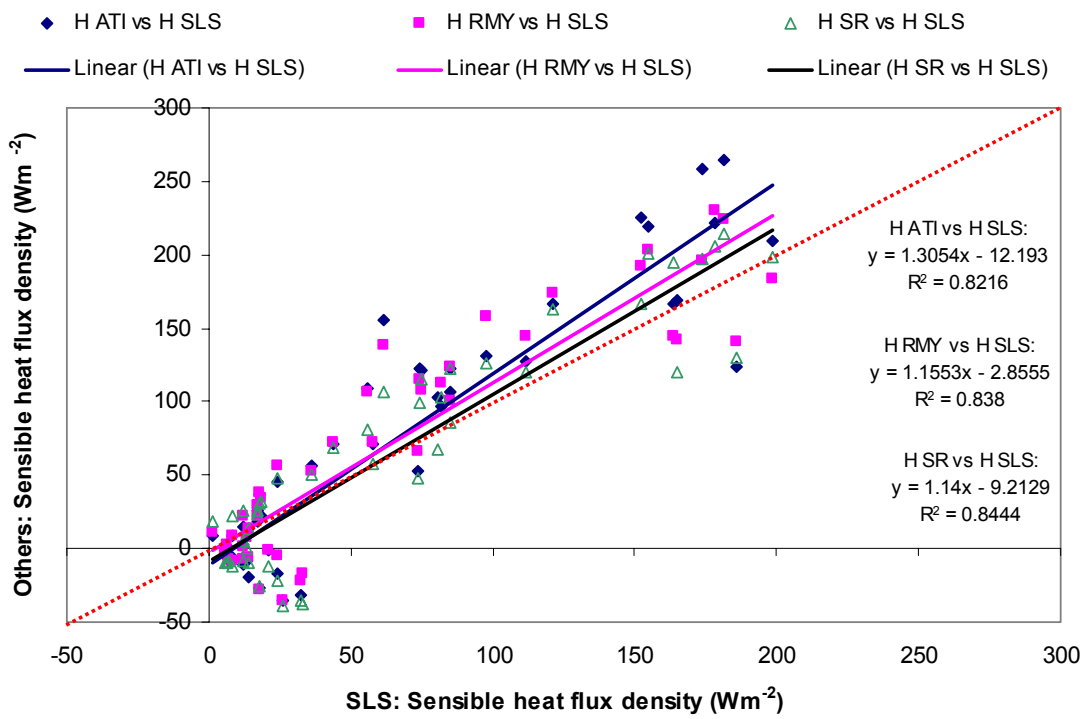

Figure 28 Sensible heat flux density estimated at a sugarcane site with incomplete canopy cover over a four-day period (DOY 275-278). On the X-axis is the sensible heat flux density estimated with the SLS, and on the Y-axis the sensible heat flux density estimated with the other systems – ATI eddy covariance, RM Young eddy covariance system and the surface renewal system (SR).

4.4.3.4 Latent heat flux density

The infra-red gas analyser (part of the ATI system) was malfunctioning during the course of this field campaign, and the latent heat flux density data therefore collected with this system, will not be shown. As the estimates of latent heat flux density (*LE*) (**Fig. 29**) of the RM Young, SR and SLS systems were all based on the simplified energy balance equation and therefore used estimates of sensible heat flux density (shown in **Fig. 27**). The *LE*s calculated using the simplified energy balance compared very well (**Fig. 29**) and reflected the good comparisons of the *H* values (**Fig. 27, 28**)

Areally-averaged estimates of *LE* (LE SLS) compared well with point-based estimates of *LE* using the eddy covariance (LE ATI EB, LE RMY) and surface renewal methods (LE SR) (**Fig. 30**). Latent heat flux densities estimated with the different methods were within 16% of each other ($R^2 > 0.93$) (**Fig. 30**). The *LE* values corresponded well despite highly variable net irradiances, and the fact that the different sensors were installed at slightly different positions in the sugarcane field.

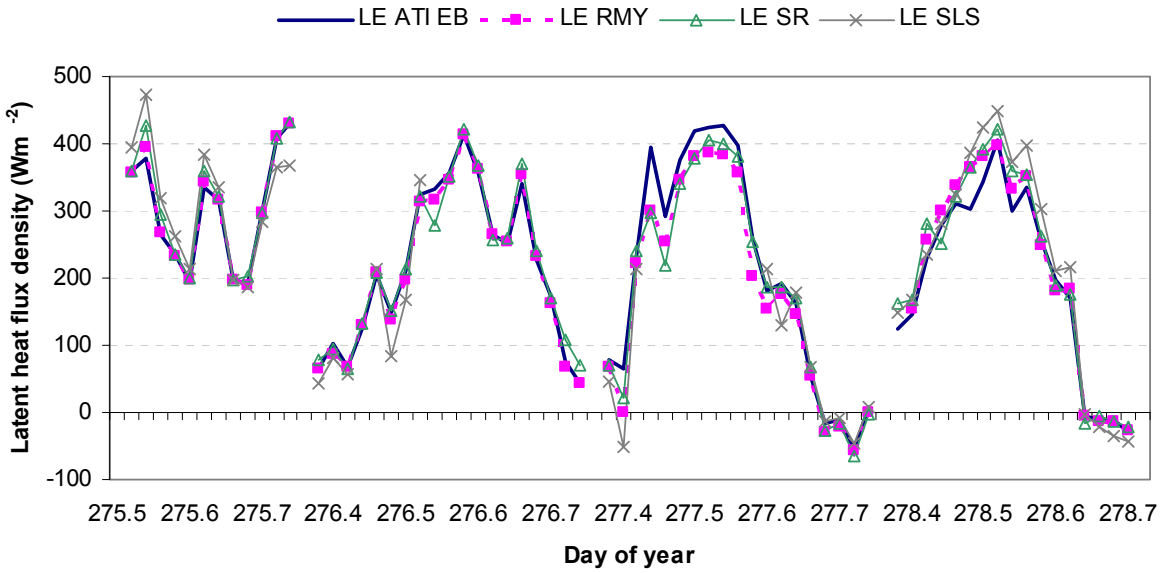

Figure 29 Latent heat flux density estimated at a sugarcane site with incomplete canopy cover over a four-day period (DOY 275-278). Latent heat flux density was estimated with the eddy covariance system (LE ATI EB) (indirect), the RM Young eddy covariance system (LE RMY), the surface renewal system (LE SR) and the surface layer scintillometer (LE SLS). Only data for the time period 08h00 to 17h00 are shown. The X-axis shows the day of year (DOY) divided into fractions of time, e.g. 275.5 refers to DOY 275 at 12h00.

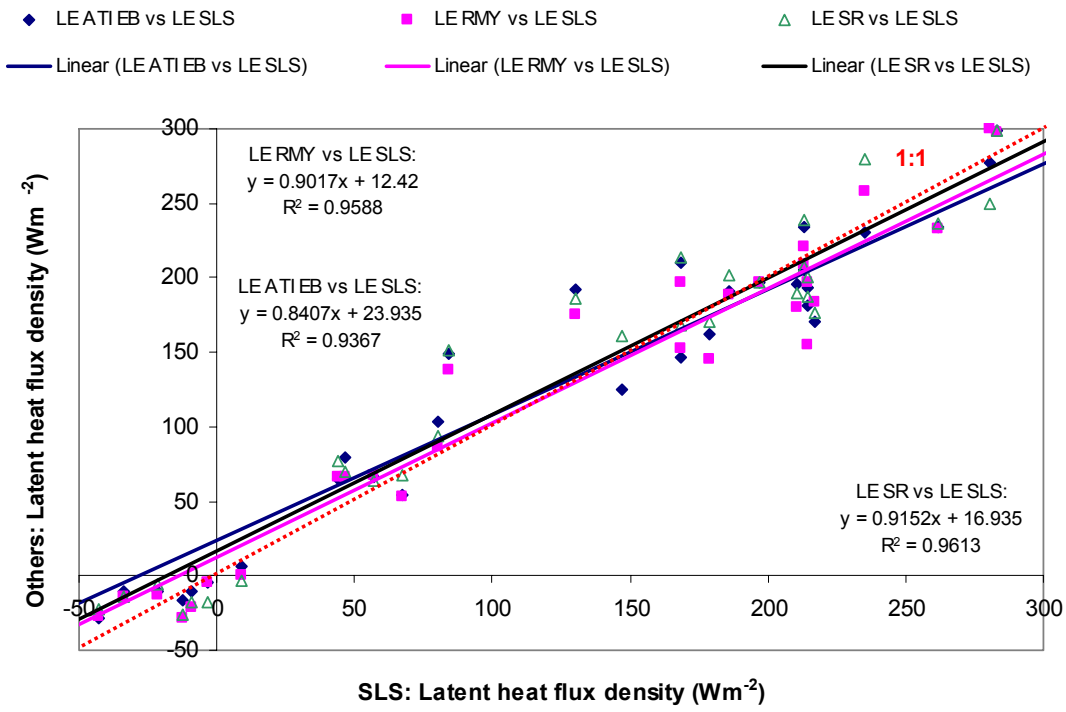

Figure 30 Latent heat flux density estimated at a sugarcane site with incomplete canopy cover over a four-day period (DOY 275-278). On the X-axis is the latent heat flux density estimated with the SLS method, and on the Y-axis the sensible heat flux density estimated with the other systems – ATI eddy covariance, RM Young eddy covariance system and the surface renewal system (SR).

4.4.3.5 Components of the energy balance of an open canopy

The components of the simplified energy balance estimated for a sugarcane field with incomplete canopy cover are shown **Fig. 31**. The soil heat flux, sensible and latent heat flux densities follow the diurnal variation in the net irradiance. Maximum mid-day net irradiances exceed 600 W m^{-2}, but soil heat flux densities remained very low (< 35 W m^{-2}). The latent heat flux densities dominated over the sensible heat flux density with mid-day *LE* values exceeding *H* values by up to 40% (160 W m^{-2}) (**Fig. 31**). This was expected since energy was available to drive transpiration, and soil moisture was available to the plants following the large rainfall events. Latent heat flux densities decreased rapidly in the afternoon, so that the *H* and *LE* values were similar, and remained that way until sunset (**Fig. 31**).

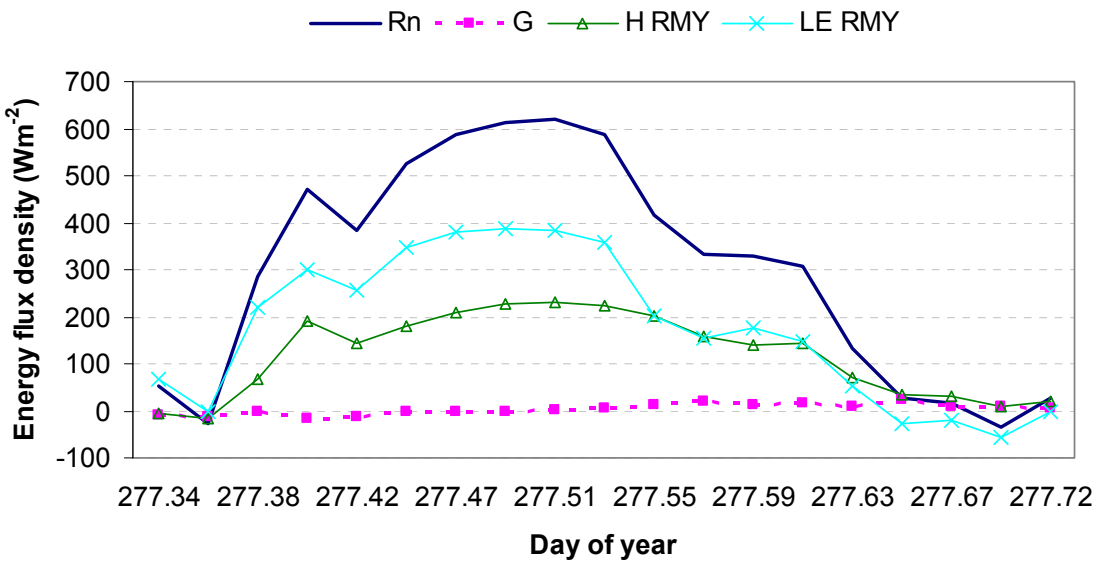

Figure 31 Energy balance components at a sugarcane site with incomplete canopy cover on 4 October 2007 (DOY 277). *Rn* refers to the net irradiance, *G* to the soil heat flux density and H RMY and LE RMY to the sensible and latent heat flux densities estimated with the RM Young eddy covariance system.

4.4.3.6 Total evaporation

4.4.3.6.1 Sub-hourly comparison

The diurnal trends in total evaporation (ET) (**Fig. 32**) estimated with the different techniques, directly reflected the latent heat flux densities estimated. Spatially averaged (ET SLS) and point-based estimates of total evaporation (ET ATI EB, ET RMY, ET SR) agreed to within 16%, with R^2 values exceeding 0.93 (**Fig. 33**). Mid-day maximum ET of up to 0.35 mm/30 min was estimated (**Fig. 32**).

4.4.3.6.2 Daily comparison

Total evaporation (ET) estimated with the micrometeorological methods and the lysimeter could only be compared at a daily time interval, as sub-daily total evaporation rates were not calculated for the lysimeter. Total evaporation estimated following a heavy rainfall event (91 mm) (e.g. DOY 274, 275), was excluded from the comparison. At the time the lysimeter was partially waterlogged, and total evaporation estimates from this system wound not have been realistic (**Table 9**).

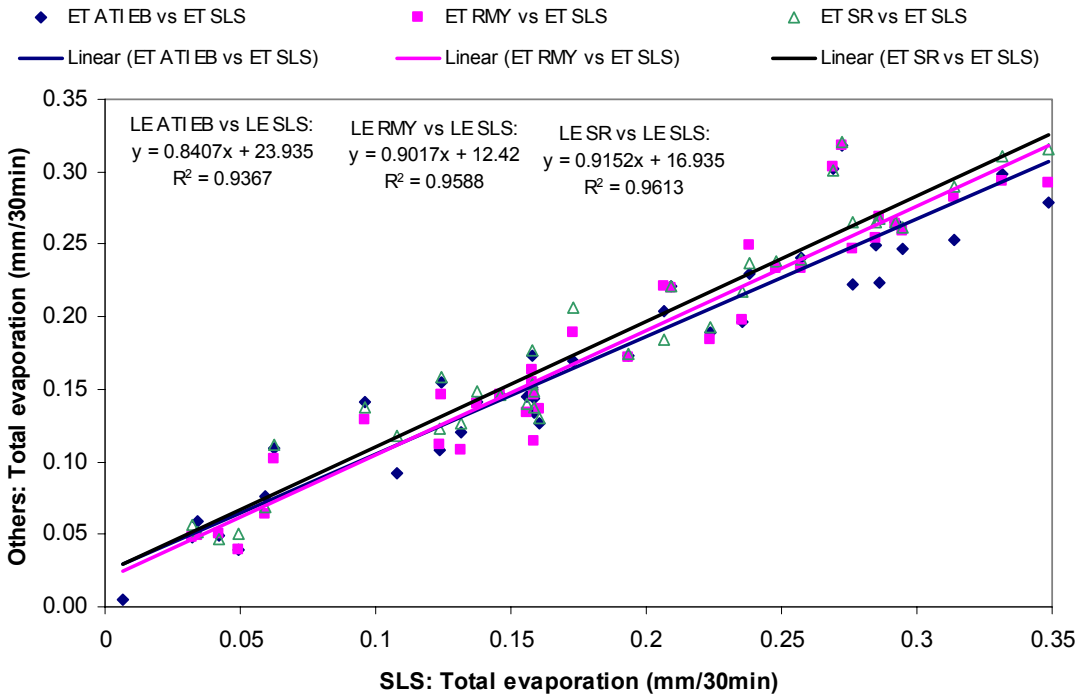

Figure 32 Total evaporation (mm/30 min) estimated at a sugarcane site with incomplete canopy cover over a four-day period (DOY 275-278). ET was estimated with the eddy covariance system (ET ATI EB) (indirect), the RM Young eddy covariance system (ET RMY), the surface renewal system (ET SR) and the surface layer scintillometer (ET SLS). Only data for the time period 08h00 to 17h00 are shown. The X-axis shows the day of year (DOY) divided into fractions of time, e.g. 275.5 refers to DOY 275 at 12h00.

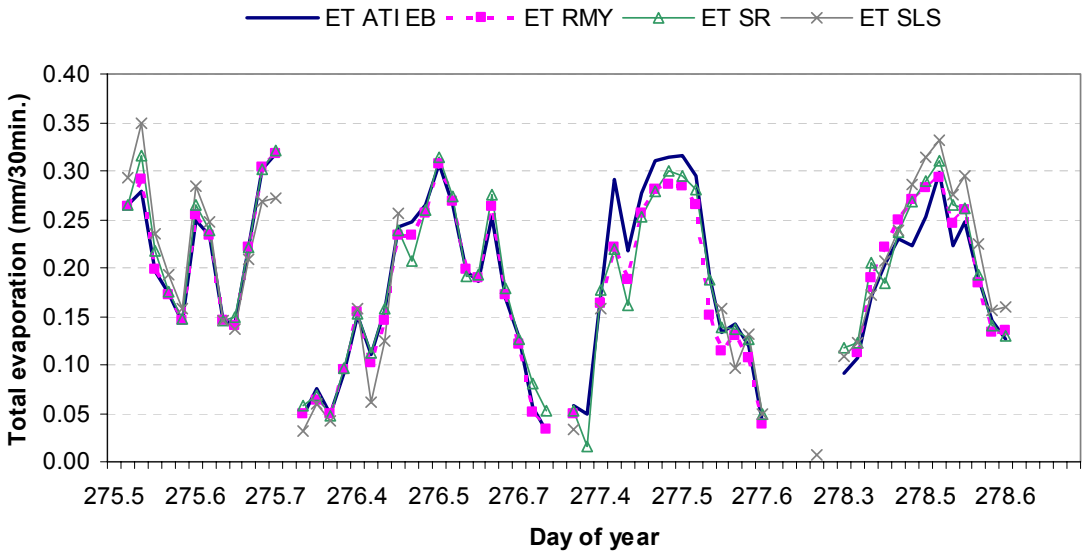

Figure 33 Total evaporation (mm/30 min) estimated at a sugarcane site with incomplete canopy cover over a four-day period (DOY 275-278). On the X-axis is the latent heat flux density estimated with the SLS method, and on the Y-axis the sensible heat flux density estimated with the other systems – ATI eddy covariance, RM Young eddy covariance system and the surface renewal system (SR).

Table 9 Daily total evaporation estimated for a sugarcane field as part of Case study 4. Total evaporation was estimated with two eddy covariance systems (ET ATI EB, ET RMY), a surface renewal system (ET SR) and a surface layer scintillometry (ET SLS) over the period 2 to 5 October 2007. Total evaporation estimates using the lysimeter are also shown.

Date	DOY	ET ATI EB	ET RMY	ET SR	ET SLS	ET Lysimeter
		mm/d	mm/d	mm/d	mm/d	mm/d
02-Oct-07	275	Incomplete dataset	Incomplete dataset	Incomplete dataset	Incomplete dataset	Data excluded
03-Oct-07	276	3.08	3.04	**3.23**	Incomplete dataset	1.19
04-Oct-07	277	3.07	2.65	2.80	Incomplete dataset	2.22
05-Oct-07	278	**2.58**	2.65	2.79	2.89	1.42
Total (DOY 275-278)		**8.72 mm**	**8.33 mm**	**8.82 mm**	**Incomplete**	**4.82 mm**

Daily estimates of ET using micrometeorological techniques (ET ATI EB, ET RMY, ET SR, ET SLS) compared well – to within 0.42 mm d^{-1}, for all days with complete data sets (**Table 9**). Days with incomplete data sets were excluded from the comparison. Total evaporation from a wet sugarcane canopy with incomplete canopy cover and following 91 mm of rainfall, ranged between 2.58 mm d^{-1} (DOY 278) and 3.23 mm d^{-1} (DOY 276) on partly cloudy days (**Table 9**). Total evaporation estimated with the field scale lysimeter was generally less, up to 2.04 mm d^{-1} (DOY 276), when compared with the other methods (ET ATI EB, ET RMY, ET SR, ET SLS) (**Table 9**). Following the 91 mm of rainfall, the lysimeter would have been partially waterlogged and the sugarcane plants would respond to these conditions through reduced transpiration. This is reflected in the lower total evaporation rates calculated for the lysimeter, when compared to the micrometeorological total evaporation estimates.

Over a period of three days (DOY 276-178), the accumulated ET estimated with the different micrometeorological systems (ET ATI EB, ET RMY, ET SR, ET SLS) were within 0.49 mm of each other (**Table 9**). The accumulated ET estimated with the lysimeter was up to 45% less than these ET estimates, because of reduced transpiration rates.

4.4.4 Summary and conclusions

Despite the incomplete canopy cover of the sugarcane site studied, the soil heat flux density was generally a small fraction of the net irradiance (< 15%). The low *G* values were not the result of a well developed canopy cover, but of the heavy mulch (tops) with which the soil was covered.

Sensible heat flux densities estimated from areally-averaged and point-based measurements were within 30% of each other, with the areally-averaged SLS estimates generally slightly lower. Latent heat flux densities estimated from areally-averaged and point-based measurements compared well (to within 16%). The areally-averaged estimates of *LE* generally exceeded the point-based *LE* estimates.

Over 30 min time intervals, ET estimated with the SLS, ECEB, RMY and SR methods were within 16% of each other ($R^2 > 0.93$).

On a daily basis, ET estimated with the ATI EB, SLS, RMY, SR methods were within 0.42 mm d^{-1} of each other, but exceeded the lysimeter ET estimates because of reduced transpiration rates due to waterlogged conditions in the lysimeter.

In general: *Total evaporation estimated with different point-based and areally-averaged micrometeorological methods applied over an incomplete sugarcane canopy, compared well. However, lysimeter ET estimates were significantly lower, possibly because of the heavy rainfall at the start of the measurement period and the sugarcane plants response to waterlogged conditions in the lysimeter.*

4.5 Case study 5: Short heterogeneous surface/aerodynamically rough canopy

4.5.1 Introduction

A number of indigenous and or invaded areas have short (< 2 m), heterogeneous (species rich) and aerodynamically rough canopies. Because of the heterogeneous and sometimes aerodynamically rough nature of these canopies, not all techniques for estimating total evaporation may be applied successfully in these situations. Hence the importance of assessing the suitability of a range of techniques for estimating total evaporation from these surfaces.

Aim of case study:

- *Investigate the suitability of different micrometeorological techniques in estimating total evaporation from short heterogeneous and aerodynamically rough vegetation.*

-

4.5.2 Materials and methods

4.5.2.1 Site description

Two sites were selected to investigate the suitability of micrometeorological techniques in estimating total evaporation from short heterogeneous and aerodynamically rough vegetation as part of Case study 5. The first site consisted of an extensive area covered with grasses and shrubs (**Fig. 34**). The site was situated in the Vumbuka Reserve at the AECI industrial complex at Umbogintwini, (30°01'02.82''S, 30°53'44.72''E), about 25 km south of Durban. The average canopy height was estimated at 0.99 m. The grass and shrub canopy was dominated by *Cynodon* grass which remained green and maintained a high leaf index throughout the period of measurement (early winter).

The second site consisted of an extensive area completely invaded by *Chromolaena* odorata (**Fig. 35**). A site was selected in the Hluhluwe game reserve, KwaZulu-Natal (28.078° S, 32.1° E, 132 m a.m.s.l.), where the *Chromolaena* was dominant in the lower lying areas, but had also spread higher up slope of the "koppies". In this area, coastal bushveld/grassland vegetation was the native vegetation. *Chromolaena* is also known as triffid weed or "parrafienbos". The *Chromolaena* at the

research site covered an area of approximately 2.5 ha. The average *Chromolaena* canopy height at the time of measurement was 1.5 m. The *Chromolaena* plants were severely wilted throughout the field campaign due to a very severe drought in the area at the time.

4.5.2.2 Techniques applied

The suitability of three different techniques was tested at both the grass/shrub site and at the *Chromolaena* site during two separate field campaigns. Fluxes from two eddy covariance systems were compared against fluxes from the surface renewal systems (SR), and the surface layer scintillometer (SLS). The surface layer scintillometer estimated areally-averaged fluxes, whereas the other techniques estimated fluxes based on point measurements.

At the grass/shrub dominated canopy, the modified Applied Technologies Inc. (ATI) eddy covariance system was installed at a height of 2.7 m above ground and the RM Young sonic anemometer (also part of eddy covariance systems) was installed at a height of 2.69 m (**Table 10**). Fine wire thermocouples as part of the surface renewal systems were installed at five heights (1.45, 1.9, 2, 2.69 and 3.02 m). Only data from the 1.45 m height are shown in this report. The average weighted height of the dual laser beam of the surface layer scintillometer was 1.5 m above the ground. Continuous total evaporation (ET) measurements took place from 23 June to 10 July 2006. Occasional gaps in the EC and SLS data sets do exist.

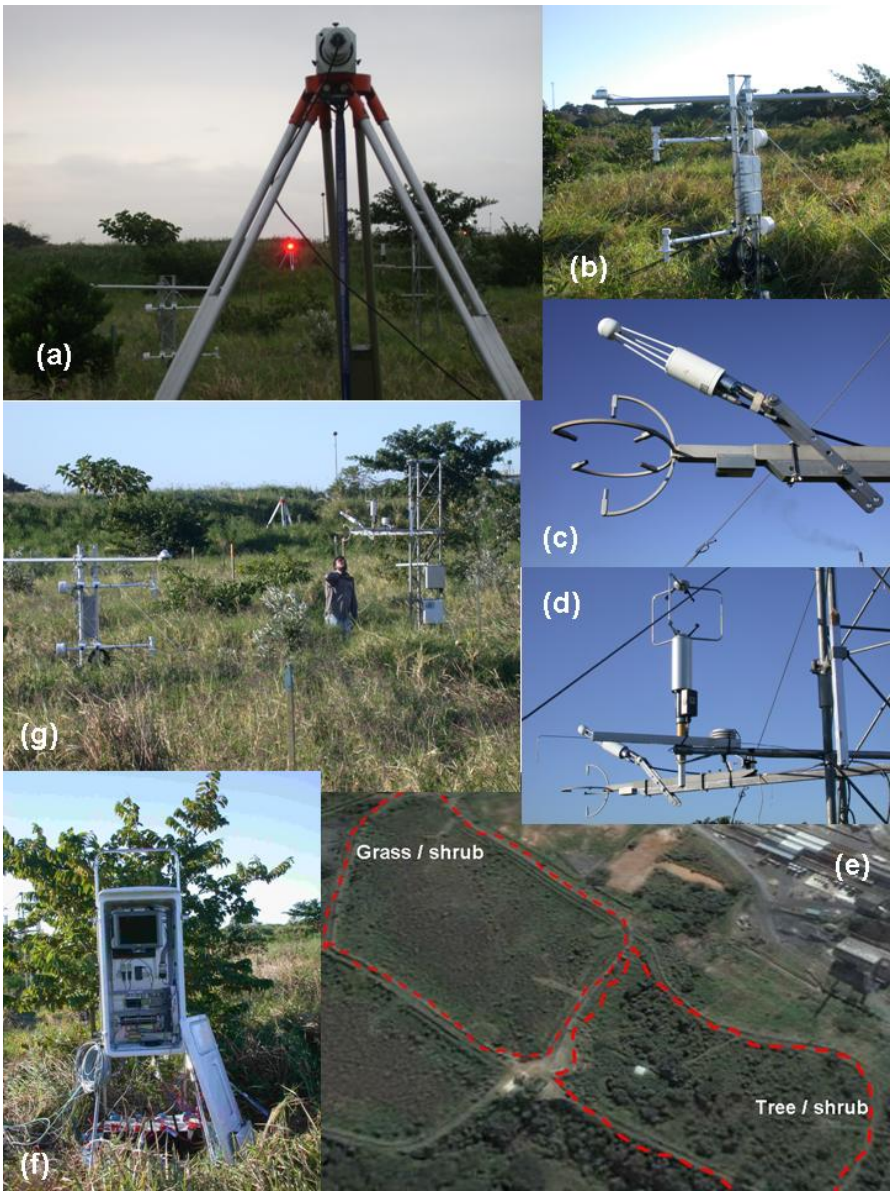

Figure 34 The grass/shrub site (e) instrumented with techniques to measure total evaporation. (a) A laser scintillometer receiver mounted on a tripod (in the foreground) with laser beam from the receiver sensor visible in the back, (b) The OEBMS system as part of the Scintec surface layer scintillometer, used to measure solar radiation, net radiation and a temperature and water vapour pressure at two heights, (c) The infrared gas analyser (top) and sonic anemometer (bottom) from the ATI eddy covariance system, (d) A RM Young sonic anemometer, with thermocouple arm in the foreground, (f) The controlling electronics and software of the ATI modified system, (g) Spatial distribution of equipment at the grass/shrub site.

Similarly, instrumentation was installed at the *Chromolaena* research site (**Table 10**). An In Situ Flux systems eddy covariance system was however used instead of an Applied Technologies Inc. (modified) system. Continuous flux and total evaporation measurements took place from 4 to 11 April 2006.

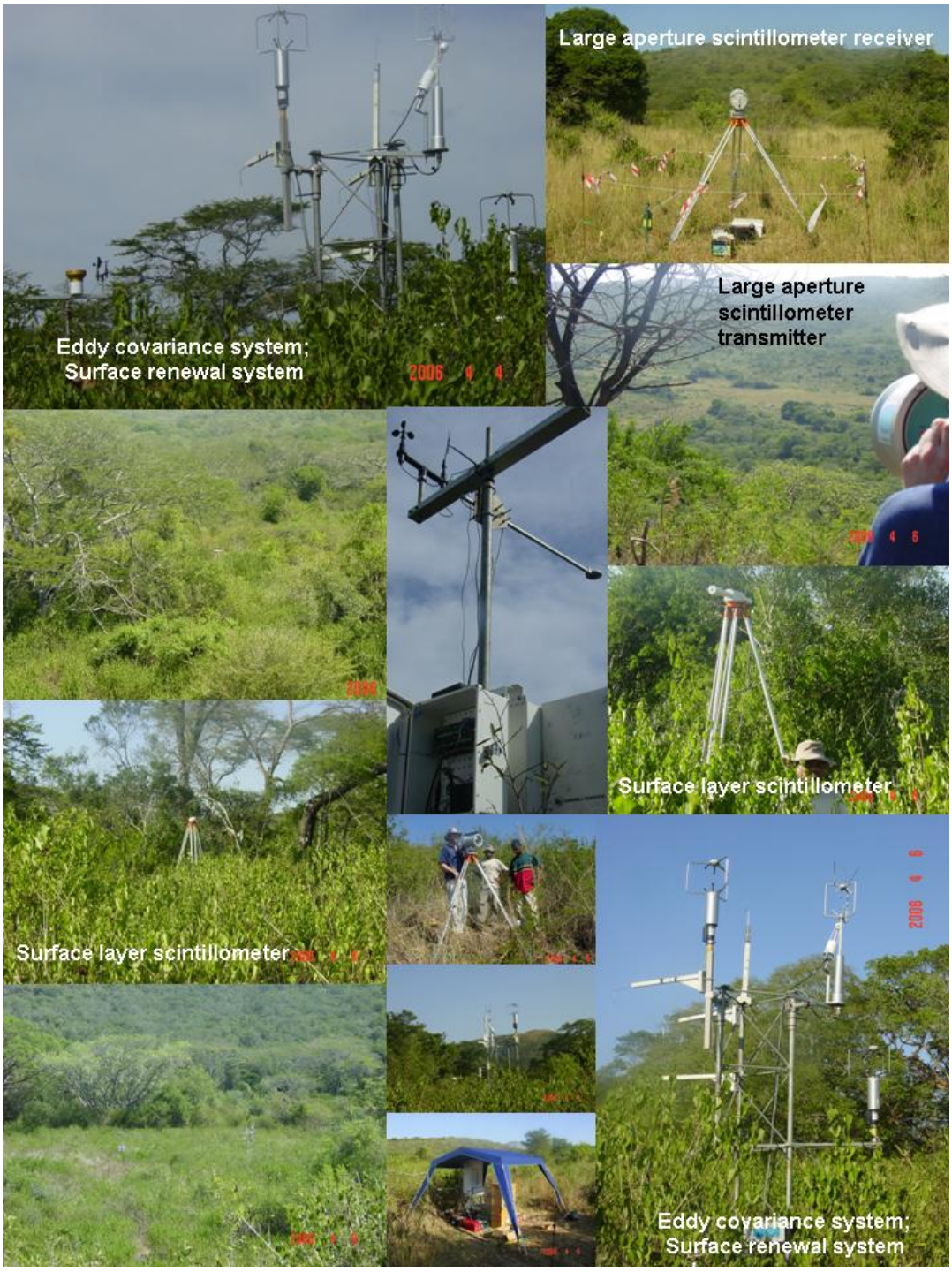

Figure 35 The *Chromolaena* site instrumented with equipment to study the total evaporation within the Hluhluwe nature reserve from 4 to 11 April 2006 as part of Case study 5.

Table 10 Summary information on the techniques applied in Case study 5 at a short, heterogeneous and aerodynamically rough canopy – including a grass/shrub dominated research site and a *Chromolaena* invaded site. The techniques applied include the modified Applied Technologies Inc. eddy covariance system (ATI), the RM Young eddy covariance system (RMY), the surface renewal system (SR) and the Surface layer scintillometer (SLS).

	Grass/shrub research site			
Techniques tested	Eddy covariance (Modified Applied Technologies Inc.)	Eddy covariance (RM Young)	Surface renewal	Surface layer scintillometry
Abbreviation	EC	RMY	SR	SLS
Measurement period	23 June 2006 – 10 July 2006	22 June 2006 – 10 July 2006	22 June 2006 – 10 July 2006	20 June 2006 – 10 July 2006
Data used in comparisons	Partly cloudy: 25 and 26 June 2006 Sunny: 8 and 9 July 2006			
Sampling type	Point measurement	Point measurement	Point measurement	Spatial, areal average
Output interval	30 min	2 min averaged to 30 min	2 min averaged to 30 min	2 min averaged to 30 min
Installation height/s	2.7 m	2.69 m	1.45 m	4.25 m
Make and model of sensors (if applicable)	ATI sonic anemometer and Licor Infra-red gas analyser	RM Young sonic anemometer	Chromal-constantan thermocouples	Scintec dual beam laser scintillometer
Additional	Net radiometer, REBS soil heat flux plates, Chromal-constantan thermocouples, Complete automatic weather station with Solarimeter, RM Young windsentry, Vaisala Temperature and Humidity sensor, Tipping bucket raingauge			
	Chromolaena odorata			
Techniques tested	Eddy covariance (In Situ Flux systems)	Eddy covariance (RM Young)	Surface renewal	Surface layer scintillometer
Abbreviation	EC	RMY	SR	SLS
Measurement period	4-11 April 2006			
Data used in comparisons	6-7 April 2006 (sunny) 8,11 April 2006 (cloudy)			
Output interval	30 min	2 min averaged to 30 min	2 min averaged to 30 min	2 min averaged to 30 min
Installation height/s	3 m	2.6 m, 3 m	2.85 m	3 m
Make and model of sensors (if applicable)	In Situ Flux system with R3 Gill sonic anemometer, and Licor 7500 Infra-red gas analyser	RM Young sonic anemometer	Chromal- constantan thermocouples	Scintec Dual beam SLS
Additional	Net radiometer, REBS soil heat flux plates, Chromal-constantan thermocouples, complete automatic weather station with Solarimeter, RM Young windsentry, Vaisala temperature and humidity sensor, tipping bucket raingauge			

4.5.3 Results

Two sunny and two cloudy days were selected for detailed analysis of energy fluxes and total evaporation from each of the sites. At the grass/shrub site, the partly cloudy days 25, 26 June 2006 (DOY 176, 177) and the sunny days 8 and 9 July 2006 (DOY 189, 190) were selected. At the *Chromolaena* site, the sunny days 6 and 7 April 2006 (DOY 96, 97) and the cloudy days 8 and 11 April 2006 (DOY 98, 101) were selected.

4.5.3.1 Climatic conditions

Measurements at the grass/shrub site were conducted in winter, and hence the climatic conditions reflect what is expected at the time of year. Average daily air temperatures over the four days studied ranged between 13.47 and 16.93°C, with a maximum air temperature of 22.9°C recorded on DOY 190. Little rain fell over the four days (0.2 mm), but solar irradiances were low and ranged between 4.82 (cloudy) and 12.97 MJ m^{-2} (sunny). Windspeed at this site was generally low with the daily average windspeed 2.1 m s^{-1}.

Measurements at the *Chromolaena* site were conducted in autumn during a severe drought in the Hluhluwe game reserve. Daily average air temperatures ranged between 21.57 and 26.19°C, with maximum air temperatures of 38.19°C recorded on DOY 96. No rainfall fell on the four days studied, but 2.7 mm of rain fell in the days prior to the measurements. The wind speed at the site was low (average daily 0.84 m s^{-1}). Solar irradiances ranged between 7.34 on cloudy days and 19.4 MJ m^{-2} on sunny days.

4.5.3.2 Net radiation

Net irradiances reached maximum mid-day values of around 340 W m^{-2} on sunny days at the grass/shrub site, which was about 30% less than the mid-day maximum solar radiation values (**Fig. 36a & b**). The soil heat flux density, accounted for only about 2% of the net irradiance (**Fig. 36a & b**), throughout the measurement period. This was due to the high leaf area indices (LAIs) of the grass/shrub vegetative cover, which completely shaded the soil.

The maximum mid-day net irradiance values measured at the *Chromolaena* site were approximately 577 W m^{-2} and accounted for 73% of the solar radiation on a sunny day (**Fig. 36c & d**). Similarly to the grass/shrub site, only a small fraction (< 10%) of the net irradiance (**Fig. 36c & d**) was partitioned into energy for heating of the soil (G). The *Chromolaena* plants nearly covered the soil completely. At both the grass/shrub and *Chromolaena* sites, most of the energy was available to heat the air (H) and drive evaporation (LE).

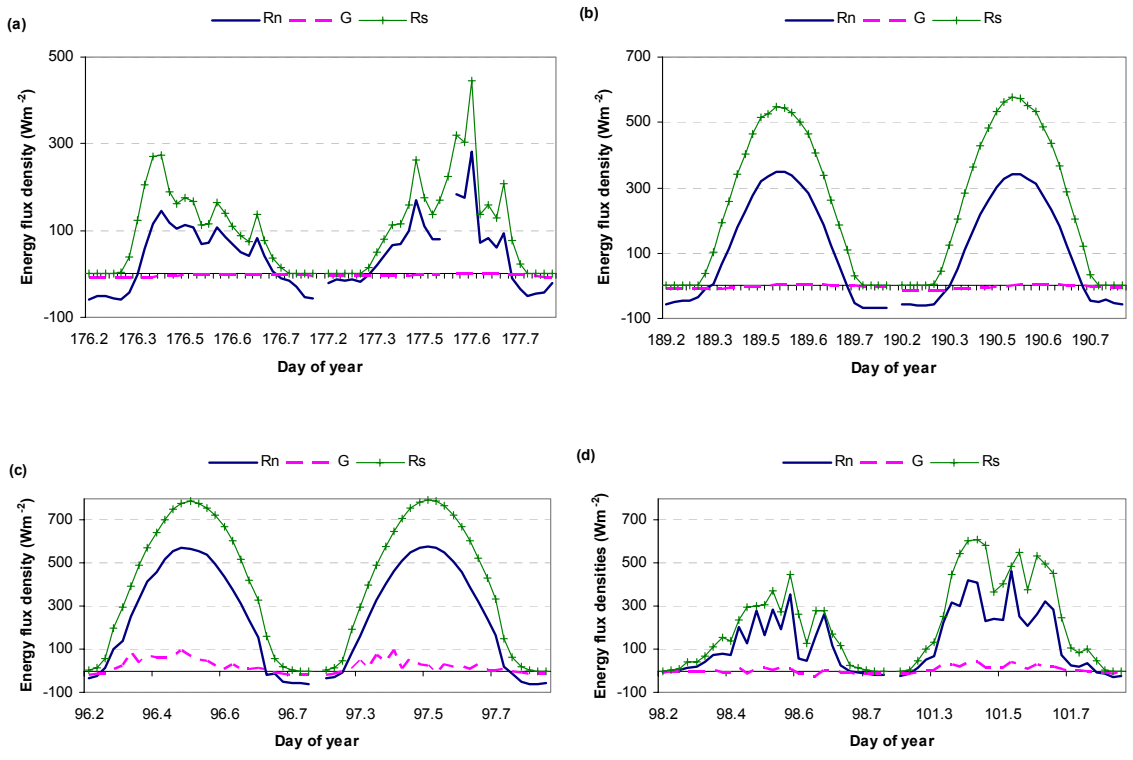

Figure 36 Solar radiation (Rs), net irradiance (*Rn*) and soil heat flux density (G) estimated at the short, heterogeneous and aerodynamically rough surfaces as part of Case study 5. a & b - Data for the grass/shrub site for four days (DOY 176-177, 189-190). Data for the time period 05h00 to 19h00 are shown. c & d – Data for the *Chromolaena* site for four days (DOY 96 to 98, 101). Data for the time period 06h00 to 19h00 are shown. The X-axis shows the day of year (DOY) divided into fractions of time, e.g. 176.5 refers to DOY 176 at 12h00.

4.5.3.3 Sensible and latent heat flux density: Grass/shrub site

The sensible heat flux densities estimated with the different methods at the grass/shrub site, showed a good agreement, both in the diurnal pattern (**Fig. 37**) and in the magnitude of the fluxes (**Fig. 37, 38**). Areally-averaged estimates of sensible heat flux density (H SLS) were within 5% of sensible heat flux estimates with the eddy covariance systems (H ATI, H RMY) (**Fig. 38**). Point-based estimates of sensible heat flux density using the surface renewal technique were up to 25% lower than the spatial estimates of *H* (**Fig. 37, 38**), with the biggest flux differences estimated on sunny days (**Fig. 37**).

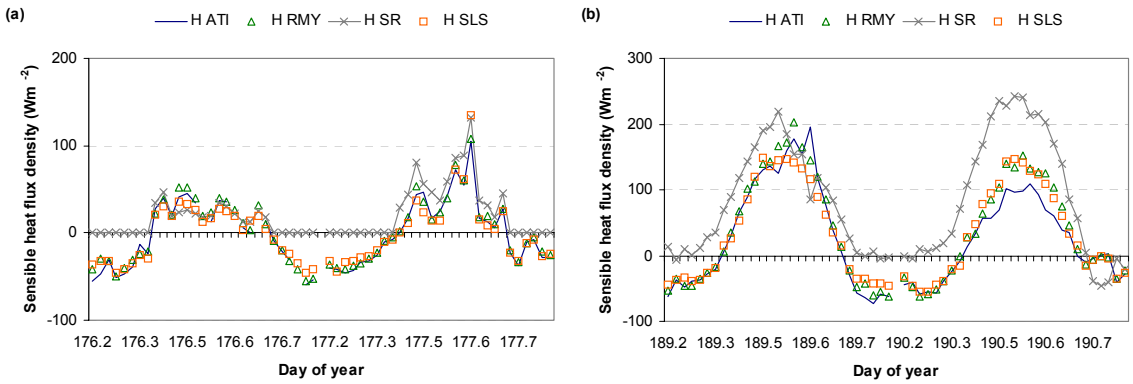

Figure 37 Sensible heat flux densities measured at the short, heterogeneous and aerodynamically rough surfaces as part of Case study 5. a & b - Data for the grass/shrub site for four days (DOY 176-177, 189-190). Data for the time period 05h00 to 19h00 are shown. Sensible heat flux density was measured with the Eddy covariance systems (ATI and RMY), a surface renewal system and a surface layer scintillometer – H ATI, HRMY, H SR and H SLS respectively. The X-axis shows the day of year (DOY) divided into fractions of time, e.g. 176.5 refers to DOY 176 at 12h00.

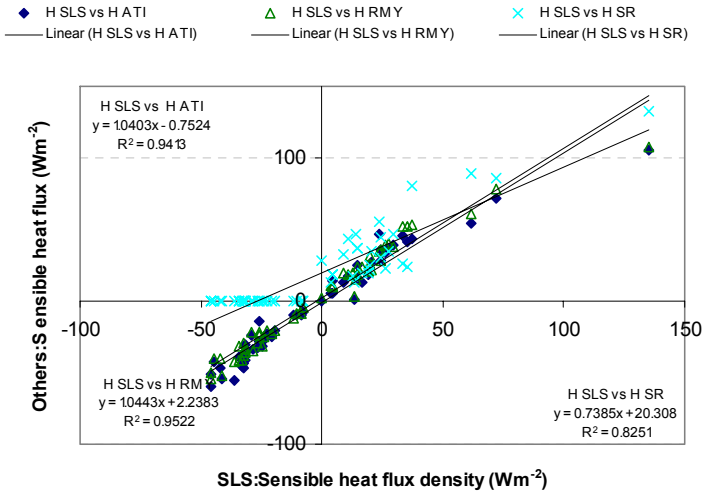

Figure 38 Sensible heat flux densities measured at the short, heterogeneous and aerodynamically rough surfaces as part of Case study 5. Data are shown for the grass/shrub site for four days (DOY 176-177, 189-190). On the X –axis the sensible heat flux densities estimated with the surface layer scintillometer (H SLS) are shown, and are compared to the sensible heat flux densities estimated with the eddy covariance systems (H ATI and H RMY) and a surface renewal system (H SR) which are shown on the Y-axis.

Indirect estimates of *LE* using eddy covariance systems (LE ATI EB, LE RMY) compared well with *LE* estimates made with the surface renewal (H SR) and scintillometer systems (H SLS) on cloudy days (e.g. DOY 176, 177) (**Fig. 39, 40**). On a sunny day (DOY 190) the latent heat flux density estimates with the RMY system and the spatial estimates of *LE* (LE SLS) compared very well, both in the diurnal trend (**Fig. 39**) and the magnitude of the fluxes (**Fig. 40**). Indirect estimates of *LE* with the modified ATI system (LE ATI EB) and *LE* estimates with the surface renewal system differed greatly from the spatial estimates of *LE* (LE SLS) (**Fig. 40**). In general, spatial estimates of *LE* were within 15% ($r^2 > 0.82$) of *LE* estimates with the surface renewal system and indirect estimates of *LE* with the eddy covariance systems (**Fig. 40**). A very poor relationship (slope=0.25 and r^2=0.68) existed between direct estimates of *LE* (LE ATI) and spatial estimates of *LE* (LE SLS) (**Fig. 40**), and other point-based estimates of *LE* (LE RMY, LE SR).

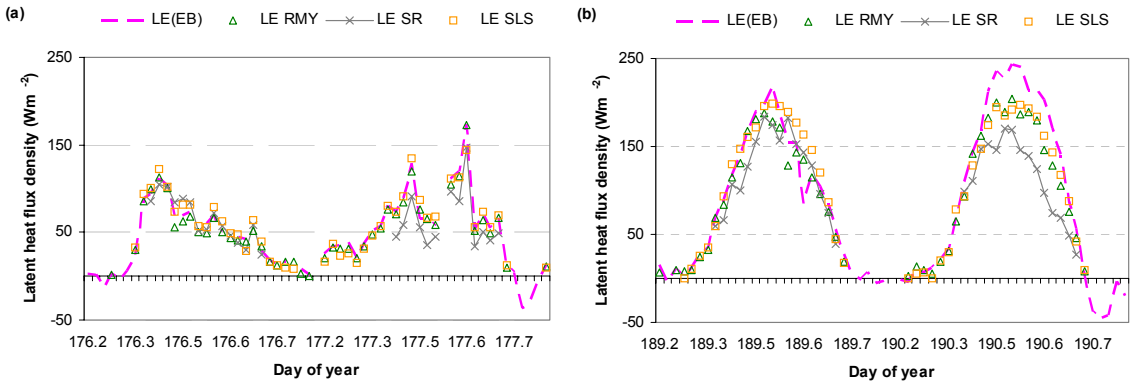

Figure 39 Latent heat flux densities measured at the short, heterogeneous and aerodynamically rough surfaces as part of Case study 5. a & b - Data for the grass/shrub site for four days (DOY 176-177, 189-190). Data for the time period 05h00 to 19h00 are shown. Latent heat flux density was measured with the Eddy covariance systems (H ATI, H ATI EB and H RMY), a surface renewal system (H SR) and a surface layer scintillometer (H SLS). The X-axis shows the day of year (DOY) divided into fractions of time, e.g. 176.5 refers to DOY 176 at 12h00.

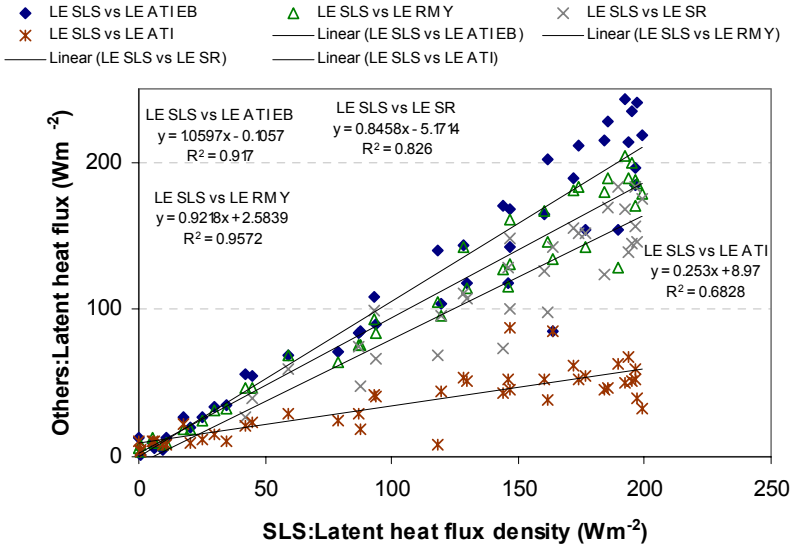

Figure 40 Latent heat flux densities measured at the short, heterogeneous and aerodynamically rough surfaces as part of Case study 5. Data are shown for the grass/shrub site for four days (DOY 176-177, 189-190). On the X –axis the latent heat flux densities estimated with the surface layer scintillometer (LE SLS) are shown, and are compared to the sensible heat flux densities estimated with the eddy covariance systems (LE ATI, LE ATI EB and LE RMY) and a surface renewal system (LE SR), shown on the Y-axis.

4.5.3.4 Sensible and latent heat flux density: Chromolaena site

The diurnal trends in the latent (LE) and sensible heat flux densities (H) estimated at the *Chromolaena* site using different techniques compared favourably on sunny (DOYs 96 to 97) and on cloudy days (DOYs 98, 101) (**Fig. 41**). However, differences in the magnitude of the fluxes existed (**Figs. 41, 42**). In general, the *H* values estimated with scintillometer (H SLS) were up to 35% less than the *H* values measured with the other techniques (r^2 >0.73) (**Fig. 42a**). Also, the *LEs* estimated with the scintillometer (LE SLS) were up to 27% less than the surface renewal estimates (LE SR) (**Fig. 42b**). The SLS latent heat flux density estimates were very similar (slope=1.06) to the indirect estimate of *LE* using the RM Young eddy covariance system (**Fig. 42b**).

During the initial data analysis the magnitude of the *H* values measured with the scintillometer were significantly different to the *H*'s measured with all other techniques. Upon close inspection it was discovered that measurements by all techniques, including the scintillometer took place in the roughness sub-layer, and not in the inertial sub-layer as assumed. Equations specific to the inertial sub-layer were initially used in the calculation of *H*'s estimated with the scintillometer. But, in fact different equations applying to the surface roughness layer should have been applied. Upon correction/recalculation of the H SLS values, the agreement between techniques was significantly improved. Note: The initial incorrect *H* and *LE*s estimated for the SLS system are not shown in this report.

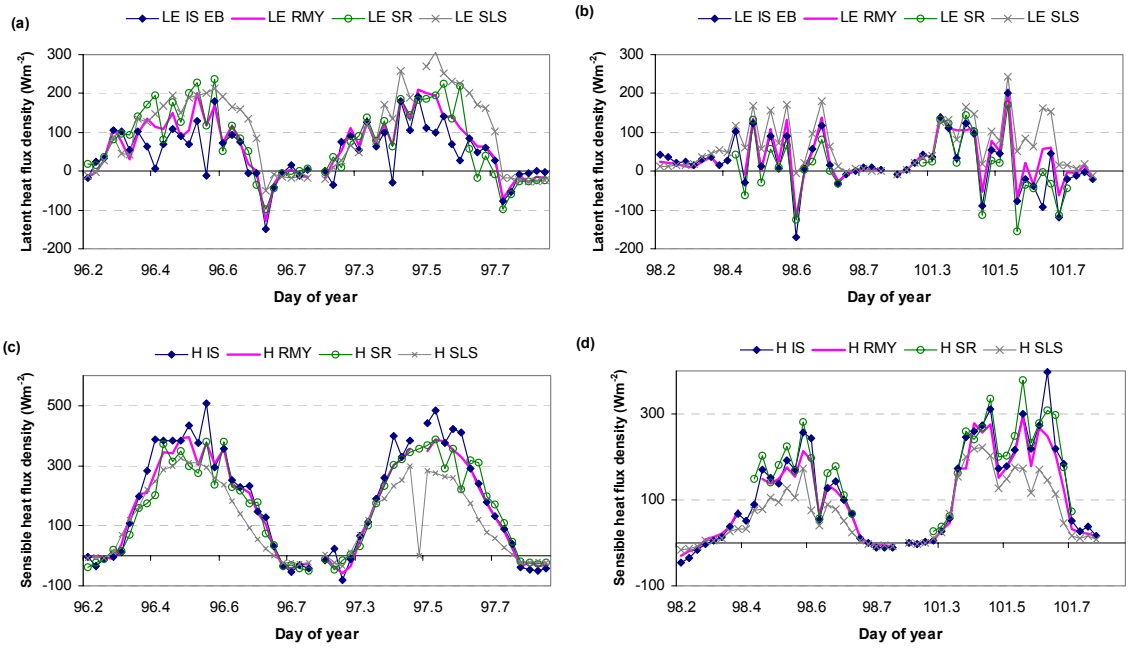

Figure 41 Latent (LE) and sensible heat flux densities (H) measured at the short, heterogeneous and aerodynamically rough *Chromolaena* surface as part of Case study 5. a & b – Indirect estimates of latent heat flux densities estimated with the In Situ Flux system (LE IS EB) and estimates of *LE* with the RM Young eddy covariance system (LE RMY), the surface renewal system (LE SR) and the surface layer scintillometer (LE SLS). c & d - Estimates of sensible heat flux densities using the In Situ Flux system (H IS), the RM Young eddy covariance system (H RMY), the surface renewal system (H SR) and the surface layer scintillometer (H SLS). Data are shown for four days (DOY 96 to 98, 101), for the periods 06h00 to 19h00. The X-axis shows the day of year (DOY) divided into fractions of time, e.g. 97.5 refers to DOY 97 at 12h00.

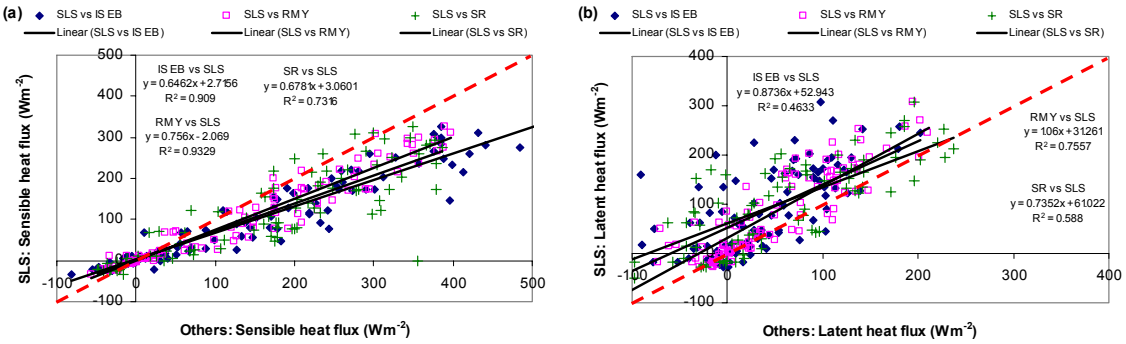

Figure 42 a - Sensible and b - Latent heat flux densities measured at the short, heterogeneous and aerodynamically rough *Chromolaena* canopy as part of Case study 5. Data are shown for four days (DOY 96 to 98, 101). On the Y–axis the sensible and latent heat flux densities estimated with the surface layer scintillometer (H SLS, LE SLS) respectively, are shown. These data are compared to the sensible heat flux densities estimated with the other systems: eddy covariance systems (_IS EB, _RMY) and the surface renewal system (_SR), shown on the Y-axis.

4.5.3.5 Total evaporation

Available (non-zero, and corresponding) thirty minute estimates of total evaporation (ET) (using spatial and point-based methods) were added for each day studied. These "sub-daily" total evaporation estimates were compared in **Table 11** (grass/shrub site) and **Table 12** (*Chromolaena* site). **Table 11** shows that the spatial estimates of total evaporation (ET SLS) were within 20% of the ET estimates from point-based methods at the grass/shrub site. The exception was direct estimates of ET using the eddy covariance system, which were 62% lower than the spatial estimates of ET. It is suspected that the Infra-red gas analyser malfunctioned, and these data should therefore be ignored.

At the *Chromolaena* site, differences in ET estimated with the spatial and point-based methods, over a four-day period, were higher than that at the grass/shrub site – up to 39% (**Table 12**). The highest estimates of ET were recorded with the scintillometer. All other estimates were very similar (**Table 12**).

Table 11 The total evaporation (mm/period) estimates for the grass/shrub surface on two cloudy (DOYs 176-177) and two sunny days (DOYs 189-190). "Sub-daily" estimates of ET were calculated from the available corresponding values. ET estimates were calculated for the Eddy covariance systems, a surface renewal system and a surface layer scintillometer. NOTE: Since the direct ET estimates with the ATI Eddy covariance system were significantly lower than the other ET estimates, it was suspected that the infra-red gas analyser as part of this system might have been malfunctioning during the field campaign, and it is suggested that the data be interpreted with caution.

Year	DOY	Total evaporation				
		Eddy covariance (ATI)	Eddy covariance (ATI EB)	Eddy covariance (RMY)	Surface renewal	Scintillometer
		mm/period	mm/period	mm/period	mm/period	mm/period
2006	176	0.326	0.472	0.494	0.512	0.558
2006	177	0.406	0.823	0.803	0.611	0.838
2006	189	0.574	1.562	1.488	1.429	1.675
2006	190	0.490	1.956	1.640	1.264	1.648
SUM (DOY 176-177, 189-190)		1.796	4.814	4.424	3.816	4.720
ET % SLS		0.381	1.020	0.937	0.808	1.000

Table 12 The total evaporation (mm/period) estimates for the *Chromolaena* surface on two cloudy (DOYs 98, 101) and two sunny days (DOYs 96 to 97). "Sub-daily" estimates of ET were calculated from the available corresponding values. ET estimates were calculated for the Eddy covariance systems, a surface renewal system and a surface layer scintillometer.

Year	DOY	Total evaporation			
		Eddy covariance (ATI EB)	Eddy covariance (RMY)	Surface renewal	Scintillometer
		mm/period	mm/period	mm/period	mm/period
2006	96	1.007	1.244	1.580	1.671
2006	97	1.035	1.345	1.422	1.949
2006	98	0.535	0.564	0.278	0.828
2006	101	0.659	0.742	0.589	0.857
SUM (96 to 98, 101)		3.236	3.895	3.870	5.304
ET % SLS		0.610	0.734	0.730	1.000

4.5.4 Summary and conclusions

In many instances, latent and sensible heat flux densities estimated above a short heterogeneous surface using both point and spatial methods, compared well diurnally. However, the magnitude of these fluxes varied, especially on sunny days.

Generally spatial estimates of sensible and latent heat flux densities exceeded point-based estimates thereof. Direct estimates of ET using the ATI eddy covariance system were significantly lower than other ET estimates (up to 61% of the SLS) at the grass/shrub site, and caution should be taken when using these data as the infra-red gas analyser might have malfunctioned during data collection.

4.6 Case study 6: Tall heterogeneous surface/aerodynamically rough canopy

4.6.1 Introduction

A number of indigenous, invaded areas and or agroforesty type surfaces have tall (> 2 m), heterogeneous (species rich) and aerodynamically rough canopies. Because of the heterogeneous and sometimes aerodynamically rough nature of these canopies, not all techniques for estimating total evaporation may be applied successfully in these situations. It was therefore considered important to investigate the suitability of a range of techniques for total evaporation estimation from these surfaces.

This project complemented work undertaken by the CSIR aimed at modelling the soil-plant-atmosphere system of two rehabilitated settling dams at an industrial complex, quantifying the long-term water balance and assessing the extent of deep drainage from these dams (Dye, 2006).

Aim of case study:

- *To determine the suitability of a range of micrometeorological techniques in estimating total evaporation from a tall heterogeneous surface/tall aerodynamically rough canopy.*

4.6.2 Materials and methods

4.6.2.1 Site description

An extensive area, dominated by trees and shrubs, was selected for the field work. The site was situated on dam 2 within the Vumbuka Reserve at the AECI industrial complex at Umbogintwini, (30°01'07.79''S, 30°53'51.31''E) (**Fig. 43**) about 25 km south of Durban. The average canopy height was 4.14 m. The trees at this site were still relatively young and had not developed a closed canopy. Continuous total evaporation (ET) measurements took place from 23 June to 10 July 2006.

4.6.2.2 Techniques applied

Table 13 summarises the techniques used to study the energy fluxes and total evaporation from this tall heterogeneous surface (or tall aerodynamically rough canopy) consisting of a combination of trees and shrubs (hereafter called tree/shrub).

The suitability of three different techniques was tested at this site: (1) the eddy covariance technique – with and without infra-red gas analyser, (2) the surface renewal technique, and (3) the scintillometry technique. The In situ (IS) flux systems eddy covariance system was installed at a height of 7.4 m, and the RM Young sonic anemometer (as part of an independent eddy covariance system) was installed at 7.4 m. Thermocouples, as part of the surface renewal technique, were installed at five heights (3.7, 4.25, 6.9, 7.4 and 9.5 m). The average weighted height of the dual laser beam of the surface layer scintillometer was 7 m above the ground.

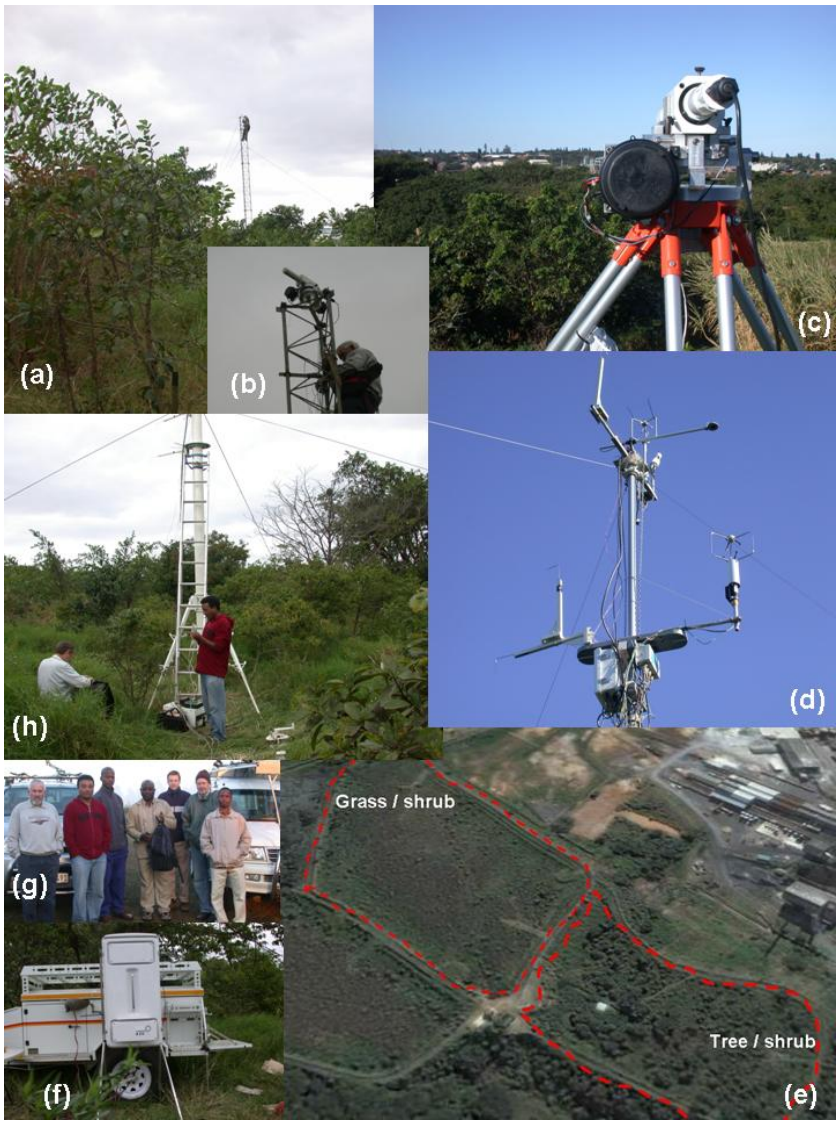

Figure 43 The tree/shrub covered site (e) instrumented with techniques to measure total evaporation. (a) A lattice mast towering out above the trees and shrubs. The surface layer scintillometer (SLS) receiver sensor was mounted on top of this lattice mast, (b) Dr. Colin Everson busy finalising the installation of the SLS receiver sensor, (c) The SLS transmitter sensor was mounted on top of the roof of a small building, to provide an unobstructed line of sight to the receiver sensor mounted on top of the lattice mast, (d) Sensors mounted on top of the 15 m telescopic mast include: thermocouples, sonic anemometers, a net radiometer, and an infra-red gas analyser, (f) the trailer, in the background, used to house the power supply powering a number of systems and in the foreground, the In Situ Flux box housing the controlling electronics and software for the eddy covariance system, (g) Project team members ready to leave to start the installation of sensors and (h) Team members busy mounting sensors onto the telescopic mast.

Table 13 Summary information on the techniques tested at the tall heterogeneous canopy dominated by trees and shrubs as part of Case study 6. IS refers to the In Situ Flux eddy covariance system, RMY to the RM Young eddy covariance system, SR refers to the surface renewal technique and SLS to the surface layer scintillometer method.

Techniques applied	Tree and shrub research site			
	Eddy covariance (In Situ Flux system)	Eddy covariance	Surface renewal	Scintillometer (surface layer)
	IS	RMY	SR	SLS
Measurement period	22 June to 10 July 2006			
Data used in comparisons	Cloudy to partly cloudy: 25 Jun. and 3 Jul. 2006 (DOYs 176 and 184) Sunny: 24 and 30 Jun. 2006 (DOYs 175 and 181)			
Sampling type	Point measurement	Point measurement	Point measurement	Spatial measurement (areal average)
Output interval	30 min	2 min averaged to 30 min	2 min averaged to 30 min	2 min averaged to 30 min
Installation height/s	7.4 m	7.4 m	4.5 m	7 m
Make and model of sensors (if applicable)	In Situ Flux with R3 Gill sonic anemometer, and Licor 7500 Infra-red gas analyser	RM Young model 8100 sonic anemometer	Chromal- constantan thermocouples	Scintec dual beam laser scintillometer
Additional	Net radiometer, REBS soil heat flux plates, Chromal-constantan thermocouples, Complete automatic weather station with Solarimeter, RM Young windsentry, Vaisala Temperature and Humidity sensor, Tipping bucket raingauge			

4.6.3 Results

Energy fluxes and total evaporation estimated with the different techniques were compared for two partly cloudy (25 Jun. and 3 Jul. 2006 - DOY 176, 184) and two sunny days (24 and 30 Jun. 2006 - DOY 175, 181). Similarities and differences in the sensible, latent heat flux densities and total evaporation measured are discussed. Only data for the time period 05h00 to 19h00 are shown.

4.6.3.1 Climatic conditions

Measurements took place in winter. Daily average air temperatures on the four days studied ranged between 14.55 and 19.26°C. Maximum temperatures up to 27.36°C were measured on DOY 184. The wind speed was generally low (average 2.15 m s^{-1}) and 0.4 mm rain fell on DOY 181. Solar irradiances ranged between 4.82 MJ m^{-2} on a cloudy day (DOY 176) and 12.38 MJ m^{-2} on a sunny day (DOY 175) and were indicative of the cool winter conditions during the measurement period.

4.6.3.2 Net radiation and soil heat flux density

The net irradiances (*Rn*) measured at the tree/shrub site reached maximum mid-day values of around 350 W m^{-2} on sunny days during winter (e.g. DOYs 175 and 181) (**Fig. 44**). On a very cloudy day (e.g. DOY 176), the maximum mid-day net irradiances values were 40% less than those of a sunny day (only about 100 W m^{-2}) (**Fig. 44**). These *Rn* values represented single point measurements above the tree/shrub surface.

The soil heat flux density (G) accounted for a small fraction of the net irradiances (about 8%), as the soil surface was nearly completely shaded by vegetation (**Fig. 44**). Therefore, about 92% of the net irradiance was available energy (*Rn* - G) that could be partitioned between the sensible (H) and latent heat flux densities (LE). The soil heat flux density estimates were based on a single point measurement.

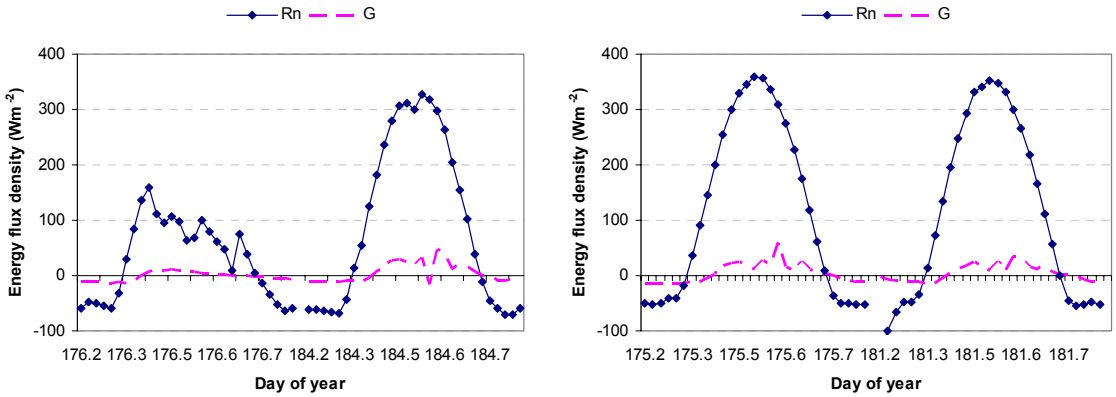

Figure 44 Net irradiances (*Rn*) and soil heat flux densities (G) measured at the tall heterogeneous site dominated by trees and shrubs as part of Case study 6. Data are shown for two cloudy (DOYs 176, 184) and two sunny days (DOYs 175, 181). Data are shown for the periods 05h00 to 19h00. The X-axis shows the day of year (DOY) divided into fractions of time, e.g. 176.5 refers to DOY 176 at 12h00.

4.6.3.3 Sensible and latent heat flux density

4.6.3.3.1 A comparison of selected days (diurnal trends)

Mid-day maximum sensible heat flux density values measured with all techniques were generally less than 200 W m^{-2} (**Figs. 45, 46**). However, mid-day maximum latent heat flux densities estimated with the different techniques generally exceeded 200 W m^{-2} on sunny days (**Figs. 47, 48**). Latent heat flux densities therefore generally dominated over sensible heat flux densities at this site during the study period.

Sensible heat flux densities estimated with four different techniques showed a reasonable agreement in their diurnal trend for both cloudy (DOYs 176, 184) and sunny days (DOYs 175, 181) (**Fig. 49**). Sensible heat flux density values estimated with the In Situ Flux systems eddy covariance system (H IS) occasionally tended to be higher than those measured with the other techniques (e.g. DOY 184) (**Fig. 49**). In contrast, the sensible heat flux densities from surface renewal (H SR) and the RM Young eddy covariance system (H RMY) were slightly lower than sensible heat flux estimates with the other methods (e.g. DOYs 184, 175) (**Fig. 49**).

The diurnal variation in the sensible heat flux densities estimated with the In Situ Flux systems eddy covariance system (H IS) did not always agree favourably with estimates from the other techniques, especially on cloudy days (e.g. DOY 176.4 to 176.6 and DOY 184.5 to 184.6) (**Fig. 49**). The differences in *H* could suggest a problem with the sonic transducers of the sonic anemometer, or a difference in the response of the different techniques to atmospheric changes.

Sensible heat flux densities estimated with two eddy covariance systems (using different sonic anemometers) (H IS, H RMY), compared well on sunny days (**Fig. 49**). On cloudy days the sensible heat flux densities estimated with the RM Young sonic anemometer (H RMY)) were slightly less than the *H*'s estimated with the In Situ Flux system (H IS) and the *H*'s estimated with the surface layer scintillometer (H SLS) (**Fig. 49**). Generally, the spatial estimates of sensible heat flux density (H) estimated with the surface layer scintillometer (H SLS) compared very well with the *H*'s estimated with the eddy covariance method (H IS, H RMY) (**Fig. 49**).

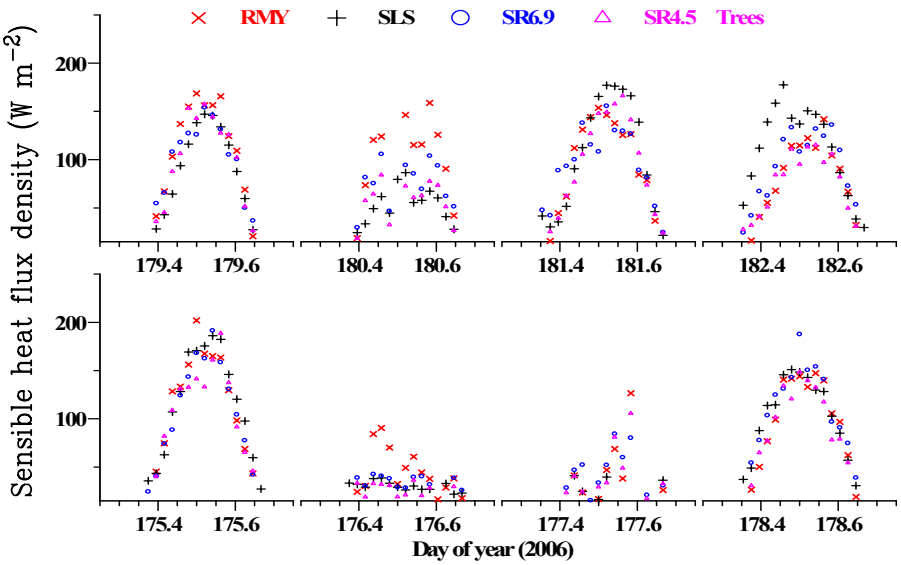

Figure 45 Diurnal variation in sensible heat flux densities estimated at the tree/shrub site as part of Case study 6. Sensible heat flux density was estimated with the eddy covariance system (RMY), the surface layer scintillometer (SLS), and surface renewal systems (SR at two heights). Data are shown for the period 24 June to 1 July 2006. The X-axis shows the day of year (DOY) divided into fractions of time, e.g. 176.5 refers to DOY 176 at 12h00.

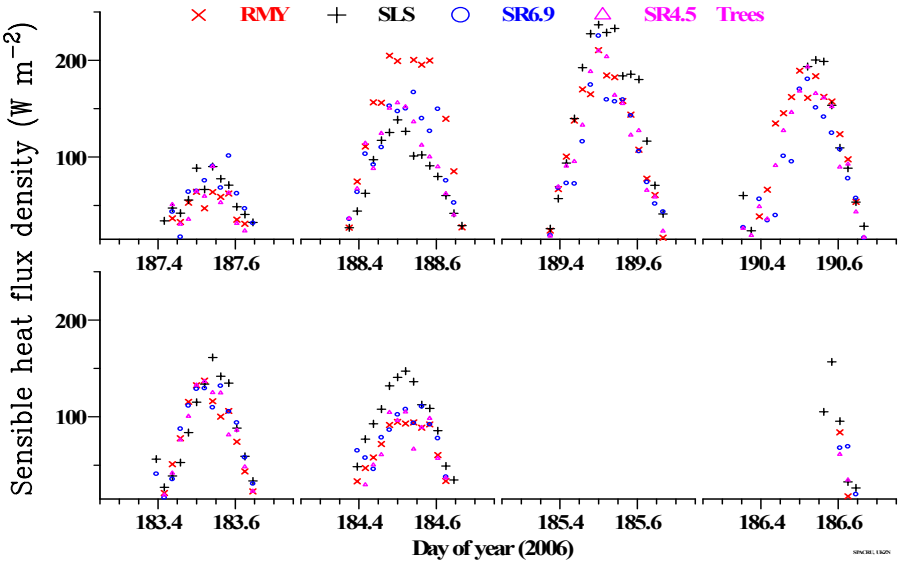

Figure 46 Diurnal variation in sensible heat flux densities estimated at the tree/shrub site as part of Case study 6. Sensible heat flux density was estimated with the eddy covariance system (RMY), the surface layer scintillometer (SLS), and surface renewal systems (SR at two heights). Data are shown for the period 2 to 9 July 2006. The X-axis shows the day of year (DOY) divided into fractions of time, e.g. 176.5 refers to DOY 176 at 12h00.

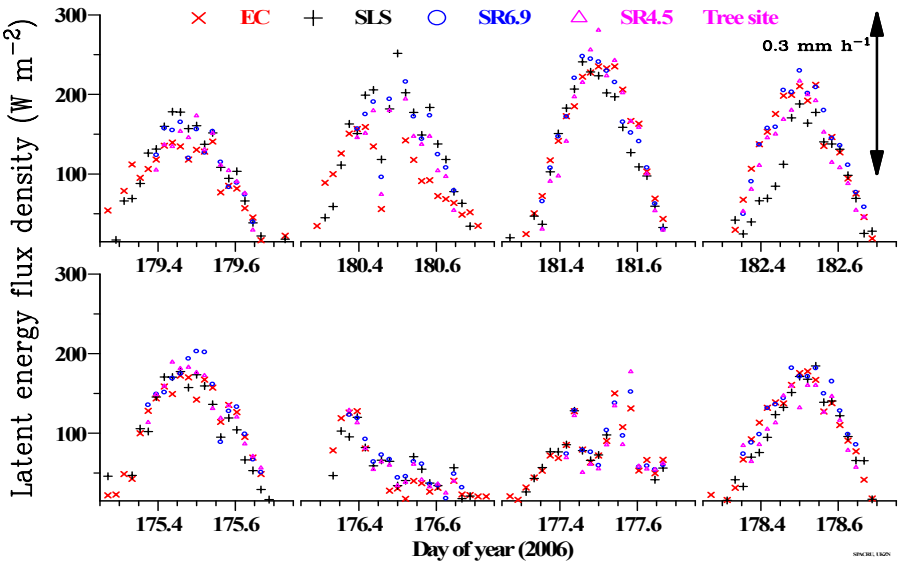

Figure 47 Diurnal variation in latent heat flux densities estimated at the tree/shrub site as part of Case study 6. Latent heat flux density was estimated with the eddy covariance system (RMY), the surface layer scintillometer (SLS), and surface renewal systems (SR at two heights). Data are shown for the period 24 June to 1 July 2006. The X-axis shows the day of year (DOY) divided into fractions of time, e.g. 176.5 refers to DOY 176 at 12h00.

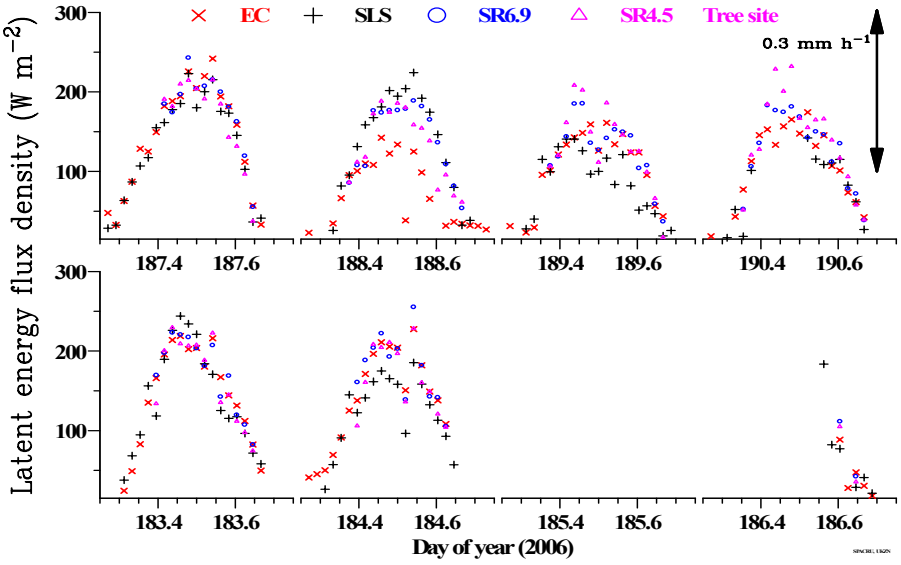

Figure 48 Diurnal variation in latent heat flux densities estimated at the tree/shrub site as part of Case study 6. Latent heat flux density was estimated with the eddy covariance system (RMY), the surface layer scintillometer (SLS), and surface renewal systems (SR at two heights). Data are shown for the period 2 to 9 July 2006. The X-axis shows the day of year (DOY) divided into fractions of time, e.g. 176.5 refers to DOY 176 at 12h00.

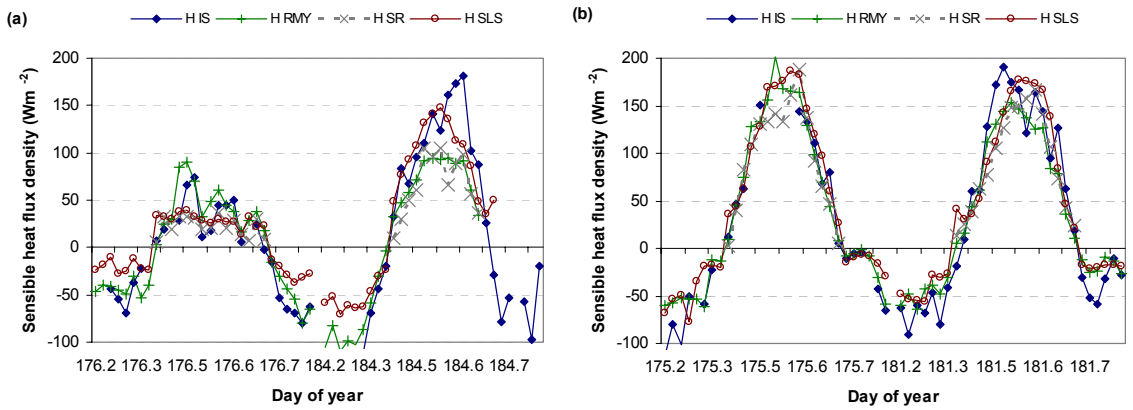

Figure 49 Sensible heat flux density measured at the tree/shrub site as part of Case study 6. Data are shown for two cloudy (DOYs 176, 184) and two sunny days (DOYs 175, 181). Sensible heat flux density was measured with the In Situ Flux systems eddy covariance system (H IS), the RM Young eddy covariance system (H RMY), the surface renewal system (H SR) and surface layer scintillometer (H SLS). Data are shown for the periods 05h00 to 19h00. The X-axis shows the day of year (DOY) divided into fractions of time, e.g. 176.5 refers to DOY 176 at 12h00.

Estimates of *H* from the surface renewal method (H SR) also compared well with those of the surface layer scintillometer method (H SLS) (**Fig. 49**). Occasionally the *H*'s estimated with the surface renewal method were less than those estimated with the surface layer scintillometer method (**Fig. 49**).

The diurnal trend in the latent heat flux densities estimated with the different methods showed good agreement for both cloudy and sunny days (**Fig. 50**). The latent heat flux densities were not specifically over- or underestimated by any one method during the measurement period. This was clear from the latent heat flux densities for both the sample days displayed in **Fig. 50** and for the entire measurement (**Figs. 47, 48**). The direct (LE IS) and indirect estimates of latent heat flux densities (LE IS EB, LE RMY) using different eddy covariance systems compared well (**Fig. 50**). However, the *LE* estimates showed slight diurnal differences (**Fig. 50**).

Point-based estimates of latent heat flux density (LE) with the RM Young eddy covariance (LE RMY) and surface renewal methods (LE SR) compared very well with spatial estimates of latent heat flux density using a surface layer scintillometer (LE SLS) (**Fig. 50**). Diurnal patterns of the direct estimates of latent heat flux density using the In Situ Flux eddy covariance system (LE IS) compared reasonably well with the *LE*s estimated with the surface layer scintillometer (LE SLS) (**Fig. 50**). However the direct estimates of *LE* (LE IS) showed a greater diurnal variation than the latent heat flux densities estimated with the surface layer scintillometer (LE SLS), especially on sunny days (**Fig. 50**).

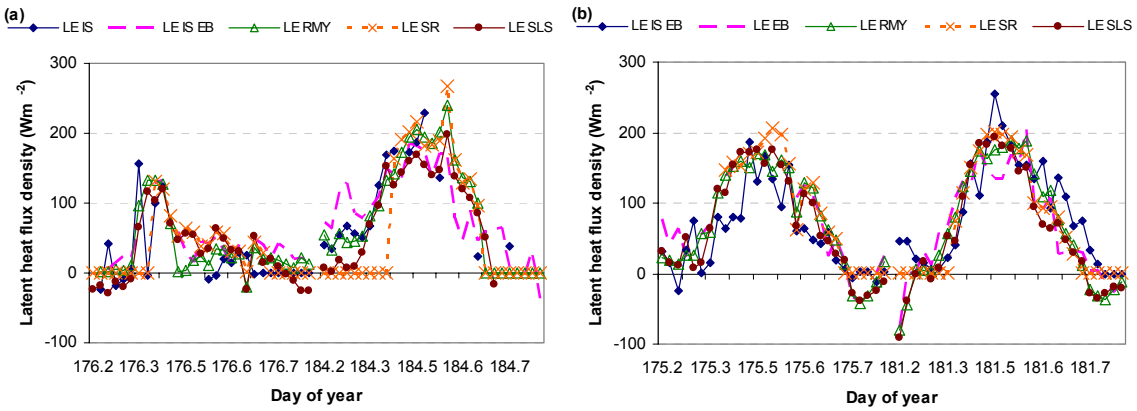

Figure 50 Latent heat flux density measured at the tree/shrub site as part of Case study 6. Data are shown for two cloudy (DOYs 176, 184) and two sunny days (DOYs 175, 181). Latent heat flux density was measured with the In Situ Flux systems eddy covariance system (LE IS, LE IS EB), the RM Young eddy covariance system (LE RMY), the surface renewal system (LE SR) and surface layer scintillometer (LE SLS). Data are shown for the periods 05h00 to 19h00. The X-axis shows the day of year (DOY) divided into fractions of time, e.g. 176.5 refers to DOY 176 at 12h00.

4.6.3.3.2 A comparison of the complete data set (scatter plots)

Latent heat flux densities, estimated at 30 min intervals with three different methods, were compared for the entire sampling period (**Fig. 51**). The latent heat flux densities estimated with the eddy covariance (LE RMY) and surface renewal methods (LE SR) compared well with the *LE*s estimated with the surface layer scintillometer (LE SLS) (R^2 = 0.8 and 0.84 respectively) (**Fig. 51**). The R^2 reflected the differences in the diurnal variation in the latent heat flux densities estimated with the different techniques. The latent heat flux densities estimated with the RM Young eddy covariance and surface renewal systems (LE RMY) and LE SR) were 10 and 9% respectively lower when compared to the surface layer scintillometer *LE*s (LE SLS) (**Fig. 51**).

The *H*'s estimated with the surface renewal system compared well to the *H*'s of the surface layer scintillometer system (H SLS) (R^2 = 0.78, slope = 0.8) (**Fig. 52**). However, the sensible heat flux densities (*H*'s) estimated with the eddy covariance system (H RMY) compared better to these *H* estimates (H SLS) (R^2 = 0.86, slope = 1.0) (**Fig. 52**). The sensible heat flux densities estimated with the surface renewal method (H SR) were underestimated by about 19%, when compared to the *H*'s estimated with the surface layer scintillometer (H SLS) (**Fig. 52**).

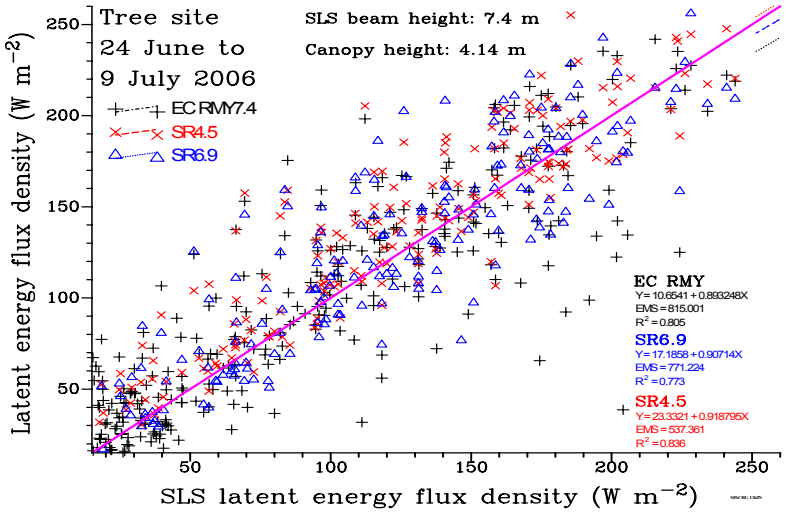

Figure 51 Latent heat flux densities at the tree/shrub site as part of Case study 6. Latent heat flux density for the SLS (surface layer scintillometer) method is plotted on the X-axis, and latent heat flux densities for the EC (RM Young eddy covariance) and SR (surface renewal at two heights) methods on the Y-axis. Data are shown for the period 24 June to 9 July 2006.

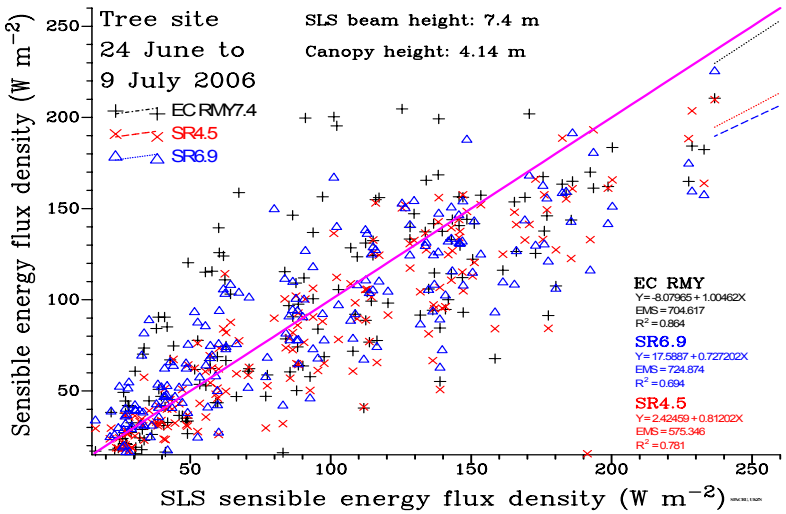

Figure 52 Sensible heat flux densities at the tree/shrub site as part of Case study 6. Sensible heat flux density for the SLS (surface layer scintillometer) method is plotted on the X-axis, and sensible heat flux densities for the EC (RM Young eddy covariance) and SR (surface renewal at two heights) methods on the Y-axis. Data are shown for the period 24 June to 9 July 2006.

4.6.3.4 Total evaporation

The total evaporation rates (mm/30 min) estimated with the different methods generally showed good agreement (**Fig. 53**). However, differences were apparent in the diurnal patterns of total evaporation. No single method consistently under- or overestimated the total evaporation (**Fig. 53**). "Sub-daily" estimates of total evaporation were calculated from the available and coincident data and are shown in **Table 14**. Point-based total evaporation estimates (ET IS, ET IS EB, ET RMY, ET SR) were generally within 15% of the spatial total evaporation estimates (ET SLS). This was also the case when ET was accumulated over a four-day period (**Table 14**). Direct estimates of ET using the In Situ Flux eddy covariance system (ET IS) were generally less than the ET estimated with the surface layer scintillometer (ET SLS). Indirect estimates of total evaporation using the surface renewal system (ET SR) and another eddy covariance system (ET RMY) exceeded the spatial estimate of total evaporation (ET SLS) by up to 25% (**Table 14**).

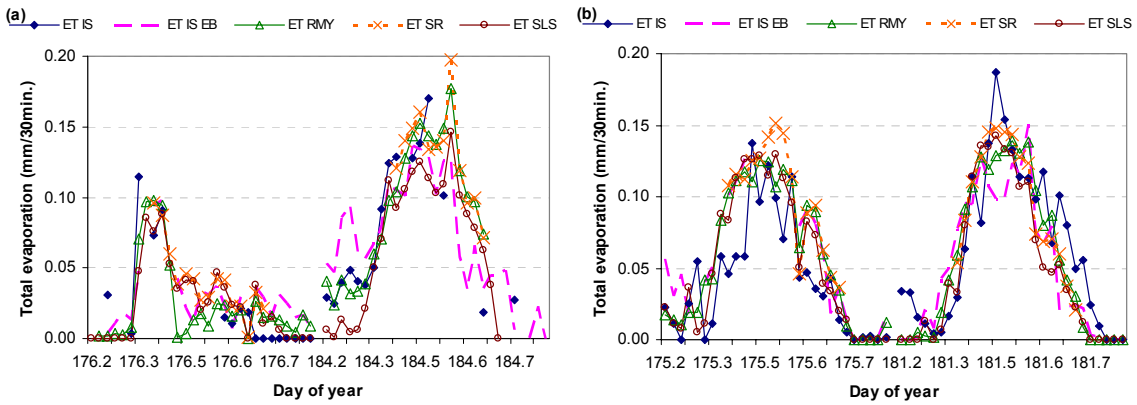

Figure 53 Total evaporation (mm/30 min) estimated at the tree/shrub site as part of Case study 6 is shown for two cloudy (DOYs 176, 184) and two sunny days (DOYs 175, 181). Total evaporation was measured with the In Situ Flux systems eddy covariance system (ET IS, ET IS EB), the RM Young eddy covariance system (ET RMY), the surface renewal system (ET SR) and surface layer scintillometer (ET SLS). Data are shown for the periods 05h00 to 19h00. The X-axis shows the day of year (DOY) divided into fractions of time, e.g. 176.5 refers to DOY 176 at 12h00.

Table 14 Total evaporation estimated at the tree/shrub site as part of Case study 6. Data are shown for two cloudy (DOYs 176, 184) and two sunny days (DOYs 175, 181). Total evaporation was measured with the In Situ Flux systems eddy covariance system (ET IS, ET IS EB), the RM Young eddy covariance system (ET RMY), the surface renewal system (ET SR) and surface layer scintillometer (ET SLS). Total evaporation represent sub-daily estimates calculated from available and corresponding 30 min data points. Many data points were missing on DOY 176 and 184 for the In situ eddy covariance system (IS ET), so data were excluded.

Year	DOY	In situ eddy covariance (ET IS)	In situ eddy covariance (ET IS EB)	RM Young eddy covariance (ET RMY)	Surface renewal (ET SR)	Surface layer scintillometer (ET SLS)
		mm/period	mm/period	mm/period	mm/period	mm/period
2006	174	0.680	0.911	1.075	1.103	0.989
2006	176	Not available	0.538	0.442	0.610	0.578
2006	181	1.642	1.378	1.573	1.540	1.397
2006	184	Not available	1.155	1.526	1.565	1.245
Sum (DOY 174, 176, 181, 184) in mm		Not calculable	3.982	4.615	4.819	4.210
ET % of SLS		Not calculable	194.60	109.63	114.47	100.00

4.6.4 Summary and conclusions

The sensible heat flux densities estimated with different techniques based on point and spatial estimates compared well under both sunny and cloudy conditions.

The sensible heat flux densities estimated with the eddy covariance system (H IS) occasionally exceeded the sensible heat flux densities estimated with the other techniques. In contrast, the sensible heat flux densities estimated with the surface renewal (H SR) and eddy covariance system (H RMY), were occasionally less than the sensible heat flux densities estimated with the other techniques.

The latent heat flux densities estimated with the different techniques compared well, but differences existed in the diurnal patterns of the latent heat flux densities estimated with the different techniques.

No single method consistently over- or under estimated the total evaporation measured above the tree and shrub canopy for the period 23 June to 9 July 2006.

In general: *Estimates of total evaporation from point-based and spatially based systems compared well and are suitable methods to estimate total evaporation from tall heterogeneous surfaces.*

4.7 Case study 7: Open water surface

4.7.1 Introduction

Evaporation is one of the main components of the energy and water balances of dams and is a major source of water loss. Estimates of the amount and rate of evaporation from open water surfaces are required in water resources management for a variety of purposes, such as the design of storage reservoirs, catchment water balance studies, municipal and industrial water supply, irrigation of agricultural lands, and management of wet lands (Brutsaert, 1982; Marsh and Bigras, 1988; Finch, 2001). However, studies of open water evaporation from fresh water systems are generally biased towards reservoir and larger lakes and relatively few investigations have been conducted for dams and ponds (Rosenberry *et al*., 2007).

In South Africa, a number of methods are routinely used to estimate evaporation from dams or water bodies. These methods include the water balance equation, mass transport equation, simple energy budget methods like the Penman potential evaporation equation (Penman, 1948) and the Penman-Monteith reference evapotranspiration method (Allen *et al*., 2006) and Priestley-Taylor method (Priestley and Taylor, 1972), which are based on meteorological data, and pans e.g. the class A-pan and the Symon's tank. Other methods used else where include Bowen ratio energy budget (BREB) method, and eddy covariance (EC) method (Rosenberg *et al*., 1983).

The Penman equation, as well as the Penman-Monteith and Priestly Taylor methods, generally gives accurate estimates of open water evaporation, if representative meteorological data are available for use in the calculations. However, as Everson (1994) reported, if the measurements of land-based weather stations do not represent conditions over open water surfaces, large errors in the estimation of evaporation, could be introduced in the evaporation estimates. To determine uncertainties in evaporation estimates from water surfaces, Everson (1994) compared evaporation estimates with the Bowen ratio energy balance method with evaporation estimates from the Penman method, class A-pans and the Symon's tanks.

Aims of case study:

- *To determine the suitability of a range of micrometeorological techniques in estimating evaporation from an open water surface*

-*Compare evaporation estimates of traditionally reference type methods with that from micrometeorological methods.*

4.7.2 Materials and methods

4.7.2.1 Site description

Field work was conducted at the Midmar Dam (29° 30'S, 30°10'E, 985 m) in the KwaZulu-Natal Midlands from 29 June to 13 July 2007 (DOY 180-194). The dam is relatively small, with a surface area of 1793.15 ha and net capacity of 235.42 million m^3 (DWAF, 2007). Most of the equipment was installed on a 3 m scaffolding structure that was erected about 20 m from the water's edge, close to Hobie Point (**Fig. 1, 40**). The automatic weather station and scintillometer receiver sensors were installed in close proximity to the Department of Water Affairs and Forestry offices at Midmar, where a Symon's pan is also installed and continuously monitored. The dominant wind directions at Midmar are East south east (100°) and North West (310°).

Notes:
- *Measurements in support of a PhD student, Nile Eltayeb, continued for an additional two weeks, but these data sets are not shown here.*
- *Occasional power failures resulted in short gaps in the surface renewal, eddy covariance and scintillometry data.*

4.7.2.2 Techniques applied

Different systems for estimating evaporation were installed at Midmar Dam as part of Case study 7. These included (1) a Scintec boundary layer scintillometer, (2) an In Situ Flux eddy covariance system, (3) an eddy covariance system using an RM Young sonic anemometer, (4) Four sets of thermocouples for the surface renewal systems, (5) Two Infra-red temperature sensors, and (6) three different types of Bowen ratio systems: a - two fine wire thermocouples and two aspirated psychrometers installed at different heights; b – two Vaisala temperature/humidity sensors installed at different heights; c - an oscillating system with Vaisala temperature/humidity sensors installed at two heights) (**Table 15)**. The results of the first four systems were contrasted with estimates of evaporation from the Symon's tank and Penman equation.

Net irradiance was measured with a single net radiometer (NR-Lite, Kipp & Zonen). The heat stored in the water was estimated from measurements with eight painted type-E sealed thermocouples together with four heat flux plates installed at different depths below the water surface. These sensors were mounted onto a float system enabling the measurement of water temperature at consistent depths below the water surface (**Fig. 54**, **Table 15**). **Table 15** gives more information on the systems applied at the open water surface.

Heat stored in the water was calculated from 2 minute measurements of water temperature and heat fluxes. The heat storage term exhibited very high variability at this short time interval due to varying temperatures sensed by the thermocouples as turbulent waves continued to pass them. The heat storage term was therefore smoothed to remove some of this variation. This was done by applying a 60 minute running mean to the 2 minute heat storage data. The two minute data were subsequently averaged to a 30 minute interval which was used in the evaporation calculations.

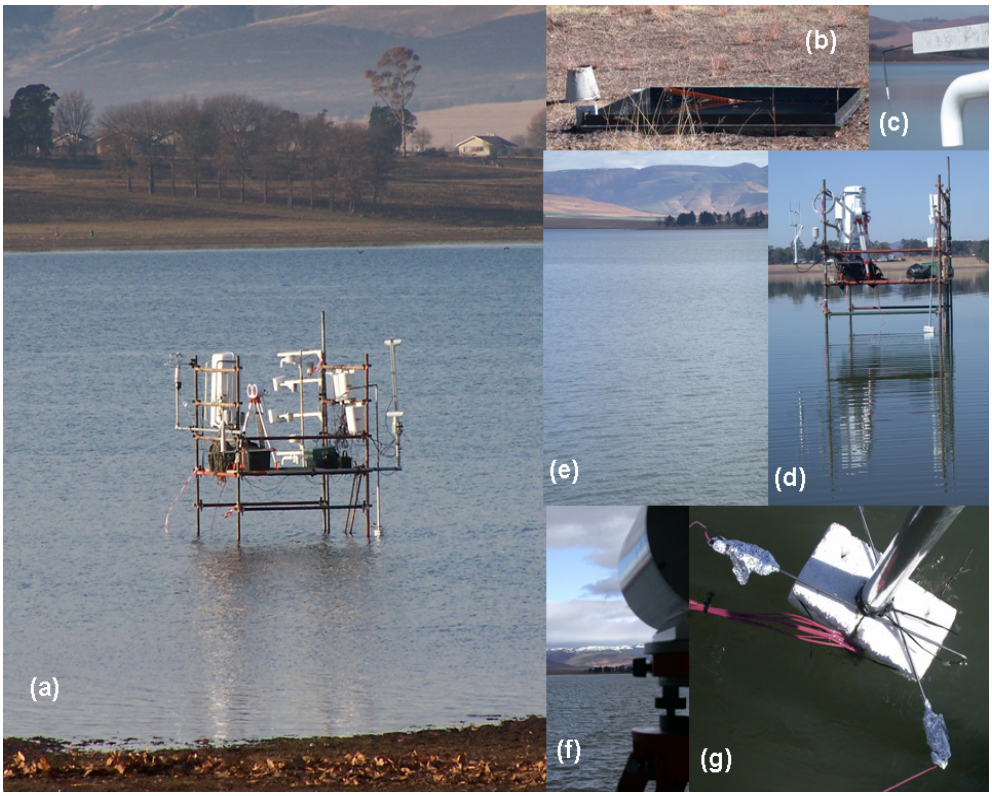

Figure 54 The open water research site used in Case study 7. (a) Scaffolding mounted in the water provided a good platform to work on and mount numerous systems, used in the study. (b) The Symon's pan at the DWAF offices, Midmar. (c) Fine wire thermocouple mounted on a short Bowen ratio arm, and a Bowen ratio arm with an aspirated psychrometer and thermocouple. (d) All systems mounted in the water on a calm day with hardly any wind. Note the smooth water surface. (e) View over the water from the scintillometer receiver sensor. The scaffolding tower with all the systems is installed in the water just to the left of the trees at the back. (f) The receiver sensor of the scintillometer, with snow on the Drakensberg mountain range in the background. (g) The float with fine wire thermocouples mounted onto it, to determine water temperature at constant but different depths below the water surface.

Table 15 Summary information on the techniques applied to estimate evaporation from an open water surface as part of Case study 7. Instrumentation was installed at the Midmar Dam, just outside Howick. The systems installed included: the In Situ Flux systems eddy covariance system (with sonic anemometer and an infra-red gas analyser); the RM Young eddy covariance system; the surface renewal systems where a number of thermocouples were used; the boundary layer scintillometer; Different Bowen ratio system (oscillating system, system where two vaisala sensors were used, and a system with aspirated psychrometers); and the Infra-red thermometer system.

Techniques tested	Eddy covariance (In Situ Flux systems)	Eddy covariance (RM Young 8100)	Surface Renewal	Boundary Layer Scintillometer (Scintec)	Bowen ratio (Oscillating)	Bowen ratio (Vaisala)	Bowen ratio (Aspirated psychrometer)	Infra-red
Measurement period	29 June to 13 July 2007 (DOY 180-194)							
Data used in comparisons	All	All	All	All	All	All	All	All
Output interval	30 min	2 min	2 min	2 min	2 min	2 min	2 min	2 min
Abbreviation used	EC IS (with IRGA) and EC EB (without IRGA)	EC RMY	SR	BLS	BR O	BR V	BR AP	IR
Installation height/s	IRGA and Sonic at 1.94 m above water	2.47 m above water	0.96, 1.52, 1.98, 2.45 m above water	Transmitter 2.065 m above water; Receiver 1.76 m above soil surface; Path length 2.5 km Effective height 8.99 m	1.72, 2.75 m above water	2.45 m	0.94, 2.45 m	2.45 m
Make and model of sensors (if applicable)	In Situ Flux with R3 Gill sonic anemometer, and Licor 7500 Infra-red gas analyser	RM Young 8100 sonic anemometer	Unshielded Type E (Chromal-constantan) fine wire thermocouples	BLS900 Scintec scintillometer	Vaisala HMP sensors	CS500	Make and model	Apogee
Additional measurements	Net radiometer NR-Lite Model 240,-110 (Kipp and Zonen) installed at 2.44 m above water; Soil thermocouples at 6 depths below water surface: 20, 40, 80, 160, 320, 550 mm; 4 REBS soil heat flux plates installed at 2 depths below water surface: 20 and 47 mm; Automatic weather station: Raingauge installed at 1.3 m above short grass; CS500 temperature/RH sensor at 1.9 m above grass; Solarimeter at 2 m above grass and Windspeed/direction sensor at 2.1 m above short grass.							

4.7.3 Results

Energy fluxes and evaporation from an open water body were measured from 29 June to 13 July 2007 (DOY 180-194) using different micrometeorological systems. Only data for the time period 08h00 to 17h00 are shown and compared.

4.7.3.1 Climatic conditions

The measurements coincided with a very cold spell in winter when daily average air temperatures ranged between 7.42 and 14.74°C on DOY 183 and 197 respectively. Minimum temperatures as low as 0.71°C (DOY 190) and maxima as high as 27.39°C (DOY 197) illustrated the wide range of temperature conditions experienced during the experiment. Only 0.1 mm of rainfall was measured over the entire measurement period (DOY 180-200). Daily total solar irradiances ranged between 8.39 and 14.41 MJ m^{-2}. Daily average wind speeds were generally low and ranged between 0.96 and 3.23 m s^{-1}, but maximum wind speeds as high as 10.27 m s^{-1} were recorded.

4.7.3.2 Net radiation and heat stored in the water

Net irradiance above water and the heat stored in water body are shown in **Fig. 55**. On a sunny day in winter (e.g. DOY 193), mid-day maximum net irradiance (*Rn*) values were as high as 430 W m^{-2} and followed the same diurnal trend as the solar irradiance (Rs) values. The heat stored in the water (G) followed fluctuations in the net irradiance (**Fig. 55**). *G* was negative early in the morning and in the late afternoon, but generally positive during day time (**Fig. 55**). The heat stored in the water generally accounted for up to 40% of the net irradiance during mid-day on sunny days (e.g. DOY 181, 187).

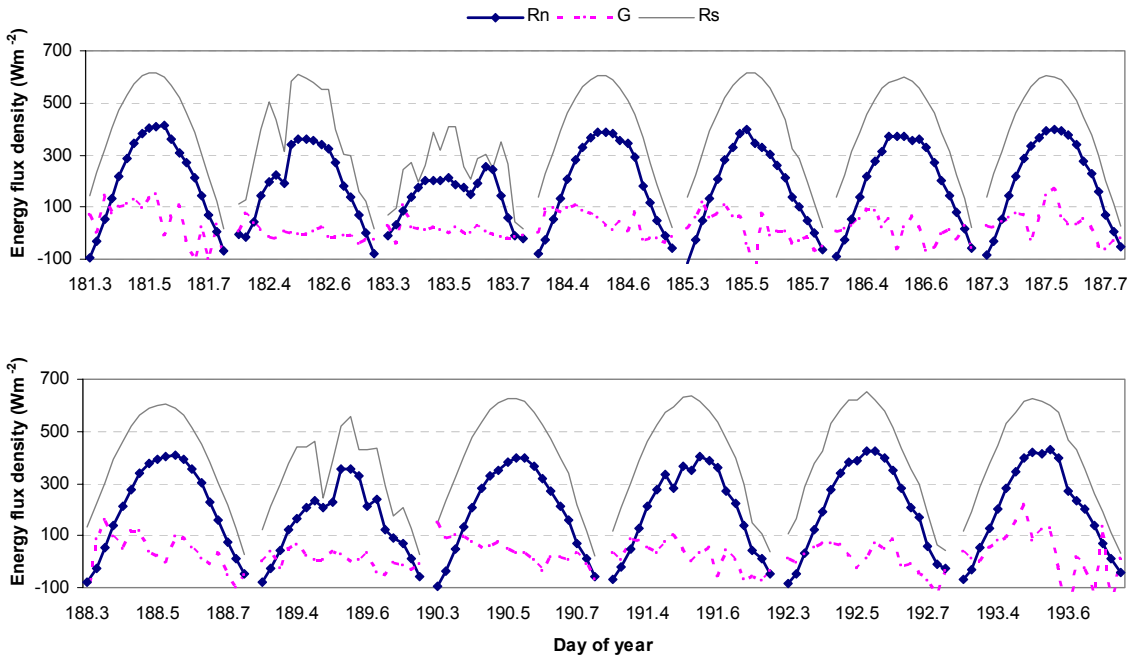

Figure 55 Net irradiance (*Rn*), solar radiation (Rs) and heat stored in water (G) measured at a water surface as part of Case study 7, over the period 30 June to 12 July 2007. Only data for the period 08h00 to 17h00 are shown. The X-axis shows the day of year (DOY) divided into fractions of time, e.g. 181.5 refers to DOY 181 at 12h00.

4.7.3.3 Sensible heat flux density

The sensible heat flux densities (H) of the open water surface were very low (generally less than 40 W m^{-2}) throughout the study period (**Fig. 56**). The sensible heat flux density values normally reached positive peaks early in the morning (between 09h00 and 10h00). Thereafter the *H* values became smaller and towards the afternoon were generally negative (**Fig. 56**). Estimates of *H* with the RM Young sonic anemometer (H RMY) and the surface renewal methods (H SR) compared well (**Fig. 56**) partly because of the initial calibration of the surface renewal data against the RMY data. However, the sensible heat flux estimates of both these system were frequently significantly different from the *H* values calculated with the In Situ Flux eddy covariance system (H IS) and the scintillometer (H LAS) (**Fig. 56**). The *H* values calculated with the scintillometer were the highest of all methods. Linear regressions between the *H* values estimates (30 min time intervals) with the scintillometer (H LAS) and that of the other methods (H IS, H RMY, H SR) showed very poor agreement (**Fig. 57**), with R^2 values of less than 0.43. The *H* values estimated with all the methods did however show similar diurnal patterns.

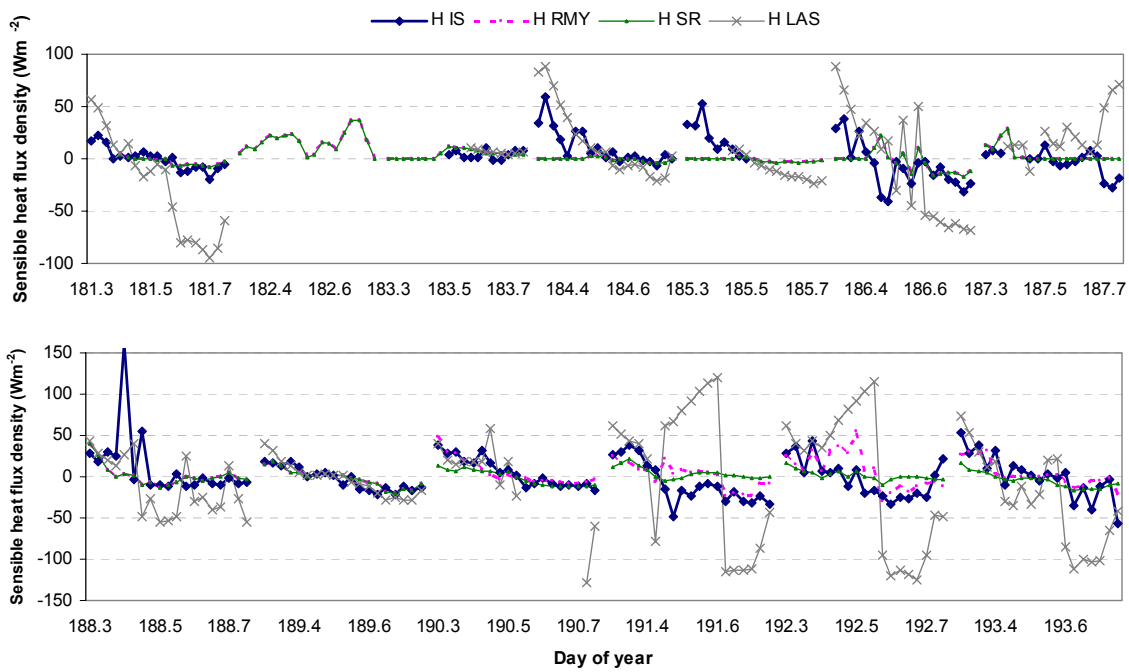

Figure 56 Sensible heat flux density (H) values estimated at the open water surface as part of Case study 7. Sensible heat flux density was measured with the In Situ Flux eddy covariance system (H IS), an RM Young eddy covariance system (H RMY), a surface renewal system (H SR) and a boundary layer scintillometer (H LAS). Data shown are for the period 30 June to 12 July 2007. Only data for the period 08h00 to 17h00 are shown. The X-axis shows the day of year (DOY) divided into fractions of time, e.g. 181.5 refers to DOY 181 at 12h00.

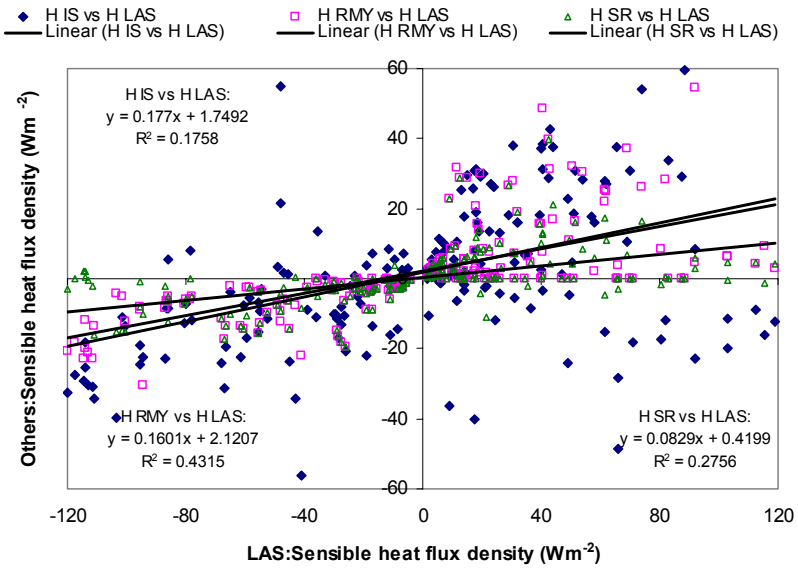

Figure 57 Sensible heat flux densities estimated at the open water surface as part of Case study 7, over the period 30 June to 12 July 2007. On the X-axis sensible heat flux densities estimated with the boundary layer scintillometer (H LAS) are shown, and on the Y-axis, sensible heat flux densities estimated with the In Situ Flux and RM Young eddy covariance systems (H IS, H RMY) and the surface renewal system (H SR).

4.7.3.4 Latent heat flux density

The latent heat flux densities (*LE*s) estimated with the different techniques compared very well and followed similar diurnal trends (**Fig. 58**). *Direct estimates of LE with the In Situ Flux eddy covariance system did not show any agreement with the LEs from the other systems and the data are therefore not shown here.* Towards the end of the measurement period (e.g. DOY 191-193), there was a slightly larger difference between the *LE* values estimated with the different systems. The point-based estimates of *LE* (LE IS EB, LE RMY, LE SR) compared favourably with the spatially averaged estimates of *LE* (LE LAS) (**Fig. 58, 59**). The *LE*s generally agreed to within 9% of each other, and R^2 values exceeded 0.9 (**Fig. 59**). Spatial estimates of *LE* using the scintillometer (LE LAS) generally exceeded all other estimates of *LE* (**Fig. 58, 59**).

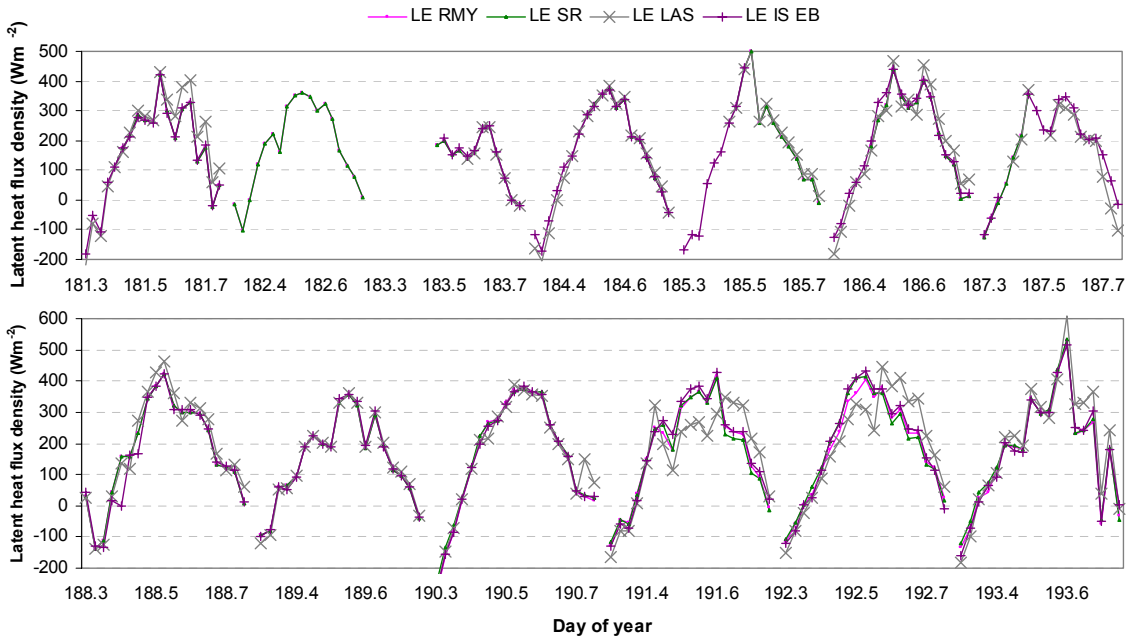

Figure 58 Latent heat flux density (LE) values estimated at the open water surface as part of Case study 7. Latent heat flux density was measured with the In Situ Flux eddy covariance system (LE IS EB), an RM Young eddy covariance system (LE RMY), a surface renewal system (LE SR) and a boundary layer scintillometer (LE LAS). Data shown are for the period 30 June to 12 July 2007. Only data for the period 08h00 to 17h00 are shown. The X-axis shows the day of year (DOY) divided into fractions of time, e.g. 181.5 refers to DOY 181 at 12h00.

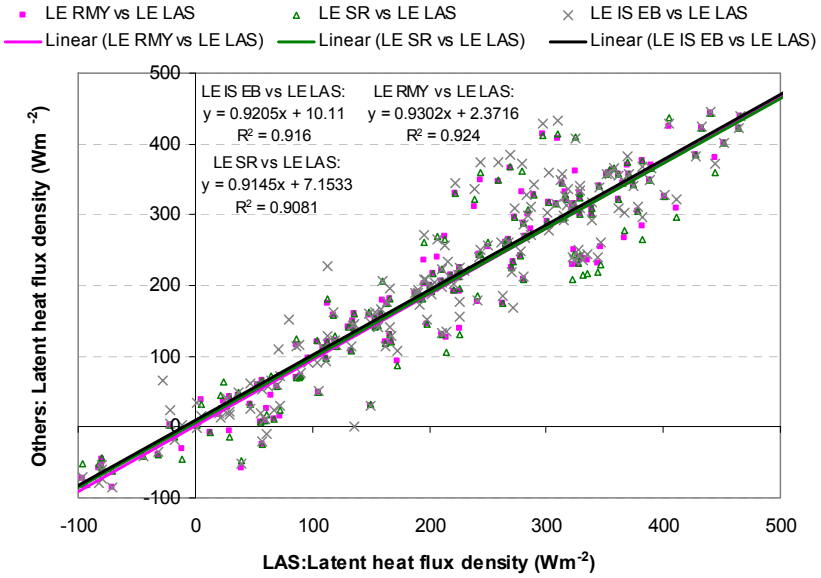

Figure 59 Latent heat flux densities estimated at the open water surface as part of Case study 7, over the period 30 June to 12 July 2007. On the X-axis latent heat flux densities estimated with the boundary layer scintillometer (LE LAS) are shown, and on the Y-axis, latent heat flux densities estimated with the In Situ Flux and RM Young eddy covariance systems (LE IS EB, LE RMY) and the surface renewal system (LE SR).

4.7.3.5 Evaporation

Open water evaporation (E) from a water surface (mm/30 min), estimated with different methods, agreed very favourably (**Fig. 60**). Estimates of E with these methods showed a similar diurnal pattern (**Fig. 60**), with slightly bigger differences in E estimated towards the end of the measurement period as temperature increased. Evaporation rates were the highest during mid-day, with mid-day evaporation values occasionally exceeding 0.3 mm/30 min (**Fig. 60**).

Spatial estimates of evaporation using a scintillometer (E LAS) and the point-based estimates of evaporation with two eddy covariance systems (E IS EB, E RMY), generally agreed to within 9% (**Fig. 60**). The spatial estimates of evaporation using the scintillometer (E LAS) were generally the highest (**Fig. 60**).

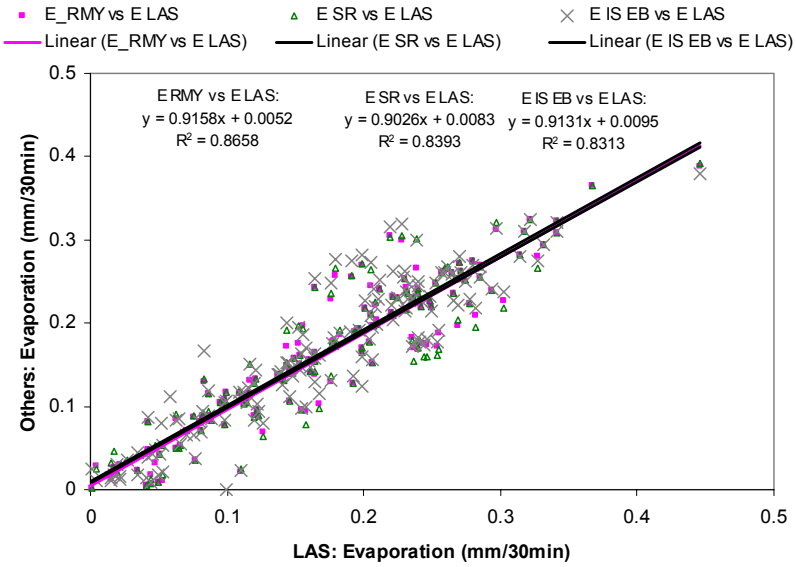

Figure 60 Evaporation (mm/30 min) estimated at the open water surface as part of Case study 7, over the period 30 June to 12 July 2007. On the X-axis the evaporation estimated with the boundary layer scintillometer (E LAS) is shown, while the Y-axis shows evaporation estimated with the In Situ Flux and RM Young eddy covariance systems (E IS EB, E RMY) and the surface renewal system (E SR).

Daily evaporation was calculated for the water surface used in Case study 7, for the period DOY 188 to 193. Estimates with different micrometeorological methods, a Symon's pan, the Penman equation and the Priestley-Taylor equation are compared in **Table 16**. Estimates of evaporation from the different micrometeorological systems (EIS EB, E RMY, E SR, E LAS) were very similar, and over a six-day period, within 5% or 1.1 mm of each other (**Table 16**). The highest evaporation rates were recorded with the boundary layer scintillometer (E LAS). The evaporation estimates with the Symon's pan were very similar to these estimates (to within 7% of the E LAS estimate), but slightly less (**Table 16**). The scintillometer estimated evaporation was 16.07 mm and the Symon's pan estimated evaporation 15.0 mm (**Table 16**). Estimates of evaporation with the Penman and Priestley-Taylor equations exceeded that estimated with the scintillometer over a six-day period (the Penman estimate was noticeably higher at 46.47%).

Table 16 Evaporation (mm d^{-1}) estimated for the open water surface studied in Case study 7. Evaporation was estimated with different methods – the eddy covariance method (EC, ECEB, RMY), surface renewal method (SR), the scintillometer (LAS), Symon's tank and the Penman and Priestley-Taylor equations. Data shown here are for the period DOY 188 to 193. Symons pan data shown here have not been audited.

Date	DOY	Evaporation						
		IS Eddy covariance	RMY Eddy covariance	Surface renewal	Boundary layer scintillometer	Symon's tank	Penman	Priestley-Taylor
		mm/d	mm/d	mm/d	mm/d	mm/d	mm/d	mm/d
07/07/2007	188	2.50	2.64	2.64	2.84	2.00	3.88	3.25
08/07/2007	189	2.18	2.17	2.17	2.17	3.00	3.22	2.42
09/07/2007	190	2.48	2.49	2.52	2.55	2.00	3.70	3.08
10/07/2007	191	2.76	2.62	2.57	2.55	2.00	4.38	3.24
11/07/2007	192	2.90	2.76	2.82	2.94	3.00	4.44	3.24
12/07/2007	193	2.62	2.60	2.69	3.02	3.00	3.92	3.16
7-12 July 07	Sum (188-193)	15.45	15.28	15.40	16.07	15.00	23.54	18.39
	E % LAS	96.16	95.05	95.85	100.00	93.33	146.47	114.43

4.7.4 Summary and conclusions

Heat stored in the water, as measured at 2 min intervals, was highly variable and had to be smoothed for use in the evaporation calculations. Heat stored sometimes accounted for up to 40% of the net radiation at mid-day on sunny days.

Sensible heat flux densities estimated with all the techniques were very small and generally less than 40 W m^{-2}. Sensible heat flux densities estimated with a boundary layer scintillometer, differed from the other sensible heat flux estimates. Latent heat flux densities estimated with all techniques were within 9% of each other.

Daily evaporation estimates with micrometeorological methods compared well to Symon's pan values (within 7%). Evaporation calculated with the Penman equation was significantly higher than all other estimates – over a 6 day period by up to 46.47%.

In general: *Estimates of evaporation from the traditionally used Symon's pan* ***(when well maintained)*** *compared well with estimates of evaporation from more complex systems, during low evaporative (winter) times. Estimates of evaporation with the Penman equation significantly exceeded evaporation estimates with the micrometeorological methods, and sources of error or causes of differences need to be investigated.*

Chapter 5: Guidelines for the Estimating Evaporation

5.1 Introduction

The fourth objective of this project was the "Development of guidelines for the complementary use of measurement and estimation techniques". A simple Decision Support System (DSS), in EXE format, was created and is aimed at (a) aiding users in the selection of a suitable technique for the estimation of total evaporation from a specific surface and (b) providing users with basic information on the selected technique(s).

5.2 How to use the Guidelines Decision Support System?

The programme developed to assist in the selection of a suitable technique for total evaporation estimation, is a simple Decision Support System. It was developed in the Visual Mind™ software programme (Business Edition, version 9.1.0.13). The Guidelines DSS runs through a web browser installed on the computer. The EXE file (on the CD included) needs no installation, but simply needs to be copied to any position on the PC, and then executed.

The user is prompted with simple questions that ultimately lead to the selection of a suitable technique for estimating evaporation. The first question the user is asked is whether the technique to be used is known to the user. If that is the case, the user can select the technique from a list (**Fig. 61**). More information on the specific technique can be obtained by opening or downloading an associated PDF file, which takes the form of a technique specific fact sheet.

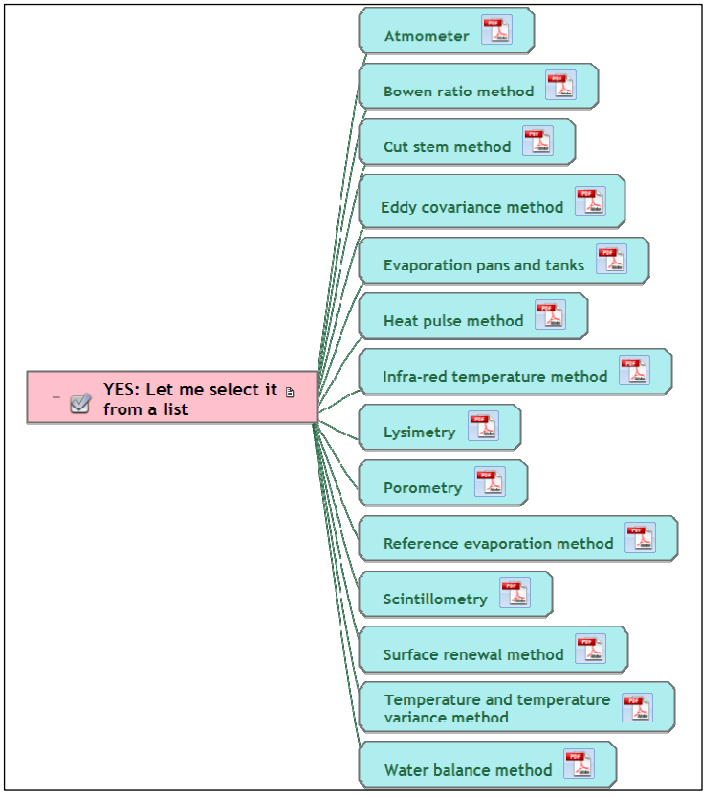

Figure 61 Selecting a suitable method for estimating evaporation from a list of available/known methods in the Guidelines DSS

If the user is unsure of the suitable method for total evaporation estimation (as listed in **Fig. 61**), the user is guided in the selection of a suitable technique through a set of questions, first of all relating to the dominant surface to be studied:

- Is it a bare soil surface?
- Is it an open water surface?
- Is it a vegetated or partly vegetated surface?

If the user wants to study a dominant surface consisting mainly of bare soil, the user is likely interested in estimating soil evaporation only, and therefore only techniques used to determine soil evaporation can be selected. To narrow down the selection of a suitable technique, the user is also prompted on the area of the bare soil surface to be studied (**Fig. 62**). Based on these, suitable techniques are suggested.

If the user is interested in studying evaporation from an open water body, the user is prompted with questions relating to the properties of the open water body. First of all, what the shape of the water body is like: whether the open water body is a dam or lake-like OR river or canal-like (**Fig. 63**). Secondly, the user is prompted on the area of the water body.

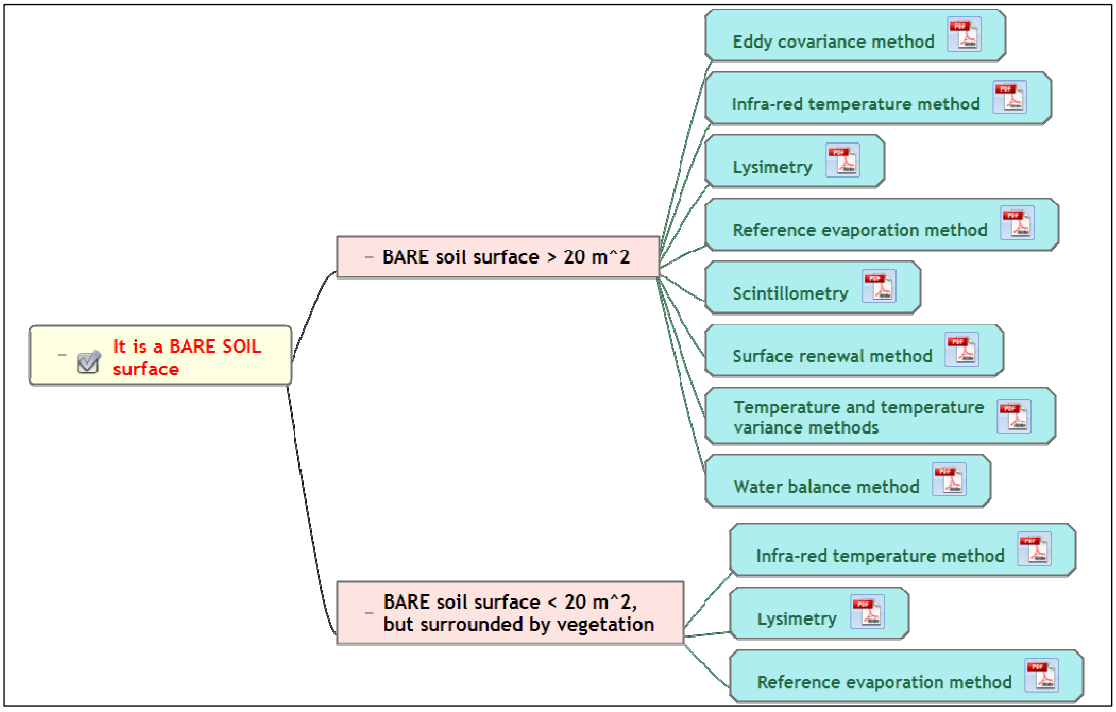

Figure 62 Selecting a suitable method to estimate evaporation from a bare soil surface of variable size – more or less than 20 m^2 – using the Guidelines DSS.

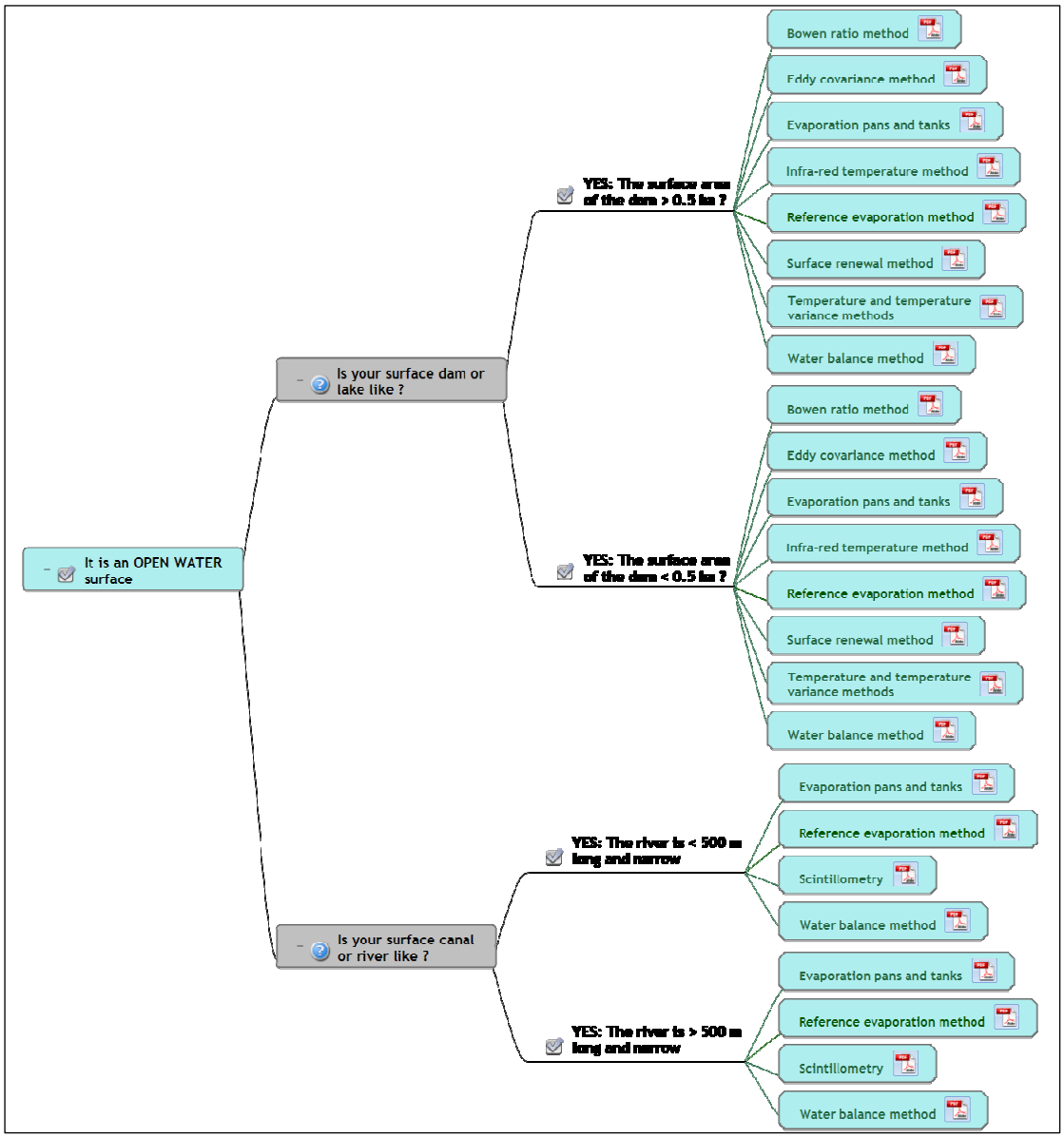

Figure 63 Selecting a suitable method to estimate evaporation from an open water body of variable shape and area using the Guidelines DSS.

If the user is interested in studying a vegetated or partly vegetated surface, the user is likely interested in either estimating total evaporation from that surface, or transpiration from individual plants or stands of plants. To assist the user in selecting the appropriate technique, the user is prompted with questions relating to the composition of plants (homogeneous or heterogeneous), crop cover (complete or incomplete cover) and the fetch:height ratio. Depending on the surface conditions, a number of techniques will be suggested. For example for a surface consisting of different species, a number of techniques are available to estimate total evaporation (**Fig. 64**).

If the surface is homogeneous or covered by an agricultural crop, the user can select whether to estimate total evaporation or transpiration only (**Fig. 65, 66**). If the user wants to determine transpiration only, the user needs to make a selection based on the canopy cover and the fetch to height ratio (**Fig. 65**). But, if the user wants to estimate total evaporation, the user needs to select the fetch to height ratio only (**Fig. 66**).

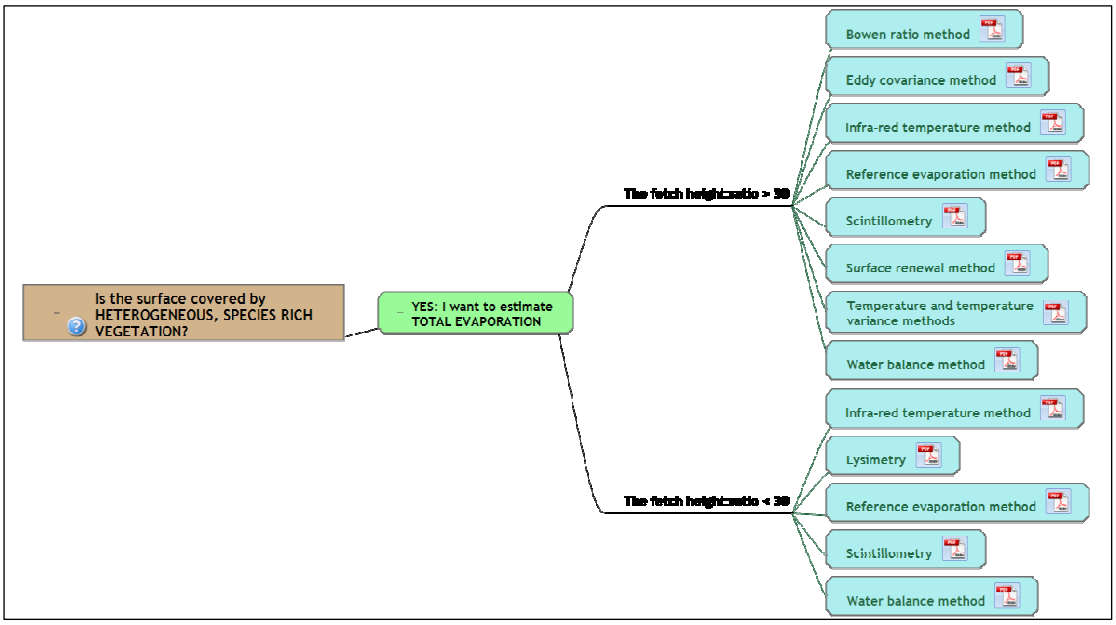

Figure 64 Selecting a suitable method to estimate total evaporation from a heterogeneous surface, rich in different plant species, based on different fetch:height ratios, using the Guidelines DSS.

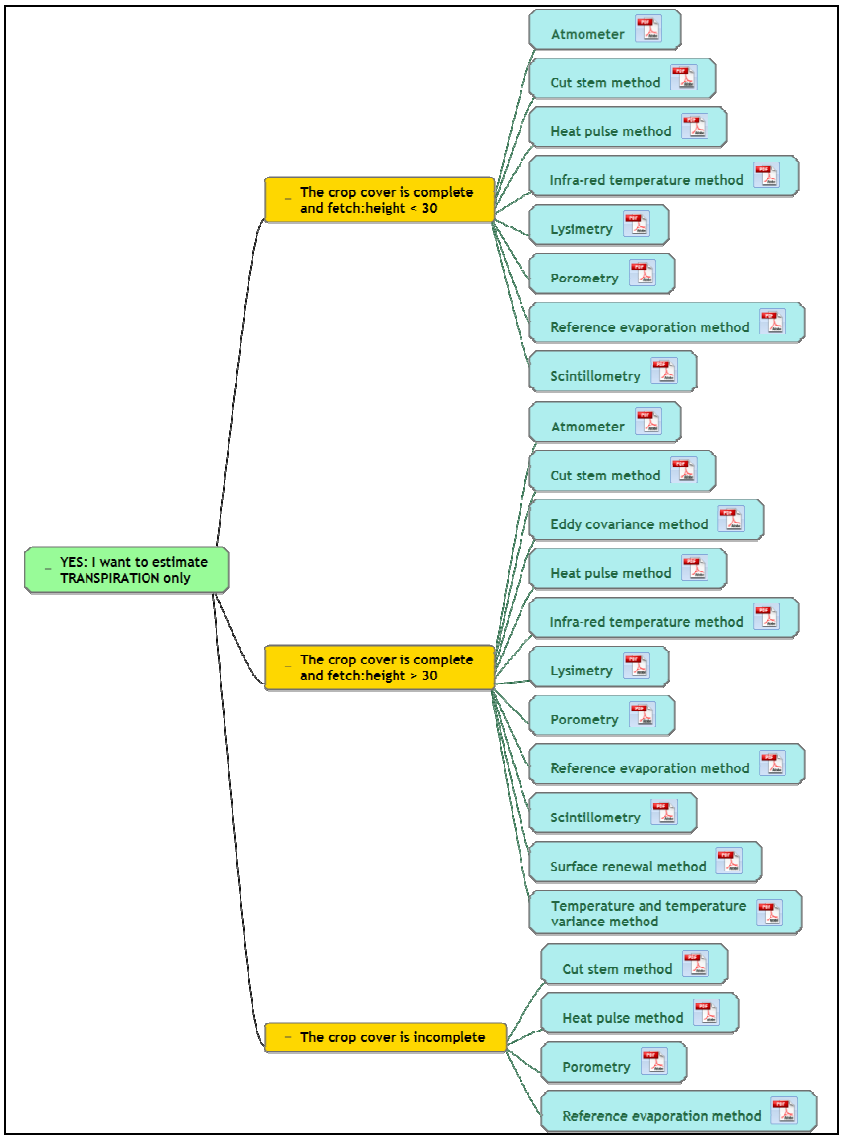

Figure 65 Selecting a suitable method to estimate transpiration of a homogeneous surface or agricultural crop, using the Guidelines DSS.

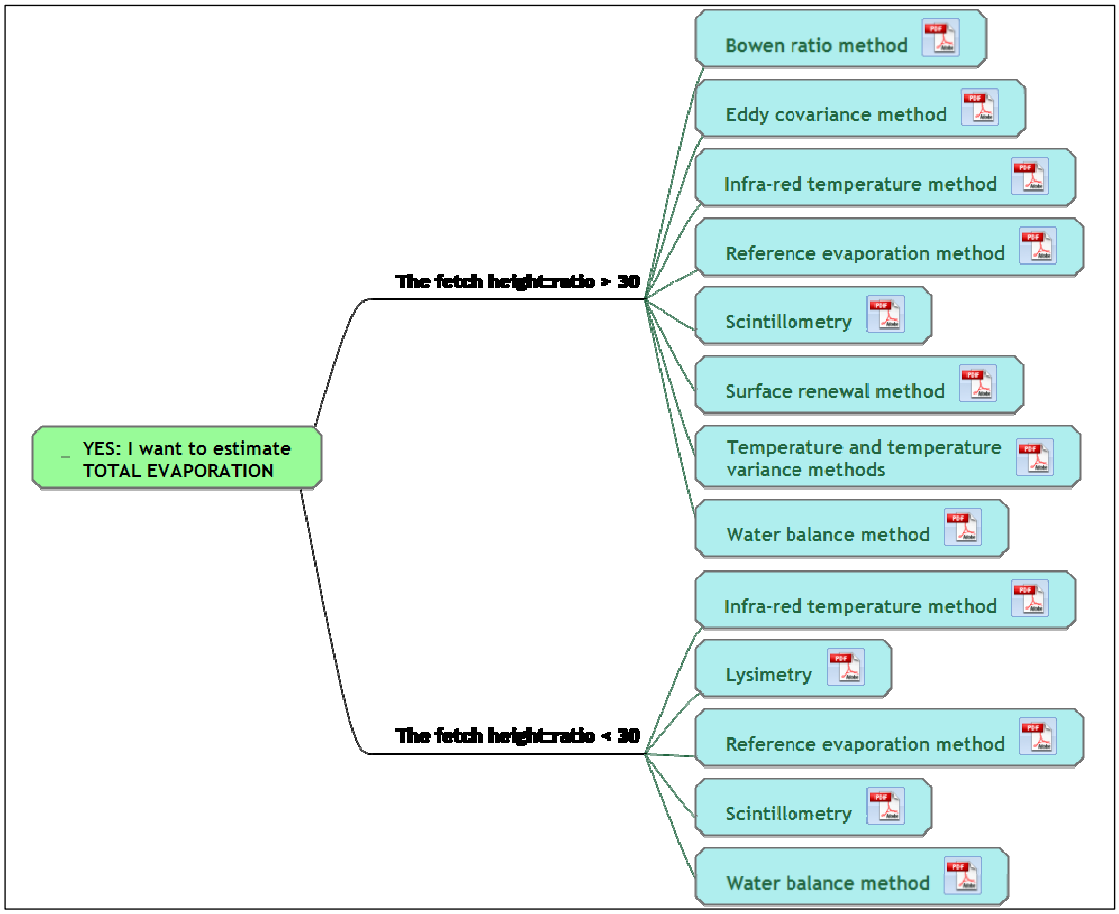

Figure 66 Selecting a suitable method to estimate total evaporation of a homogeneous surface or agricultural crop, using the Guidelines DSS.

5.3 Technique specific fact sheets

More information on the specific technique can be obtained by opening or downloading an associated PDF file from the Guidelines DSS. This PDF takes the form of a technique specific fact sheet. The user can download a fact sheet for each of the following techniques:

- *Atmometer (Fact sheet 1)*
- *Bowen ratio method (Fact sheet 2)*
- *Cut stem method (Fact sheet 3)*
- *Eddy covariance method (Fact sheet 4)*
- *Evaporation pans and tanks (Fact sheet 5)*
- *Heat pulse method (Fact sheet 6)*
- *Infra-red method (Fact sheet 7)*
- *Lysimetry (Fact sheet 8)*
- *Porometry (Fact sheet 9)*
- *Reference evaporation method (Fact sheet 10)*
- *Scintillometry (Fact sheet 11)*
- *Surface renewal method (Fact sheet 12)*
- *Temperature and temperature variance method (Fact sheet 13)*
- *Water balance method (Fact sheet 14)*

All the Fact sheets are included in Appendix 1.

Each fact sheet contains basic information on the specific technique or method, including information on the:

- *Type of method*
- *Spatial scale for application*
- *Averaging period*
- *Theoretical basis*
- *Main assumption*
- *Measurements required*
- *Minimum set of sensors required*
- *Fetch:height requirements (where applicable)*
- *Suitable surfaces for application*
- *Advantages and disadvantages of method*
- *Supplier*
- *References to method*

In addition to this information, it is stated whether the method provides an estimate of (a) transpiration, evaporation, total evaporation or reference evaporation, (b) the approximate cost of a system, (c) ease of use of the method, (d) whether historical data are or can be used, or whether new data are collected, (e) whether the method is more suited to operational application or research and (f) whether this method is simple or complex.

5.4 How to reference this Guidelines Decision Support System?

The Guidelines document can be distributed freely. However, please acknowledge the researchers involved in the development, and the Water Research Commission as the funding agent. Please use the following reference:

Jarmain, C., Clulow, A.D., Mengistu, M.G., Everson, C., Gush, M.B. and Savage, M.J. 2008. Guidelines for the selection of an appropriate evaporation estimation technique. Decision Support System designed as part of a Water Research Commission funded project, K5/1567.

5.5 Queries or suggestions

For any queries relating to this decision support system "Guidelines for the selection of an appropriate evaporation estimation technique", please contact *Dr. Caren Jarmain*, at cjarmain@csir.co.za.

Chapter 6: CONCLUSIONS AND RECOMMENDATIONS

Evaporation estimation remains one of the important challenges for the agricultural and environmental sciences. Determination of reliable and representative evaporation data is an important issue of atmospheric research with respect to applications in agriculture, catchment hydrology and the environmental sciences, not only in South Africa but also elsewhere in the world. Techniques for long-term measurements of evaporation at different time scales and from different climatic regions are not yet readily available, though a number of different methods are available for shorter term measurements. Methods like the scintillometer and temperature-based aerodynamic methods are becoming more popular and hold great potential for long-term application and estimation of evaporation over different spatial scales. The scintillometer has the advantage of the large areal representation of the measurements and real-time monitoring but the method is costly. The temperature-based methods, such as the surface renewal method, have low cost and low power requirements. In some cases real-time estimations of evaporation are possible for the temperature-based methods.

Eight possible areas for future research and activities are presented here in relation to the progress made in the current programme of research:

1. There is a dearth of technologists trained in the area covered by this research project. This has negative long-term consequences. This project attempted to address this through conducting a training workshop. This should be aggressively pursued through regularly conducting similar workshops. Different agencies within South Africa are using different methods – hopefully there can be some sharing of knowledge and data and working towards a common approach in future.

2. The aspect of fetch and the footprint of evaporation estimates were not the main focus of this report. However, these important aspects must receive continuing attention especially since more and more research is being conducted on indigenous and invasive vegetation. Some of the sites chosen for evaporation measurement were at the limit of inadequate fetch and this aspect needs to be considered in more detail in relation to footprints. For example only one footprint model was applied in this research.

3. The lack of energy balance closure is another area that has frustrated energy balance methods and the consequential estimation of evaporation. This aspect needs further research, which should also involve the estimation of evaporation from the high frequency measurements of water vapour pressure using an approach similar to the SR approach for high frequency air temperature.

4. The contribution and importance of advected energy (local and regional) to the energy balance of arid environments, especially where total evaporation from riparian zones needs to be estimated, also need to be assessed. With an increased interest in these arid environments and especially the water use requirements of ground water dependent ecosystems, it is important to understand limitations of micrometeorological systems if applied under these environmental conditions.

5. Ground-based methods for estimating evaporation will always be in demand. These measurements are required to validate the remote estimates determined using spatial methods. The merging of these technologies will see much progress in the near future for near real time water resources management.

6. Water resources management on a catchment scale is normally based on catchment water balance modelling. Advances in technologies like the microwave scintillometry system which provides estimates of evaporation over several kilometres (~15 km) can provide opportunities for improved catchment water balance modelling. Estimated and measured evaporation from small catchments can be compared directly for the first time ever. Especially when linked to remotely sensed data, this combination of measurement and modelling could hold great potential and needs to be investigated.

7. A complete, on site, real-time, sub-hourly, inexpensive and simple method for estimation evaporation has not yet been achieved. It has been suggested that high frequency air temperature-based methods, of which the surface renewal method is one, may pave the way for evaporation stations from which real-time and sub-hourly estimates may be obtained relatively inexpensively. It is in this area that future research should also be continued.

8. Especially for water resources management of dams and reservoirs, a real-time, sub-hourly, inexpensive and simple method for estimation evaporation is required. Since the size of the dam or reservoir can differ greatly, and so also the water quality, all affecting evaporation rates, it is in this area that future research should also be continued.

Chapter 7: References

Abezghi T.W., 2003. Estimation of reference evaporation and comparison with Et-gauge evaporimeter. M.Sc. Agric. Thesis, University of Natal, 166 pp.

Allen R.G., Pereira L.S., Raes D., Smith M., 1998. Crop evaporation: Guidelines for computing crop water requirements, FAO Irrigation and Drainage Paper no. 56. Food and Agriculture Organization of the United Nations, Rome, Italy. ISBN 92-5-104219-5.

Allen R.G., Pruitt W.O., Wright J.L., Howell T.A., Ventura F., Snyder R., Itenfisu D., Steduto P., Berengena J., Yrisarry J.B., Smith M., Pereira L.S., Raes D., Perrier A., Alves I., Walter I., Elliott R., 2006. A recommendation on standardized surface resistance for hourly calculation of reference ET_o by the FAO56 Penman-Monteith method. Agric. Water Manage. 81, 1–22.

Anandakumar K., 1999. Sensible heat flux over a wheat canopy: optical scintillometer measurements and surface renewal analysis estimates. Agric. For. Meteorol. 96, 145-156.

Bezuidenhout C.N., Lecler N.L., Gers C. and Lyne P.W.L., 2006. Regional based estimates of water use for commercial sugar-cane in South Africa. Water SA 32 (2). ISSN 0378-4738.

Bosman H.H., 1990. Methods to convert American Class A-pan and Symon's tank evaporation to that of a representative environment. Water SA 16 (4), 227-236.

Bowen ratio definition at http://earthstorm.mesonet.org/materials/b.php accessed on 19 March 2008 at 11:41.

Bowen I.S., 1926. The ratio of heat losses by conduction and by evaporation from any water surface. Physical Review 27, 779-787.

Bristow K.L., de Jager J.M., 1981. A proposed technique to measure evapotranspiration using micrometeorological methods. Water SA 7 (1), 49-53.

Brueckner A.E., 1944. Transpiration studies of some Natal thornveld trees. S. Afr. J. Sci. 41, 186-193.

Brutsaert W.H., 1982. Evaporation Into the Atmosphere. Theory, History, and Applications. D. Reidel Publishing Co, Dordrecht, Holland. 299 pp.

Burger, C. 1999. Comparative evaporation measurements above commercial forestry and sugarcane canopies in the KwaZulu-Natal Midlands. Unpublished M.Sc. Agric. Thesis, University of Natal, Pietermaritzburg, KwaZulu Natal, South Africa.

Burgess S.S.O., Adams M.A., Turner N.C., Beverly C.R., Ong C.K., Khan A.A.H., Bleby T.M., 2001 An improved heat pulse method to measure low and reverse rates of sap flow in woody plants. Tree Physiol. 21, 589-598.

Castellvi F., 2004. Combining surface renewal analysis and similarity theory: A new approach for estimating sensible heat flux. Water Resour. Res. 40 W05201 doi:10.1029/2003WR002677, 1-20.

Castellvi F., Martinez-Cob A., Perez-Coveta O., 2006. Estimating sensible and latent heat fluxes over rice using surface renewal. Agric. For. Meteorol. 139, 164-169.

Cava D., Contini D., Donateo A., Martano P., 2008. Analysis of short-term closure of the surface energy balance above short vegetation. Agric. For. Meteor., in press.

Cellier P., Olioso A., 1993. A simple system for automated Bowen ratio measurement. Agric. For. Meteorol., 66, 81–92.

Clulow A.D., 2008. The long-term measurement of total evaporation over Acacia mearnsii using large aperture scintillometry. Unpublished M.Sc. thesis, University of KwaZulu Natal, Pietermaritzburg, South Africa.

Dalton J. 1801. On the constitution of mixed gases; on the force of steam or vapour from water or other liquids in different temperatures, both in a Torricellian Vacuum and in air; on evaporation: and on the expansion of gases by heat. Mem. Lit. Phil. Soc., 5, 366-535.

De Clercq W.P., Fey M.V.(eds). 2007. Land use impacts on salinity in Western Cape waters. Draft final report to the Water Research Commission on Water Research Commission Project No. K5/1503.

Drexler J.Z., Snyder R.L., Spano D., Paw U K.T., 2004. A review of models and micrometeorological methods used to estimate wetland evapotranspiration. Hydrological Processes 18, 2071-2101.

Du Preez C.M.R., 1964. Die transpirasie van ´n aantal Karoobossoorte. Unpublished M.Sc. Thesis, University of the Orange Free State, Bloemfontein, South Africa.

DWAF, 2007. Information on South African dams. Hydrological services, Department of Water Affairs and Forestry. Available at http://www.dwaf.gov.za/hydrology/dwafapp2_wma/. Accessed October 29, 2007.

Dye P.J., 2006. Evaluation of managed vegetative cover for the dams area, Vumbuka reserve, KwaZulu-Natal: Modelling the slimes dam water balance under grass-and tree-dominated vegetation. CSIR Report no. CSIR/NRE/ECO/ER/2006/0193/C, Pretoria, South Africa.

Dye P.J., Le Maitre, D.M., Jarmain, C., Everson, C.S., Gush, M.B., and Clulow, A. Submitted to the WRC. Development of a system of simplified models of vegetation water use based on the principle of limits to ET in different categories of vegetation. Water Research Commission, Pretoria. Draft.

Dye P.J., Bosch J.M., 2000. Sustained water yield in afforested catchments - the South African experience. In: von Gadow K., Pukkala T., Tomé M. (eds), Sustainable Forest Management. Kluwer Academic Publishers, Dordrecht, The Netherlands , pp. 99–120.

Dye P.J., Olbrich B.W., 1993. Estimating transpiration from 6-year-old Eucalyptus grandis trees: development of a canopy conductance model and comparison with independent sap flux measurements. Plant Cell Environ. 16, 45–53.

Dye P.J., Poulter A.G., Soko S. and Maphanga D. 1997b. The determination of the relationship between transpiration rate and declining available water for Eucalyptus grandis. Water Research Commission Report No. 441/1/97, Pretoria, South Africa.

Dye P.J., Soko S., Maphanga D., 1997a. Intra-annual variation in water use efficiency of three clones in Kwa Mbonambi, Zululand. CSIR report ENV/P/C 97048, Pretoria, South Africa.

Dye P.J., Soko S., Poulter A.G., 1996. Evaluation of the heat pulse velocity method for measuring sap flow in Pinus patula. J. Exp. Bot. 47, 975–981.

Dye, P.J., Gush, M.B., Everson, C.S., Jarmain, C., Clulow, A.D., Mengistu, M. and Geldenhuys, C. 2007. Report on alternative modelling approaches to determine water use for stands of indigenous tree species. Deliverable report of WRC project K5/1462: Water use in relation to biomass of indigenous tree species in woodland, forest and/or plantation conditions.

Dye, P.J., Gush, M.B., Everson, C.S., Jarmain, C., Clulow, A.D., Mengistu, M., Geldenhuys, C., Wise, R., Scholes, R., Archibald, A., Savage, M. 2008. Water use in relation to biomass of indigenous tree species in woodland, forest and/or plantation conditions. Report to the Water Research Commission.

Everson C.S., 1979. Autecological studies on *Philippia evansii* M.E.BR. with particular reference to water relations. Unpublished M.Sc. Thesis, University of Natal, Pietermaritzburg, South Africa.

Everson, C.S., 1994. Investigating the feasibility of using Bowen ratio technology to measure evaporation from the Orange River. CSIR, Divion of Forest Science and Technolgy Report Number FOR-C 238.

Everson C.S., 1999. Evaporation from the Orange river: Quantifying open water resources. Report to the Water Research Commission. WRC report no. 683/1/99, Pretoria, South Africa.

Everson C.S., 2001. The water balance of a first order catchment in the montane grasslands of South Africa. J. Hydrol. 241, 110-123.

Everson, C.S., Clulow, A. and Mengistu, M. 2008. Feasibility Study On The Determination of Riparian Evaporation in Non-Perennial Systems: Report on the Early Summer and Summer Field Trips. Deliverable No. 1 & 2, CSIR, Natural Resources and the Environment, Water Research Commission Project K5/775.

Everson, C.S., Ghezehei, S., Gush, M.B. and Everson, T. 2007. Agroforestry Systems For Improved Food Production Through The Efficient Use Of Water: Deliverable 9 – 2007. Measurements Of Water Dynamics, Soil Fertility And Plant Productivity. Deliverable No. 9 submitted to the Water Research Commission, Project K5/1480.

Everson C.S., Molefe G.L., Everson T.M., 1998. Monitoring and modelling components of the water balance in a grassland catchment in the summer rainfall area of South Africa. Water Research Commission Report No. 493/1/98, Pretoria, South Africa.

Finch J.W., 2001. A comparison between measured and modelled open water evaporation from a reservoir in south-east England. Hydrol. Process. 15, 2771-2778.

Finnigan J. J., Clement R., Malhi Y., Leuning R., Cleugh H.A., 2003. A re-evaluation of long-term flux measurement techniques part I: averaging and coordinate rotation. Boundary-Layer Meteorol. 107, 1573-1472.

Foken T., 2006. 50 years of the Monin–Obukhov similarity theory. Boundary-Layer Meteorol. 119, 431–447.

Fritschen, L.J., Fritschen, C.L., 2005. Bowen ratio energy balance method. In: Hatfield, J.L., Baker, J.M. (Eds), Micrometeorology in Agricultural Systems Agronomy Monograph no. 47. pp. 397-405.

Gay L.W., Greenberg R.J., 1985. The AZET battery powered Bowen ratio system. Proc. 17th Conf. Agric. For. Meteorol. 7, 329–334.

Green G.C., Clothier B.E., 1988. Water use of kiwifruit vines and apple trees by the heat-pulse technique. J. of Exp. Bot. 39 (198), 115-123.

Green G.C., Burger W.P.J., Conradie, 1974. Lysimetric determination of citrus tree evapotranspiration. Agrochemophysica 6,35-42.

Ham J.M., Heilman J.L., 2003. Experimental test of density and energy-balance corrections on carbon dioxide flux as measured using open-path eddy covariance. Agron. J. 95, 1393-1403.

Heilman J.L., Brittin C.L., Neale C.M.U., 1989. Fetch requirements for Bowen-ratio measurements of latent and sensible heat fluxes. Agric. For. Meteorol. 44, 261-273.

Henrici M., 1940. The transpiration of different plant associations in South Africa. Part 1 – Transpiration of Karroo bushes. Union of South Africa. Department of Agriculture and Forestry Science Bulletin No. 185. (Plant Industry Series No. 39).

Henrici M., 1942. Transpiration of grasses in the sour mountain grassveld of the Drakensberg in comparison with the water loss of indigenous forests. S. Afr. J. Sci. 39, 155-163.

Hensley M., Anderson J.J., Botha J.J., van Staden P.P., Singels A., Prinsloo S., du Toit A., 1997. Modelling the water balance on benchmark ecotopes. Water Research Commission Report No. 508/1/9, Pretoria, South Africa.

Hill R.J., 1992. Review of optical scintillation methods of measuring the refractive-index spectrum, inner scale and surface fluxes. Waves in Random and Complex Media 2, 179-201.

Huschke R.E., 1959 (Editor). Glossary of Meteorology, Am. Meteorol. Soc., Boston, Massachusetts, USA, 638 pp.

Hutson J.L., Green G.C., W.S. Meyer, 1980. A weighing lysimeter facility at Roodeplaat for crop evapotranspiration studies. Water SA 6, 41-45.

Jackson R.D., Idso S.B., Reginato R.J., Pinter Jr. P.J., 1981. Canopy temperature as a drought stress indicator. Water Resour. Res. 17, 1133-1138.

Jarmain C., Everson C.S., 2002. Comparative evaporation measurements above commercial forestry and sugarcane canopies in the KwaZulu-Natal Midlands. CSIR Report no. ENV-C-S 2002-005, Pretoria, South Africa.

Jarmain, C. 2003. Potential for using trees to limit the ingress of water into mine workings: A comparison of total evaporation and soil water relations for Eucalyptus and grassland. Unpublished PhD (Agrometeorology) Thesis, University of Natal, Pietermaritzburg, KwaZulu Natal, South Africa.

Jarvis P.G., 1976. The interpretation of the variations in leaf water potential and stomatal conductance found in canopies in the field. Philosophical Transactions of the Royal Society of London B. 273, 593-610.

Kite G., Droogers P., 2000. Comparing estimates of actual evapotranspiration from satellites, hydrological models, and field data: A case study from Western Turkey. International Water Management Institute Research Report no. 42, 32 pp.

Lewis, J.M. 1995. The Story behind the Bowen ratio. Bulletine of the American Meteorological Society 76 (2), 2433-2443.

Lightbody, K.E., 1993. Use of a stem steady state heat energy balance technique for the measurement of sap flux in Eucalyptus grandis. M.Sc.Agric. thesis, Department of Agronomy, University of Natal. Pp 113.

Liu H., Randerson J.T., Lindfors J., Massman W.J., Foken T., 2006. Consequences of incomplete surface energy balance closure for CO_2 fluxes from open-path CO_2/H_2O infrared gas analysers. Boundary-Layer Meteorol 120, 65-85.

Lukangu, G., 1998. Bowen ratio and surface temperature techniques for measuring evaporation from cabbages. M.Sc.Agric., University of Natal. Pp. 166.

Marsh P., Bigras S.C., 1988. Evaporation from Mackenzie delta lakes, N.W.T., Canada. Arctic and Alpine Research 20 (2), 220-229.

Marshall D.C., 1958. Measurement of sap flow in conifers by heat transport. Plant Physiol. 33, 385–396

McKenzie, R.S. and A. R. Craig, 2001. Evaluation of river losses from the Orange River using hydraulic modelling. J. Hydrol. 241, 62-69.

Mengistu M G, 2003. The use of infrared thermometry for irrigation scheduling of cereal rye (*Secale cereale L.*) and annual ryegrass (*Lolium multiflorum Lam*.). Unpublished M.Sc. Agric. Thesis, University of Natal, Pietermaritzburg, KwaZulu Natal, South Africa. pp 109.

Mengistu M.G., Savage M.J., 2006. Estimation of evapotranspiration from different plant canopy surfaces using a surface renewal method. Oral presentation to the Combined Congress 2006, South African Society of Crop Production/Soil Science Society of South Africa, 23 to 26 Jan. 2006, Durban, South Africa.

Mengistu M.G., Savage M.J., 2007. Evapotranspiration measurement for a silvopastoral system consisting of *Jatropha* and Kikuyu grass. Paper presentation to the Combined Congress 2006, South African Society of Crop Production/Soil Science Society of South Africa, 29 Jan to 1 Feb. 2007, Badplaas, South Africa.

Mengistu, M.G., 2008. Heat and energy exchange above different surfaces using surface renewal. Unpublished PhD thesis, University of KwaZulu-Natal, Pietermaritzburg, South Africa. Pp. 151.

Mes M.G., Aymer-Ainslie K.M., 1935. Studies on the water relations of grasses. 1. Themeda triandra Forsk. S. Afr. J. Sci. 32, 280-304.

Meyers T.P., Baldocchi D.D., 2005. Current micrometeorological flux methodologies with applications in agriculture. In: Hatfield, J.L., Baker, J.M. (Eds), Micrometeorology in Agricultural Systems Agronomy Monograph no. 47, pp. 381-396.

Olbrich B.W., 1994. The application of the heat pulse velocity technique to the study of transpiration from *Eucalyptus grandis*. Unpublished PhD thesis, University of the Witwatersrand, Johannesburg, South Africa.

Olivier F.C., Singels A., 2007. Effect of a trash blanket on irrigation water use efficiency of sugar cane. ISSCT XXVIth congress Durban, South Africa 29th July - 2nd August 2007.

Olivier F.C., Lecler N.L., Singels A., Van Antwerpen R., 2006. Increasing water use efficiency and yield of irrigated sugarcane by means of good agronomic practices. Deliverable 4: Progress Report On Plant Crop Field Trials. A Report For The Water Research Commission Project K5/1577/4, Pretoria, South Africa.

Paw U K.T., 1992. Development of models for thermal infrared radiation above and within plant canopies. J. Photogrammetry Remote Sens. 47, 189-203.

Paw U K.T., Brunnet Y., 1991. A surface renewal measure of sensible heat flux density. In: Preprints, 20th Conference on Agricultural and Forest Meteorology, 10-13 September, Salt Lake City, UT. American Meteorological Society, Boston, MA, pp. 52-53.

Paw U K.T., Brunnet Y., Collineau S., Shaw R.H., Maitani T., Qui J., Hipps L., 1992. On coherent structure in turbulence within and above agricultural plant canopies. Agric. For. Meteorol. 61, 55-68.

Paw U, K.T., Snyder, R.L., Spano, D., Su, H.-B., 2005. Surface renewal estimates of scalar exchange. In: Hatfield, J.L., Baker, J.M. (Eds), Micrometeorology in Agricultural Systems Agronomy Monograph no. 47. Pp. 455-483.

Paw U K.T., Snyder R.L., Spano D., Su H.B., 2005. Surface renewal estimates of scalar exchange. In: Hatfield J.L., Baker J.M. (Eds), Micrometeorology in Agricultural Systems Agronomy Monograph no. 47, pp. 455-483.

Paw U K.T., Qiu J., Su H.B., Watanabe T., Brunnet Y., 1995. Surface renewal analysis: a new method to obtain scalar fluxes without velocity data. Agric. For. Meteorol. 74, 119-137.

Penman H.L., 1948. Natural evaporation from open water, bare soil and grass. Proc. Royal Soc. London A193, No. 1032, 120-145.

Priestley C.H.B. and Taylor R.J. 1972. On the assessment of surface heat flux and evaporation using large-scale parameters. Monthly Weather Review 100: 81–92.

Qui J., Paw U K.T., Shaw R.H., 1995. Pseudo-wavelet analysis of turbulence patterns in three vegetation layers. Boundary-Layer Meteorol. 72, 177-204.

Ritchie J.T., 1972. A simple method of estimating the soil water balance. Agric. Meteorol. 28, 1-7.

Roberts J., 1977. The use of tree-cutting techniques in the study of the water relations of mature *Pinus sylvestris L*. Journal of Experimental Botany 28 (104), 751-76.

Rosenberg N.J., Blad B.L., Verma S.B., 1983. Microclimate: The Biological Environment. 2nd edition. Wiley, New York, USA, 495 pp.

Rosenberry D.O., Winter T.C., Buso D.C., Likens G.E., 2007. Comparison of 15 evaporation methods applied to a small mountain lake in the northern USA. J.Hydrol. 340, 149-156.

Savage M.J., 2007. Sensible heat estimation using a high frequency temperature-based method above various canopies. Paper presentation to the 13th SANCIAHS Conference, 6 to 7 September, Cape Town, South Africa.

Savage, M.J., 2008. Estimation of evaporation using a dual-beam surface layer scintillometer and component energy balance measurements. Agric. For. Meteorol. In press.

Savage, M.J. and Vermeulen, K. 1983. Microclimate modification of tall moist grasslands of Natal by spring burning. Journal of Range Management 36, 172-174.

Savage M.J., Abezghi T., Johnston M.A., 2002. Atmospheric emittance minus crop emittance under clear skies for calculating grass reference evaporation and comparison with an automation ET-Gage Atmometer reference evaporation. Combined SASHS and SASCP congress, 15th to the 17th January 2002, Pietermaritzburg, South Africa.

Savage M.J., Everson C.S., Metelerkamp B.R. 1997. Evaporation measurement above vegetated surfaces using micro-meteorological techniques. Water Research Commission Report No. 349/1/97, Pretoria, South Africa. ISBN No: 1 86845 363 4.

Savage M.J., Everson C.S., Odhiambo G.O., Mengistu M.G., Jarmain C., 2004. Theory and practice of evaporation measurement, with a special focus on SLS as an operational tool for the estimation of spatially-averaged evaporation, Water Research Commission Report No. 1335/1/04, Pretoria, South Africa. ISBN 1-77005-247-X.

Savage M.J., Heilman J.L., McInnes K.J., Gesch R.W., 1995. Placement height of eddy correlation sensors above a short grassland surface. Agric. For. Meteorol. 74, 195-204.

Savage M.J., McInnes K.J., Heilman J.L., 1996. The "footprints" of eddy correlation sensible heat flux density and other micrometeorological measurements. S. Afr. J. Sci. 92, 137-142.

Savage M.J., Mengistu M.G., 2006. Evaporation estimation using a high frequency temperature-based method and the simplified energy balance. Paper presentation to the South African Society of Atmospheric Sciences, Bloemfontein, South Africa.

Savage M.J., Odhiambo G.O., Mengistu M.G., Everson C.S., Jarmain, C., 2005. Theory and practice of evaporation measurement, with special focus on surface layer scintillometry as an operational tool for the estimation of spatially-averaged evaporation. Oral presentation to the 12th SANCIAHS Conference, 5 to 7 th September 2005, Midrand, Gauteng.

Scholes R.J., Savage M.J.S., 1989. Studying water in the soil-plant-atmosphere continuum: a bibliographic guide to techniques. South African National Scientific Programmes Report No. 163.

Schotanus P., Nieuwstadt F.T.M., de Bruin H.A.R., 1983. Temperature measurement with a sonic anemometer and its application to heat and moisture fluctuations. Boundary-Layer Meteorol. 26, 81-93.

Scintec, 2006. Scintec boundary layers scintillometer user manual for BLS450, BLS900 and BLS2000 (including BLSDMI/1 option). Scintec AG. 56 pp. www.scintec.com

Singels A., Kennedy A.J., Bezuidenhout C.N., 1998. IRRICANE: A simple computerised irrigation scheduling method for sugarcane, Proc. S. Afr. Sug. Technol. Ass. 72, 117-122.

Slavik B., 1974. Methods of studying plant water relations. Springer-Verlag, Berlin, Heidelberg, New York.

Smith D.M., Allen S.J., 1996. Measurement of sap flow in plant stems. J. of Experimental Botany, 47 (305), 1833-1844.

Snyder R.L., Spano D., Paw U K.T., 1996. Surface renewal analysis for sensible heat and latent heat flux density. Boundary-Layer Meteorol. 77, 249-266.

Spano D., Snyder R.L., Duce P., Paw U K.T., 2000. Estimating sensible and latent heat flux densities from grape vine canopies using surface renewal. Agric. For. Meteorol. 104, 171-183.

Stanhill G., 2002. Is the Class A evaporation pan still the most practical and accurate meteorological method for determining irrigation water requirements? Agric. For. Meteorol. 112, 233–236.

Stannard D.I., 1997. A theoretically based determination of Bowen-ratio fetch requirements. Boundary-Layer Meteorol. 83, 375-406.

Stannard D.I., Blanford J.H., Kustas W.P., Nichols W.D., Amer S.A., Schmugge T.J., Weltz M.A., 1994. Interpretation of surface flux measurements in heterogeneous terrain during the Monsoon '90 experiment. Water Resour. Res. 30, 1227-1239.

Sverdrup H.U., 1943. On the ratio between heat conduction from the sea surface and the heat used for evaporation. Ann. N. Y. Acad. Sci. 68, 81-88.

Swanson R.H., Whitfield D.W.A., 1981. A numerical analysis of heat pulse velocity theory and practice. J. Exp. Bot. 32, 221–239.

Swinbank W.C., 1951. The measurement of vertical transfer of heat and water vapour by eddies in the lower atmosphere. J. Met. 8, 135-145.

Tanner B.D., Greene J.P., Bingham G.E., 1987. A Bowen ratio design for long term measurements. Am. Soc. Agric. Eng. Tech. Paper no. 87 2503, Am. Soc. Agric. Eng., St. Joseph, MI.

Thiermann V., 1992. A displaced-beam scintillometer for line-averaged measurements of surface layer turbulence. 10th Symposium on turbulence and diffusion. Portland, Oregon, USA.

Thiermann V., Grassl, H., 1992. The measurement of turbulent surface-layer fluxes by use of bichromatic scintillation. Boundary-Layer Meteorol. 58, 367-389.

Tillman J. E., 1972. The indirect determination of stability, heat and momentum fluxes in the atmospheric boundary layer from simple scalar variables during dry unstable conditions, J. Appl. Meteorol. 11, 783–792.

Twine T.E., Kustas W.P., Norman J.M., Cook D.R., Houser P.R., Meyers T.P., Prueger J.H., Starks P.J., Wesely M.L., 2000. Correcting eddy-covariance flux underestimates over a grassland. Agric. For. Meteorol. 103, 279-300.

Tyagi N.K., Sharma D.K., Luthra S.K., 2000. Determination of evapotranspiration and crop coefficients of rice and sunflower with lysimetry. Agric. and Water Management 45, 41–54.

Van Atta C.W., 1977. Effect of coherent structures on structure functions of temperature in the atmospheric boundary layer. Arch. Mech. 29, 161-171.

Van Zinderen Bakker E.M. (Jnr.), 1971. Ecological investigations on rain forests of the Eastern Orange Free State, Unpublished M.Sc. thesis, University of the Orange Free State, Bloemfontein, South Africa.

Weinmann H., le Roux M., 1946. A critical study of the torsion balance of measuring transpiration. S. Afr. J. Sci. 42:147-153.

Wiles L., Everson C.S., Jewitt G.P.W., Blight J.J., 2005. Total Evaporation Estimation from Sugarcane using the Scintillation Technique, Proc. of the 12th SANCIAHS Symposium, Midrand, SA.

Wiles, L.W., 2008. Total evaporation estimation from sugarcane using the scintillation technique. M.Sc., School of Bioresources Engineering and Environmental Hydrology, University of KwaZulu-Natal, Pietermaritzburg, South Africa. Pp 126.

Williams R., Zangvil A., Karnieli A., 1984. A portable evaporimeter for rapid measurement of the evaporation rate of water. Agric. For. Meteor. 32, 217–224.

Wilson K., Goldstein A., Falge E., Aubinet M., Baldocchi D., Berbigier P., Bernhofer C., Ceulemans R., Dolman H., Field C., Grelle A., Ibrom A., Law B.E., Kowalski A., Meyers T., Moncrieff J., Monson R., Oechel W., Tenhunen J., Valentini R., Verma S., 2002. Energy balance closure at FLUXNET sites. Agric. For. Meteorol. 113, 223-243.

Zhang C., Shaw R.H., Paw U K.T., 1992. Spatial characteristics of turbulent coherent structures within and above an orchard canopy. In Precipitation Scavenging and Atmosphere-Surface Exchange, Vol. 2, coordinators Schwartz, S.E., Slinn, W.G.N., Hemisphere Publishing Co., Washington, USA, pp 41-75.

Appendix 1

Fact sheet 1: Atmometer and ET gauge method

Atmometer and ET gauge method

ET_o, R5000-R15 000, 1, N, O, S [1]

- *Type of method:* Direct estimate
- *Reference to method:* Williams, R., Zangvil, A., Karnieli, A., 1984. A portable evaporimeter for rapid measurement of the evaporation rate of water. *Agric. For. Meteor.* 32, 217–224.
- *Spatial scale:* < 0.01 m²
- *Measurement distance/area:* 1 m above the surface
- *Averaging period:* Hourly and daily
- *Theoretical basis/comment on method:* An atmometer, or ET gauge, is a canvas-covered ceramic evaporation plate mounted on a water reservoir. The canvas covering controls the evaporation rate simulating the rate of evaporation from a healthy leaf in a well-watered situation. The green canvas that covers the plate mimics the solar radiation absorption characteristics of a plant leaf. Water is provided to the ceramic plate by suction through a plastic supply tube and the amount of water drawn to the plate depends on wind speed, sunlight and relative humidity. As water evaporates from the ET gauge, the water level in the reservoir and sight tube on the outside of the reservoir decreases.
- *Assumptions:* Water evaporation from the atmometer surface is not restricted or limited
- *Measurements required:* Differences in reservoir depth
- *Minimum set of sensors required:* Manual atmometer or electronic Et-gage connected to the pulse port of a datalogger/event recorder

- *Applications over:* Grassland and agricultural crops
- *Don't apply over:* Water, tall canopies (forest), and heterogeneous surfaces
- *Advantage of method:* Simple, low cost
- *Disadvantage of method:* Actual total evaporation needs to be calculated from reference evaporation using an independent measurement or crop factor. Very sensitive to wind and thus instrument placement and exposure is critical.
- *Supplier:* Delta-T Devices
- *References to application in SA:* Savage M.J., Abezghi T. and Johnston M.A. 2002. Atmospheric emittance minus crop emittance under clear skies for calculating gross reference evaporation and comparison with an automation ET-Gage Atmometer reference evaporation. Combined SASHS and SASCP congress, 15th to the 17th January 2002.

[1] E,T,ET,ETo (E/Evaporation, T/Transpiration, ET/Evapotranspiration, ETo/Reference evaporation), cost of equipment, ease of use (1 easy, 4 difficult)., N/H new or historical data, R/O research or operational purposes, S/C relatively simple or complex method

Fact sheet 2: Bowen ratio energy balance method

Bowen ratio energy balance method

E or ET, R70 000, 3, N, R, C [1]

- *Type of method:* Energy balance $Rn-G-H-LE=0$

  where R_n is the net irradiance, G is the soil heat flux density, H is the sensible heat flux density, and LE is the latent heat flux density

- *Reference to method:* Heilman J.L., Brittin C.L. and Neale C.M.U. 1989. Fetch requirements for Bowen-ratio measurements of latent and sensible heat fluxes. Agric. For. Meteorol. 44:261-273.

- *Spatial scale:* Field

- *Measurement distance/area:* Profile measurement, Vertical separation distance 1-2 m, fetch > 30:1

- *Averaging period:* 20 minutes

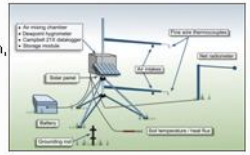

- *Theoretical basis/comment on method:* By definition R_n-G=H+LE

  where $LE=\frac{Rn-G}{1+\beta}$ $1+\beta\neq 0$, $\beta=\frac{\gamma(\Delta T)}{(\Delta e)}=\frac{H}{LE}$

  and β is the Bowen ratio, γ is the psychrometric constant (kPa °C-1), ΔT is the vertical temperature difference (K), Δe is the vertical difference in water vapour pressure (kPa)

- *Assumptions:* The Bowen ratio energy balance technique assumes a shortened energy balance, finite air temperature and water vapour pressure differences and similarity of the transfer coefficients $K_v=K_h$. The transport is one-dimensional and steady state conditions exist.

- *Measurements required:* Net radiation, soil heat flux, soil temperature, soil moisture content, profile measurements of water vapour pressure, air temperature.

- *Minimum set of sensors required:* Net radiometer, soil heat flux plates, soil averaging thermocouples, soil water content sensor, air temperature sensors, dewpoint or humidity sensors.

- *Fetch : Height*
  >30:1 (Ideal 100:1)

- *Applications over:*
  Agricultural crops (sugarcane), plantation trees (wattle, eucalyptus), indigenous vegetation (grassland, fynbos, *Phragmites* reeds, wetlands)

- *Don't apply over:*
  Very tall and rough canopies

- *Advantage of method:*
  Well-established and relatively inexpensive

- *Disadvantage of method:*
  It is assumed that $K_v=K_h$. This is generally true during neutral and unstable atmospheric conditions near the surface, but may not be true during stable (inversion) conditions

- *Supplier:*
  Campbell Scientific Inc. (www.campbellsci.com)

- *Reference to application in SA:*
  Savage, M.J., Everson, C.S. and Metelerkamp, B.R. 1997. Evaporation measurement above vegetated surfaces using micro-meteorological techniques. Water Research Commission Report No. 349/1/97, p248. ISBN No: 1 86845 363 4.

[1] E,T,ET,ETo (E/Evaporation, T/Transpiration, ET/Evapotranspiration, ETo/Reference evaporation), cost of equipment, ease of use (1 easy, 4 difficult)., N/H new or historical data, R/O research or operational purposes, S/C relatively simple or complex method

Fact sheet 3: Cut stem method

Cut stem method

T, R3 000, 1, N, R, S [1]

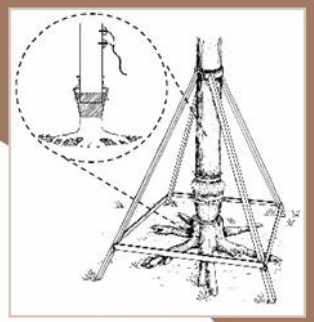

▪ *Type of method:*	Destructive weight measurement of a plant part
▪ *Reference to method:*	Roberts, J. 1977. The Use of Tree-cutting Techniques in the Study of the Water Relations of Mature *Pinus sylvestris L. Journal of Experimental Botany*, Vol. 28, No.104, pp. 751-76.
▪ *Spatial scale:*	Plant
▪ *Measurement distance/area:*	Destructive weight measurements of a plant part (e.g. branch, stem)
▪ *Averaging period:*	Hourly, daily
▪ *Theoretical basis/comment on method:*	The change in observed weight per unit time is equal to the transpiration rate of the particular plant or part thereof. This method provides an estimate of transpiration rate only and excludes other types of evaporation such as soil evaporation
▪ *Assumptions:*	The cut plant continues to transpire normally after cutting has taken place
▪ *Measurements required:*	Weight changes over time
▪ *Minimum set of sensors required:*	High precision scale

▪ *Used with:*
Trees, shrubs

▪ *Don't apply over:*
Plants with a small stem diameter

▪ *Advantage of method:*
Simple

▪ *Disadvantage of method:*
Provides an estimate of transpiration per plant or plant part only; sampling is destructive

▪ *Suppliers*
Information not available

▪ *References to application in SA:*
Olbrich, B.W. 1994. The application of the heat pulse velocity technique to the study of transpiration from Eucalyptus grandis. PhD thesis, University of the Witwatersrand, Pp. 122.

[1] *E,T,ET,ETo (E/Evaporation, T/Transpiration, ET/Evapotranspiration, ETo/Reference evaporation), cost of equipment, ease of use (1 easy, 4 difficult)., N/H new or historical data, R/O research or operational purposes, S/C relatively simple or complex method*

Fact sheet 4: Eddy covariance method

Eddy covariance method

E or ET, R70 000 –R250 000, 4, N, R, C [1]

- *Type of method:* Direct method (2 sensors) or energy balance method (1 sensor)

$$Rn - G - H - LE = 0$$

where R_n is the net irradiance, G is the soil heat flux density, H is the sensible heat flux density, and LE is the latent heat flux density (equivalent of ET).

- *Reference to method:* Meyers, T.P. and Baldocchi, D.D. 2005. Current micrometeorological flux methodologies with applications in agriculture. In: Hatfield, J.L., Baker, J.M. (Eds), Micrometeorology in Agricultural Systems Agronomy Monograph no. 47. pp. 381-396.
- *Spatial scale:* Field
- *Measurement distance/area:* Point measurement – eddy sizes of > 15 cm in diameter
- *Averaging period:* Usually between 20 and 60 minutes
- *Theoretical basis/comment on method:* The eddy covariance method provides a direct measure of the vertical turbulent flux of a scalar entity of interest (F_s) across the mean horizontal stream lines, providing that fast response sensors (~10 Hz) are available to estimate wind vector and scalar entity of interest (sensible heat, water vapour, and carbon dioxide). A 3-D sonic anemometer is used to obtain the orthogonal wind vectors and sonic temperature. An open path H_2O/CO_2 infrared gas analyzer is used to measure water vapour and carbon dioxide concentrations respectively. For a sufficiently long averaging period of time over horizontally uniform surface, the flux is usually expressed as:

$$F_s = \rho_a \overline{w's'}$$

where w is the vertical wind speed and s is the concentration of the scalar of interest. The primes indicate fluctuation from a temporal average (i.e. $w' = w - \overline{w}$) and the over bar represents a time average. The vertical wind speed is responsible for the flux across a plane above a horizontal surface.

- *Assumptions:* Assumes turbulent transfer of water vapor at sample point only, and that corrections for water vapor transfer in turbulence (at time scales less than ~0.1 seconds or greater than the selected averaging time) are acceptable.
- *Measurements required:* Direct estimate of ET: sonic anemometer and infrared gas analyzer
  Indirect estimate of ET: net radiation, soil heat flux, soil temperature, soil moisture content, sonic anemometer
- *Minimum set of sensors required:* Direct estimate of ET: three dimensional wind speed, sonic temperature , infrared gas analyzer
  Indirect estimate of ET: net radiometer, soil heat flux plates, soil averaging thermocouples, soil water content sensor, three dimensional wind speed, sonic temperature

- *Fetch : Height*
  > 30:1 (Ideally 100:1)
- *Applications over:*
  Agricultural crops (sugarcane), plantation trees (wattle, eucalyptus), indigenous vegetation (grassland, fynbos, *Phragmites*, wetlands), open water surface
- *Don't apply over:*
  Very rough canopies
- *Advantage of method:*
  If water vapour covariance is measured, it provides a direct estimate of LE, and, if Rn, G and H are measured at the same time, energy balance closure can be computed to provide some verification of the measurements.
- *Disadvantage of method:*
  High cost, complexity and the sensitivity of instruments to damage, and requires high maintenance to obtain good results
- *Supplier:*
  Campbell Scientific Inc., Gill Instruments Ltd
  Li-Cor Biosciences, Applied technologies, Inc.
- *Reference to application in SA:*
  Savage, M.J., Everson, C.S., Metelerkamp, B.R. 1997. Evaporation measurement above vegetated surfaces using micro-meteorological techniques. Water Research Commission Report No. 349/1/97, p248. ISBN No: 1 86845 363 4.

[1] E,T,ET,ETo (E/Evaporation, T/Transpiration, ET/Evapotranspiration, ETo/Reference evaporation), cost of equipment, ease of use (1 easy, 4 difficult)., N/H new or historical data, R/O research or operational purposes, S/C relatively simple or complex method

Fact sheet 5: Infra-red temperature method

Infra-red temperature method

E or ET, R40 000, 2, N, O, S [1]

- *Type of method:* By definition energy balance: $R_n - G - H - LE = 0$

  where R_n is the net irradiance, G is the soil heat flux density, H is the sensible heat flux density, LE is the latent heat flux density
- *Reference to method:* Jackson, R.D., Idso, S.B., Reginato, R.J. and Pinter Jr., P.J. 1981. Canopy temperature as a drought stress indicator. Water Resour. Res. 17, 1133-1138.
- *Spatial scale:* Field
- *Measurement distance/area:* Arial measurement (< 25 m²)
- *Averaging period:* 30 minutes and hourly
- *Theoretical basis/comment of method:* Canopy surface temperature is measured using an infra-red thermometer and Ficks Law is applied to estimate sensible heat flux density. Air temperature, wind speed and a stability correction is required.
- *Assumptions:* Temperature measurement is representative of the plant / canopy / surface temperature
- *Measurements required:* Areal measurement of canopy temperature, air temperature and windspeed.
- *Minimum set of sensors required:* Infra-red thermometer, air temperature sensor, anemometer, net radiometer, soil heat flux plates, soil averaging thermocouples, soil water content sensor

- *Applications over:* Agricultural crops, water, homogeneous vegetation
- *Don't apply over:* Heterogeneous surface
- *Advantage of method:* Simple
- *Disadvantage of method:* Evaporation estimates applicable to field of view of the sensor only
- *Supplier:* Apogee, Everest
- *References to application in SA:* Mengistu M.G. 2003. The use of infrared thermometry for irrigation scheduling of cereal rye (secale cereale L.) and annual ryegrass (lolium multiflorum Lam.). M.Sc. Agric. Thesis, University of Natal. Pp 109.

[1] E,T,ET,ETo (E/Evaporation, T/Transpiration, ET/Evapotranspiration, ETo/Reference evaporation), cost of equipment, ease of use (1 easy, 4 difficult)., N/H new or historical data, R/O research or operational purposes, S/C relatively simple or complex method

Fact sheet 6: Lysimetry

Lysimetry

E or ET, R100 000, 2, N, R, S [1]

Type of method:	Water budget
Reference to method:	Tyagi N.K., Sharma D.K. and Luthra S.K. 2000. Determination of evapotranspiration and crop coefficients of rice and sunflower with lysimeter. *Agriculture and Water Management* **45**: 41–54.
Spatial scale:	Field
Measurement distance/area:	Field lysimeter: < 10 m² Micro-lysimeter < 1 m²
Averaging period:	Field lysimeter: usually 20 to 60 minutes Micro-lysimeter: usually daily
Theoretical basis/comment on method:	$ET = \rho_w (\delta V/\delta t) / A_{lysimeter}$ where ρ_w is the density of water, $\delta V/\delta t$ the weight change of the soil volume, $A_{lysimeter}$ the area of the lysimeter.
Assumptions:	Water budget = 0, interface between soil and air at base of lysimeter does not affect drainage, there is no lateral flow of soil water. The lysimeter is constructed so that the soils correspond closely to soils under natural conditions.
Measurements required:	Rainfall, drainage, weight change
Minimum set of sensors required:	Rain gauge, lysimeter, drainage bucket

- *Applications in:*
  Agriculture crops, citrus, and other open and closed canopy
- *Don't apply with:*
  Deep rooted trees.
- *Advantage of method:*
  Direct method to estimate water loss
- *Disadvantages of method:*
  Construction is difficult; it is not portable; labour intensive; represents only a small area; soil volume is enclosed so not directly represent surrounding conditions; microlysimeters only provide a measure of soil evaporation.
- *Supplier:*
  Information not available
- *References to application in SA:*
  Olivier F.C. and Singels A. 2007. Effect of a trash blanket on irrigation water use efficiency of sugar cane. ISSCT XXVIth congress Durban, South Africa 29th July - 2nd August 2007.

[1] E,T,ET,ETo (E/Evaporation, T/Transpiration, ET/Evapotranspiration, ETo/Reference evaporation), cost of equipment, ease of use (1 easy, 4 difficult)., N/H new or historical data, R/O research or operational purposes, S/C relatively simple or complex method

Fact sheet 7: Evaporation pans and tanks

Evaporation pans and tanks

ET_o, R10 000 - R15 000, 1, N , O, S [1]

- *Type of method:* Directly measures a change in water level over time for a sample of open water in a "pan" with well-specified dimensions and siting
- *Reference to method:* Allen, R.G., Pereira, L.S., Raes, D. and Smith, M. 1998. Crop evapotranspiration – Guidelines for computing crop water requirements – FAO Irrigation and drainage paper 56. ISBN 92-5-104219-5.
- *Spatial scale:* Field
- *Measurement distance/area:* A-pan: 1.13 m²
- *Averaging period:* Hourly and daily
- *Theoretical basis/comment on method:* An evaporation pan is used to hold water during observations for the determination of the quantity of evaporation at a given location. Pans are of varying sizes and shapes, the most commonly used being circular or square. The best known of the pans are the "Class A" evaporation pan and the "Sunken Colorado Pan. In Europe, India and South Africa, a Symon's Pan (Symon's Tank) is used. The Class A evaporation pan is a universally used standard-sized pan with a diameter of 1.2 m and a depth of 250 mm. When installed, it is elevated 150 mm off the ground. The operating water level is 175 – 200 mm deep; therefore, the water level in the pan is kept 50 – 75 mm from the rim. A stilling well located on the side of a Class A pan has a level sensor which is used to record water depths. The measurements can be taken automatically. If precipitation occurs in the 24-hour period, it is taken into account in calculating the evaporation. Additional measurement of rainfall is therefore required. The Symon's tank is similar to Class A pan but has a larger reservoir.
- *Assumptions:* Assumes measured evaporation from pans can be calibrated against actual evaporation from adjacent area; calibration is transferable between locations and climates.
- *Measurements required:* The amount of evaporation per time unit (the difference between the two measured water depths) and rainfall
- *Minimum set of sensors required:* Evaporation pan, rain gauge

- *Applications over:* Grassland, agricultural crops, water
- *Don't apply :* Over rough canopies, in very cold places, in places with rainfall events of > 55 mm (for a 203mm rain gauge), where the Class A Evaporation pan will likely overflow
- *Advantage of method:* Simple, low cost, easy maintenance.
- *Disadvantage of method:* Provide reference estimate of evaporation only and a crop coefficient or factor is required to estimate ET; the aerodynamic roughness of water surface is different from a vegetative surface; evaporation is dependent on pan exposure
- *Supplier:* ICT International Pty Ltd www.ictinternational.com.au
- *References to application in SA:* Bosman, H.H. 1990. Methods to convert American Class A-pan and Symon's tank evaporation to that of a representative environment. *Water SA*, 16, 227-236.

[1] E,T,ET,ETo (E/Evaporation, T/Transpiration, ET/Evapotranspiration, ETo/Reference evaporation), cost of equipment, ease of use (1 easy, 4 difficult), NH new or historical data, R/O research or operational purposes, S/C relatively simple or complex method

Fact sheet 8: Porometry

Porometry

T, variable cost, 2, N, R, S [1]

- *Type of method:* Direct measurement of leaf transpiration, measured from humidity increase in a chamber temporarily enclosing transpiring leaves/shoots.
- *Reference to method:* Jarvis, P.G. 1976. The interpretation of the variations in leaf water potential and stomatal conductance found in canopies in the field. Philosophical Transactions of the Royal Society of London B. 273, 593-610.
- *Spatial scale:* Leaf to plant
- *Measurement distance/area:*
- *Averaging period:* Hourly
- *Theoretical basis/comment on method:*

There are different types of porometers:

1. Mass flow (air under pressure forced through leaf)
2. Dynamic (rate of change of vapour pressure in cup attached to leaf)

In this type, a small chamber containing a fast response humidity sensor is sealed to the leaf surface. Dry air is pumped through the chamber to achieve a pre-set humidity, then the time required for the chamber humidity to rise to some other preset value is measured.

3. Null balance (adjust flow of dry air to maintain cuvette vapor pressure constant)

In this system a chamber is attached to a leaf (or a leaf is enclosed in a chamber) and the flow of dry air through the chamber is controlled such that the humidity in the chamber remains constant. The change in air flow is measured to calculate conductance.

4. Steady state (measure the vapour flux and gradient near a leaf)

There are a variety of ways to define "steady state". This porometer measures diffusion through a pathway. Other porometers that are "steady state" monitor the time versus the reading until nothing is changing or is "Steady". This method is more similar to the null balance porometer.

- *Assumptions:* Assumes that the enclosed leaves / shoots in the chamber do not significantly alter transpiration rate; steady state conditions
- *Measurements required:* Stomatal conductance or resistance
- *Minimum set of sensors required:* Porometer

- *Applications:* Suitable for individual leaves
- *Don't apply over:* Plants with very small leaves
- *Advantage of method:* Direct measurement of leaf transpiration
- *Disadvantage of method:* Up-scaling to plant and field level is required
- *Supplier:* Decagon
- *References to application in SA:* Dye, P.J. and Olbrich, B.W. 1993. Estimating transpiration from 6-year-old *Eucalyptus grandis* trees: development of a canopy conductance model and comparison with independent sap flux measurements. Plant, Cell and Environment. 16, 45-53.

[1] E,T,ET,ETo (E/Evaporation, T/Transpiration, ET/Evapotranspiration, ETo/Reference evaporation), cost of equipment, ease of use (1 easy, 4 difficult)., N/H new or historical data, R/O research or operational purposes, S/C relatively simple or complex method

Fact sheet 9: Reference evaporation method

Reference evapotranspiration method

ET_o, R36 000, 2, N and H, O, S [1]

Type of method:	Semi-empirical, based on a combination of the shortened energy balance equation and aerodynamic transfer formulas
Reference to method:	Allen, R.G., Pruitt, W.O., Wright, J.L., Howell, T.A., Ventura, F., Snyder, R., Itenfisu, D., Steduto, P., Berengena, J., Yrisarry, J.B., Smith, M., Pereira, L.S., Raes, D., Perrier, A., Alves, I., Walter, I., Elliott, R. 2006. A recommendation on standardized surface resistance for hourly calculation of reference ETo by the FAO56 Penman-Monteith method. Agric. Water Manage. 81, 1–22.
Spatial scale:	Field
Measurement distance/area:	Point
Averaging period:	Hourly and daily
Theoretical basis/comment on method:	This method allows the calculation of a short grass (0.1 m) and taller crop (0.5 m) reference evaporation from standard weather station data. For non-reference crops, actual total evaporation is estimated by multiplying the reference evaporation by a crop factor K_c.
Assumptions:	The crop is not short of water or nutrients, is extensive and totally covers the soil surface.
Measurements required:	Solar radiation, air temperature, wind speed, and relative humidity and latitude, longitude and altitude
Minimum set of sensors required:	Pyranometer, air temperature and relative humidity sensor, anemometer.

Fetch : Height 100:1 (all directions)
Applications over: Grassland, agricultural crops, water Used in different models (e.g. SWB, SWAP, etc.)
Advantage of method: Simple, low cost, low power consumption, low maintenance
Disadvantage of method: Crop factor / coefficient required to convert reference evaporation to actual total evaporation
Supplier: Campbell Scientific Inc. (www.campbellsci.com)
References to application in SA: Abezghi, T.W. 2003. Estimation of reference evaporation and comparison with Et-gage evaporimeter. M.Sc. Agric. Thesis, University of Natal. Pp. 166.

[1] E,T,ET,ETo (E/Evaporation, T/Transpiration, ET/Evapotranspiration, ETo/Reference evaporation), cost of equipment, ease of use (1 easy, 4 difficult), N/H new or historical data, R/O research or operational purposes, S/C relatively simple or complex method

Fact sheet 10: Sap flow techniques

Sap flow techniques

T, R45 000, 3, N, R, C [1]

Type of method:	Direct sap flow or heat pulse method
Reference to method:	Smith, D.M. and Allen, S.J. 1996. Measurement of sap flow in plant stems. Journal of Experimental Botany, 47 (305), 1833-1844.
Spatial scale:	Plant
Measurement distance/area:	Measurements made in or surrounding the stem of plants (< 200 mm)
Averaging period:	Hourly
Theoretical basis/comment on method:	The transpiration rate of a plant is monitored by evaluating the rate at which sap flows through the conducting tissues (xylem). A sap flow system either utilises heater and temperature probes which are inserted into the stem or roots, or an external heater surrounding them. Sap absorbs / transfers heat and induces temperature changes in the sensors. Various sap flow measurement methods exist. The Heat Pulse Velocity method utilises a heater probe inserted into the sapwood, with thermocouples inserted downstream and sometimes upstream of the heater to measure temperature changes resulting from the heat pulse. The Thermal Dissipation Probe method utilises an upper needle containing a heater element and thermocouple, referenced to a second lower needle, both inserted into the sapwood. The Heat Field Deformation method utilises a heater and two atmospherics of thermocouples implanted symmetrically and asymmetrically into the stem. The Heat Balance method is based on the ratio between heat input and temperature rise in a pre defined space. The Stem Heat Balance method combines external heating with a soft and flexible heater together with thermo sensors.
Assumptions:	Heat and energy conservation
Measurements required:	Temperature changes in sap, cross sectional sap wood area and stem circumference at measuring point, bark thickness, wood density, sap wood wound widths
Minimum set of sensors required:	Heat probes, temperatures probes, power supply for the heater probes

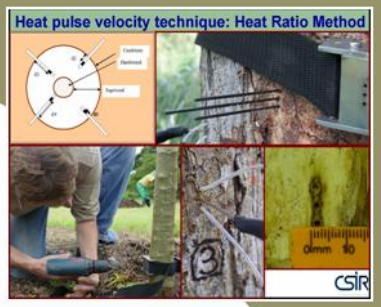

- *Used with:*
  Trees, shrubs
- *Don't apply over:*
  Plants with a small stem diameter
- *Advantage of method:*
  Very useful for calibration and validation of water and energy balance and separation of evaporation and transpiration components. It can be applied under any terrain, soil and meteorological conditions for studies of different species.
- *Disadvantage of method:*
  Measures transpiration only and uncertainties in estimating water use can occur as a result of errors made in scaling transpiration from plant to stand; Some methods are intrusive
- *Suppliers*
  CSIRO Land and Water (www.clw.csiro.au)
- *References to application in SA:*
  Dye, P.J., Soko, S., Poulter, A.G. 1996. Evaluation of the heat pulse velocity method for measuring sap flow in *Pinus patula*. *Journal of Experimental botany*, 47, 975-981.

[1] E,T,ET,ETo (E/Evaporation, T/Transpiration, ET/Evapotranspiration, ETo/Reference evaporation), cost of equipment, ease of use (1 easy, 4 difficult)., N/H new or historical data, R/O research or operational purposes, S/C relatively simple or complex method

Fact sheet 11: Scintillometry

Scintillometry

E or ET, R250 000-R500 000, 3, N, R, C [1]

- *Type of method:* Energy balance $Rn-G-H-LE=0$

  where R_n is the net irradiance, G is the soil heat flux density, H is the sensible heat flux density, LE is the latent heat flux density
- *Reference to method:* Hill R.J. 1992. Review of optical scintillation methods of measuring the refractive-index spectrum, inner scale and surface fluxes, Waves in Random and Complex Media, 2, 179-201.
- *Spatial scale:* Field, catchment
- *Measurement distance/area:* 50 – 10 000 m
- *Averaging period:* 2 to 30 minutes
- *Theoretical basis/comment on method:* A scintillometer is used to measure path-weighted sensible heat flux. It measures the intensity fluctuations of visible or infrared radiation after propagation above the plant canopy of interest. It optically measures the structure parameter of refractive index of air, C_n^2, reflecting the atmospheric turbulence structure. Depending on the aperture size, scintillometers are classified into small aperture (SLS, beam path length of 50 – 250 m) and large aperture scintillometers (LAS, beam path length of 250 m – 5km, and path length of >10 km for boundary layer scintillometers). Sensible heat flux is estimated using what is referred to as Monin-Obukhov similarity theory (MOST).
- *Assumptions:* Applies to a turbulent layer close to the surface to a surface with uniform aerodynamic roughness (MOST)
- *Measurements required:* Net radiation, soil heat flux, soil temperature and heat flux, soil moisture content, profile air temperature measurements, windspeed
- *Minimum set of sensors required:* Scintillometer, net radiometer, soil heat flux plates, soil averaging thermocouples, soil water content sensor, air temperature sensors, anemometer

- *Fetch : Height*
  Ideally 100:1
- *Applications over:*
  Grassland, agricultural crops, forests, riparian vegetation, indigenous vegetation
- *Don't apply over:*
  Open water surface
- *Advantage of method:*
  Path averaged measurement of ET
- *Disadvantage of method:*
  Saturation of signal; direction of flux requires independent measurements of air temperature and windspeed
- *Supplier:*
  Scintec, Kipp and Zonen
- *References to application in SA:*
  Savage M.J., Everson C.S., Odhiambo G.O., Mengistu M.G. and Jarmain C. 2004. Theory and practice of evaporation measurement, with a special focus on SLS as an operational tool for the estimation of spatially-averaged evaporation, Water Research Commission Report No. 1335/1/04. ISBN 1-77005-247-X.

[1] E,T,ET,ETo (E/Evaporation, T/Transpiration, ET/Evapotranspiration, ETo/Reference evaporation), cost of equipment, ease of use (1 easy, 4 difficult)., N/H new or historical data, R/O research or operational purposes, S/C relatively simple or complex method

Fact sheet 12: Surface renewal method

Surface renewal method

E or ET, R35 000, 3, N, R, S [1]

- *Type of method:* Energy balance $R_n - G - H - LE = 0$

  where R_n is the net irradiance, G is the soil heat flux density, H is the sensible heat flux density, LE is the latent heat flux density.
  There are three approaches using different calculations. The most common method is described below, the other two approaches require additional measurements of windspeed.

- *Reference to method:* Paw U, K.T., Snyder, R.L., Spano, D., and Su, H.-B. *In press.* Surface Renewal Estimates of Scalar Exchange. Refereed chapter in *Micrometeorology of Agricultural Systems*, ed. J.L. Hatfield, Agronomy Society of America.

- *Spatial scale:* Field

- *Measurement distance/area:* Point measurement at a defined height above the surface or canopy

- *Averaging period:* From 2 to 60 minutes

- *Theoretical basis/comment on method:* H is calculated from the amplitude and ramping period of high frequency air temperature measurements at a defined height using a fine wire thermocouple. The equation for H is:

  $$H = \alpha \rho c_p \frac{a}{\tau} z$$

  where α is the calibration (weighting) factor, ρ is the density of air (kg m^{-3}), c_p is the specific heat capacity of air (J $kg^{-1}K^{-1}$), a is ramp amplitude, and τ is the inverse ramp frequency (ramping period), and z is the measurement height above the ground surface (m).

- *Assumptions:* Initial calibration relationship constant for specific height above canopy

- *Measurements required:* Net radiation, soil heat flux, soil temperature, soil moisture content, high frequency air temperature

- *Minimum set of sensors required:* Net radiometer, soil heat flux plates, soil averaging thermocouples, soil water content sensor, fine wire thermocouple

- *Fetch : Height*
  10:1 to 200:1 (Ideal 100:1)

- *Applications over:*
  Agricultural crops, forests, open water surface

- *Don't apply over:*
  Very rough surface

- *Advantage of method:*
  Low cost, low power consumption
  Easy to maintain, replicate

- *Disadvantage of method:*
  Initial calibration for surface required

- *Supplier*
  Campbell Scientific Inc. (www.campbellsci.com)

- *References to application in SA:*
  Mengistu, M.G., undated. Heat and energy exchange above different surfaces using surface renewal. Draft PhD thesis submitted, University of KwaZulu-Natal, Pietermaritzburg, South Africa. Pp. 148.

[1] E,T,ET,ETo (E/Evaporation, T/Transpiration, ET/Evapotranspiration, ETo/Reference evaporation), cost of equipment, ease of use (1 easy, 4 difficult)., N/H new or historical data, R/O research or operational purposes, S/C relatively simple or complex method

Fact sheet 13: Temperature and temperature variance methods

Temperature and temperature variance methods

E or ET, R37 000, 3, N and H, R, S [1]

▪ *Type of method:*	Energy balance $R_n - G - H - LE = 0$ where R_n is the net irradiance, G is the soil heat flux density, H is the sensible heat flux density, LE is the latent heat flux density
▪ *Reference to method:*	Tillman, J. E. 1972. The Indirect Determination of Stability, Heat and Momentum Fluxes in the Atmospheric Boundary Layer from Simple Scalar Variables during Dry Unstable Conditions, *J. Appl. Meteorol.* 11, 783–792.
▪ *Spatial scale:*	Field
▪ *Measurement distance/area:*	Point measurement above surface
▪ *Averaging period:*	30 minutes
▪ *Theoretical basis/comment on method:*	Temperature variance: $H \propto \sigma T$ and u_* where σT is the temporal air temperature standard deviation and u_* is the friction velocity (m s^{-1}). H is related to the weighted average of the time history of air temperature and u_*
▪ *Assumptions:*	MOST is assumed
▪ *Measurements required:*	Net radiation, soil heat flux, soil temperature, soil water content, high frequency air temperature using a fine-wire thermocouple
▪ *Minimum set of sensors required:*	Net radiometer, soil heat flux plates, soil averaging thermocouples, soil water content sensor, air temperature sensors, windspeed

▪ *Fetch : Height*
Ideally 100:1

▪ *Applications over:*
Agriculture, water, forests, grassland

▪ *Don't apply over:*
Very rough canopies

▪ *Advantage of method:*
Simple, low cost

▪ *Disadvantage of method:*
Requires high frequency air temperature measurements; direction of flux requires independent measurements of air temperature and windspeed

▪ *Supplier:*
Campbell Scientific Inc. (www.campbellsci.com)

▪ *References to application in SA:*
Savage, M.J., 2007. Sensible heat estimation using a high frequency temperature-based method above various canopies. Paper presentation to the 13th SANCIAHS Conference, 6 to 7 September, Cape Town, South Africa.

[1] E,T,ET,ETo (E/Evaporation, T/Transpiration, ET/Evapotranspiration, ETo/Reference evaporation), cost of equipment, ease of use (1 easy, 4 difficult)., N/H new or historical data, R/O research or operational purposes, S/C relatively simple or complex method

Fact sheet 14: Water balance method

Water balance method

E or ET, cost variable, 2, N and H, R and O, S [1]

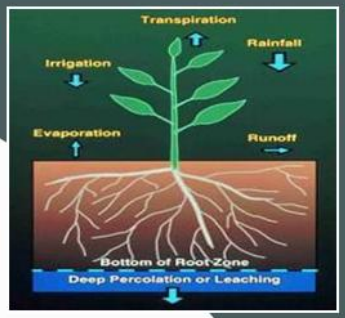

- *Type of method:* Water balance or budget
- *Reference to method:* Ritchie, J.T. (1972). A simple method of estimating the soil water balance. Agric. Meteorol. 28, 1-7.
- *Spatial scale:* Catchment or sub-catchment (field scale)
- *Measurement distance/area:* Variable
- *Averaging period:* Variable: Daily, weekly, monthly, annual
- *Theoretical basis/comment on method:* Inputs and losses of the hydrological cycle are measured or estimated using the law of conservation and mass balance system. At a daily level, the mass balance would be represented by:

  $P + CR + Irr - ET - R - D - S = 0$

  P is the amount of rainfall [mm d^{-1}], *CR* is the capillary rise from the groundwater table [mm d^{-1}] (not shown in figure), *Irr* is the irrigation dose [mm d^{-1}], *ET* is evapotranspiration [mm d^{-1}], *R* is runoff [mm d-1], *D* is drainage [mm d^{-1}], and *S* is the storage of water in the soil compartment [mm d^{-1}]. Field water balance computer models like SWB, SWAP, WAVES, etc., use the water balance approach to estimate evaporation.
- *Assumptions:*
  - All significant components of the system are included in the mass balance equation.
  - In many cases, components of the mass balance equation require estimation (such as drainage) using hydrological models.
  - Point measurements and estimates are representative of the catchment or sub-catchment
- *Measurements required:* Rainfall, runoff, soil water content, drainage, capillary rise, groundwater levels, soil properties
- *Minimum set of sensors required:* Rain gauges, weirs, soil water content sensors

- *Applications over:*
  Any surface - agricultural and others
- *Don't apply over:*
  Areas where soils, geology or groundwater information is unknown or highly heterogeneous surface
- *Advantage of method:*
  Catchment level results: limited data required for annual water balance estimates
- *Disadvantage of method:*
  Low accuracy; coarse spatial and temporal resolution
- *Supplier:*
  Hydrological models available include ACRU, Mike Basin, SWAP, SWB, WAVES
- *References to application in SA:*
  Hensley, M., Anderson, J.J, Botha, J.J., van Staden, P.P., Singels, A., Prinsloo, S. and Du Toit. A. 1997. Modelling the water balance on benchmark ecotopes. WRC Report No. 508/1/9. WRC, Pretoria.

[1] E,T,ET,ETo (E/Evaporation, T/Transpiration, ET/Evapotranspiration, ETo/Reference evaporation), cost of equipment, ease of use (1 easy, 4 difficult)., N/H new or historical data, R/O research or operational purposes, S/C relatively simple or complex method